

Conceptual Design and Assessment of Extractive Distillation Processes with Deep Eutectic Solvents

By

Ann-Joelle Minor

in partial fulfilment of the requirements for the degree of

Master of Science
in Chemical Engineering

at the Delft University of Technology,
to be defended publicly on Friday, December 18, 2020, at 1:00 PM.

Student number: 4949692
Project duration: April 20, 2020 – December 18, 2020
Thesis committee: Prof. dr. ir. André de Haan,
Prof. dr. ir. Anton. A. Kiss,
Prof. dr. ir. Costin Sorin Bildea,

Delft University of Technology, *Supervisor*
Delft University of Technology
University Politehnica of Bucharest

Preface

This work was done under the supervision of Professor André de Haan in partial fulfilment of the requirements of the Master of Science degree in chemical engineering. First, I would like to thank Professor André de Haan in this sense, for his guidance and advice concerning, not only this work but also future career orientations. I am very grateful to have benefited from researching this extremely interesting topic, and his inputs and constructive ideas that I will definitely remember also for further projects. I also would like to thank Professor Tony Kiss for being a part of my defense committee and helping me with a problem which saved a considerable amount of time! Moreover, I would like to thank Professor Costin Sorin Bildea as a member of my defence committee for investing time and his interest in my work from University Politehnica of Bucharest!

I am also thankful to my friends and colleagues for setting the ground of this fantastic journey, and a wonderful living experience in Delft, especially in the first year of the master program. I would also like to express my profound gratitude to my close friend Sohan Abhay Phadke, for proofreading as well as Michaël Lejeune for his support and motivation during these months. Last but not least, I would like to thank my family for encouraging me wholeheartedly in pursuing my goals; for their support in good and challenging times, and most importantly, for their unconditional love.

*Ann-Joelle Minor
Delft, December 2020*

Abstract

Extractive distillation with organic solvents as entrainers is one of the most commonly used separation techniques for azeotropic mixtures in the chemical industry. To reduce the large energy requirements, and the secondary pollution problems, both of which are associated with the use of organic solvents, the search for alternative entrainers has received much attention. Recently, deep eutectic solvents that are known as green and non-volatile components have been considered as entrainers for extractive distillation processes. However, research focuses mainly on vapour-liquid equilibrium measurements, and an economic comparison with the conventional organic solvents has not been done yet.

This work investigates extractive distillation with deep eutectic solvents where a conceptual process design is carried out for the separation of ethanol and water, as well as isopropanol and water with the aid of Aspen Plus as process simulator. In order to fulfil the research aim of exploring whether deep eutectic solvents reduce both cost and overall energy consumption, first, a database for the investigated deep eutectic solvents is created. Based on the effect of the deep eutectic solvents on the vapour-liquid equilibrium, choline chloride:urea (1:2) and choline chloride:triethylene glycol (1:3) are chosen for the ethanol system and isopropanol system, respectively. Subsequently, different entrainer recycle alternatives are investigated, and a sensitivity analysis of the design variables is performed. For both systems, it is found that a series of two evaporators are the most economical entrainer regeneration option. Last, a consistent comparison of the final processes with the process using the conventional organic solvents and ionic liquids is carried out. The results show that the considered deep eutectic solvents are not only beneficial in terms characteristics such as biodegradability, toxicity and selectivity, but also regarding specific energy requirements and the total annual costs. The process using conventional organic solvents is improved by at least 20.1% from an energetical perspective and by a minimum of 16.6% from an economic perspective for both systems. The replacement of ionic liquids by deep eutectic solvents also results in an energy reduction of a minimum of 6%. The additional use of heat integration further improves the final processes by 8 to 10% with respect to specific energy requirements in steam and therefore reduces the carbon footprint. Finally, it is concluded that the extractive distillation using deep eutectic solvents outperforms the process using conventional organic solvents and ionic liquids in both separations; ethanol and water, and isopropanol and water.

Table of Contents

TABLE OF CONTENTS	I
LIST OF SYMBOLS & ABBREVIATIONS.....	V
LIST OF FIGURES	IX
LIST OF TABLES	XIII
1 INTRODUCTION & MOTIVATION.....	1
2 LITERATURE REVIEW & KNOWLEDGE GAP	3
2.1 Conventional Process and Entrainer	3
2.2 Ionic Liquids	5
2.3 Deep Eutectic Solvents	6
2.3.1 Separation of Ethanol and Water	6
2.3.2 Separation of IPA and Water	7
2.3.3 Summary of the Considered Separation Systems and DESs.....	7
3 DATA & ASPEN IMPLEMENTATION OF THE DES	8
3.1 Data Collection.....	8
3.2 Validation of the Regression.....	8
3.2.1 Properties of the DESs.....	8
3.2.2 Thermodynamic Model.....	9
3.3 VLE Analysis & Feasibility of the DES as Entrainer.....	9
3.3.1 Ethanol and Water.....	10
3.3.2 IPA and Water.....	12
3.3.3 Summary & Final Choice of the DES.....	13
4 PRELIMINARY PROCESS SYNTHESIS.....	14
4.1 Separation Task & Constraints.....	14
4.2 Identification of Design Variables & Objective Functions.....	14
4.3 Black-Box Diagram.....	15
5 BASE CASE DESIGNS & PROCESS SIMULATION	16
5.1 Unit Design Specifications	16
5.1.1 Heating, Cooling and Change in Pressure	16
5.1.2 Recovery Unit.....	16
5.1.3 EDC Unit.....	17
5.2 Sensitivity Analysis.....	18
5.2.1 Entrainer and Feed Temperature of the EDC	18
5.2.2 Pressure of the EDC	19
5.2.3 Entrainer Impurity of the EDC.....	19

5.2.4	Entrainer and Feed Stage of the EDC	20
5.2.5	Reflux Ratio and Entrainer to Feed Ratio of the EDC	21
5.2.6	Number of Stages of the EDC	21
5.2.7	Regeneration: Two Evaporators.....	22
5.2.8	Regeneration: Evaporator and Stripping Column	23
5.3	Optimised Base Case Processes & Flowsheets	24
6	HEAT INTEGRATION	27
6.1	Energy Savings & Composite Curves.....	27
6.2	Heat-Integrated Aspen Flow Sheets & Process Stream Summaries.....	28
7	PREPARATIONS FOR THE ASSESSMENTS	30
7.1	Equipment Specifications.....	30
7.1.1	Separation Towers.....	30
7.1.2	Reflux Drums	31
7.1.3	Heat Exchangers and Evaporators	31
7.1.4	Pumps, Valves and Vacuum System.....	32
7.2	Utility Requirements	33
7.3	Total Annual Costs	34
7.3.1	Total Annual Production Costs.....	34
7.3.2	Total Capital Investment.....	35
8	SELECTION OF ONE BASE CASE DESIGN	36
9	PROCESS FLOW DIAGRAM & PROCESS STREAM SUMMARY	39
10	EVALUATION OF THE PROCESS USING DES	42
10.1	Properties & Characteristics.....	42
10.2	Specific Energy Requirements & Total Annual Costs	44
11	CONCLUSIONS & RECOMMENDATIONS	47
11.1	Conclusions	47
11.2	Recommendations	48
12	REFERENCES.....	49
APPENDIX A DECISIONS & HEURISTICS.....		- 1 -
APPENDIX B THEORETICAL BACKGROUND & METHODS.....		- 9 -
B.1	Process Modelling	- 9 -
B.1.1	Thermophysical Property Estimation	- 9 -
B.1.2	Thermodynamics.....	- 9 -
B.1.3	Process Simulation	- 10 -
B.1.4	Determination of Design Variables.....	- 10 -
B.2	Analysis	- 13 -
B.2.1	Pseudo-Binary Diagrams.....	- 13 -

B.2.2	Characteristics of Entrainers.....	- 13 -
B.2.2.1	Selectivity, Relative Volatility & Capacity	- 13 -
B.2.2.2	Residue Curve Maps & Minimum Entrainer Amounts.....	- 14 -
B.2.3	Data Validation	- 15 -
B.3	Utility Requirements and Classifications.....	- 16 -
B.4	Purchase Costs of the Equipment	- 17 -
APPENDIX C	SUPPLEMENT TO THE MAIN TEXT	- 20 -
C.1	Innovation Map.....	- 20 -
C.2	Literature Review	- 21 -
C.2.1	List of Publications: DESs as Entrainer in Extractive Distillation.....	- 21 -
C.2.2	Process Details of Investigated Publications	- 22 -
C.2.3	Extractive Distillation with ILs as Entrainers.....	- 24 -
C.3	Process & Property Data Collection	- 26 -
C.3.1	Pure Component Properties	- 26 -
C.3.2	Temperature-Dependent Properties.....	- 28 -
C.3.3	Vapor-Liquid Equilibrium.....	- 30 -
C.3.4	Aspen Parameters.....	- 35 -
C.4	Aspen Implementation of the DES	- 37 -
C.4.1	Data Validation	- 37 -
C.4.1.1	Residue Mean Square Deviations.....	- 37 -
C.4.1.2	Simulated VLE Curves with Data Points.....	- 38 -
C.4.2	Analysis of the Activity Coefficients.....	- 43 -
C.4.3	Residue Curve Maps	- 45 -
C.5	Preliminary Process Synthesis: Black-Box Diagrams	- 46 -
C.6	Base Case Design: Entrainer Regeneration Options.....	- 47 -
C.7	Process Simulation.....	- 49 -
C.7.1	Sensitivity Analysis.....	- 49 -
C.8	Base Case Designs	- 50 -
C.8.1	Aspen Flow Sheets before Heat Integration.....	- 50 -
C.8.2	Process Design Variables	- 55 -
C.8.3	Heat integration	- 57 -
C.8.4	Heat-Integrated Aspen Flow Sheets & Process Stream Summaries.....	- 60 -
C.8.5	Utility Summary	- 64 -
C.8.6	Equipment List & Economic Assessment.....	- 67 -
C.8.6.1	Equipment Sizing & Purchase Costs	- 68 -
C.8.6.2	Equipment Summary & Costs.....	- 77 -
C.8.6.3	Total Annual Production Costs.....	- 81 -
C.8.6.4	Total Annual Costs	- 82 -
C.9	Final DES Processes & Literature Comparison.....	- 82 -
C.9.1	Utility Summary	- 82 -
C.9.2	Flowsheets & Process Stream Summary	- 93 -
C.9.2.1	Separation Task 1.....	- 94 -

C.9.2.2	Separation Task 2.....	- 99 -
C.9.2.3	Separation Task 3.....	- 104 -
C.9.3	Equipment Specification & Economic Assessment.....	- 110 -
C.9.3.1	Equipment Sizing & Purchase Costs	- 110 -
C.9.3.1.1	Separation Task 1	- 110 -
C.9.3.1.2	Separation Task 2	- 115 -
C.9.3.1.3	Separation Task 3	- 119 -
C.9.3.2	Equipment Summary & Costs.....	- 125 -
C.9.3.2.4	Separation Task 1.....	- 125 -
C.9.3.2.5	Separation Task 2	- 128 -
C.9.3.2.6	Separation Task 3	- 131 -
C.9.3.3	Total Annual Production Costs.....	- 135 -
C.9.3.3.7	Separation Task 1.....	- 135 -
C.9.3.3.8	Separation Task 2	- 136 -
C.9.3.3.9	Separation Task 3	- 137 -
C.9.3.4	Total Annual Costs	- 139 -
C.9.3.4.10	Separation Task 1	- 139 -
C.9.3.4.11	Separation Task 2	- 139 -
C.9.3.4.12	Separation Task 3	- 139 -

List of Symbols & Abbreviations

Abbreviation	Meaning
[BF ₄] ⁻	Tetrafluoroborate anion
[Bmim] ⁺	1-butyl-3-methylimidazolium
[Cl] ⁻	Chloride anion
[Emim] ⁺	1-ethyl-3-methylimidazolium
[N(CN) ₂] ⁻	Dicyanamide anion
[OAc] ⁻	Acetate anion
A	Assumptions
alpha	Relative volatility
C	Choices
CH	Chilled water
ChCl	Choline Chloride
CW	Cooling water
DES	Deep Eutectic Solvent
DMSO	Dimethyl sulfoxide
E/F	Entrainer-to-feed ratio
EDC	Extractive Distillation Column
EG	Ethylene Glycol
f.o.b.	Free on board
GA	Glycolic acid
Gly	Glycerol
H	Heuristics
HBA	Hydrogen Bond Acceptor
HBD	Hydrogen Bond Donor
HHAL	High alarm liquid level
HP	high pressure steam
IL	Ionic liquid
IPA	Isopropanol
LA	Lactic acid
LP	Low pressure steam
MA	Malic acid
MP	Medium pressure steam
NRTL	Non-random two liquid
PDC	Purification Distillation Column
R ²	Coefficient of determination
RCMs	Residue curve maps
RF	Refrigerant
RMSD	The root mean square deviation
RR	Reflux ratio
scCO ₂	Supercritical CO ₂
SRC	Solvent Recovery Column
TEG	Triethylene glycol
TEMA	Tubular Exchanger Manufacturers Association
Ur	Urea
TAC	Total annual costs
VLE	Vapour Liquid Equilibrium

Symbol	Meaning	Unit
\dot{Q}_{HE}	Heat exchanger duty	kW
\dot{m}_w	cooling water mass flow rate	kg/s
\bar{y}	Averaged data points	
\hat{y}_1	Data points	
y_i	Simulated point	
\dot{U}_g	Vapour gas flow rate	m ³ /s
C_b	Base costs	\$
C_{BT}	Base costs for sieve trays	\$
$C_{P,liquid}$	Purchase costs liquid	\$
$C_{P,steamjet}$	Purchase costs steamjet	\$
C_P	Purchase cost	\$
C_{PL}	Cost of platforms and ladders	\$
C_T	Costs for installed trays	\$
C_v	Costs of the empty vessel	\$
C_{AP}	Total annual production costs	\$
C_{TPI}	Fixed capital investment	\$
F_{stages}	Factor stages	-
S_{liquid}	Size factor – liquid ring pump	ft ³ /min
$S_{steamjet}$	Size factor – Steam Jet ejector	lb/hr/torr
T_{cond}	Temperature precondenser	°C
W_{air}	Air leakage of equipment	lb/hr
$W_{product}$	Product flow to vacuum	lb/hr
W_{vacuum}	Flow to vacuum	lb/hr or ft ³ /min
γ_i	Activity coefficient of component i	-
τ_{ji}	Dimensionless interaction parameter	-
P_{comp}	Compressor power	kW
k_{SB}	Brown parameter	m/s
Δp	Pressure difference	kPa
ΔT	Temperature difference	°C
ΔT_{LM}	Logarithmic mean temperature difference	°C
ΔT_w	Temperature difference of the cooling water	°C
A_z	Cross-sectional area	m ²
c_p	Heat capacity	kJ/kg/K
cp_w	Heat capacity of water	kJ/kg/K
D	Diameter	ft
dT_{min}	Minimum approach temperature	°C
D_{ves}	Vessel diameter	ft
E_M	Modulus of elasticity	psi
F	Correction factor	-
f_{LTPI}	Lang factor	-
F_M	Material factor	-
F_{OP}	Plant operating factor	-
g	Gravitational acceleration constant	m/s
H	Height	m or ft or in
H	Pump head	ft
h_e	Evaporation energy of the steam	kJ/kg
h_L	Saturated liquid enthalpy	kJ/kg
h_v	Saturated vapour enthalpy	kJ/kg
I	plant cost index	-
i_{min}	Return on investment	1/year
L	Tangent-to-tangent length	m or ft or in
LD_{50}	Median letal dose 50%	[mg/kg]
m_{gas}	Stripping agent flowrate	kg/s

m_R	Refrigerant mass flowrate	kg/s
m_s	Steam mass flow rate	kg/s
M_w	Molecular weight	[g/mol]
η	Viscosity	mN-sec/m ²
N_E	Entrainer feed stage	-
N_F	Main feed stage	-
$N_{\text{freecycle}}$ or $N_{\text{recyclegas}}$	Feed stage of product recycle	-
N_{stripp}	Number of stages of stripping column	-
N_{th}	Number of stages	-
p	Operating pressure	kPa or atm
p_c	Critical pressure of a component	bar
$P_{\text{condensor}}$	Pressure condenser	kPa or atm
P_d	Design Pressure	psig
P_o	Lowest operating pressure	kPa
p_{recov}	Pressure of the recovery unit	kPa
p_{stripp}	pressure of the stripping column	kPa
p_{vap}	Vapor pressure	Pa
Q_{Cmin}	Minimum of cold utilities	kW
Q_{HE}	Heat exchanger loads	kW
Q_{hp}	Pump power	horsepower
Q_R	Refrigeration capacity	tonne
Q_{reb}	Reboiler duty	kW
R	Ideal gas constant	J/mol/K
S	Maximum allowable stress	psig
S/F	Solvent to feed mass ratio	
T	Temperature	°C
T_b	Boiling temperature	°C
T_c	Critical temperature of a component	°C
T_{evap}	Temperature of the evaporator	°C
T_F	Feed temperature	°C
$T_{\text{freecycle}}$	Temperature of the product recycle	°C
T_{gas}	Temperature of stripping agent	°C
T_m	Melting temperature	°C
T_o	Highest operating temperature	°C
T_P	Temperature of the product recycle	°C
T_{recov}	Temperature of the recovery unit	°C
T_E	Temperature of the entrainer	°C
T_d	Design temperature	°F
t_c	Corrosive allowance	in or cm
t_E	Wall thickness	in or cm
t_{EC}	Wall correction	in or cm
t_{ho}	Hold-up time	min
t_s	Actual wall thickness	in or cm
t_w	Necessary wall thickness	in or cm
U	Heat transfer coefficient	W/m ² /°C
U_{gmax}	Maximum gas velocity	m/s
V	Volume equipment	m ³ or ft ³
V_c	specific volume at critical point	cm ³ /kmol
V_{ves}	Volume of the vessel	m ³ or ft ³
W	Weight of shell and two heads	lb
w_3	Weight fraction of the entrainer	kg/kg
x_1	Mole fraction	mol/mol
x_1'	Mole fraction on entrainer free basis	mol/mol
$x_{1\text{dist}}$	Distillate purity / mole fraction	mol/mol

$X_{3\text{recyc}}$	Entrainer recycle mole fraction	mol/mol
X_E	Entrainer recycle purity	mole/mole
Z_c	compressibility factor	-
Θ	Vapor liquid surface angle	rad
ρ	density	g/cm^3
ω	acentric factor	-
Δg_{ji}	Interaction energy parameter	J/mole
$\alpha_{p_{ij}}$	Symmetrical non-randomness parameter	-

List of Figures

Main text

Figure 1: Stages and structure of this project, starting from the idea to the final evaluation of DESs. The eminent chemical engineering modelling software Aspen Plus is used to perform simulations [18].	2
Figure 2: Applications of ethanol represented in a pie chart [20].	3
Figure 3: Conventional separation of ethanol and water for the production of bioethanol.	4
Figure 4: Comparison between ChCl:GA (1:3), ChCl:EG (1:2) and ChCl:Ur (1:2) in a diagram of the vapour mole fraction of ethanol over the liquid mole fraction of ethanol on entrainer free basis (left) and the selectivity over the entrainer mole fraction (right).	10
Figure 5: Residue curve map for ethanol, water and ChCl:EG (1:2) on a mole basis. Also shown is the azeotrope of water and ethanol and the isovolatility curve (in dashed red).	11
Figure 6: IPA vapour mole fraction (left) and relative volatility (right) over liquid mole fraction on entrainer free basis for four different constant ChCl:TEG (1:3) weight fractions.	12
Figure 7: Simulation results of the activity coefficient of IPA (γ_1) (left) and water (γ_2) (middle) and the selectivity (right) as defined in Chapter B.2.2 plotted over the mole fraction of ChCl:TEG (1:3) for two different IPA mole fractions on entrainer free basis (x_1).	12
Figure 8: Black box diagram for the separation of ethanol (1) and water (2) using the process details of Bastidas <i>et al.</i> (2010) [30]. The constraints (inbox) and the design variables and unknowns (in red) are given as well. However, for this diagram, the separation efficiency of the entrainer and water has been assumed to be 100%.	15
Figure 9: Reboiler duty (blue: Q_{reb}) and mole fraction of ethanol in the distillate (orange: x_{1dist}) over the feed temperature (T_F) for two different entrainer feed temperatures (dashed and solid lines: different T_E). The pressure of the feed is 1.5 bar.	18
Figure 10: Energy requirements of the process for different condenser pressures (14, 40, 70 and 101 kPa) of the EDC. Shown are the reboiler duty (green), the requirements downstream to the EDC (blue).	19
Figure 11: Mole fraction of ethanol in the distillate (x_{1dist}) over the entrainer to feed ratio (E/F) for three different reflux ratios (RR). Left graph: entrainer feed containing 99.5 mol% of ChCl:Ur (1:2), Right graph: entrainer feed containing 98.5 mol% of ChCl:Ur (1:2).	20
Figure 12: Ethanol purity in distillate (x_{1dist}) over main feed stage (N_F) for different entrainer feed stages (N_E) (left) and reboiler duty (Q_{reb}) for two different N_E . RR is adapted to meet the purity constraint.	20
Figure 13: Ethanol purity in distillate (x_{1dist}) and reboiler duty (Q_{reb}) (right) over the reflux ratio RR for different E/F.	21
Figure 14: Reboiler duty (Q_{reb}) over the total number of stages (N_{th}) for the two different entrainer purity cases $x_E=99$ mol% (orange) and $x_E=99.5$ mol% (blue). RR and E/F are adapted to meet the constraints.	22
Figure 15: Mole fraction of the entrainer in the entrainer recycle (x_E) (left) and recovery of the entrainer (right) over the operating temperature for different operating pressures of the first evaporator.	23
Figure 16: Mole fraction of the entrainer in the entrainer recycle (x_E) (left) and recovery of the entrainer (right) over the operating temperature for different operating pressures of the second evaporator.	23
Figure 17: Energy requirements of the processes with a different entrainer recycle and regeneration unit choice. Shown are the reboiler duty (green), the total energy demand of the heat exchangers in the process (orange) and the total energy demand of the entrainer regeneration unit (blue).	24
Figure 18: Creation of four base case designs through the evaluation of different process alternatives.	25
Figure 19: Process flowsheet and additional information regarding flows, process design variables and heat exchanger duties for the base case design involving two evaporators and the EDC operating at 1 atm. The compositions are given in mole fractions.	26
Figure 20: Composite curves of the integrated process part. The hot composite curve (orange) consists of distillate cooling (left part: E07) and entrainer recycle cooling (right part: E01), and the cold composite curve is the main feed (E02). Shown are also the pinch (black line) and the minimum of cold utilities (Q_{Cmin}).	27

Figure 21: Process flowsheet and additional information regarding flows, process design variables and heat exchanger duties for the base case design involving two evaporators and the EDC operating at 1 atm after applying heat integration. The compositions are given in mole fractions.....	29
Figure 22: Total annual production costs including refrigerant, cooling water, electricity, LP, MP and HP Steam for the four different base case designs.	36
Figure 23: Equipment f.o.b. purchase costs in 10^3 \$ such as the vacuum system, heat exchanger regeneration and EDC costs for the four base case designs.	37
Figure 24: Total annual investment in 10^3 \$ for the four base case designs.	37
Figure 25: Extractive distillation of IPA and water with the IL [Emim] ⁺ [N(CN) ₂] ⁻ taken from Ma <i>et al.</i> (2019) [36]. Added equipment or equipment characteristics necessary for the economic assessment are marked in blue.....	40
Figure 26: Process flow diagram of the extractive distillation of IPA and water using ChCl:TEG (1:3). The simulation was adapted to match the literature.....	41
Figure 27: Selectivity at the entrainer mole fraction $x_3=0.6$ and the ethanol mole fraction on entrainer free basis $x_1=0.95$ (see chapter C.9.7 for choice of mole fractions). Selectivities are given for ChCl:Ur (1:2), the conventional entrainer EG and the ILs. Values were taken from an Aspen Plus simulation for EG and ChCl:Ur (1:2) and from Ge <i>et al.</i> (2008) for the ILs [40]......	42
Figure 28: Minimum entrainer amounts w_{smin} for ChCl:Ur (1:2), the conventional entrainer EG and ILs. Values were taken from an Aspen Plus simulation for EG and ChCl:Ur (1:2) and from Ge <i>et al.</i> (2008) for the ILs for the boundary condition of the ethanol fraction on entrainer free basis approaching one [40].	43
Figure 29: Selectivity (left) and minimum entrainer amount w_{smin} (right) comparison between ChCl:TEG (1:3), the conventional entrainer EG and the ILs. Values were taken from an Aspen Plus simulation for EG and ChCl:Ur (1:2) and from Zhang <i>et al.</i> (2007) for the ILs [37]......	43
Figure 30: TAC and its relative proportions of the three separation tasks: 1: separation of ethanol and water using EG and ChCl:Ur (1:2) (top left graph) 2: separation of IPA and water using IL and ChCl:Ur (1:2) (top right graph) and 3: separation of IPA and water using, DMSO, IL and ChCl:TEG (1:3) (bottom graph) [30, 31, 35, 36]. The costs of the processes of the literature, and the simulated process, as well as the simulated heat-integrated process using DES, are shown. In the equipment costs, the lang factor (4.74), factor for the delivery of the equipment (1.05), cost index factor (607.5/500) and the return of the investment ($i=0.2$) have already been included.	45

Appendix

Figure A 1: Illustration of the steps in the iterative procedure to find the optimised process design variables of the EDC. Given are the steps, the strategy to find the design variables, the initial guess and the constraints that have to be met.	- 11 -
Figure A 2: Illustration of the steps in the iterative procedure to find the optimised process design variables of the evaporator regeneration unit. Given are the steps, the strategy to determine the design variables, and the initial guess.....	- 11 -
Figure A 3: Illustration of the steps in the iterative procedure to find the optimised process design variables of the evaporator and stripping base case design. Given are the steps, the strategy to determine the design variables, the initial guess and the constraints that have to be met.	- 12 -
Figure A 4: Innovation map of hyperbranched polymers, a mixture of organic solvents and solid salts, and deep eutectic solvents.....	- 20 -
Figure A 5: Simulation results and experimental measurements for 30 wt% of ChCl:Ur (1:2) plotted in a vapour mole fraction (y_1) over the liquid mole fraction of ethanol (x_1) diagram (left), the temperature over x_1 diagram (middle), and the relative volatility (α) over x_1 diagram (right) [13].	- 38 -
Figure A 6: Simulation results and experimental measurements for 15 wt% of ChCl:TEG (1:3) plotted in a vapour mole fraction (y_1) over the liquid mole fraction of ethanol (x_1) diagram (left), the temperature over x_1 diagram (middle), and the relative volatility (α) over x_1 diagram (right) [47].	- 38 -

Figure A 7: Simulation results and experimental measurements for 20 mole% of ChCl:GA (1:3) plotted in a vapor mole fraction (y_1) over the liquid mole fraction of ethanol (x_1) diagram (left), the temperature over x_1 diagram (middle), and the relative volatility (α) over x_1 diagram (right) [43].	- 39 -
Figure A 8: Simulation results and experimental measurements for 20 mole% of ethanol on entrainer free basis plotted in a diagram of the vapour mole fraction (y_1), the temperature and the relative volatility (α) over the mole fraction of ChCl:EG (1:2) [46].	- 40 -
Figure A 9: Simulation results and experimental measurements for 20 wt% of ChCl:Ur (1:3) plotted in a vapor mole fraction (y_1) over the liquid mole fraction of ethanol (x_1) diagram (left), the temperature over x_1 diagram (middle), and the relative volatility (α) over x_1 diagram (right) [13].	- 40 -
Figure A 10: Simulation results and experimental measurements for 10 wt% of ChCl:Ur (1:3) plotted in a vapor mole fraction (y_1) over the liquid mole fraction of ethanol (x_1) diagram (left), the temperature over x_1 diagram (middle), and the relative volatility (α) over x_1 diagram (right) [13].	- 41 -
Figure A 11: Simulation results and experimental measurements for 10 wt% of ChCl:TEG (1:3) plotted in a vapor mole fraction (y_1) over the liquid mole fraction of ethanol (x_1) diagram (left), the temperature over x_1 diagram (middle), and the relative volatility (α) over x_1 diagram (right) [47].	- 41 -
Figure A 12: Simulation results and experimental measurements for 5 wt% of ChCl:TEG (1:3) plotted in a vapor mole fraction (y_1) over the liquid mole fraction of ethanol (x_1) diagram (left), the temperature over x_1 diagram (middle), and the relative volatility (α) over x_1 diagram (right) [47].	- 42 -
Figure A 13: Simulation results and experimental measurements for 3 wt% of ChCl:TEG (1:3) plotted in a vapor mole fraction (y_1) over the liquid mole fraction of ethanol (x_1) diagram (left), the temperature over x_1 diagram (middle), and the relative volatility (α) over x_1 diagram (right) [47].	- 42 -
Figure A 14: Simulation results of the activity coefficient of ethanol (γ_1) (left) and water (γ_2) (middle) and the selectivity (right) as defined in Chapter B.2.2 plotted over the mole fraction of ChCl:EG (1:2) for two different ethanol mole fractions on entrainer free basis.	- 43 -
Figure A 15: Residue curve maps for the system ethanol and water with the DES ChCl:EG (1:2) (top left), ChCl:Ur (1:2) (top right), and ChCl:GA (1:3) (bottom left) and for the system IPA and water with ChCl:TEG (1:3) (bottom right) on mass basis. The isovolatility curve and azeotropic point is also shown.	- 45 -
Figure A 16: Black box diagram for the separation of ethanol (1) and water (2) using the process details of Zhu <i>et al.</i> (2019) [35]. The constraints (in box) and the design variables and unknowns (in red) are given as well. However, for this diagram, the separation efficiency of the entrainer and water has been assumed to be 100%.	- 46 -
Figure A 17: Black box diagram for the separation of IPA (1) and water (2). The constraints (in box) and the design variables and unknowns (in red) are given as well. However, for this diagram, the separation efficiency of the entrainer and water has been assumed to be 100%.	- 47 -
Figure A 18: Reboiler duty (Q_{reb}) for different stripping agent recycle stages (N_P) and temperatures. The purity is always adapted by RR to meet the constraint of 99.7 mol% ethanol.	- 49 -
Figure A 19: Energy requirements of the evaporator (Q_{evap}) in the evaporator and stripping process and purity (x_E) and recovery of the entrainer of the recycle stream. Shown are also the purity and recovery constraints.	- 49 -
Figure A 20: Purity of the entrainer recycle stream for different total number of stages of the stripping column.	- 50 -
Figure A 21: Recovery and purity of the entrainer recycle stream over the stripping agent flowrate (n_{gas}). Shown is also the purity constraint.	- 50 -
Figure A 22: Aspen Plus flowsheet of the base case design with the EDC operating at 1 atm and using a stripping column as entrainer regeneration option [18].	- 51 -
Figure A 23: Aspen Plus flowsheet of the base case design with the EDC operating at 14 kPa and using a stripping column as entrainer regeneration option [18].	- 52 -
Figure A 24: Aspen Plus flowsheet of the base case design with the EDC operating at 14kPa and using only evaporators as entrainer regeneration option [18].	- 54 -
Figure A 25: Hot (red) and cold (blue) composite curve for the 1 atm EDC base case with two evaporators [18].	- 57 -

Figure A 26: Composite curves of the remaining to heaters using utilities (green and blue) and the condenser of the EDC for the process using two evaporators and the EDC at 1 atm. The potentially saved energy requirements are too small for profitable process heat integration and are therefore rejected.....	- 57 -
Figure A 27: Hot (red) and cold (blue) composite curve of the process using 2 evaporators and the EDC operating at 14 kPa. Less energy savings are possible than for the 1atm process [18].....	- 58 -
Figure A 28: Composite curves of the integrated process part for the process using 2 evaporators and the EDC at 14 kPa. The hot composite curve (orange) is the entrainer recycle cooling (E01), and the cold composite curve is the main feed (E02).....	- 58 -
Figure A 29: Hot (red) and cold (blue) composite curve in a diagram of the temperature over the enthalpy for the process using a stripping column and the EDC at 101 kPa [18].	- 59 -
Figure A 30: Composite curves of the integrated process part for the process using a stripping column and the EDC at 101 kPa. The hot composite curve (orange) is the vapour that needs cooling after the evaporator (E06), and the cold composite curve (blue) is the main feed (E02).	- 59 -
Figure A 31: Composite curves of the integrated process part for the process using a stripping column and the EDC at 101 kPa. The hot composite curve (orange) is the entrainer recycle cooling (E01), and the cold composite curve (blue) is the ethanol and water mixture coming from the stripping column as recycle to the EDC.	- 59 -
Figure A 32: Aspen Plus flowsheet of the heat-integrated base case design with the EDC operating at 14 kPa and using only evaporators as entrainer regeneration option [18].....	- 61 -
Figure A 33: Aspen Plus flowsheet of the heat-integrated base case design with the EDC operating at 14 kPa and the stripping column as entrainer regeneration option [18].....	- 62 -
Figure A 34: Aspen Plus flowsheet of the heat-integrated base case design with the EDC operating at 101 kPa and the stripping column as entrainer regeneration option [18].....	- 63 -
Figure A 35: Literature process of the separation of ethanol and water with the conventional solvent EG taken from Bastidas <i>et al.</i> (2010) [30]. Added equipment or equipment characteristics necessary for the economic assessment are marked in blue.	- 94 -
Figure A 36: Process flowsheet for the separation of ethanol and water using ChCl:Ur (1:2). This process is compared with the conventional process using EG.	- 95 -
Figure A 37: Process flowsheet for the separation of ethanol and water using ChCl:Ur (1:2) using heat integration.	- 97 -
Figure A 38: Literature process of the separation of ethanol and water with the IL [Emim] ⁺ [BF ₄] ⁻ taken from Zhu <i>et al.</i> (2016) [35]. Added equipment or equipment characteristics necessary for the economic assessment are marked in blue. No IL recovery constraint can be found.	- 99 -
Figure A 39: Process flowsheet for the separation of ethanol and water using ChCl:Ur (1:2). This process is compared with the process using the IL.....	- 100 -
Figure A 40: Process flowsheet for the separation of ethanol and water using ChCl:Ur (1:2) using heat integration. This process is compared with the process using the IL.....	- 102 -
Figure A 41: Literature process of the separation of IPA and water with the conventional entrainer DMSO taken from Ghuge <i>et al.</i> (2019) [31]. Added equipment or equipment characteristics necessary for the economic assessment are marked in blue.	- 104 -
Figure A 42: Literature process of the separation of IPA and water with the IL [Emim] ⁺ [N(CN) ₂] ⁻ taken from Ma <i>et al.</i> (2019) [36]. Added equipment or equipment characteristics necessary for the economic assessment are marked in blue.	- 105 -
Figure A 43: Process flow diagram of the extractive distillation of IPA and water using ChCl:TEG (1:3). The simulation was adapted to match the literature.....	- 106 -
Figure A 44: Process flowsheet for the separation of IPA and water using ChCl:TEG (1:3) and applying heat integration.....	- 108 -

List of Tables

Main text

Table 1: Statistical parameters RMSD and R^2 for the vapour fraction of ethanol / IPA, the temperature, and the relative volatility (α) of the four systems: ethanol – water – ChCl:Ur (1:2) (30 wt%), ethanol – water – ChCl:GA (1:3) (20 mol%), ethanol – water – ChCl:EG (1:2) and IPA – water – ChCl:TEG (1:3) (15 wt%). The data with the highest amount of DES was taken.....	9
Table 2: Three separation tasks of this project, including the feed flowrates and compositions and purity and recovery constraints.....	14
Table 3: The energy savings in kW and as a percentage of the overall energy requirements for the four base case designs.....	28
Table 4: Specific energy requirements of the processes of the literature using EG or IL and the simulated process as well as simulated heat integrated (HI) process using the DES ChCl:Ur (1:2) for the separation of ethanol and water. Shown are also the improvement of the DES process compared to the corresponding literature process.	44
Table 5: Specific energy requirements of the processes of the literature processes using DMSO and IL and the simulated process, as well as simulated heat integrated (HI) process using the DES ChCl:TEG (1:3) for the separation of IPA and water. Shown are also the potential savings by implementing the heat integrated process using the DES.....	45
Table 6: The possible savings in the TAC of the processes using the conventional solvent or the IL when considering the process using the DES as well as the heat integrated process using the DES.....	46
Table 7: The possible savings in the specific energy requirements in steam of the processes using the conventional solvent or the IL when considering the process using the DES as well as the heat integrated process using the DES.....	46

Appendix

Table A 1: Decisions that have been made throughout the whole project and this report. Also given is the explanation and the chapter in which this decision was made.	- 1 -
Table A 2: Listed heuristics and assumptions, the reasoning and application within this project. Heuristics were taken from Seider <i>et al.</i> (2006) or Turton <i>et al.</i> (2012) [56, 65].	- 5 -
Table A 3: Steam classes that are taken as utilities for this project, the absolute pressure, temperature and evaporation enthalpy [95].....	- 16 -
Table A 4: Characteristics of cooling water that is taken as utility in this project [95].	- 17 -
Table A 5: Characteristics of the refrigerant ammonia that is taken as a utility in this project [95].	- 17 -
Table A 6: F.o.b. purchase cost calculation of the towers; formulas and meaning. For this calculation, the head thickness is assumed to be equal to the shell thickness [56]	- 17 -
Table A 7: F.o.b. purchase cost calculation for the reflux drums [56].	- 18 -
Table A 8: F.o.b. purchase cost calculation for heat exchangers [56].	- 18 -
Table A 9: F.o.b. purchase cost calculation for evaporators [56].	- 18 -
Table A 10: F.o.b. purchase cost calculation for the liquid ring pump and steam jet ejector [56].	- 19 -
Table A 11: Advantages and disadvantages of alternative entrainers to organic solvents for the use in extractive distillations [4, 8, 10, 12].	- 21 -
Table A 12: Literature review showing the main publications about the use of DES as entrainer in extractive distillation processes. Shown are the components to be separated, the used DES, the publication and the topic of the application being divided in either the measurement of the VLE or the process design.	- 21 -

Table A 13: Details of the publications about the process design and simulation of the extractive distillation of ethanol and water using the conventional solvent ethylene glycol as entrainer (EG). *in case of mismatching units or lacking energy consumption / kg ethanol data has been changed or calculated	- 22 -
Table A 14: Details of the publications about the process design and simulation of the extractive distillation of ethanol and water using DESs as entrainer (ChCl:Ur (1:2) and ChCl:GC (1:3)). *in case of mismatching units or lacking energy consumption/kg ethanol data has been changed or calculated	- 22 -
Table A 15: Details of the publications about the process design and simulation of the extractive distillation of ethanol and water using the ILs as entrainer ([Emim] ⁺ [BF ₄] ⁻ and [Emim] ⁺ [N(CN) ₂] ⁻). *in case of mismatching units or lacking energy consumption/kg ethanol data has been changed or calculated	- 23 -
Table A 16: Details of the publications about the process design and simulation of the extractive distillation of IPA and water using the conventional entrainer DMSO. *in case of mismatching units or lacking energy consumption/kg ethanol data has been changed or calculated	- 23 -
Table A 17: Details of the publications about the process design and simulation of the extractive distillation of IPA and water using the DES ChCl:TEG (1:2) as entrainer. *in case of mismatching units or lacking energy consumption/kg ethanol data has been changed or calculated	- 23 -
Table A 18: Details of the publications about the process design and simulation of the extractive distillation of IPA and water using the ILs as entrainer ([Emim] ⁺ [N(CN) ₂] ⁻ and [Emim] ⁺ [OAc] ⁻). *in case of mismatching units or lacking energy consumption/kg ethanol data has been changed or calculated	- 24 -
Table A 19: Different studies about the use of ILs as entrainer in the extractive distillation of ethanol and water. Shown are the ILs, the essential findings, and the publication about the VLE measurement or process design.	- 24 -
Table A 20: Different studies about the use of ILs as entrainer in the extractive distillation of IPA and water. Shown are the ILs, the essential findings, and the publication about the VLE measurement or process design.	- 25 -
Table A 21: Physical and chemical properties and safety and toxicity data of ethanol, water and IPA.	- 26 -
Table A 22: Physical and chemical properties and safety and toxicity data of ChCl, Ur, and GA.	- 26 -
Table A 23: Physical and chemical properties and safety and toxicity data of EG and TEG.	- 27 -
Table A 24: Physical and chemical properties and safety and toxicity data of ChCl:Ur (1:2) and ChCl:GA (1:3).	- 28 -
Table A 25: Physical and chemical properties and safety and toxicity data of ChCl:EG (1:2) and ChCl:TEG (1:3).	- 28 -
Table A 26: Density measurements for different temperatures of ChCl:Ur (1:2) [105], ChCl:GA (1:3) [106], ChCl:EG (1:2) [107] and ChCl:TEG (1:3) at 1 atm [108].	- 29 -
Table A 27: Viscosity measurements for different temperatures of ChCl:Ur (1:2) [105], ChCl:GA (1:3) [106] and ChCl:EG (1:2) at 1 atm [109].	- 29 -
Table A 28: Vapor pressure (p_{vap}) for different temperatures for the component ChCl:Ur (1:2) [110]. This vapor pressure measurement is taken for each DESs.	- 30 -
Table A 29: Heat capacity measurements for different temperatures of ChCl:Ur (1:2) [111], ChCl:TEG (1:3) [108] and ChCl:EG (1:2) at 1 atm [63].	- 30 -
Table A 30: VLE data for the ternary system IPA (1), Water (2) and ChCl:TEG (1:3) (3) for different weight fractions of ChCl:TEG (1:3) at 1 atm [47].	- 31 -
Table A 31: VLE data for the ternary system Ethanol (1), Water (2) and ChCl:Ur (1:2) (3) for different weight fractions of ChCl:Ur (1:2) at 1 atm [13].	- 33 -
Table A 32: VLE data for the ternary system Ethanol (1), Water (2) and ChCl:EG (1:2) (3) at 1 atm [11]	- 34 -
Table A 33: VLE data for the ternary system Ethanol (1), Water (2) and ChCl:GA (1:3) (3) at 1 atm [43].	- 35 -
Table A 34: Parameters of the NRTL model for the four systems at 1 atm.	- 35 -
Table A 35: Chosen property function in Aspen for the temperature-dependent properties and the regressed parameters.	- 36 -
Table A 36: Publications with binary VLE measurements of water and DES. Listed are several HBDs that form a DES with ChCl as HBA.	- 37 -
Table A 37: RMSD of the regression of the heat capacity, the density, the viscosity and the vapor pressure for the four DESs ChCl:Ur (1:2), ChCl:EG (1:2), ChCl:GA (1:3) and ChCl:TEG (1:3)	- 37 -

Table A 38: The different regeneration technologies, and their application in the literature, advantages and disadvantages.	- 47 -
Table A 39: Process stream summary of the base case design with the EDC operating at 1 atm and using a stripping column as entrainer regeneration option.	- 51 -
Table A 40: Stream summary of the base case design with the EDC operating at 14 kPa and using a stripping column as entrainer regeneration option.	- 52 -
Table A 41: Process stream summary of the base case design with the EDC operating at 1 atm and using only evaporators as entrainer regeneration option.	- 53 -
Table A 42: Process stream summary of the base case design with the EDC operating at 14kPa and using only evaporators as entrainer regeneration option [18].	- 54 -
Table A 43: Optimised design parameters of the EDC operating at 1 atm, and the evaporators.....	- 55 -
Table A 44: Optimised design parameters of the EDC operating at 14 kPa, and the evaporators.....	- 55 -
Table A 45: Optimised design parameters of the EDC operating at 1 atm, the evaporators, and the stripping column.....	- 56 -
Table A 46: Optimised design parameters of the EDC operating at 1 atm, the evaporators, and the stripping column.....	- 56 -
Table A 47: Solutions for heat integration found by the Aspen Plus Energy Analyser for the process shown in Figure 19 using two evaporators and the EDC at 1atm [18]. Each solution shows the energy saving in percent, the payback in years, and the heat exchanger locations. Implemented solutions and rejected solutions are marked in green and red, respectively.	- 57 -
Table A 48: Solutions for heat integration found by the Aspen Plus Energy Analyser for the process shown in Figure A 24 for the process using 2 evaporators and the EDC at 14 kPa [18]. Each solution shows the energy saving in percent, the payback in years, and the heat exchanger locations. Implemented solutions and rejected solutions are marked in green and red, respectively.	- 58 -
Table A 49: Process stream summary of the heat-integrated base case design with the EDC operating at 101 kPa and using only evaporators as entrainer regeneration option.....	- 60 -
Table A 50: Process stream summary of the heat-integrated base case design with the EDC operating at 14 kPa and using only evaporators as entrainer regeneration option.	- 61 -
Table A 51: Process stream summary of the heat-integrated base case design with the EDC operating at 14 kPa and the stripping column as entrainer regeneration option.	- 62 -
Table A 52: Process stream summary of the heat-integrated base case design with the EDC operating at 101 kPa and the stripping column as entrainer regeneration option.	- 63 -
Table A 53: Summary of all utilities used for each equipment for the base case design with the 1 atm EDC and two evaporators. The equipment numbering equals the flowsheet shown in Figure 21. Additionally to this flowsheet, there is the steam jet ejector for creating the vacuum of the second evaporator, and the liquid ring pumps for creating the vacuum of the first evaporator.....	- 64 -
Table A 54: Summary of all utilities used for each equipment for the base case design with the 14 kPa EDC and two evaporators. The equipment numbering equals the Aspen flowsheet shown in Figure A 32. Additionally, there is the steam jet ejector for creating the vacuum of the second evaporator, and the liquid ring pumps for creating the vacuum of the EDC and the first evaporator.	- 65 -
Table A 55: Summary of all utilities used for each equipment for the base case design with the 1atm EDC and the stripping column. The equipment numbering equals the Aspen flowsheet shown in Figure A 33. Additionally, there are the liquid ring pumps for creating the vacuum of the evaporator and the stripping column.....	- 66 -
Table A 56: Summary of all utilities used for each equipment for the base case design with the 14kPa EDC and the stripping column. The equipment numbering equals the Aspen flowsheet shown in Figure A 33. Additionally, there are the liquid ring pumps for creating the vacuum of the EDC, the evaporator and the stripping column.	- 67 -
Table A 57: Equipment sizing of the EDC columns with all required characteristics for the four base case designs.....	- 68 -
Table A 58: Purchase costs calculation of the EDC column for the four base case designs	- 69 -

Table A 59: Equipment sizing of the stripping columns with all required characteristics for the stripping base cases.	- 69 -
Table A 60: Purchase costs calculation of the stripping column for the stripping base case designs	- 70 -
Table A 61 Equipment sizing of the reflux drums of the two evaporator base cases designs.	- 71 -
Table A 62: Equipment sizing of the reflux drums of the stripping column base cases designs.	- 72 -
Table A 63: Purchase cost calculation of the reflux drums for the four base case designs	- 73 -
Table A 64: Equipment specification and purchase cost calculation for the vacuum systems of the base case design with the 14 kPa EDC and evaporators.	- 73 -
Table A 65: Equipment specification and purchase cost calculation for the vacuum systems of the base case design with the 1 atm EDC and evaporators.	- 74 -
Table A 66: Equipment specification and purchase cost calculation for the vacuum systems of the base case design with the 14 kPa EDC and a stripping column.....	- 75 -
Table A 67: Equipment specification and purchase cost calculation for the vacuum systems of the base case design with the 1 atm EDC and a stripping column.....	- 75 -
Table A 68: Summary of the equipment, the important equipment characteristics and the costs for each equipment for the 1 atm EDC evaporators base case. The total equipment costs for the year 2019 and the total permanent investment are also given. The corresponding flowsheet can be found in Figure 21.....	- 77 -
Table A 69: Summary of the equipment, the important equipment characteristics and the costs for each equipment for the 14 kPa EDC evaporators base case. The total equipment costs for the year 2019 and the total permanent investment are also given. The corresponding flowsheet can be found in Figure A 32..	- 78 -
Table A 70: Summary of the equipment, the important equipment characteristics and the costs for each equipment for the 1atm EDC stripping base case. The total equipment costs for the year 2019 and the total permanent investment are also given. The corresponding flowsheet can be found in Figure A 34. -	- 79 -
Table A 71: Summary of the equipment, the important equipment characteristics and the costs for each equipment for the 14 kPa EDC stripping base case. The total equipment costs for the year 2019 and the total permanent investment are also given. The corresponding flowsheet can be found in Figure A 33.-	- 80 -
Table A 72: Utility consumption, and prices, and annual costs of the utilities of the base case design with the 1 atm EDC and two evaporators.....	- 81 -
Table A 73: Utility consumption, and prices, and annual costs of the utilities of the base case design with the 14kPa EDC and two evaporators.....	- 81 -
Table A 74: Utility consumption, and prices, and annual costs of the utilities of the base case design with the 1 atm EDC and the stripping column.....	- 81 -
Table A 75: Utility consumption, and prices, and annual costs of the utilities of the base case design with the 14kPa EDC and the stripping column.....	- 82 -
Table A 76: TAC calculation for the extractive distillation of ethanol and using ChCl:Ur (1:2) for the four base case designs.....	- 82 -
Table A 77: Summary of utilities for the process separating ethanol and water using EG in the literature of Bastidas <i>et al.</i> (2010) [30]. The equipment numbering equals the process flowsheet shown by Figure A 35..	- 83 -
Table A 78: Summary of utilities of the non-heat integrated process for the extractive distillation of ethanol and water with ChCl:Ur (1:2). The equipment numbering equals the process flowsheet shown by Figure A 36.	- 84 -
Table A 79: Summary of utilities of the heat integrated process for extractive distillation of ethanol and water with ChCl:Ur (1:2), the. The equipment numbering equals the process flowsheet shown by Figure A 37. -	- 85 -
Table A 80: Summary of utilities for the process separating ethanol and water using the IL [Emim] ⁺ [BF ₄] ⁻ in the literature of Zhu <i>et al.</i> (2016) [35]. The equipment numbering equals the process flowsheet shown by Figure A 38.	- 86 -
Table A 81: Summary of utilities of the non-heat integrated process for the extractive distillation of ethanol and water with ChCl:Ur (1:2). The equipment numbering equals the process flowsheet shown by Figure A 39.....	- 87 -
Table A 82: Summary of utilities of the heat integrated process for the extractive distillation of ethanol and water with ChCl:Ur (1:2). The equipment numbering equals the process flowsheet shown by Figure A 40.-	- 88 -

Table A 83: Summary of utilities for the process separating IPA and water using DMSO in the literature of Ghuge <i>et al.</i> (2017) [31]. The equipment numbering equals the process flowsheet shown by <i>Figure A 41</i>	- 89 -
Table A 84: Summary of utilities for the process separating IPA and water using the IL [Emim] ⁺ [N(CN) ₂] ⁻ in the literature of Ma <i>et al.</i> (2019) [36]. The equipment numbering equals the process flowsheet shown by <i>Figure A 42</i>	- 90 -
Table A 85: Summary of utilities of the non-heat integrated process for the extractive distillation of IPA and water with ChCl:TEG (1:3). The equipment numbering equals the process flowsheet shown by <i>Figure A 43</i>	- 91 -
Table A 86: Summary of utilities of the heat integrated process for the extractive distillation of IPA and water with ChCl:TEG (1:3). The equipment numbering equals the process flowsheet shown by <i>Figure A 44</i>	- 92 -
Table A 87: Process stream summary for the separation of ethanol and water using ChCl:Ur (1:2). This process is compared with the conventional process using EG.....	- 95 -
Table A 88: Process stream summary for the separation of ethanol and water using ChCl:Ur (1:2) using heat integration.....	- 97 -
Table A 89: Process stream summary for the separation of ethanol and water using ChCl:Ur (1:2). This process is compared with the process using the IL.....	- 100 -
Table A 90: Process stream summary for the separation of ethanol and water using ChCl:Ur (1:2) using heat integration.....	- 102 -
Table A 91: Process stream summary for the separation of IPA and water using ChCl:TEG (1:3).....	- 107 -
Table A 92: Process stream summary for the separation of IPA and water using ChCl:TEG (1:3) and applying heat integration.....	- 108 -
Table A 93: Equipment specification of the EDC of the simulated process using ChCl:Ur (1:2) and the literature process using EG [30]. Data given by the literature is marked in green.....	- 110 -
Table A 94: Equipment f.o.b. purchase costs of the EDC of the simulated process using ChCl:Ur (1:2) and the literature process using EG [30].....	- 111 -
Table A 95: Equipment specification of the reflux drum of the simulated process using ChCl:Ur (1:2) and the literature process using EG [30].....	- 111 -
Table A 96: Equipment purchase costs of the reflux drum of the simulated process using ChCl:Ur (1:2) and the literature process using EG [30].....	- 112 -
Table A 97: Equipment specification and f.o.b. purchase costs of the vacuum system of the simulated process using ChCl:Ur (1:2) and the literature process using EG [30]. Data given by the literature is marked in green.....	- 112 -
Table A 98: Equipment specification of the SRC used for the solvent recovery of EG by Bastidas <i>et al.</i> (2010) [30]. Data given by the literature is marked in green.....	- 113 -
Table A 99: Equipment purchase costs of the SRC used for the solvent recovery of EG by Bastidas <i>et al.</i> (2010) [30].....	- 114 -
Table A 100: Equipment purchase costs of the reflux drum of the SRC used for the solvent recovery of EG by Bastidas <i>et al.</i> (2010) [30].....	- 115 -
Table A 101: Equipment specification of the EDC of the simulated process using ChCl:Ur (1:2) and the literature process using the IL [EMIM] ⁺ [BF ₄] ⁻ for the ethanol and water system [35]. Data given by the literature is marked in green.....	- 115 -
Table A 102: Equipment f.o.b. purchase costs of the EDC of the simulated process using ChCl:Ur (1:2) and the literature process using the IL [EMIM] ⁺ [BF ₄] ⁻ for the ethanol and water system [35].....	- 116 -
Table A 103: Equipment specification of the reflux drum of the simulated process using ChCl:Ur (1:2) and the literature process using the IL [EMIM] ⁺ [BF ₄] ⁻ for the ethanol and water system [35].....	- 116 -
Table A 104: Equipment purchase costs of the reflux drum of the simulated process using ChCl:Ur (1:2) and the literature process using the IL [EMIM] ⁺ [BF ₄] ⁻ for the ethanol and water system [35].....	- 117 -
Table A 105: Equipment specification and f.o.b. purchase costs of the vacuum system of the simulated process using ChCl:Ur (1:2) and the literature process using the IL [EMIM] ⁺ [BF ₄] ⁻ for the ethanol and water system [35].....	- 118 -

Table A 106: Equipment specification of the EDC separating IPA and water of the simulated process using ChCl:TEG (1:3) and the literature process using the conventional solvent DMSO and the IL [Emim] ⁺ [N(CN) ₂] ⁻ [31, 36]. Data given by the literature is marked in green.	- 119 -
Table A 107: Equipment f.o.b. purchase costs of the EDC separating IPA and water of the simulated process using ChCl:TEG (1:3) and the literature process using the conventional solvent DMSO and the IL [Emim] ⁺ [N(CN) ₂] ⁻ [31, 36].	- 120 -
Table A 108: Equipment specification of the reflux drum of the simulated process using ChCl:TEG (1:3) and the literature process using the conventional solvent DMSO and the IL [Emim] ⁺ [N(CN) ₂] ⁻ for the IPA and water system [31, 36].	- 120 -
Table A 109: F.o.b. purchase costs of the reflux drum of the simulated process using ChCl:TEG (1:3) and the literature process using the conventional solvent DMSO and the IL [Emim] ⁺ [N(CN) ₂] ⁻ for the IPA and water system [31, 36].	- 121 -
Table A 110: Equipment specification and f.o.b. purchase costs of the vacuum system of the simulated process using ChCl:TEG (1:3) and the literature process using the IL [Emim] ⁺ [N(CN) ₂] ⁻ for the IPA and water system [36]. Data given by the literature is marked in green.	- 122 -
Table A 111: Equipment specification of the SRC used for the solvent recovery of DMSO by Ghuge <i>et al.</i> (2010) [31]. Data given by the literature is marked in green.	- 123 -
Table A 112: Purchase cost of the SRC used for the solvent recovery of DMSO by Ghuge <i>et al.</i> (2010) [31]. ...	- 124 -
Table A 113: Equipment purchase costs of the reflux drum of the SRC used for the solvent recovery of DMSO by Ghuge <i>et al.</i> (2010) [31].	- 124 -
Table A 114: Summary of the equipment, the important equipment characteristics and the costs for each equipment for literature process of Bastidas <i>et al.</i> (2010) using EG [30]. The total equipment costs for the year 2019 and the total permanent investment are also given.	- 125 -
Table A 115: Summary of the equipment, the important equipment characteristics and the costs for each equipment for simulated non-heat-integrated DES process. The total equipment costs for the year 2019 and the total permanent investment are also given.	- 126 -
Table A 116: Summary of the equipment, the important equipment characteristics and the costs for each equipment for simulated heat-integrated DES process. The total equipment costs for the year 2019 and the total permanent investment are also given.	- 127 -
Table A 117: Summary of the equipment, the important equipment characteristics and the costs for each equipment for literature process of Zhu <i>et al.</i> (2016) using the IL [Emim] ⁺ [BF ₄] ⁻ [35]. The total equipment costs for the year 2019 and the total permanent investment are also given.	- 128 -
Table A 118: Summary of the equipment, the important equipment characteristics and the costs for each equipment for simulated non-heat-integrated DES process. The total equipment costs for the year 2019 and the total permanent investment are also given.	- 129 -
Table A 119: Summary of the equipment, the important equipment characteristics and the costs for each equipment for simulated heat-integrated DES process. The total equipment costs for the year 2019 and the total permanent investment are also given.	- 130 -
Table A 120: Summary of the equipment, the important equipment characteristics and the costs for each equipment for literature process of Ghuge <i>et al.</i> (2017) using the conventional solvent DMSO [31]. The total equipment costs for the year 2019 and the total permanent investment are also given.	- 131 -
Table A 121: Summary of the equipment, the important equipment characteristics and the costs for each equipment for literature process of Ma <i>et al.</i> (2019) using the IL [Emim] ⁺ [N(CN) ₂] ⁻ [36]. Total equipment costs for the year 2019 and the total permanent investment are also given.	- 132 -
Table A 122: Summary of the equipment, the important equipment characteristics and the costs for each equipment for simulated non-heat-integrated DES process. The total equipment costs for the year 2019 and the total permanent investment are also given.	- 133 -
Table A 123: Summary of the equipment, the important equipment characteristics and the costs for each equipment for simulated heat-integrated DES process. The total equipment costs for the year 2019 and the total permanent investment are also given.	- 134 -

Table A 124: Utility consumption, and prices, and annual production costs of the extractive distillation of ethanol and water using EG simulated by Bastidas <i>et al.</i> (2010) [30].	- 135 -
Table A 125: Utility consumption, and prices, and annual production costs of the extractive distillation of ethanol and water using ChCl:Ur (1:2) for the non-heat integrated process.	- 135 -
Table A 126: Utility consumption, and prices, and annual production costs of the extractive distillation of ethanol and water using ChCl:Ur (1:2) for the heat integrated process.	- 135 -
Table A 127: Utility consumption, and prices, and annual production costs of the extractive distillation of ethanol and water using the IL [Emim] ⁺ [BF ₄] ⁻ simulated by Zhu <i>et al.</i> (2016) [35].	- 136 -
Table A 128: Utility consumption, and prices, and annual production costs of the extractive distillation of ethanol and water using ChCl:Ur (1:2) for the non-heat integrated process.	- 136 -
Table A 129: Utility consumption, and prices, and annual production costs of the extractive distillation of ethanol and water using ChCl:Ur (1:2) for the heat integrated process.	- 137 -
Table A 130: Utility consumption, and prices, and annual production costs of the extractive distillation of IPA and water using the IL [Emim] ⁺ [N(CN) ₂] ⁻ simulated by Ma <i>et al.</i> (2019) [36].	- 137 -
Table A 131: Utility consumption, and prices, and annual production costs of the extractive distillation of IPA and water using DMSO simulated by Ghuge <i>et al.</i> (2017) [31].	- 137 -
Table A 132: Utility consumption, and prices, and annual production costs of the extractive distillation of IPA and water using ChCl:TEG (1:3) for the non-heat integrated process.	- 138 -
Table A 133: Utility consumption, and prices, and annual production costs of the extractive distillation of IPA and water using ChCl:TEG (1:3) for the non-heat integrated process.	- 138 -
Table A 134: TAC calculation for the extractive distillation of ethanol and water of the literature using IL, and the non-heat-integrated and heat-integrated process using ChCl:Ur (1:2).	- 139 -
Table A 135: TAC calculation for the extractive distillation of ethanol and water of the literature using IL, and the non-heat-integrated and heat-integrated process using ChCl:Ur (1:2).	- 139 -
Table A 136: TAC calculation for the extractive distillation of IPA and water of the literature using IL, and the non-heat-integrated and heat-integrated process using ChCl:TEG (1:3).	- 139 -

1 Introduction & Motivation

Driven by the need for a sustainable future, the chemical industry aims to innovate processes to reduce the energy requirements, the associated carbon footprint, and the handling of harmful components with the constraint of economic competitiveness [1, 2]. Extractive distillation is one of the main separation techniques for close-boiling or azeotropic mixtures which is a difficult task in the chemical process industry [3]. In this separation method, another component, called entrainer, is added to increase the relative volatilities of the desired components [3, 4]. Yet, extractive distillation faces challenges such as a large solvent consumption, low efficiency, and high energy consumption. As such, it is not uncommon that the extractive distillation contributes to more than 50% of the total operating costs [1, 5]. The most convenient way to improve overall efficiency and reduce energy consumption is the entrainer selection [4, 6]. Currently, organic solvents are mostly used as entrainers with a production of more than 10 million tons each year [7]. However, the traditional organic solvents often possess disadvantages such as high volatility, accumulation in the atmosphere, non-biodegradability, secondary pollution problems, flammability and high energy consumption of the extractive distillation [8, 9].

Consequently, researchers have been investigating alternatives to overcome these issues. Mainly, these investigations focused on the addition of solid salts, hyperbranched polymers and ionic liquids (ILs), which reduce the energy requirements of the extractive distillation due to the increase to higher relative volatilities [4, 8, 10]. The addition of dissolved salts is used industrially for the separation of ethanol and isopropanol (IPA) [11]. Hyperbranched polymers offer unique characteristics such as polydispersity and a high level of polymer branching, both of which can be tailored [12]. Ionic liquids (ILs) consist of asymmetric anions and large organic cations and have attracted much attention due to their negligible volatility and tuneable properties [8, 10, 13, 14]. In spite of that, some drawbacks of these alternatives have been discovered such as the complex synthesis and high costs of ILs, non-availability and high costs of hyperbranched polymers, and corrosion, recyclability and dissolution problems for the addition of solid salts (for a comparison see Table A 11) [8, 12, 14].

First studied in 2003 by Abbott *et al.*, deep eutectic solvents (DESs) – often also called “low melting temperature mixtures” – have recently gained attention as entrainers for extractive distillation processes [4, 15]. DESs are usually derived from renewable resources and consists of two or three components which create hydrogen bond interactions with each other [16]. Typically, a hydrogen bond donor (HBD) and hydrogen bond acceptor (HBA) form a eutectic mixture with a lower melting point than that of each individual component. DESs have advantages such as non-volatility, non-flammability, simple preparation, low price and high biodegradability, and therefore have a great potential to overcome the above-stated issues with conventional organic solvents and the alternative entrainers to become industrially relevant [4, 9, 17]. To this aim, extractive distillation with DESs as the entrainer must be economically viable and advantageous over the other investigated alternatives. As explained with greater detail in the literature review (chapter 2), the research progress is – by far – not elaborated enough to prove this. Only a few separation systems have been investigated, process designs and simulations are scarce, and most importantly, a consistent economic comparison between DESs and conventional organic solvents as well as an alternative entrainer has not been performed. Conveniently, the literature offers several process designs with ILs, which are therefore chosen as the alternative entrainer in the process evaluation of DESs. The innovation map, which identifies the key inventions of

this new technology, is shown for the alternative entrainers and DESs in *Figure A 4*. The scope of this project can be narrowed by the following research question:

Are deep eutectic solvents as entrainers improving the overall energy requirements and economic attractiveness of an extractive distillation process compared to the conventional organic solvents and ionic liquids?

Starting from this question, this report goes through a number of stages that discuss and decide among several process alternatives, until the final process using DESs is obtained. For this final design, flowsheets and process stream summaries are given, and it is evaluated and compared to the process using conventional entrainers and ILs in terms of total annual costs (TAC) and specific overall energy requirements (chapter 10). In *Figure 1*, the necessary stages of finding these values are given, which simultaneously detail the structure of this report.

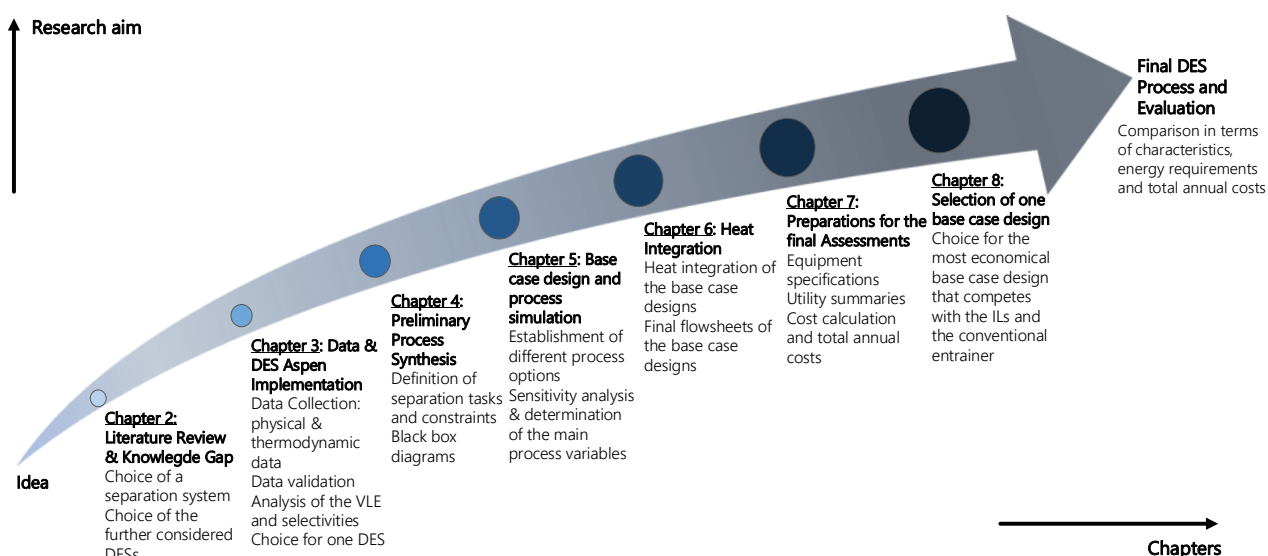


Figure 1: Stages and structure of this project, starting from the idea to the final evaluation of DESs. The eminent chemical engineering modelling software Aspen Plus is used to perform simulations [18].

Along with these stages, numerous heuristics are applied, which help together with the assumptions to make decisions. These heuristics (H), assumptions (A) and choices (C) are numbered and summarized in Appendix A. In Appendix B the methods and theoretical background for the results of the main chapters are given. Finally, Appendix C gives further details, additional information and results that are appended to the main text chapters. In that section, flowsheets, equipment and cost calculation tables are given to the reader to be able to trace all investigations.

With this information and with the stages shown in *Figure 1*, it is assured that:

1. the most promising DES is selected among all experimentally investigated DESs of the literature
2. the most economically attractive process alternative is chosen for the processes using DESs
3. the processes of the literature and the simulated processes using DES can undergo a fair comparison by using adapted process flowsheets, with the same utility constraints and economic equations

In the following chapter, the separation systems are chosen, and the conventional processes are explained.

2 Literature Review & Knowledge Gap

This literature review is given to familiarise with the current related research investigations, highlight the knowledge gap and opportunities, and therefore outline the importance of this research project. Many extractive distillation processes use organic solvents as entrainers. Some systems have already been analysed in terms of suitability to replace those organic solvents by DESs. Also, within this thesis, a separation system has to be found, where the feasibility and potential benefit of replacing the organic solvents by DESs as entrainers is investigated. For this, the literature presence of properties and *ternary* VLE data of the DES and the separation system is indispensable to obtain a validated process (more information in chapter C.4.1). Therefore, it is crucial to find out, which DES and separation systems were investigated, which data has been experimentally researched and potentially, which process using DES as entrainer has already been designed. With this knowledge, the most promising DESs, according to literature, can be chosen.

Regarding the separation system, a summary of researches about VLE measurements of DESs systems and the process design of the extractive distillation is given Table A 12 in the appendix. It can be summarised as follows:

- Most investigations are about VLE measurements and process designs, and simulations are scarce (only four processes)
- Only four separation systems have been studied: ethanol and water, isopropanol and water, allyl alcohol and water, and acetonitrile
- ChCl:Ur (1:2) is the most investigated DES

Therefore, further process designs and simulations have to be done to evaluate the performance of DESs as entrainers. Since the ethanol-water separation system represents the classic example, it is taken into consideration for this project (C 2). Also, the IPA and water separation system is well investigated in terms of the VLE, and only one process has been designed yet so that this system is explored in this work (C 6). However, for the systems allyl alcohol & water and acetonitrile & water, publications about the process with conventional solvents or alternative entrainers are absent, which makes a final comparison between the DES, the organic solvent, and the IL difficult. For this reason, these systems are rejected (C 1).

2.1 Conventional Process and Entrainer

Since it was decided to design the separation of ethanol and water, and IPA and water, it is necessary to give the background information about the production process of ethanol and the current separation system with the conventional entrainers. This is used later to evaluate DESs as entrainers.

Anhydrous ethanol is a basic chemical and has a wide range of applications, e.g. as a chemical reagent, fuel, organic solvent or raw material for many other important chemicals. With a global bioethanol production of 100.2 billion litres, it is mostly used for the automotive and transportation sector, which can be seen in the pie chart in Figure 2 [8, 19].

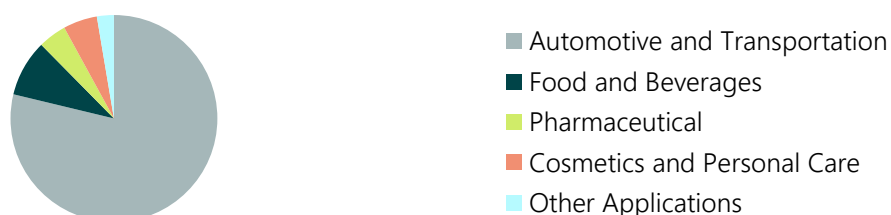


Figure 2: Applications of ethanol represented in a pie chart [20].

As a useful fuel additive, ethanol must meet the purity requirements, which is at least 99 wt% according to the standards (EN 15376, ASTM D 4806). In the production process by either fermentation of sugars or catalytic hydration of ethylene, a mixture of ethanol and water is often obtained. However, this purification is not possible through an ordinary distillation process as ethanol and water form a minimum boiling azeotrope with an azeotropic composition around 96 wt% [5, 21]. Therefore, the conventional process involves an extractive distillation column, which can be seen in the traditional separation process in Figure 3.

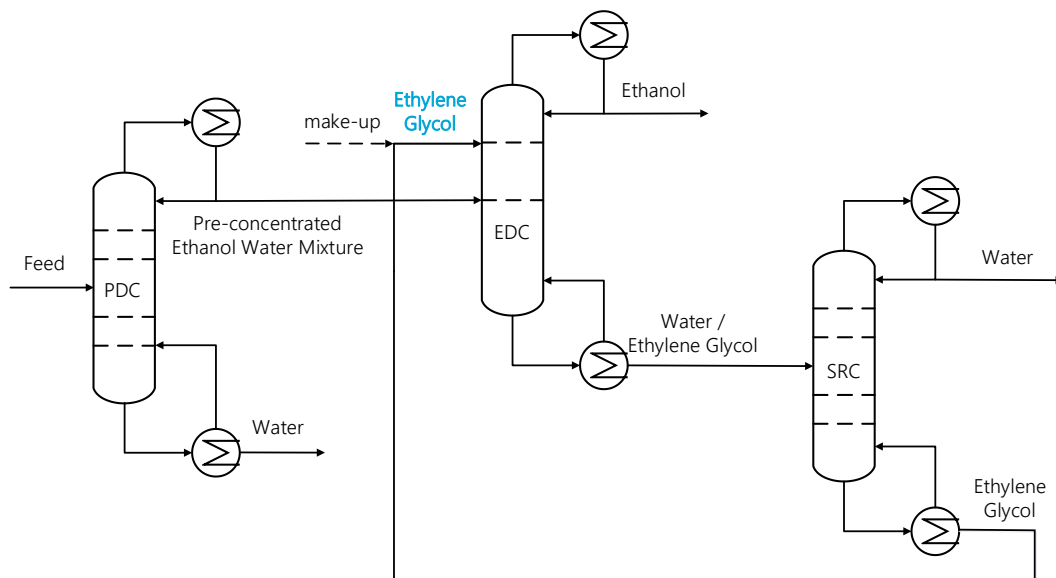


Figure 3: Conventional separation of ethanol and water for the production of bioethanol.

It can be seen that the aqueous mixture is preliminarily purified by a purification distillation column (PDC). Usually, a maximum of 85 mol% ethanol is obtained [5]. For a higher purification level approaching the azeotropic composition at 89.4 mol%, ordinary distillation is not considered as an effective separation method. In this work, the PDC step is not considered. In the second purification step, azeotropic distillation, pressure-swing distillation, pervaporation, liquid-liquid extraction, adsorption, extractive distillation or hybrid separation methods can be used [5, 14, 22]. Among those, the most promising technologies for the separation of ethanol and water are adsorption with molecular sieves and extractive distillation [23]. Despite both having a similar energy consumption, the latter is preferably used in industry [5, 14]. In the extractive distillation column (EDC), the most used entrainer in the industry is ethylene glycol (EG) [5, 14, 24]. EG, as heavy entrainer, is added at the top of the extractive distillation column. In the solvent recovery column (SRC), EG is purified and recycled. For this, ordinary or vacuum distillation are applied [5].

IPA is a basic chemical and widely used in paint, dye, and the pharmaceutical industry as well as a cleaning agent [25, 26]. In its production process from water and propene by hydrogenation, or by fermentation of cellulosic materials, mixtures of IPA and water can be found and need to be dehydrated [27, 28]. Also, when used as a cleaning agent, IPA has to be recovered from the waste solvent stream containing mostly IPA and water [26]. A separation of IPA and water through ordinary distillation is impossible due to the formation of a minimum boiling azeotrope [29]. The azeotropic composition is 68.7 mol% at 1 atm, with a temperature of 80.1°C [26]. There are two conventional separation processes, azeotropic distillation with the light entrainer cyclohexane and extractive distillation with the heavy entrainer dimethyl sulfoxide (DMSO) [28]. Extractive distillation is superior from an economical and technical point of view, and the process includes the EDC and SRC, which was shown in Figure 3 by replacing EG with DMSO [25].

The exact design parameters of the conventional process and the feed flowrates, purity levels and recovery levels vary by different publications. In *Table A 13* and *Table A 16* in the appendix, the process details that have been found in the literature are listed for the extractive distillation of ethanol and water using EG and IPA and water using DMSO, respectively. Eventually, the publication containing information such as reboiler and condenser duties can be taken as a reference to evaluate the performance of the process using the DES as entrainer. The process of Bastidas *et al.* (2010) is, therefore chosen for the separation of ethanol and water (C 8) [30]. For IPA and water, the process of Ghuge *et al.* (2017) is chosen for the final comparison of the DES with DMSO (C 9) [31].

2.2 Ionic Liquids

As ILs are used for the final comparison and process evaluation of DESs, it is necessary to find a suitable process in the literature. Also, ILs are very similar to DESs, and some researchers even consider DESs to be a subgroup of ILs with choline as cation and chloride and the HBD as the anion [32]. Thus, the behaviour of DESs in the equilibrium system might be explained by the same mechanisms as ILs (see Chapter 3.3).

In 2003, the extractive distillation using ILs got firstly proposed by Lei's group, to combine the characteristic "easy operation" of a liquid solvent with the advantage of the high separation ability of a solid salt and evaluate their suitability for large-scale production processes [33]. Since then, many ILs have been investigated, and more details about the findings can be found in the appendix in *Table A 19* for ethanol and water and in *Table A 20* for IPA and water. The main findings about the VLE, process simulation and process optimisation are similar and summarised in the following:

- Regarding the cation: imidazolium-based ionic liquids show the best performance in a solvent screening [34]: 1-ethyl-3-methylimidazolium ([Emim]⁺) has a shorter chain length compared to 1-butyl-3-methylimidazolium ([Bmim]⁺) which is beneficial for a higher selectivity [35].
- Regarding the anion, the relative volatility is enhanced by the following order: chloride anion ([Cl]⁻) ≈ acetate anion ([OAc]⁻) > dicyanamide anion ([N(CN)₂]⁻) > tetrafluoroborate anion ([BF₄]⁻) [21, 34, 36]. The IL with [Cl]⁻ shows a strong salting-out effect [37–39] but the high viscosity complicates the process [21, 34, 35, 39, 40]. Some researchers considered [OAc]⁻ as most promising, while others state that its low decomposition temperature (T_d) is a considerable disadvantage for the regeneration unit [10, 21, 35, 40].
- Regarding a process design and simulation for the separation, [Emim]⁺[BF₄]⁻, [Bmim]⁺[BF₄]⁻ and [Emim]⁺[N(CN)₂]⁻ were used as entrainers for the separation of ethanol and water [12, 35, 41]. The process details can be found in *Table A 15* in the appendix. For the separation of IPA and water, [Emim]⁺[OAc]⁻ and [Emim]⁺[N(CN)₂]⁻ were implemented as entrainers [28, 36, 42]. The process details can be found in *Table A 18* in the appendix.

For ethanol and water, the process designed by Zhu *et al.* (2016) is chosen for the comparison with the DES, as the publication contains the necessary details [35] (C 8). For the IPA and water system, Chen *et al.* (2017) concluded that compared to DMSO, the IL [Emim]⁺[OAc]⁻ could not significantly reduce the costs because of the high boiling point and low degradation temperature [28, 42]. For this reason, [Emim]⁺[N(CN)₂]⁻ has been implemented in a process by Ma *et al.* (2019), where no final comparison to the conventional solvents has been done [36]. Thus, this process is chosen as a reference to evaluate the DES (C 9).

2.3 Deep Eutectic Solvents

This chapter gives the main findings of the investigations about DESs for the extractive distillation of ethanol and water, and IPA and water listed in Table A 12. Moreover, the knowledge gap is elaborated.

2.3.1 Separation of Ethanol and Water

In 2014, Rodriguez *et al.* firstly investigated the VLE of water, ethanol and four different DESs, namely ChCl:malic acid (MA) (1:1), ChCl:lactic acid (LA) (1:2), ChCl:glycolic acid (GA) (1:3) and ChCl:GA (1:1). It was found, that except for ChCl:LA (1:2), all investigated DESs are able to break the azeotrope and that ChCl:GA (1:3) has the highest effect on the relative volatility. Thus, it was declared to be the most promising DES among the four investigated ones [43]. Subsequently, Ma *et al.* (2017) studied the use of ChCl:GA (1:3) as entrainer in the separation process of ethanol and water through a process simulation and a batch extractive distillation experiment. The optimisation was carried out with a heat exchanger network, resulting in a 46.23% and 37.0% energy reduction compared to the process with the conventional solvent and an investigated IL, respectively [8].

Gjineci *et al.* (2015) measured and simulated the VLE of ChCl:urea (Ur) (1:2) and ChCl:triethylene glycol (TEG) (1:3) and found that ChCl:Ur (1:2) proves better suitability for this system [13, 17]. As the VLE for only small weight fractions of DES was measured with relative volatilities close to one, Peng *et al.* (2017) conducted the measurements for higher weight fractions [13]. Subsequently, Han *et al.* (2018) designed and simulated the separation process of ethanol and water using ChCl:Ur (1:2) [44]. It was concluded that the total annual costs (TAC) were reduced by 14.61% compared to the conventional process with EG. Also, Pan *et al.* (2019) and Shang *et al.* (2019) designed and simulated the process in Aspen Plus to evaluate the use of ChCl:Ur (1:2) as entrainer in the large-scale production of ethanol [4, 45]. They concluded that ChCl:Ur (1:2) is more suitable as entrainer than glycerol and an investigated IL [45]. In Table A 14 in the appendix, the process details that have been found in the literature for the extractive distillation of ethanol and water using DESs (ChCl:Ur (1:2) and ChCl:GA (1:3)) are listed.

Next to the mentioned two process simulations, the effect of adding ChCl to the conventional solvent was investigated. Zhang *et al.* (2019) measured the VLE of ChCl:EG in various ratios. In all cases, the formation of the DES proved to be advantageous by increasing the activity coefficient of ethanol and reducing the activity coefficient of water, therefore improving the relative volatility [11].

As stated above, some DESs were already compared to each other, which concludes that ChCl:LA (1:2), ChCl:(MA) (1:1), ChCl:GA (1:1), and ChCl:TEG (1:3) can be eliminated as compared to ChCl:Ur (1:2), ChCl:GA (1:3) and ChCl:EG (1:2) (C 5). However, there are still missing investigations before DESs can be stated as advantageous compared to the other alternatives:

- No solvent screening and comparison between all investigated DESs: ChCl:Ur (1:2), ChCl:GA (1:3) and ChCl:EG (1:2) have not been compared to each other
- No statement about the most promising DES for the separation of ethanol and water
- Small number of process designs and simulations using DESs as entrainer
- No consistent economic comparison with EG and ILs

Hence, the comparison between the DESs ChCl:Ur (1:2), ChCl:GA (1:3) and ChCl:EG (C 3) is done within this project. As the technical and economic evaluation through process simulation is crucial for potential use in industrial-scale applications, the process design, simulation and optimisation of the most advantageous DES is carried out. Finally, a consistent economic comparison to EG and IL is performed within this project.

2.3.2 Separation of IPA and Water

In 2015, the VLE of IPA and water was firstly measured with a DESs by Rodriguez *et al.* [27]. Unfortunately, the investigated DESs ChCl:LA (1:3) and ChCl:GA (1:3) were not able to break the azeotrope within the measured range up to 10 mol% [27]. Zhang *et al.* (2017) investigated the effect of adding ChCl to glycerol for the extractive distillation of IPA and water (ChCl:Gly (2:1)) [29]. The mass fraction to break the azeotrope between IPA and water is much smaller than when glycerol is used as a single component [29]. Zhang *et al.* (2018) added ChCl in different ratios to EG and reported that its addition is enhancing the relative volatilities [46]. Jiang *et al.* (2019) performed a solvent screening which showed that ChCl:TEG (1:3) has the highest solvent power among the 28 investigated DESs [47]. Therefore, Jiangs' group also measured the VLE of this system and found that the azeotropic point could be eliminated at a considerably lower weight fraction compared to all other alternatives [47].

The only process design and simulation was done by De *et al.* (2019) [25]. The group compared three different entrainers with each other: glycerol, glycerol+MgCl₂ and ChCl:Gly (1:3). The TAC, specific energy consumption, entrainer quantity and CO₂ emissions were used for the evaluation, and it was found that glycerol+MgCl₂ is the most promising. However, the disadvantages of the use of a salt listed (see Table A 11) were not taking into account. ChCl:Gly (1:3) also showed a significant reduction in those parameters compared to glycerol. The process details can be found in Table A 17 in the appendix [47].

In contrast to ethanol and water, a solvent screening has been done and ChCl:TEG (1:3) was found to be most promising. Even though this DES has the highest solvent power, it was not implemented into a process design and simulation in the literature yet. Moreover, the only simulation results that were found (DES: ChCl:Gly) were not compared to the process using the conventional entrainer DMSO. Thus, for the evaluation of DESs in the extractive distillation of IPA and water, it is crucial to conduct the process design and simulation and compare the results to DMSO and another alternative entrainer (IL) (C 7).

2.3.3 Summary of the Considered Separation Systems and DESs

A summary of the above-stated decisions, the separation systems that were taken for the evaluation of the DES and the further investigated DESs is given below.

DES as entrainer for an extractive distillation process			
✗ Acetonitrile & water	✗ Allyl alcohol & water	✓ Ethanol & water	✓ IPA & water
		✗ ChCl:TEG (1:3)	✗ ChCl:EG (1:2)
		✗ ChCl:LA (1:2)	✗ ChCl:LA (1:3)
		✗ ChCl:MA (1:1)	✗ ChCl:Gly (2:1)
		✗ ChCl:GA (1:1)	✗ ChCl:GA (1:3)
		✓ ChCl:Ur (1:2)	✓ ChCl:TEG (1:3)
		✓ ChCl:EG (1:2)	
		✓ ChCl:GA (1:3)	

3 Data & Aspen Implementation of the DES

As DESs are not predefined components in Aspen, a user-defined component has to be implemented. This involves the collection of data, the implementation of data into Aspen Plus and the regression of parameters (see methods in chapter B.1.1). Generally, a data collection is necessary for a design project for each involved component. Therefore, chapter 3.1 provides physical and thermodynamic data, including VLE measurements of the literature. Subsequently, the data regression and simulation is validated in chapter 3.2 (for methods see chapter B.2.3). Finally, the data can be analysed and evaluated by performing simulations (chapter 3.3). This includes a feasibility assessment in terms of investigating the residue curve maps (RCMs) and the comparison of the different pre-selected DESs with respect to the entrainer selection criteria given in the methods (for methods see chapter B.2). Also, mechanisms of the DES in the corresponding separation system (IPA or ethanol system) are analysed. Hence, the final DES is selected.

3.1 Data Collection

The data collection include the normal boiling and freezing temperature, molecular weight, chemical structure, solubility information, hazard statements and the LD₅₀ value. In *Table A 21*, *Table A 22* and *Table A 23*, the data is given for individual components: ethanol, IPA, water, ChCl, Ur, GA, and TEG. The same data is given for the DESs in the molecular ratio in *Table A 24* and *Table A 25*. The density (ρ) and viscosity (η) is given as a function of the temperature in *Table A 26* and *Table A 27*. The vapour pressure (p) is negligible for each DES, and the data was taken from the measurements of ChCl:Ur (1:2) as a function of the temperature (*Table A 28*). Moreover, thermodynamic properties such as the heat capacity and the VLE are given in *Table A 29*, *Table A 30*, *Table A 31*, *Table A 32*, and *Table A 33*. The functions of the mentioned properties in terms of the temperature are given together with the regressed parameters (*Table A 35*). The NRTL parameters are provided by *Table A 34*.

3.2 Validation of the Regression

For the process simulation, it is crucial that each DES is implemented in Aspen and that its properties and VLE behaviour are predicted accurately. Thus, the following two chapters analysis the regression of properties and the VLE.

3.2.1 Properties of the DESs

For the temperature-dependent properties of the DESs, a regression with a temperature-dependent function available in Aspen Plus was required. The root mean square deviation (RMSD) of this regression for the four different DES is given in *Table A 37* in the appendix which overall shows that the temperature-dependent properties of the DESs can be predicted accurately.

The boiling temperature of ChCl:TEG (1:3) cannot be found in the literature. Therefore, it is estimated by Aspen Plus after implementing the DES as a user-defined component. The estimated boiling temperature (250°C) is higher than that of ChCl:Ur (1:2) (172.45 °C) and ChCl:EG (1:2) (165.85°C). There are three reasons, by which this estimation can be validated:

1. Mechanisms of boiling a DES: According to Delgado-Mellado *et al.* (2018) and Wenjun *et al.* (2018), the hydrogen bonding breaks first, which is why the hydrogen bond-ability plays a significant role [48, 49]. ChCl:TEG (1:3) has one of the highest hydrogen bonding abilities.

2. As the HBD has a lower decomposition/boiling temperature than choline chloride as HBA, it is majorly determining when the DES components start decomposing/boiling. TEG has a relatively high boiling temperature (285°C) compared to EG (197°C).
3. The property estimation gives a critical temperature of 425.95°C, which is also acceptable when comparing to the data (437.52°C).

Thus, this estimated boiling temperature is taken for ChCl:TEG (1:3).

3.2.2 Thermodynamic Model

For the validation of the thermodynamic model, the RMSD and R^2 were calculated for the vapour fraction of ethanol / IPA, the temperature, and the relative volatility. Those parameters can be seen in Table 1. The VLE curves, including the simulation and the data for mole fractions, temperatures and relative volatilities are given in the appendix by Figure A 5 to Figure A 13.

Generally, it can be seen that all R^2 values are lying mostly above 0.9 and always above 0.6, suggesting a good fit of the NRTL model. Also, the deviation parameter is in an acceptable range for the vapour fraction and relative volatility. Expectedly, the deviation of the relative volatility is higher than for the vapour fraction of ethanol because the relative volatility includes both components – ethanol and water – inherently. Indicated by both statistical measures, it can be seen that the temperature prediction is the most inaccurate regression. Furthermore, between the different systems, there are differences in the goodness of the fit. It seems that for the Ethanol-water-ChCl:Ur (1:2) system, the NRTL model predicts the data very well, while for IPA-water-ChCl:TEG (1:3) system, the prediction is less reliable.

Table 1: Statistical parameters RMSD and R^2 for the vapour fraction of ethanol / IPA, the temperature, and the relative volatility (alpha) of the four systems: ethanol – water – ChCl:Ur (1:2) (30 wt%), ethanol – water – ChCl:GA (1:3) (20 mol%), ethanol – water – ChCl:EG (1:2) and IPA – water – ChCl:TEG (1:3) (15 wt%). The data with the highest amount of DES was taken.

	RMSD_{y1} [mol]	R^2_{y1}	RMSD_T [K]	R^2_T	RMSD_{α}	R^2_{α}
ChCl:Ur (1:2)	0.027	0.987	0.624	0.981	0.776	0.964
ChCl:GA (1:3)	0.017	0.994	4.60	0.618	0.338	0.973
ChCl:EG (1:2)	0.01	0.921	3.527	0.743	0.214	0.947
ChCl:TEG (1:3)	0.131	0.995	4.839	0.648	0.564	0.879

The VLE data regression is difficult due to the negligible vapour pressure of the DES and the associated higher error. The IPA system is even more difficult in the regression of the data because of the complex behaviour of the VLE: For small ethanol liquid mole fractions, the relative volatility shows the typical increasing trend by increasing the DES amounts while for higher ethanol mole fractions, the relative volatility is smaller for higher DES amounts. Similar observations were found by the literature, and more details are given in the appendix (see chapter 0). As the RMSD for the relative volatility is above 0.6, the NRTL model is considered to predict the VLE accurate enough. However, the lower accuracy of the IPA-water-ChCl:TEG (1:3) system is kept in mind in the process evaluation, where MP steam is taken instead of LP steam due to the low-temperature trend of the simulation (see chapter 8).

3.3 VLE Analysis & Feasibility of the DES as Entrainer

For the separation of ethanol and water, the different DESs and their effect on the VLE is assessed. Based on that, it is decided for one DES in chapter 3.3.3. For the separation of IPA and water, the impact of the chosen DES, ChCl:TEG (1:2), is investigated. For both systems, the feasibility via RCMs is also assessed.

Equations for selectivities (S), and relative volatilities and theoretical background related to this assessment and RCMs are given in the methods in chapter B.2.

3.3.1 Ethanol and Water

For the separation of ethanol and water, the DESs ChCl:Ur (1:2), ChCl:GA (1:3) and ChCl:EG (1:2) were pre-selected. Their different effect on the VLE is discussed in the following Figure 4, where the VLE is plotted at the right, and the selectivity with increasing entrainer amounts is plotted at the left graph.

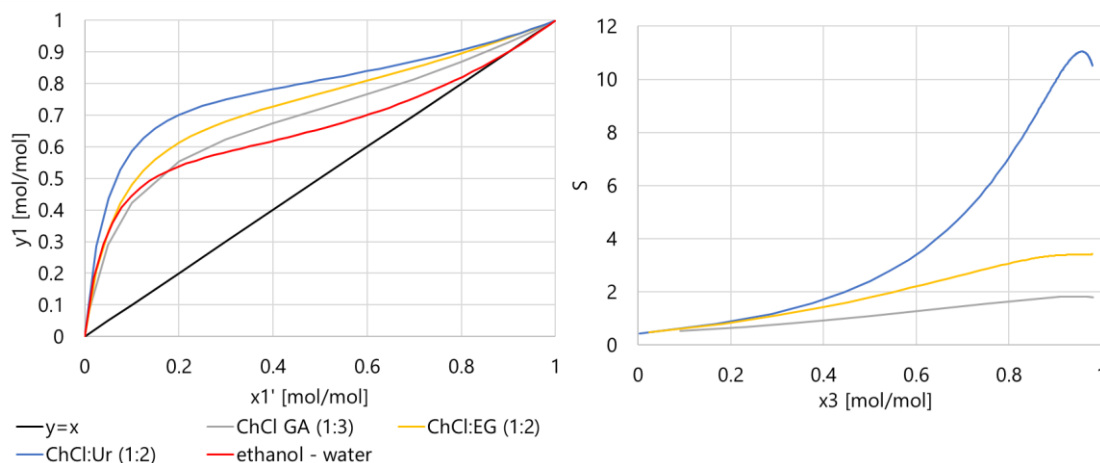


Figure 4: Comparison between ChCl:GA (1:3), ChCl:EG (1:2) and ChCl:Ur (1:2) in a diagram of the vapour mole fraction of ethanol over the liquid mole fraction of ethanol on entrainer free basis (left) and the selectivity over the entrainer mole fraction (right).

Expectedly, an increased DES amount enhances the relative volatility. This is due to the salting-out effect of the DES [8]. The differences between the DESs shown in Figure 4 can be related to the hydrogen bonding ability of the individual DES. Generally, the hydrogen bonding interactions between the HBD and the HBA of the DES are energetically favoured as compared to the lattice energies of the pure components resulting in the freezing point depression. The ions show high vibrational freedom, low symmetry and delocalisation, which is why the crystalline phases are destabilised [17]. A high hydrogen-bonding ability is causing a strong deviation from the ideality, which is beneficial for the selectivity. Thus, it can be stated that a higher polarity is often related to higher selectivities [50].

In Figure 4, it can be seen that ChCl:Ur (1:2) shows a higher separation capability than ChCl:GA (1:3) and ChCl:EG (1:3). The following reasons can be found:

1. Shang *et al.* (2019) investigated σ -profiles and showed that ChCl:Ur (1:2) has a broad profile outside the nonpolar region and high peaks, which proves the high polarity and selectivity [45]. The σ -profiles are divided into the HBD, nonpolar and HBA region. According to his group, the peak at $-0.017 \text{ e-}/\text{\AA}^2$ for ChCl/Urea (1:2) in the hydrogen bond donor region can result in a preferred interaction with the peak of water in the hydrogen bond acceptor region ($0.015 \text{ e-}/\text{\AA}^2$) [45]. More information is given in the appendix, where it can be seen that the activity coefficient for water in the presence of DES is even below one due to the strong attractive forces (see chapter C.4.2).
2. From a molecular point of view looking at the structural formula of the molecules (database Table A 25): A smaller molecule reduces the steric effect and therefore increases the separation factor [21, 34]. Water is less likely to partition in an entrainer with a higher steric effect [34]. Thus, the interaction between water and a small molecule of DES is stronger, which shifts the ethanol equilibrium more into the vapour phase [34].

3. Certain functional groups are improving the HBD ability [10]. The amino and hydroxyl group have a strong polar character and can act as both HBA and HBD. Therefore, it is not surprising that ChCl:Ur as a small molecule with two amino groups and one hydroxyl group has the highest selectivity. ChCl:EG (1:2) shows a lower separation capability as it is slightly longer and has two hydroxyl groups only. ChCl:GA (1:3) has a carboxyl and hydroxyl group (see Table A 24). Therefore, it can build strong hydrogen bonds with water but also form an intermolecular hydrogen bonding as dimeric species [51–53].

Another point to consider is the capacity and feasibility of the system. In general, the increase of the selectivity often goes in hand with the reduction of the capacity [50]. The non-ideality of the mixture is beneficial for high selectivities, but this often results in limited miscibility. Liquid phase demixing is a substantial disadvantage for extractive distillation processes [50]. Therefore, the solvent power as a product of capacity and selectivity is often used to evaluate the suitability of the entrainers [10, 50]. Fortunately, the DES systems are not prone to form a miscibility gap, which can also be seen in the RCMs. Thus, it is not necessary to make a compromise between selectivity and capacity.

As described in the methods in chapter B.2.2.2, RCMs can be used to confirm the DESs feasibility as entrainer for extractive distillation processes. The RCMs of the systems with ChCl:Ur (1:2), ChCl:GA (1:3) and ChCl:EG (1:2) on a mass basis are shown in the appendix (Figure A 15).

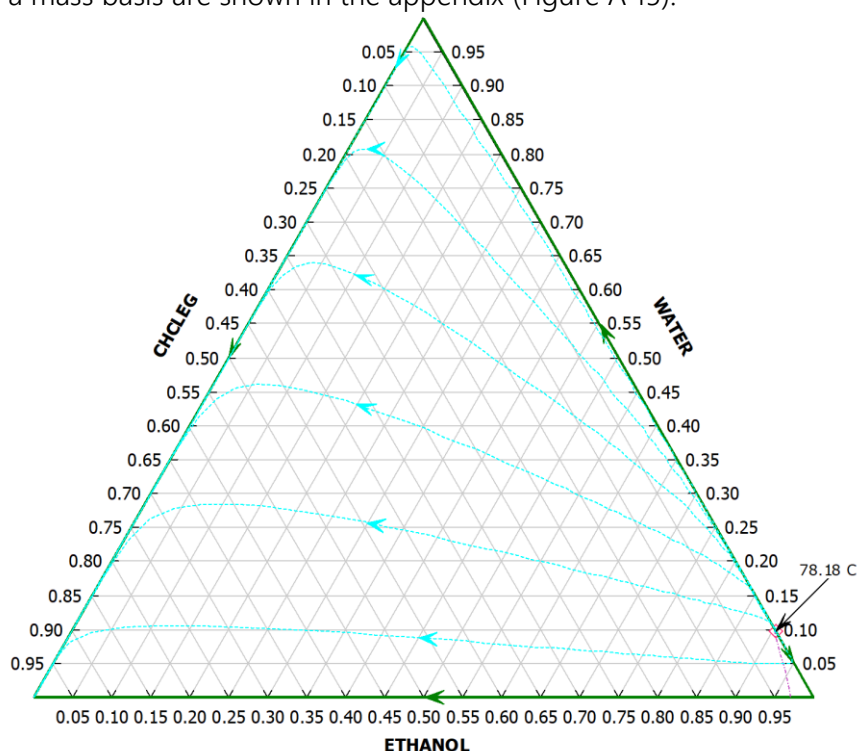


Figure 5: Residue curve map for ethanol, water and ChCl:EG (1:2) on a mole basis. Also shown is the azeotrope of water and ethanol and the isovolatility curve (in dashed red).

In Figure 5, it can be seen that DESs as entrainers for the separation of ethanol and water is possible according to the general feasibility criterion stated by Gerbaud *et al.* (2019) (see methods in chapter B.2.2.2) [54]. There are no distillation boundaries or other azeotropes visible, which shows that pure ethanol, water and the DES can be obtained [45]. According to Serafimov's classification scheme, the system belongs to the class 1.0-1a with the minimum boiling azeotrope as an unstable node, ethanol and water as saddle points and the DES as stable node [8, 55]. Moreover, the isovolatility curve moves towards the water-free side by the gradual addition of the DES. It shows the minimum entrainer amount to be approximately 3.5 mol% of ChCl:EG (1:2). The shown RCMs are very similar to the ones shown in

the literature by Ma *et al.* (2017) and Han *et al.* (2018) [8, 44], further proving the reliability of the Aspen implementation of the DESs.

3.3.2 IPA and Water

As in the previous for the ethanol and water system, the separation with ChCl:TEG (1:3) is feasible (see RCM in Figure A 15). In chapter 3.2.2, it was outlined that the system of IPA, water and DES is different than that with ethanol and shows an untypical behaviour. This is further demonstrated in Figure 6.

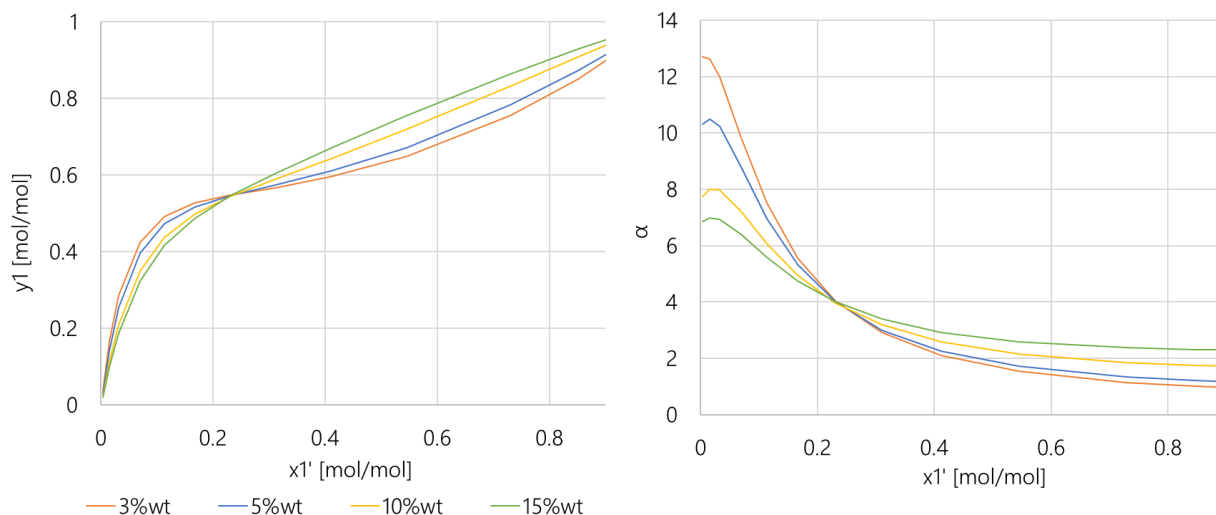


Figure 6: IPA vapour mole fraction (left) and relative volatility (right) over liquid mole fraction on entrainer free basis for four different constant ChCl:TEG (1:3) weight fractions.

It can be seen that at an IPA mole fraction of 0.22, there is an inversion of the behaviour. High IPA concentrations show the typical salting-out effect of the DES, while for smaller IPA concentrations the relative volatility decreases with increasing DESs weight fraction. It is also interesting to see that for this system, ChCl:TEG (1:3) is considered as the best entrainer which is entirely different for the separation of ethanol and water (see literature review chapter 2). To explain this behaviour, the activity coefficients are considered and shown in Figure 7.

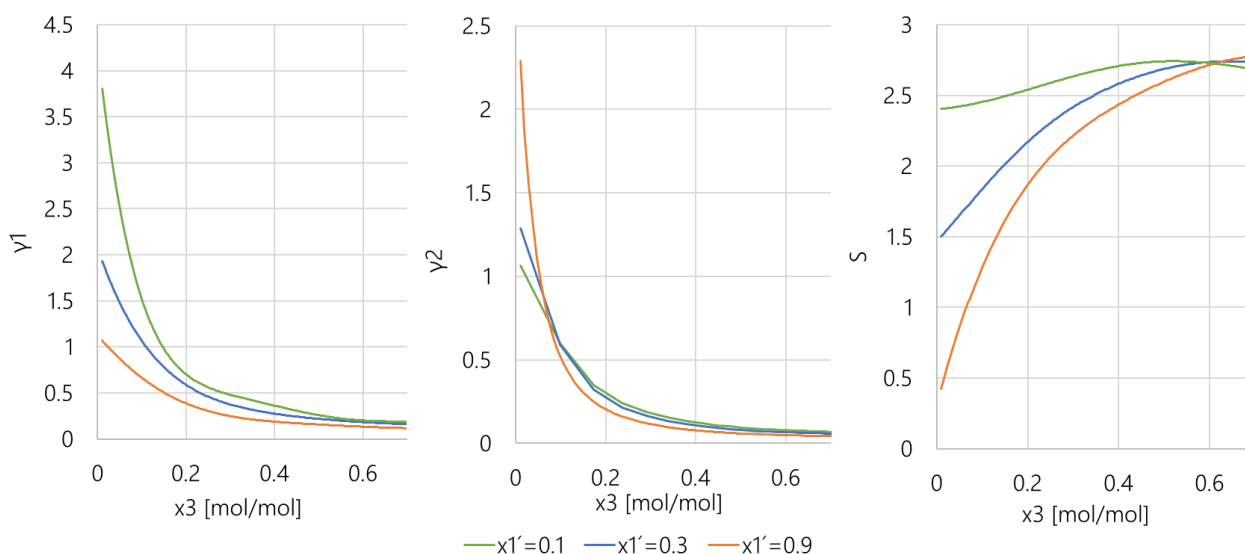


Figure 7: Simulation results of the activity coefficient of IPA (γ_1) (left) and water (γ_2) (middle) and the selectivity (right) as defined in Chapter B.2.2.1 plotted over the mole fraction of ChCl:TEG (1:3) for two different IPA mole fractions on entrainer free basis (x_1').

In Figure 7, it can be seen that both the activity coefficient of IPA (γ_1) as well as for water (γ_2) shows a negative deviation from the ideality. Therefore, the DES strengthens the attractive forces. In a solvent screening, Jiang *et al.* (2019) investigated the σ -profiles [47]. It was shown that IPA has even a stronger HBD ability than water. Thus, to become a good entrainer, the selected DES should have a strong HBA ability which is contrary to the ethanol and water system. According to Jiang's group, the DESs with a high solvent power automatically have almost no HBD ability but a strong HBA ability [47]. ChCl:TEG (1:3) has two ether and hydroxyl groups that can accept hydrogen bonds and therefore shows those matching profiles. The strong HBA ability of ChCl:TEG (1:3) gives this DES perfect suitability for the IPA and water system but a weak match for ethanol and water. Water also has a strong HBD ability, which is why it can also form hydrogen bonding with the DES. This also explains why the activity coefficient of water shows the negative deviation similarly as for the ethanol and water system. More detailed information regarding the analysis of Figure 7 can be found in the appendix (see chapter C.4.2).

3.3.3 Summary & Final Choice of the DES

There are no substantial disadvantages for any system, and all have a capacity high enough to be fully miscible. The comparison between the ethanol and IPA system and the summary of the analysis is shown below.

<u>Analysis of the effect of the DES to the separation system</u>	
Ethanol & water	IPA & water
<ul style="list-style-type: none"> ✓ The separation of ethanol and water is feasible with all considered DES. ✓ The best DES should have a strong HBD ability to interact with water as strongest HBA. ✓ ChCl:Ur (1:2) has the highest selectivity and lowest minimum entrainer due to a strong HBD ability proven by σ-profiles, the small molecule size and the amino and hydroxyl functional group. ✓ ChCl:Ur (1:2) is therefore chosen. 	<ul style="list-style-type: none"> ✓ The separation of ethanol and water with the only considered DES ChCl:TEG (1:2) is feasible. ✓ The best DES should have a strong HBA ability to interact with IPA as strongest HBD which is proven for ChCl:TEG.

Therefore it is decided to exclude ChCl:GA (1:3) and ChCl:EG (1:2) from further consideration because of the considerable lower selectivity (C 4).

4 Preliminary Process Synthesis

In the previous chapters, the data has been collected, the DESs have been successfully implemented in Aspen Plus, the feasibility has been proven, the most suitable DES has been selected, and the mechanisms have been studied. In this chapter, the process design stage is started, which begins with a preliminary process synthesis, according to Seider *et al.* (2006) [56]. It includes a black-box diagram with the compositions of each flow. For this, it is necessary to specify the separation task and the constraints. Accordingly, it is also essential to identify the design variables and the associated trade-offs.

4.1 Separation Task & Constraints

For the final fair comparison between the process using DES and the process of the literature, the exact feed and product flowrates and purity and recovery constraints must match. The separation task and constraints are therefore defined by the publication, which is used to compare and evaluate the designed DES process. In chapter 2, it was decided that the conventional solvent and the IL are taken for the evaluation of the performance of the DES process.

The separation tasks consisting of the feed flowrates, compositions, purities and recovery constraints (taken from each publication) are shown in Table 2.

Table 2: Three separation tasks of this project, including the feed flowrates and compositions and purity and recovery constraints.

Separation of ethanol and water		Separation of IPA and water
1 Comparison with process using EG of Bastidas <i>et al.</i> (2010) [30]	2 Comparison with process using IL of Zhu <i>et al.</i> (2016) [35]	3 Comparison with process using DMSO and IL of Ghuge <i>et al.</i> (2017) and Ma <i>et al.</i> (2019) [31, 36]
Feed: 245 kmol/h, 88.5 mol% ethanol, 11.5 mol% water Ethanol product purity: 99.7 mol% Recovery of ethanol: 99.9% Recovery of DES: 99%	Feed: 100 kmol/h, 85 mol% ethanol, 15 mol% water Ethanol product purity: 99.9 mol% Recovery of ethanol: 99.9% Recovery of DES: 99%	Feed: 100 kmol/h, 50 mol% ethanol, 50 mol% water Ethanol product purity: 99.9 mol% Recovery of ethanol: 99.9% Recovery of DES: 99%

For the separation of ethanol and water, the process details of Bastidas *et al.* (2010), and Zhu *et al.* (2016) were taken [30, 35]. Two different simulations have to be performed as those flowrates and constraints are varying in the publication. For the separation of IPA and water, the process details of Ma *et al.* (2019), and Ghuge *et al.* (2017) were taken [31, 36]. In the case of IPA and water, the feed flow rates and compositions are the same, and the constraints vary only marginal. Those separation tasks are visualised by decision C 8 and C 9 in the appendix. Concluding, three separation tasks need to be simulated to guarantee a fair comparison of the process using DES to the conventional and ILs process.

4.2 Identification of Design Variables & Objective Functions

For the process design, it is crucial to identify all design degrees of freedom. The design parameters include the reflux ratio (RR), entrainer-to-feed ratio (E/F), main feed stage (N_F), entrainer feed stage (N_E), number of stages (N_{th}), EDC pressure (p_{EDC}) and the entrainer recycle purity (x_E) [35]. Because of this considerable number of design parameters, it is necessary to investigate their individual impact on the process (see chapter 5) [6]. Subsequently, they have to be chosen in a way to guarantee the best possible economic potential by also keeping other factors in mind, such as the environmental impact or

operability. As an objective function, the TAC or CO₂ emissions can be taken to optimise the process. However, this iterative computational optimisation algorithm is often a time-consuming undertaking. For the research question of this project, it is sufficient to minimise the overall energy consumption, and, if necessary, develop some cases for the economic comparison. Therefore, the controllability or CO₂ emissions are out of scope. The overall energy consumption as objective function mainly consists of the reboiler duty and the entrainer regeneration energy demand. Meanwhile, a reasonable limit to this minimisation should be applied in order to keep the capital costs bounded. This is done through a combination of heuristics, short-cut rules and a sensitivity analysis, which is presented in chapter 5. Further information and explanation regarding this decision are given in the methods in the appendix (see chapter B.1.4).

4.3 Black-Box Diagram

The feed flowrates and constraints have been given by the separation tasks in the previous chapters. For a typical black-box diagram, a perfect recovery of the solvent is usually assumed. Thus, there is no trace of entrainer in the product, and no make-up stream is needed [56]. Next to this, for the black box diagram, it must be defined whether the process is done continuously or in batch operation mode. As both product chemicals are commodity chemicals which are required in largescale, a continuous operation mode is selected according to Seiders *et al.* (2006) (H 1) [56]. All heuristics used for the process creation are summarised in Table A 2 in the appendix (see Appendix A). The black box diagram of separation task 1 is shown in the following figure. Black box diagrams of the separation tasks 2 to 3 are shown in the appendix by Figure A 16 and to Figure A 17.

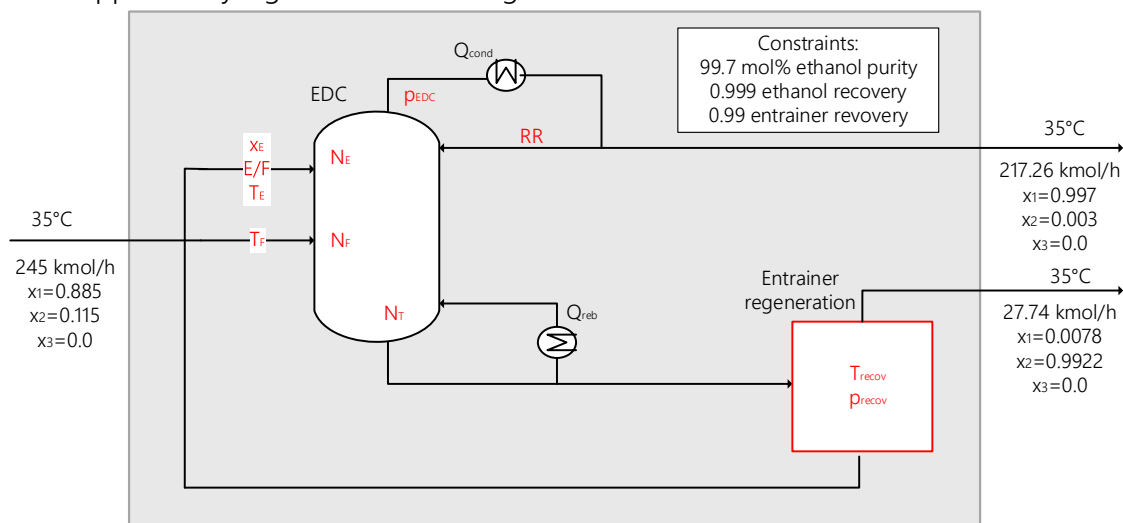


Figure 8: Black box diagram for the separation of ethanol (1) and water (2) using the process details of Bastidas *et al.* (2010) [30]. The constraints (inbox) and the design variables and unknowns (in red) are given as well. However, for this diagram, the separation efficiency of the entrainer and water has been assumed to be 100%.

As can be seen, the input and output flowrates and the constraints, as stated in chapter 4.1, are given. The streams are assumed to enter and leave the system with a temperature of 35°C (assumption (A 1)). The separation is a direct split, as the products ethanol or IPA are the most volatile components. Furthermore, the design variables, as defined in the previous chapter, are marked in red. It is also known that an extractive distillation column is used which is why this unit operation is not given as a box. However, the purification of the entrainer is not further specified yet, which is why it is given as a red box in the black box diagram [54]. The further specification of this unit operation is discussed in the following chapter.

5 Base Case Designs & Process Simulation

This chapter aims to specify the unit operations and perform a sensitivity analysis within the process simulation for the development of one or several base case designs. The final goal of the development of base case designs is to establish the most economical process version that can compete with the process using conventional solvents or ILs. The decisions are summarised in *Table A 1* in the appendix.

5.1 Unit Design Specifications

Several process alternatives for the recovery unit are evaluated, and heuristics are applied for the temperature and pressure change blocks. With this chapter, all necessary unknowns needed for the process simulation are determined. The heuristics that are applied were given in *Table A 2*, together with the reasoning and application.

5.1.1 Heating, Cooling and Change in Pressure

The near-optimal temperature difference and pressure drop in a heat exchanger are chosen according to heuristic (H 2 & H 3) [56]. The pressure drop of pipelines and valves and the temperature change across a pump for liquids is neglected ((A 2) and H 4). Moreover, when a pressure change needs to be applied for a gas stream, it is more profitable to condense the gas and use a pump instead of a compressor because of the huge power requirement of the gas compression (H 5) [56].

5.1.2 Recovery Unit

So far, the non-volatility of the DESs was stated as a strong advantage since the product ethanol will not be contaminated, and the emission into the atmosphere will be prevented [32]. The downside of this is that the hydrophilic DESs end up in the aqueous environment, and the regeneration of the DESs can be difficult and especially energy demanding. Indeed, in the literature, it is stated that this step can be more challenging than expected and recovery options have to be thoroughly assessed to achieve an economic and technically feasible process [10, 32, 57, 58]. The water might be discharged as an effluent which is why its quality is important. However, this and the treatment of the wastewater will not be considered in this project (C 18).

According to Seider *et al.* (2006), liquid mixtures should be separated using distillation, enhanced distillation methods, extraction, stripping, adsorption or crystallisation dependent on the phase of the streams and the properties of its chemical species (H 7) [56]. As the first option, distillation should always be considered. However, the conventional distillation can be excluded as the non-volatile entrainer would break down the columns counterflow [58]. Moreover, Shang *et al.* (2019) decided against a recovery column because of the thermal stability of ChCl:Ur (1:2) [45]. For these reasons, the research focuses on stripping, evaporation, crystallisation and extraction, where the evaluation is visualised in the decision *Table A 1* together with the choices [58]. For weighting those different options, the purification processes for ILs in the literature are considered, as ILs are similar to DESs and the DESs process options are not well investigated yet.

In *Table A 38*, all considered options, the advantages, disadvantages and references are listed. The considered options are extraction with a solvent and supercritical CO₂ (scCO₂), induced phase separation by CO₂ and salts, adsorption, evaporation, stripping, and membrane separations such as nanofiltration, reverse osmosis, and pervaporation. Because of the scarce adsorption and desorption data in the literature for both ILs and DESs, absorption can directly be rejected (C 11) [59].

On a molecular level, the interaction ability of the DES with water determines how effective a particular method can be [59]. The strong hydrophilia of the considered DESs further complicates its purification from water [60, 61]. Therefore, extraction with an organic solvent, which on the positive side avoids huge energy requirements, would, however, be very problematic (C 10). Moreover, due to possible cross-contamination, it diminishes the green aspect of DESs [59]. In contrast, extraction with scCO₂ is a green process but is very costly to pressurise the CO₂ [41, 59]. Again, this process might be impossible for the separation of the hydrophilic DESs from water and is mostly applied for capturing organic components in the second phase containing scCO₂ [57]. Thus, both options can be dismissed for the systems considered in this project.

Induced phase separation by pressurised CO₂ was reported to be possible for this type of separation by Peng *et al.* (2010) [60]. In this technique, crystalline compounds in the form of gas hydrates are formed under suitable temperature and pressure conditions. In those gas hydrates, the non-volatile compound can be caged and separated mechanically from the formed water hydrates. Subsequently, the DESs can be recovered by readapting the temperature and pressure conditions. However, this method can only be applied for a specific initial concentration range of the entrainer, and maximum 73% of the IL was recovered by Peng *et al.* (2010) [60, 61]. Therefore, this technology can possibly not meet the recovery constraint and is rejected (C 12).

Because of the high energy consumption, membrane separation techniques can be a good alternative [59]. Haerens *et al.* (2010) investigated nanofiltration, reverse osmosis and pervaporation for the separation of ChCl:EG (1:2) from water [32]. The group found that all three methods give only a limited purification of the DES, and additionally, a large membrane area would be required [32]. Therefore, this recovery option is not further considered either (C 13).

The rejection of the main solvent regeneration possibilities explains why evaporation and stripping are the benchmark methods in the literature [10, 62]. One or a series of two evaporators under vacuum conditions has been variously applied for the separation of DESs or ILs from water because of the simplicity and the thermal stability of the DES / ILs [4, 8, 35, 36, 41, 42, 45, 62–64]. The decrease in pressure and increase in temperature makes the evaporation of water possible. Using a combination of an evaporator and a stripping column has the advantage of milder conditions and has therefore also been used widely as well [12, 28, 42, 58]. However, when stripping with nitrogen or gas, additional VLE data must be present. Jongmans *et al.* (2013) propose stripping with the overhead product of the EDC column [57]. The group compared different solvent regeneration technologies and came to the conclusion that indeed the purification involving only evaporation, and evaporation and stripping with the overhead product are the most promising technologies [57].

Concluding, it can be stated that either evaporation or evaporation and stripping with the overhead product is the best alternative for the DESs recycle stream. Those two options represent the first two base case designs (C 15). The establishment of the operating conditions of those equipment's and the exact purity constraint for the DESs recycle is done in chapter 5.2.

5.1.3 EDC Unit

The design variables of the EDC were identified in chapter 4.1. Necessary for the process simulation is the choice of the condenser and the pressure drop of the EDC. According to H 6, a pressure drop of 0.1 psi (0.7 kPa) can be assumed [65]. Commonly a total condenser is chosen, except if the product is required in vapour condition [65]. Therefore, a total condenser is chosen for the base case design involving only evaporation. For the stripping column, the stripping agent needs to be gaseous, which is why a partial condenser is selected for this base case design (C 19).

5.2 Sensitivity Analysis

In the previous chapter, two different base cases have already been established, which was visualised in Table A 1: First, the regeneration unit involving only evaporation, and second, the evaporation and stripping purification. The whole chapter illustrates the process simulation at the example of the separation task 1, which was shown in the black box scheme in Figure 8. It was decided to determine the necessary design parameters by a combination between specific heuristics, short-cut rules and sensitivity analysis (see chapter 4.2 and B.1.4). The approach of this optimisation procedure and the step-by-step method are illustrated in Figure A 1 for the EDC, Figure A 2 for the two evaporators regeneration units and Figure A 3 for the evaporator and stripping column regeneration unit. Further details of the simulation input and model of the columns can be seen in the methods in the appendix (see chapter B.1.4).

5.2.1 Entrainer and Feed Temperature of the EDC

The heat balance of the distillation column is strongly influenced by T_F [66]. In general, mostly, the feed conditions are designed to be saturated to match the columns trays conditions [65]. Placing a feed preheater can minimise the reboiler duty (Q_{reb}) strongly and definitely minimises the overall utility requirements when another hot process stream can be used to preheat the feed. However, when the T_F is increased above the boiling point, water also evaporates and causes the distillate purity (x_{1dist}) to drop. This can be seen in Figure 9 [66].

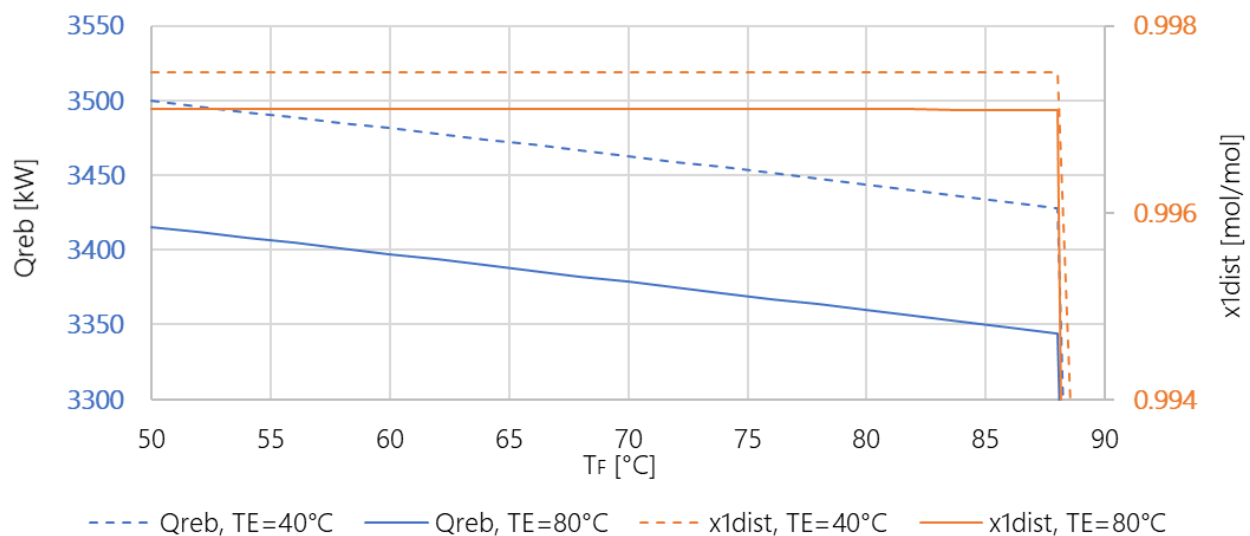


Figure 9: Reboiler duty (blue: Q_{reb}) and mole fraction of ethanol in the distillate (orange: x_{1dist}) over the feed temperature (T_F) for two different entrainer feed temperatures (dashed and solid lines: different T_E). The pressure of the feed is 1.5 bar.

Figure 9 also shows that Q_{reb} firmly falls when T_F is above the boiling point. Due to the strong decrease in purity, the RR and E/F has to be increased to meet the constraint still (see chapter 5.2.5). Therefore, a T_F close to the boiling point is used such that the feed enters the column as a saturated liquid [8].

Another essential variable is T_E which is also shown in Figure 9. It can be seen that a higher T_E reduces the reboiler duty but also goes in hand with a reduction in the distillate purity. This occurs because part of the heavy component water also vaporises at the stage of the entrainer feed, which increases the amount of water in the distillate [67]. As the Q_{reb} is approximately constant when adapting RR to meet the purity constraint, a decision cannot easily be made. Therefore, Doherty and Malone (2001) gave a guideline to set T_E 5–10 °C lower than the temperature of distillate [68].

5.2.2 Pressure of the EDC

The pressure of the EDC column is a key design variable as it influences majorly other design variables [56]. Lowering the pressure in this separation task has the following advantages:

- Lowering the temperature levels and therefore the reduction in Q_{reb} , the possibility to use low-pressure steam and avoidance of possible partial decomposition of the DES [69]
- Increase in the relative volatility between ethanol and water and therefore a possible reduction in the required stages [70]
- Decreasing the E/F and therefore an additional decrease in Q_{reb} (see chapter 5.2.5) and the energy demand of the regeneration unit [71]

However, the pressure has a lower bound, since for too low temperatures, a costly refrigerant has to be taken, and the operating and capital costs of the vacuum system become high [72]. To condense the distillate product with cooling water of 20°C assuming an approach temperature difference of 10°C, the pressure must be above 11 kPa (see chapter 7.2). However, below 14 kPa, a two-stage steam jet ejector must be taken, which is why the lowest bound defined for this separation task is 14 kPa [56]. Thus, four different pressure cases are evaluated in terms of total energy requirements. This can be seen in Figure 10, in which, as an example, the base case involving only evaporation is taken.

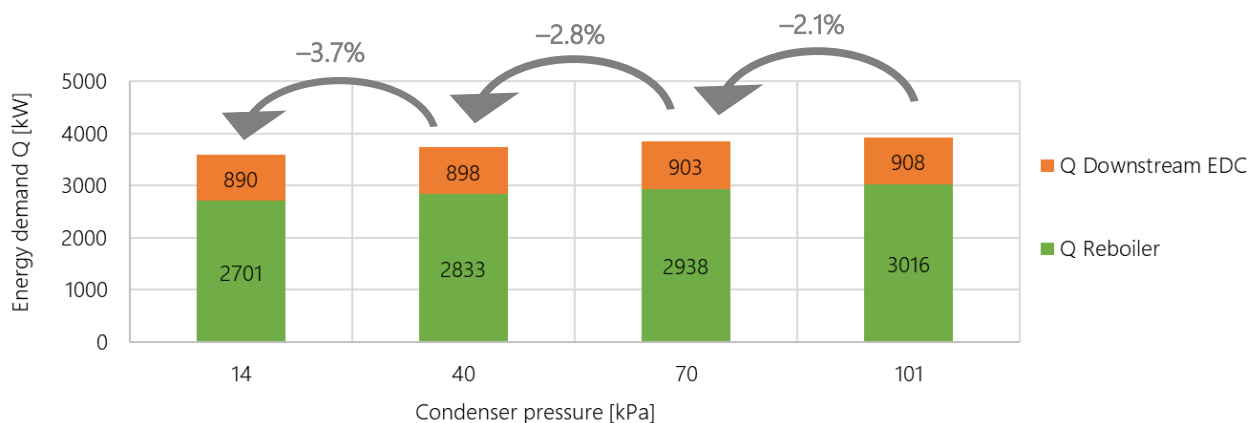


Figure 10: Energy requirements of the process for different condenser pressures (14, 40, 70 and 101 kPa) of the EDC. Shown are the reboiler duty (green), the requirements downstream to the EDC (blue).

As can be seen, a decrease in pressure of approximately 30 kPa decreases the total energy requirement by approximately 100 kW. The reboiler duty falls because of the reasons mentioned above. Also, energy requirements downstream to the EDC reduce as less entrainer has to be used so that the streams become smaller (for E/F see chapter 5.2.5). As this effect is even increasing for lower pressures, the pressure case of 14 kPa is taken for further evaluation. However, without the calculation of the additional capital and operational costs for the vacuum system, the benefit as compared to the process at atmospheric pressure cannot be proven. Therefore, both cases will be further assessed in terms of economic analysis (C 16) (see chapter 8).

5.2.3 Entrainer Impurity of the EDC

According to Shang *et al.* (2019), it is not necessary to feed pure entrainer, which ultimately would make the recovery of the entrainer more challenging [45]. However, there is a minimum entrainer purity that is necessary to meet the ethanol product purity constraint, which is illustrated in Figure 11.

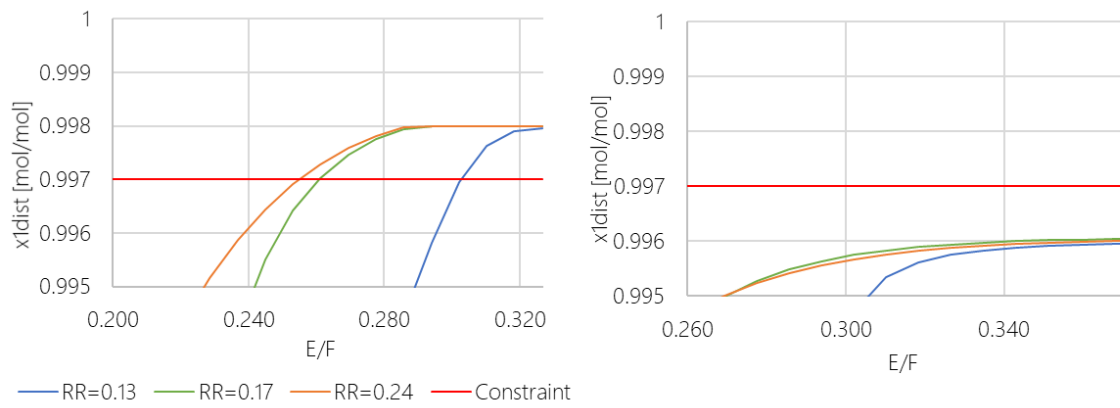


Figure 11: Mole fraction of ethanol in the distillate (x_{1dist}) over the entrainer to feed ratio (E/F) for three different reflux ratios (RR). Left graph: entrainer feed containing 99.5 mol% of ChCl:Ur (1:2), Right graph: entrainer feed containing 98.5 mol% of ChCl:Ur (1:2)

As can be seen, even when increasing RR and E/F , the product purity constraint shown as a red line cannot be met when the entrainer contains 1.5 mol% of water. This can be explained by the fact that too much of this water evaporates into the distillate [45]. Therefore, there is always a certain maximum ethanol distillate purity that can be achieved for each entrainer purity. The maximum entrainer impurity for this separation task amounts 1.1 mol%. The impurities of 0.5 and 1 mol% were chosen and further evaluated in terms of the energy requirements (see chapter 5.3) (C 17).

5.2.4 Entrainer and Feed Stage of the EDC

The feed stages N_F and N_E are determining the rectifying, extractive, and stripping sections. They influence the feasibility of the separation as the composition profiles of the different sections must meet [73]. In Figure 12, the influence of N_F and N_E are shown.

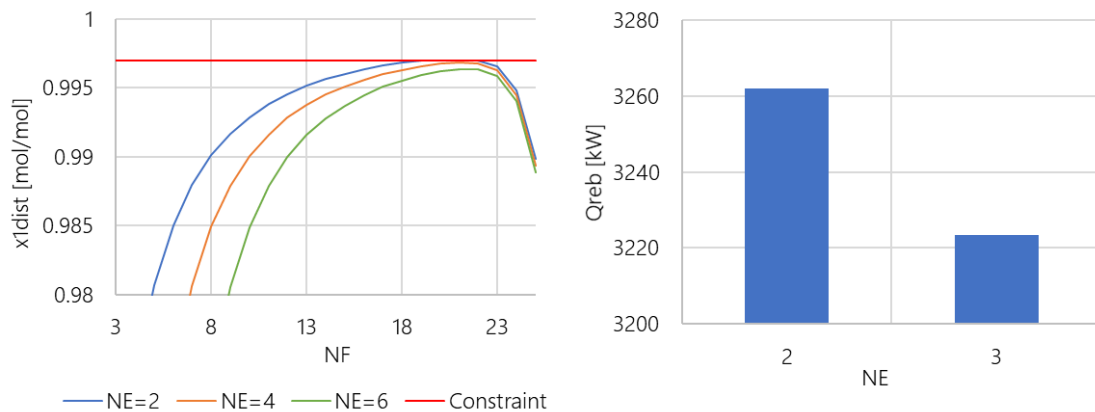


Figure 12: Ethanol purity in distillate (x_{1dist}) over main feed stage (N_F) for different entrainer feed stages (N_E) (left) and reboiler duty (Q_{reb}) for two different N_E . RR is adapted to meet the purity constraint.

It can be observed that there is a range of N_F for which the purity is the highest. This range depends on N_E and is close to the reboiler. Thus, most separation work is done in the rectifying section as a high ethanol content zone [67].

Concerning N_E , it can be seen that there is only a small range for which the purity constraint can be met. Evaluating those two stages in terms of the energy demand, it can be seen that feeding the entrainer at the second stage requires more energy than at the third. This can be explained by the vaporisation of water close to the condenser so that RR or E/F must be adapted to meet the purity constraint. This ultimately increases Q_{reb} . Thus, N_F and N_E were chosen according to this analysis in an iterative loop with E/F , RR , and N_{th} [67].

5.2.5 Reflux Ratio and Entrainer to Feed Ratio of the EDC

In conventional distillation processes, the economic trade-off is done between the N_{th} and RR as the most significant design variables [74]. The RR increases the energy consumption of the distillation column and therefore, the operating costs, while the N_{th} increases the capital costs [70]. Usually, 1.1 to 1.5 times the minimum RR is taken [72].

When designing an extractive distillation process, the theoretical relations between the design variables change, and these rules of thumb cannot always be taken anymore. For instance, in the extractive distillation, there exists a maximum RR next to the typical minimum RR, which limits the feasibility of the azeotropic separation and can be seen in Figure 13 on the left. This maximum value arises because of a dilution effect: With increasing RR, the impact of the entrainer diminishes, which can also be seen in the graph. Therefore, E/F and RR are dependent on each other and for both a minimum value exists.

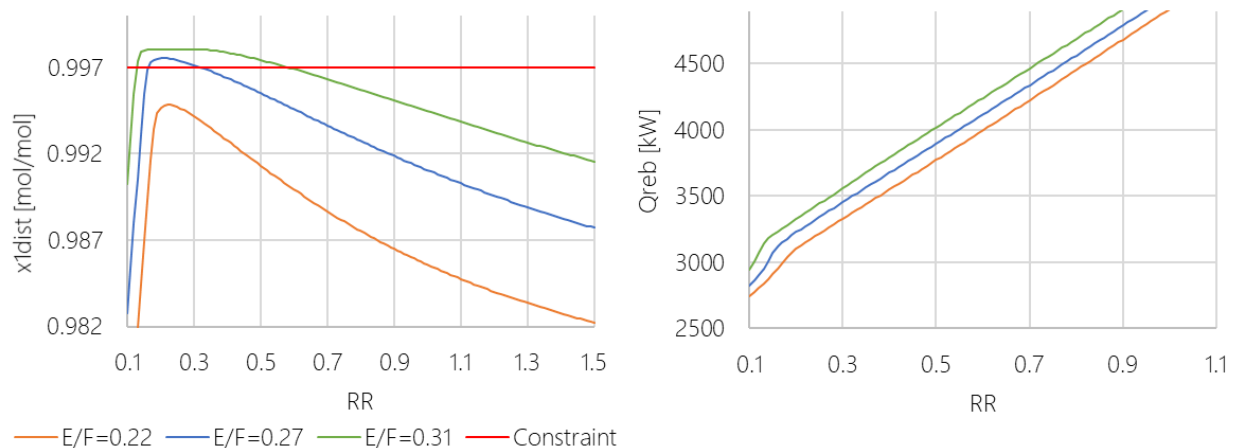


Figure 13: Ethanol purity in distillate (x_{1dist}) and reboiler duty (Q_{reb}) (right) over the reflux ratio RR for different E/F.

In Figure 13 on the right, one can see that both E/F and RR increase Q_{reb} . The increase of both variables increases the liquid flow in the column. Contrary to the increase of RR, the increase of E/F does not imply a higher amount to be vaporised in the reboiler. However, the reboiler duty still increases due to the rise in the temperature levels.

Many researchers state the RR and E/F are the most crucial design variables for energy requirements and economic profitability of the extractive distillation [6, 75]. Gil *et al.* (2008) state that RR should be minimum and E/F should be adapted to meet the purity requirement [67]. This would also be suggested by the right graph of Figure 13, in which it can be seen that RR has a much stronger relative influence on Q_{reb} than E/F. However, it was also found that a much bigger relative increase in E/F is required in order to meet the purity constraint. Indeed, when varying E/F and adapting RR to meet the purity constraint, an approximately equal Q_{reb} can be seen. Furthermore, one can state that when increasing E/F:

- the temperature levels increase so that required utilities become more expensive
- higher energy demand downstream to the EDC due to higher amounts to be purified
- The range of feasible RR increase resulting in an increase the operational stability [6]

Because of the first two points, it is decided to rather adapt the RR to meet the purity requirement. However, because of the controllability, E/F is chosen higher than the lowest amount possible.

5.2.6 Number of Stages of the EDC

The energy reduction of the reboiler is investigated when increasing N_{th} by five. This is shown in Figure 14, in which Q_{reb} is shown for the two different impurity cases described in chapter 5.2.3.

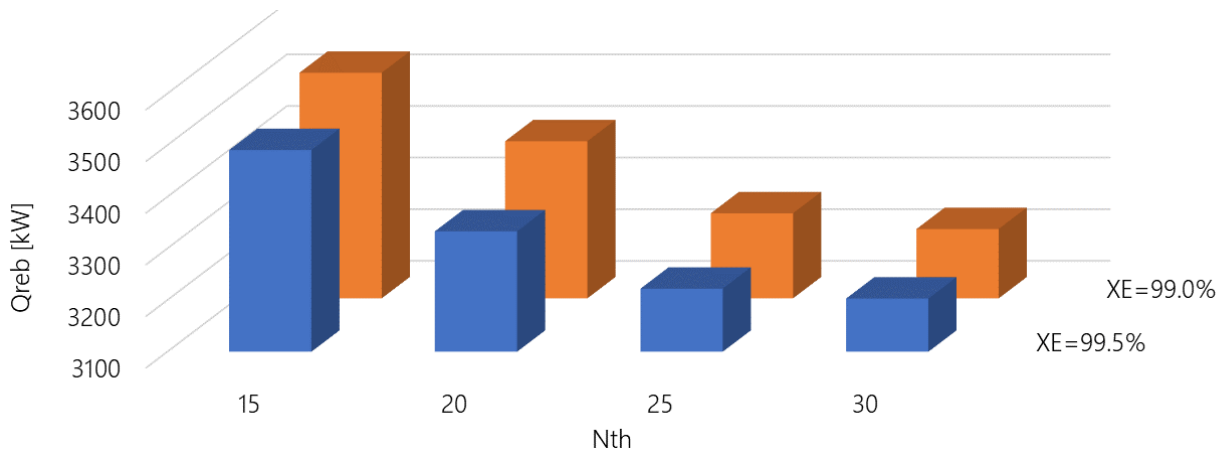


Figure 14: Reboiler duty (Q_{reb}) over the total number of stages (N_{th}) for the two different entrainer purity cases $x_E=99$ mol% (orange) and $x_E=99.5$ mol% (blue). RR and E/F are adapted to meet the constraints.

As can be seen, a smaller entrainer purity leads to a substantial reboiler energy increase. It was explained in chapter 5.2.3 that with increasing entrainer purity, the ethanol purity in the distillate increases. Thus, less RR and E/F are required in order to meet the constraint, which reduces Q_{reb} . However, the total energy requirements can still be smaller for the case of $x_E=0.99$ mol% as the entrainer purification can be assumed to be less energy demanding which will be further discussed in the overall comparison in chapter 5.3.

Figure 14 also shows that the effect of the increase in stages is not constant over the stages. As the stages increase, also the pressure drop over the column increases. The effect of the pressure was shown in chapter 5.2.2 and explains why, at some point, increasing N_{th} could even have a negative impact on Q_{reb} [70, 76]. The N_{th} was chosen in a way that less than 1% of the energy requirement can be saved by a five-stage increase. For the given example, the N_{th} of 30 can be found in both cases. As the minimum N_{th} for the cases of $x_E=99.5$ and 99 mol% equals 12 and 14, respectively, this result matches the conventional determination of N_{th} by 2-3 times the minimum N_{th} [41].

5.2.7 Regeneration: Two Evaporators

It was decided in chapter 5.1.2 that simple evaporation is a considered option for the entrainer regeneration. The following sensitivity analysis chapter guides through all steps of the procedure (Figure A 2) for the case of $x_E=99.5$ mol% and $p_{EDC}=101$ kPa.

It can be shown that one evaporator is not enough to meet the purity and recovery constraint. Therefore, two evaporators in series are used. Moreover, it was demonstrated by Ma *et al.* (2019) that two evaporators could be more economical than one [36]. This group also showed that it is best to operate the first evaporator at the highest and the second evaporator at the lowest possible pressure to meet the constraints [36].

The operating conditions of the two evaporators have to be adapted iteratively. A sensitivity analysis for the first evaporator and the case of $x_E=99.5$ mol% is shown in Figure 15 in which the purity and recovery of the entrainer recycle (after the second evaporator) are investigated.

As can be seen, the operating conditions of the first evaporator do not influence the entrainer mole fraction of the recycle stream. However, it decides about the possible recovery of the DES. As expected, higher pressures and temperatures result in the vaporisation of the DES in the first evaporator, so that the recovery constraint cannot be met. In this case, the highest possible pressure of 2 kPa is chosen as explained above. Another advantage of this choice is also that a two- instead of three-stage steam jet ejector or a liquid ring pump can be selected [56].

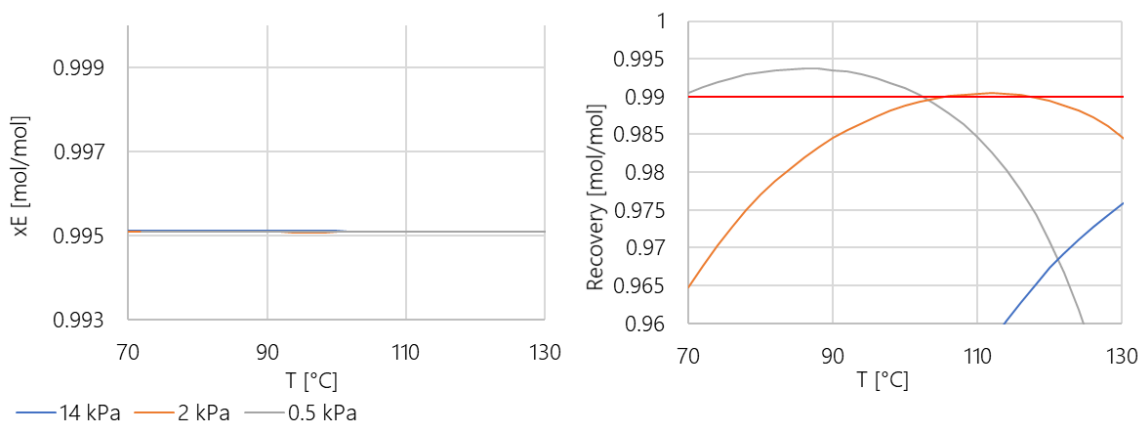


Figure 15: Mole fraction of the entrainer in the entrainer recycle (x_E) (left) and recovery of the entrainer (right) over the operating temperature for different operating pressures of the first evaporator.

The sensitivity analysis concerning the second evaporator can be seen in Figure 16.

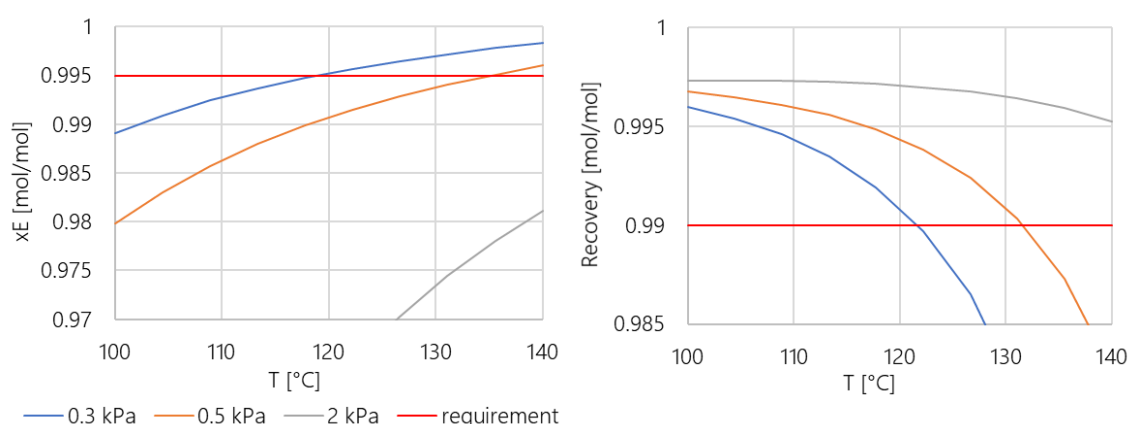


Figure 16: Mole fraction of the entrainer in the entrainer recycle (x_E) (left) and recovery of the entrainer (right) over the operating temperature for different operating pressures of the second evaporator.

The operating conditions of the second evaporator strongly influence the entrainer purity and recovery. In this example, it can be seen that for 0.5 kPa, a minimum temperature of 135°C is required to achieve the necessary DES purity. However, a maximum temperature of 131°C is allowed to meet the recovery constraint. Thus, only smaller operating pressures are possible.

5.2.8 Regeneration: Evaporator and Stripping Column

Next to the previous regeneration solution, it was decided in chapter 5.1.2 to use a combination of an evaporator and a stripping column with the EDC product as the stripping agent. As a difference to the previous base case design, the EDC condenser is now set as a partial condenser (see C 19). The following paragraphs explain all steps of the procedure (Figure A 4) briefly as the design variables have been already analysed in more detail in the previous chapter.

The pressure of the stripping column is increased to 2 kPa, where a liquid ring pump can be taken for obtaining the vacuum conditions. The pressure of the evaporator adapted to the highest pressure possible and the minimum pressure for the evaporator is the pressure for which cooling water of 20°C can be taken.

As ethanol is used as the stripping agent, this stream of water and ethanol has to be recycled to the EDC to not lose the product. Thus, the stage and temperature of this recycle – called product recycle in the following – need to be determined. Similarly, as for the main feed temperature and stages that were shown in chapter 5.2.1 and 5.2.4, the energy requirements are the lowest when the conditions and concentrations of the recycle feed match those of the stage. This is also shown in Figure A 18 in the

appendix, where Q_{reb} is plotted for different feed stages of this stream (N_P =stages of product recycle), and temperatures while RR is adapted to meet the ethanol purity constraint.

As shown in chapter 5.2.7 for the evaporator base case, the recovery of the entrainer decreases over the temperature while the purity increases. There is a temperature range for the evaporator between 150 and 161 °C that can be chosen to meet both requirements (see details in *Figure A 19*). The energy requirements increase by increasing temperature so that the lowest temperature is selected.

Concerning the total number of stages for the stripping column, the influence of increasing the stages of the stripping column on x_E is investigated (*Figure A 20*). A similar approach as before is taken: The stage, where an increase by one stage results in less a 0.1% increase in purity is selected.

As the flow rate of the stripping agent increases, the purity increases strongly in the beginning and finds a maximum. The recovery slightly decreases, which can be seen in *Figure A 21* in the appendix. Seider *et al.* (2006) recommend taking 1.1 times the minimum flowrate [56].

5.3 Optimised Base Case Processes & Flowsheets

Additional to the two different regeneration options, four other cases have been established: First, two different pressure cases for the EDC, and second, two different DES recycle purities. The energy requirements of the pressures cases have been shown in chapter 5.2.2, where it was concluded, that the cases have to be compared in terms of an economic analysis (see chapter 8).

The overall energy requirements of the two different recycle purity cases, and regeneration unit choices can be seen in *Figure 17*.

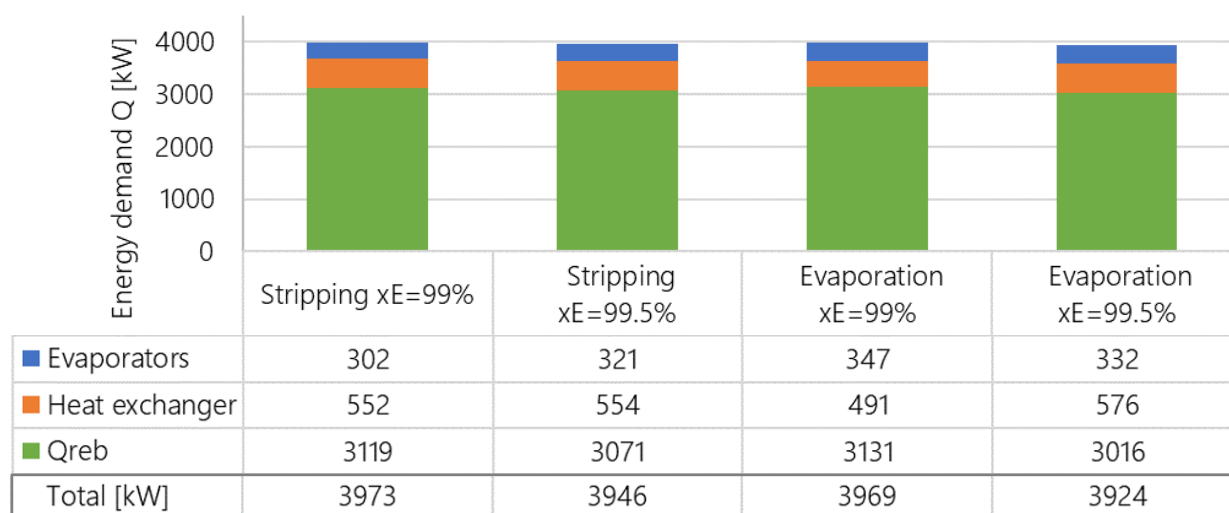


Figure 17: Energy requirements of the processes with a different entrainer recycle and regeneration unit choice. Shown are the reboiler duty (green), the total energy demand of the heat exchangers in the process (orange) and the total energy demand of the entrainer regeneration unit (blue).

It can be seen that in terms of the different regeneration units, there are no significant differences between the two regeneration options. Even though one might expect that the energy requirement for two evaporators is much higher, the first evaporator is the most energy demanding and therefore dominant for the requirements, which is why the energy reduction for stripping is only small. However, the second evaporator operates at a much higher degree of vacuum than the first evaporator, which increases the capital costs. The equipment differs, which is why a decision can be made with economic analysis (see chapter 8).

Contrary to the two regeneration unit options and the different pressure cases of the EDC, the different impurities can directly be evaluated without the need for an economic comparison, as the

equipment does not change. In *Figure 17*, it can generally be observed that the contribution of the energy requirements downstream of the EDC is relatively low. Expectedly, for higher purities, the energy requirements for the EDC are smaller and higher downstream to the EDC. There are nevertheless no differences in evaporation duties as there is a balance between bigger flowrates and higher required temperatures for the lower and higher DES concentrated streams, respectively. However, the heat exchanger before the evaporators have higher duties for the lower purity case because of the higher loads. In total, the higher purity case shows a lower energy demand, as the EDC contribution is more significant. Therefore, the higher purity case is selected in the following (C 17).

Concluding, there are four base case designs that are evaluated in chapter 8: two different regeneration options and two different pressure cases. This is visualised in *Figure 18*.

Base case designs of the extractive distillation using DES					
Entrainer Regeneration Options	✗ Extraction and induced phase separation	✗ Adsorption	✗ Membrane processes	✗ Vacuum distillation	✓ Evaporation ✓ Stripping
Simulation Options	✗ Recycle DES 99 mol%	✓ Recycle DES 99.5 mol%	✓ EDC at 101 kPa	✓ EDC at 14 kPa	
Base case designs	1 Evaporators EDC at 101 kPa	2 Evaporators EDC at 14 kPa	3 Stripping EDC at 101 kPa	4 Stripping EDC at 14 kPa	

Figure 18: Creation of four base case designs through the evaluation of different process alternatives

On the following page, the flowsheet of the base case with the EDC operating at 1atm and the evaporators is given exemplary. The Aspen Plus flowsheets of the other three base case designs are given by *Figure A 22* to *Figure A 24* in the appendix. Process stream summaries for all four base case designs are provided by *Table A 39* to *Table A 42*. The design variables of the four processes are shown in *Table A 43* to *Table A 46* in the appendix.

As can be seen in *Figure 19*, additional information regarding the EDC, evaporator and exchanger duties is given. For 11 equipment devices, heat is supplied or taken by utilities, which are shown in the figure. This is not very efficient and results in higher production costs and CO₂ emissions than necessary. Therefore, the following chapter is about heat integration within the process.

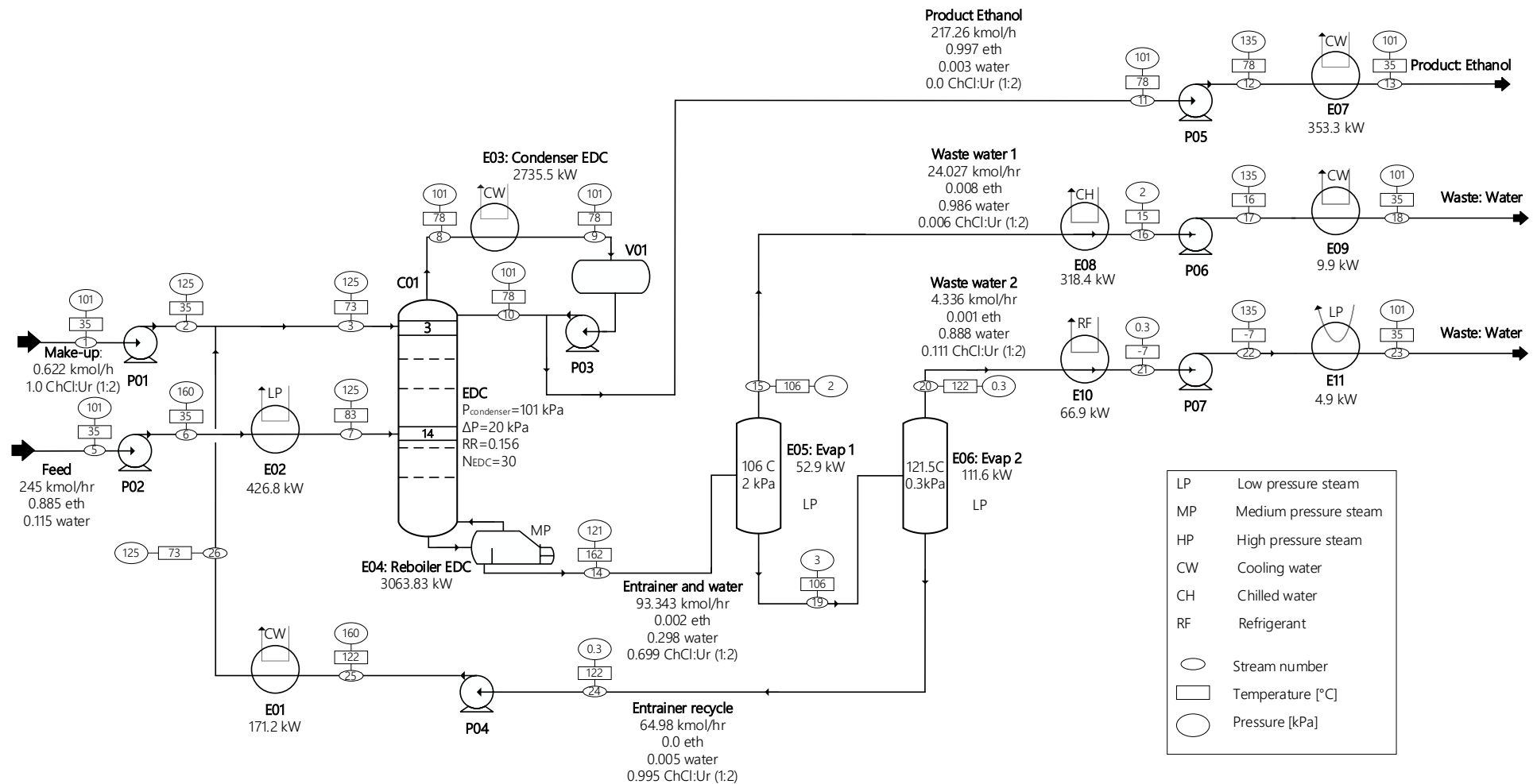


Figure 19: Process flowsheet and additional information regarding flows, process design variables and heat exchanger duties for the base case design involving two evaporators and the EDC operating at 1 atm. The compositions are given in mole fractions.

6 Heat Integration

Heat exchangers between process streams are implemented into the optimised processes of the previous chapter. Eventually, the flow diagrams that were shown in the last chapter are modified by process heat exchangers and are given newly at the end of this chapter.

6.1 Energy Savings & Composite Curves

The following analysis is exemplary for the 1 atm EDC base case involving only evaporators, where the flowsheet was given by Figure 19. For this process, approximately 750 kW can be saved by heat integration, which can be seen at the overall composite curve of the entire process (see Figure A 25). However, for achieving an economical design, there must be a balance between the capital costs in terms of the number of heat exchangers and the operating costs in terms of utility requirements. Many heat exchangers in this process have only minimal duties (see process flowsheet Figure 19). Implementing an additional process heat exchanger is, in many cases not profitable. Hence, the Aspen Plus Energy Analyser tool was used to give the most economical heat integration solutions, that have payback periods of less than five years. The result of this can be seen in the Appendix in *Table A 47*, in which not only the energy savings are given but also the payback period and energy costs savings according to Aspen Plus. Thus, the options with a payback period of fewer than five years were considered, which are explained in the following (A 3).

The two economical solutions are heat integration between the feed as cold stream, and the distillate and entrainer recycle as hot streams. This is shown in Figure 20 in terms of the composite curves. It can be seen that the entrainer can be completely cooled down without any need of an additional cooler. However, the distillate needs an extra cooler with a duty of ~90 kW (Q_{cmin}). The feed can be fully heated up and does not need an additional heater. In total, a duty of ~425 kW is saved in utilities.

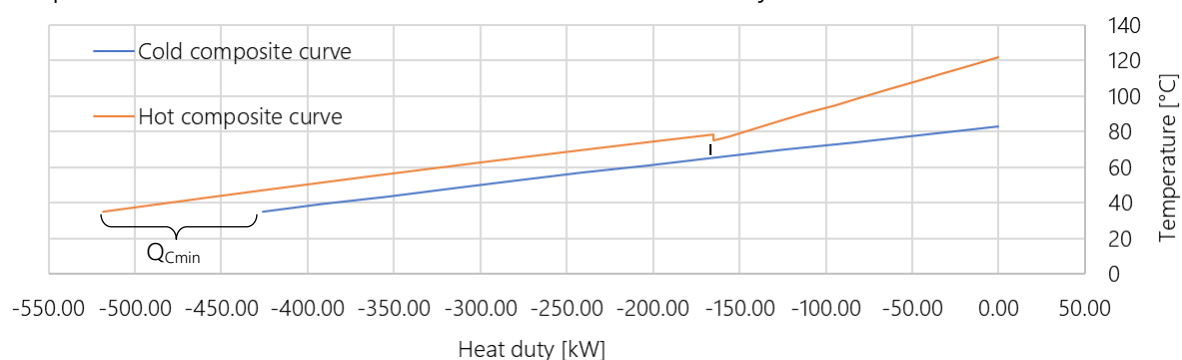


Figure 20: Composite curves of the integrated process part. The hot composite curve (orange) consists of distillate cooling (left part: E07) and entrainer recycle cooling (right part: E01), and the cold composite curve is the main feed (E02). Shown are also the pinch (black line) and the minimum of cold utilities (Q_{cmin}).

The corresponding process that was previously shown in Figure 19 has other heat exchangers. Heat integration is possible with the condenser of the EDC. However, this would have a payback time of over five years (see *Table A 47*). The corresponding composite curves for these possible but small energy savings are also shown in Figure A 26 in the appendix. The possible energy savings and total energy that is saved in utilities by heat integration are summarized below in Table 3 for all base case designs. In the following, the other base case designs are briefly explained. Additional information and details can be found in the appendix.

Table 3: The energy savings in kW and as a percentage of the overall energy requirements for the four base case designs.

Base case design	Possible Energy Savings [kW]	Integrated Energy Savings [kW]
2 Evaporators, EDC 101 kPa	~550	428
2 Evaporators, EDC 14 kPa	~300	205
Stripping, EDC 101 kPa	~450	403
Stripping, EDC 14 kPa	~500	397

As can be seen in Figure 3, fewer utility savings are possible for the 2 evaporators base case design with the EDC operating at 14 kPa. The reason for that is that the distillate leaves the EDC already at 35°C because of the pressure reduction. Therefore, this stream cannot be used to heat the main feed, and solely the entrainer recycle is used for this aim. Consequently, there is much less heat integration possible (see the composite curve in Figure A 27 and solutions in Table A 48). The composite curve for the applied heat integration is shown in Figure A 28.

In the base case design involving the stripping column and EDC at 1 atm, the entrainer recycle that leaves the stripping column is not able to supply as much heat as for the base cases before. The reason for that is that it is already close to its target temperature (E01: ~55 kW). Heat integration is done with the product recycle instead of the feed (see composite curve Figure A 31 ~55kW). No additional heater or cooler is implemented as only a small additional duty is required that can be supplied by the reboiler. As the evaporator is designed at a much higher pressure than for the 2 evaporator base cases (see methodology Figure A 3), the vapour wastewater can be used for heat integration with the main feed. The vapour can be fully condensed without a need of an extra cooler (see composite curve Figure A 30). However, the feed still needs 80kW of heating which cannot be supplied profitably by any other process stream. As the EDC reboiler needs MP steam (see chapter 7.2), it is more profitable to add a further pre-heater that can use LP steam [69]. The base case design of the stripping regeneration and an EDC operating at 14kPa is very similar than the case before. As can be seen in Table 3, for both base case designs, 400 kW are saved in utilities.

6.2 Heat-Integrated Aspen Flow Sheets & Process Stream Summaries

In Figure 21, the heat integrated process flow diagram, including additional information such as heat exchanger duties, is given for the 2 evaporator base case design with the EDC operating at atmospheric pressure. As can be seen, by the comparison between the flowsheet shown in Figure 19, E01, E02, and E07 are used for heat integration. As stated above the feed can be fully heated to the target temperature without the need for an extra heat exchanger. Similarly, no additional cooler is required for the entrainer recycle. The heat integrated Aspen Plus flowsheets are shown for the other base case designs in the appendix in Figure A 32, Figure A 33 and Figure A 34. Process stream summaries are given for all base case designs in Table A 49 to Table A 52.

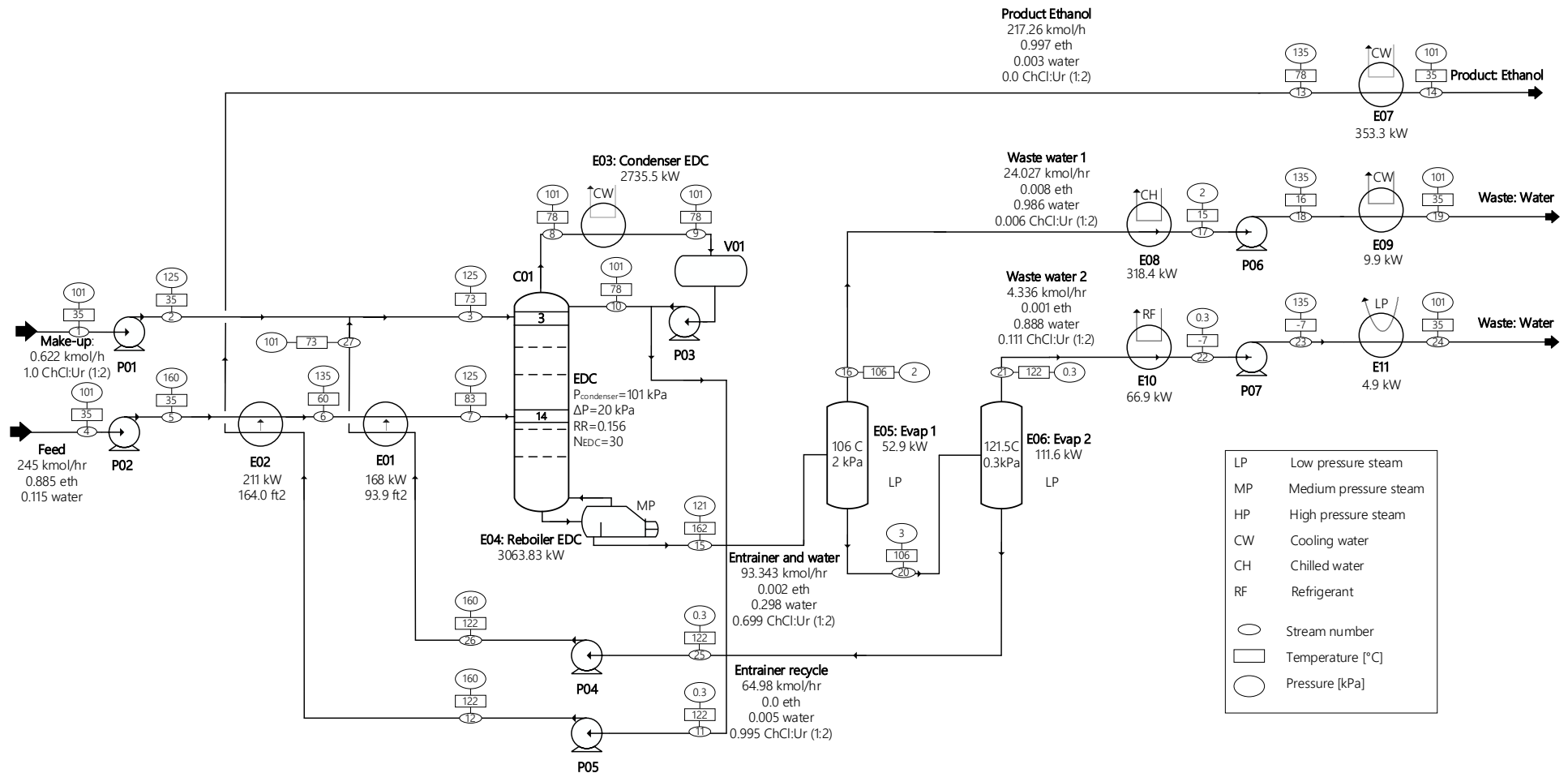


Figure 21: Process flowsheet and additional information regarding flows, process design variables and heat exchanger duties for the base case design involving two evaporators and the EDC operating at 1 atm after applying heat integration. The compositions are given in mole fractions.

7 Preparations for the Assessments

As described, the assessment is not only done in terms of energy requirements but also from an economic perspective. For the final evaluation of both, base case designs and the extractive distillation processes with DESs, the equipment has to be specified to a certain degree, a utility summary is required, and the economic method has to be known. Those preparations are given in the following.

7.1 Equipment Specifications

This chapter will explain the choices made in the equipment design. These choices were made with heuristics given in Seider *et al.* (2006) or Turton *et al.* (2019), which are further added to the heuristics Table A 2 [56, 65]. It is important to note that the equipment design limited to the needed characteristics for the assessments.

7.1.1 Separation Towers

There are two different columns; the EDC and the stripping column. For the economic analysis, the type as well as the dimensions of the column, need to be determined.

Concerning the type of the column, either packed or trayed columns are used for the distillation and stripping column. The mass transfer area for trays is provided by the gas bubbles, while for packed columns it is created through the liquid coating of the surface and vapour passing it countercurrent. Tray columns are easier to clean than packed columns which makes them more suitable for fouling-prone systems. Also, the potential flow maldistribution that might occur for packings because of the uneven liquid distribution across the cross-section is less likely to happen. Packed columns, on the other hand, are characterised by a lower pressure drop and might therefore be especially beneficial for vacuum operations. Also, for corrosive and foaming systems or systems when a low liquid hold-up is required, packings may be advantageous [56, 65]. The final decision for packed or trayed columns can only be made in consideration of many factors and at a stage with more experimental data. At this stage, it is sufficient to choose a trayed column, as according to Seider *et al.* (2006), it is usually preferred for initial phases (C 20) [56]. Because of the liquid maldistribution, trayed columns are also preferred for diameters of more than 0.9 meter, which is the case for all base case designs (see below). Moreover, the stripping column operating under vacuum is very short so that the pressure drop is not necessary a decision factor. The simplest and least expensive tray type with the lowest pressure drop are sieve trays, which therefore chosen (C 21). According to H 11, the diameter of the sieve tray should be 0.6 cm.

Concerning the dimensions of the column, the tower height, diameter, wall thickness and weight are required for the economic assessment. As the number of trays is set, the height and tangent to tangent length can be calculated with the tray spacing. According to H 12, the tray spacing is 0.5 meters and at the space at the top and bottom 1.2 and 1.8 meters, respectively. The method for determining the diameter is based on avoiding flooding and weeping in the column. It contains the calculation of the flooding capacity factor, the flooding velocity and the active area. As those characteristics are different on each tray, the calculation is done by Aspen Plus by the tray sizing tool where the operating range is set to 80% of flooding and the active area amounts 90% (H 13). A diameter is found, and it is checked by Aspen tray rating that the flooding parameter is in between 0.4 and 0.8 such that flooding and weeping are avoided (H 13). For the weight of the towers, the wall thickness, design pressure and temperature and the maximum allowable stress are required. The equations for this calculation are taken from Seider

et al. (2006) and given along with the results in Table A 57 for the EDCs for the four base case designs. In Table A 57 and Table A 58, these results are given for the stripping columns for the stripping base cases [56].

For the final evaluation of the processes using DESs, three processes were created for the three separation tasks (see chapter 4.1). The EDC specification of those and the processes of the literature are given in Table A 93, Table A 101, and Table A 106 for separation task 1, 2, and 3, respectively.

7.1.2 Reflux Drums

The reflux drum of the distillation column needs to separate the reflux stream from the product stream continuously and thereby smooth out fluctuations by maintaining its liquid level. For the two different regeneration options, there are two different types of reflux drums needed. The two-evaporator base case design requires a reflux drum to separate the liquid product stream from the liquid reflux stream. For the stripping base case design, the reflux drum separates the vapour from the liquid stream continuously. The required reflux drum dimensions are the same as for the towers.

According to H 14, the reflux drums are horizontal in a cylindrical shape. For the liquid stream separation, the volume of the reflux column V_{ves} can be determined over the liquid flowrate \dot{V}_L ($V_{ves} = \frac{t_{ho}\dot{V}_L}{0.5}$) by assuming a hold-up time t_{ho} of 5 minutes and a fill of 50% (H 15). For the vapour-liquid reflux drum, the diameter D_{ves} is determined starting from the maximum gas velocity u_{gmax} , which can be calculated by the Souder's Brown equation ($u_{gmax} = k_{SB}\sqrt{\frac{\rho_l - \rho_g}{\rho_g}}$). This equation is set equal to the actual velocity of the gas, that can be expressed in terms of the vapour gas flow rate \dot{v}_g divided by the cross-sectional area ($\frac{\dot{v}_g}{A_z}$). Taking an vapor liquid surface angle Θ of 4.429 rad that is calculated over the assumption A 5 that the high alarm liquid level (HHAL) is equal to 0.8 D_{ves} , the cross-sectional area A_z can be expressed in terms of the vessel diameter as follows: $A_z = \frac{D_{ves}^2}{8}(2\pi - \theta - \sin\theta) = 0.3518 D_{ves}^2$. Thus, it can be solved for the diameter of the vessel ($D_{ves} = \sqrt{\frac{\dot{v}_g}{0.3518 u_{gmax}}}$). The optimum length to diameter ratio is three (H 14), such that for both, liquid-liquid reflux drum and vapour-liquid reflux drum, the overall dimensions can be calculated. The same equations as for the tower is required to calculate the vessel weight. However, the vessel thickness is calculated slightly differently as there is no need to account for the effect of wind for huge heights of towers.

The final results for the sizes of the reflux drums are given along with the equations in Table A 62 for the stripping base cases and in Table A 61 for the evaporators base cases. For the above-mentioned final processes using DES and the processes of the literature using ILs and the conventional solvents, the reflux drum dimensions can be found in Table A 95, Table A 103, and Table A 108 for separation task 1,2, and 3, respectively.

7.1.3 Heat Exchangers and Evaporators

The design of a shell-and-tube heat exchanger is an iterative process as the diameters, tube length, tube layout, baffle type and spacing, and the numbers of tube and shell passes influence the heat-transfer coefficients and pressure drops which are on the other hand also required to determine those geometries. Only a simplified procedure is done to obtain the necessary characteristics for the economic assessment. Thus, the use of heuristics is again required, and the heat transfer coefficients need to be approximated in a very simplified manner.

According to H 16, both process and utility heat exchange can be done in a shell-and-tube heat exchanger in countercurrent flow, if the area is above 100 ft². The shell-and-tube heat exchanger design is standardized by the Tubular Exchanger Manufacturers Association (TEMA) [65]. Typically, they are designed as a 16-ft long tube with an outside diameter of ¾-in and a 1-in tube pitch in triangular spacing (H 17). The shell can be designed with different inside diameters which are chosen according to the required area. A floating tube sheet is chosen as the – often occurring – big temperature difference can cause failure for a fixed head (C 22) [65]. According to H 18, the tube side is for fouling, corrosive, scaling, and high-pressure fluids and the shell side for viscous, evaporating or condensing fluids. Thus, cooling water is in the tube side and steam in the shell side. As the refrigerant is at a much higher pressure than the process stream that is condensed after the evaporators, the refrigerant is placed in the tubes [65].

For areas below 100 ft², a double pipe heat exchanger is commonly chosen for process and utility streams that are not evaporating (C 23) [56]. For the reboiler of the EDC, a kettle reboiler is usually chosen [56]. Concerning the evaporator, the specific type has to be determined. Long-tube vertical evaporators (rising film) and horizontal tube evaporators are the most popular choice [56, 65]. Forced circulation and agitated film heat exchangers are for special systems like high viscous solutions and therefore, more expensive [41, 58]. At this stage, it is enough to choose a horizontal evaporator, which can also be revised in terms of experiments at a later stage (C 24).

For the economic analysis, the required area of the heat exchanger is of importance. As the duty can be calculated according to $Q = F U \Delta T_{LM} A$, the area is determined from an energy balance. As can be seen, the correction factor F for the countercurrent flow, the heat transfer coefficient U , and the logarithmic mean temperature difference ΔT_{LM} must be known for this. According to H 19, F can be taken as 0.9 for a conservative estimate [65]. In H 20 the heat transfer coefficients are estimated for different systems. The logarithmic mean temperature difference is usually calculated by $\Delta T_{LM} = \frac{\Delta T_1 - \Delta T_2}{\ln(\frac{\Delta T_1}{\Delta T_2})}$. However, this equation is not correct for curved T-Q lines which happens when the heat capacity changes significantly for the temperature. A curved T-Q line occurs in this process, as streams containing the nonvolatile entrainer are condensed. Therefore, if possible, ΔT_{LM} is taken from Aspen Plus, that calculated this variable numerically.

The calculated areas are given in the equipment summaries in Table A 68 to Table A 71 for the four base case designs. The areas for the non-heat integrated final processes, the heat-integrated final processes and the processes of the literature are given in Table A 114 to Table A 123 in equipment summary tables.

7.1.4 Pumps, Valves and Vacuum System

According to H 21, centrifugal pumps should preferably be used for a flow rate range between 3 and 1135 m³/h. Rotary pumps are less common but can be used for flow rates down to 0.2 m³/h. Next to the type of the pump, the essential characteristics for a pump are the flow rate and the pump head. The pump head can be calculated by $H = \Delta p / \rho_L g$, where Δp is the pressure difference, ρ_L the density of the stream, and g the gravitational acceleration constant.

Concerning the pressure reduction, valves that reduce the pressure to ambient pressure are neglected for the purpose of this project (C 25). Concerning the vacuum system, Seider *et al.* suggest using a liquid ring pump for pressures down to 2 kPa and a steam jet ejector for pressures down to 0.26 kPa (H 22) [56]. The liquid ring pump compresses the vacuum gas to the ambient pressure while the steam jet ejector uses a flow of pressurized steam to remove the vacuum gas [65]. As a vacuum device

with fewer stages is more economical, the lowest stages possible are taken according to the necessary suction pressure [56]. For the base case designs, the following equipment is chosen according to the mentioned heuristics.

- A one-stage liquid ring pump is used for the low-pressure case EDC (14 kPa) and the evaporator of the stripping base cases (45 kPa)
- An oil-sealed liquid ring pump is used for the stripping column (2 kPa), and the first evaporator of the evaporator stripping base cases (2 kPa)
- A three-stage steam jet ejector is used for the second evaporator of the two evaporator base cases (0.3 kPa)

The most important characteristic for defining the costs of the vacuum system is the vapour flowrate to the device. This flowrate is composed of the air that leaks into the equipment and the volatile product. Air leakage W_{air} occurs via gasket joints, fissures in the vessel walls and porous welds. The mass flow rate can be estimated by equation (1), where V is the volume of the equipment and p the operating pressure [42, 56].

$$W_{air} = 5 + V^{0.66} (0.0298 + 0.03088 \ln(p) - 0.0005733 (\ln(p))^2) \quad (1)$$

V in ft^3 , p in $torr$, W in lb/hr

Accompanied by the air, the volatile product further increases the load of the vacuum system. In order to reduce this load and the product loss, the gas should first pass through a precondenser before entering the vacuum equipment. The flowrate of product loss can be estimated by a flash calculation around W_{air} and the total product flow at the temperature of the precondenser. Finally, the flowrate to the vacuum system can be determined by adding both, the air leakage flowrate W_{air} and the product flowrate $W_{product}$.

With this, the required characteristics of the equipment piece are determined, and the results can be found along with the costs in Table A 64 to Table A 67 for the four base case designs. For the final processes that are evaluated and the processes of the literature, these characteristics are given by Table A 97, Table A 105, and Table A 110 for the separation task 1, 2 and 3 respectively.

7.2 Utility Requirements

For the calculation of the utility requirements, the conditions of the utilities have to be known. These conditions are taken from Seider et al (2006) or Turton *et al.* (2019), and they are summarised for steam, cooling water, chilled water and refrigerant in Table A 3, Table A 4, and Table A 5 [56, 65]. Detailed information is given in the methodology in chapter B.3. Near-optimal approach temperatures have already been given in chapter 5.1.1 by H 2.

Regarding the refrigerant, temperature levels are typically used as classification. In this project, a temperature of -13°C is sufficiently low enough for all processes [56]. A suitable refrigerant for this temperature level is ammonia as can be seen by H 9 [65]. The mass flow rate of the refrigerant can be calculated according to equation (19) in the methodology, involving enthalpies of the saturated vapour and liquid [77]. The capacity is calculated according to equation (20), which is based on H 8, stating that a ton of refrigeration is the removal of 127000 kJ/h [65]. Cooling water was preferably used because of the comparably low costs and designed to not exit the heat exchanger with a higher temperature than 40°C according to H 7. In the low-pressure base case design, the upper temperature of the cooling water of the condenser is limited by the optimal approach temperature. Equation (18) is used to calculate the cooling water amount. For heating LP, MP and HP steam is used (Table A 3). According to H 10 also for the steam jet ejector system, MP steam is used to create the vacuum (see chapter 7.1.4). For the steam

jet ejector, equation (17) is used to calculate the amount of steam. For the heaters, the steam flow rate is calculated according to equation (16) involving the enthalpy of evaporation. The hydraulic power for pumps is taken from the aspen simulation (equation (14)). The calculation of the motor power is done by assuming an efficiency of 80% (A 4), which lies within the typical range for centrifugal pumps (see equation (15)) [78]. With this information, the utility requirements can be calculated. The summary of the required utilities for the equipment shown in the Aspen flowsheets are given for the four base case designs by Table A 53 to Table A 56 and for the finalised processes using DESs and the process of the literature using conventional solvents by Table A 77 to Table A 86.

7.3 Total Annual Costs

For the comparison of both, the different base case designs and the final processes with the literature processes, an economic assessment is carried out. For this, the total annual costs (TAC), as a measure for economic goodness, are commonly used to compare several process alternatives. It considers the fixed capital investment C_{TPI} , the total annual production costs C_{AP} as well as a reasonable return on investment (i_{min}) which is taken to 0.2, according to Seider *et al.* (2006) (A 6) [56].

$$C_{TAC} = C_{AP} + i_{min} C_{TPI} \quad (2)$$

Profitability measures such as the net present value or the investor's rate of return are not considered as the purpose at this early stage is only to compare different processes [56]. Sales revenues are also not calculated as only a small part of the ethanol / IPA production process is considered. In the following, the contributions from the total annual production costs and fixed capital investment are explained.

The TAC calculation for the base case designs is given by Table A 76. For the final processes and the processes of the literature, the TAC calculation is shown in Table A 134, Table A 135, and Table A 136 for separation task 1, 2, and 3, respectively.

7.3.1 Total Annual Production Costs

The total annual production costs consist of direct costs and indirect costs such as the operating overhead, property taxes and insurance costs. The direct costs are divided into variable costs such as feedstock costs, utility costs and waste treatment costs and semi-variable costs such as are labour related operations and maintenance costs [79]. In this report, for the total annual production costs, only the annual utility costs are taken into account as only the comparability to the other processes is essential. Usually, the utility costs have a significant contribution to the product selling price, and they might vary for the different base case designs and entrainer usage [56]. The costs for the make-up stream are neglected as a high recovery of above 99% was assumed according to the separation tasks. The cooling utility for the precondenser of the vacuum system is neglected (A 7). As the utility flowrates \dot{m} are given, as explained in chapter 7.2, the utility costs (C_{AP}) can be calculated as follows:

$$C_{AP} = \text{price} \cdot \dot{m} \cdot F_{OP} \quad (3)$$

The factor F_{OP} is the plant operating factor which is chosen according to Seider *et al.* (2006) as $330/365=0.9$ (A 8) [56].

The considered prices for the utilities are given along with the results for all four base cases by Table A 72 to Table A 75 in the appendix. For the final processes with and without heat integration and the processes of the literature, these costs are given in Table A 124 to Table A 126 for separation task 1, Table A 127 to Table A 129 for separation task 2, and Table A 130 to Table A 133 for separation task 3.

7.3.2 Total Capital Investment

The fixed capital investment costs (C_{TPI}) of a plant are a one-time expense for the overall design construction of that plant. It is divided into direct module expenses and indirect module expenses. The lang factor method is used in this project, which applies a factor F_{LTPI} to the free onboard (f.o.b.) purchase costs C_{pi} as can be seen by the formula [56]. The reported accuracy of this method is about 35%.

$$C_{TPI} = 1.05 f_{LTPI} \sum_i \frac{I_i}{I_{bi}} C_{pi} \quad (4)$$

The lang factor f_{LTPI} is a factor to include other direct costs such as costs of installation, piping, control instrumentation, service facilities and buildings and some indirect costs such as supervision, construction, legal expenses, and contingency. The working capital, which is operating costs for the early operation of the plant, is not included. In the case of a fluids processing plant, the lang factor equals 4.74 (A 9) [56]. The equation is multiplied by a factor of 1.05 to account for the delivery of the equipment. By the chemical engineering plant cost index (I) ratio, the equations are updated from the date of Seider *et al.* (2006: $I_{bi}=500$) to 2019 ($I_i=607.5$) [56, 80].

The purchase costs the equipment are calculated based on standard equations described by Seider *et al.* (2006) [56]. For simplicity, and because of the lack of data and cost equations for stainless steel, carbon steel was used for all equipment pieces, which should definitely be revised at a later stage of the project (material factor $F_M=1$) (A 10). The cost equations for calculating the f.o.b. purchase costs are given in Table A 6 for towers, Table A 7 for reflux drums, Table A 8 for heat exchangers, Table A 9 for evaporators and Table A 10 for steam jet ejectors and liquid ring pumps. The precondensers costs are neglected (A 7). All other pumps have been neglected as the powers and size factors are too low to apply the cost equations, and the cost contribution of pumps is generally small (A 11).

The results are given by Table A 58 and Table A 60 for the EDC for the four different base case designs. For the reflux drums, the f.o.b. purchase costs are given by Table A 63. The results for all heat exchangers and evaporators are given by Table A 68 to Table A 71. The vacuum systems costs for the liquid ring pump and steam jet ejector are given for the four base cases by Table A 64 to Table A 67. Overall summaries of the equipment purchase costs for the four base case designs can be found by Table A 68 to Table A 71 in the appendix.

For the final processes and the processes of the literature, the costs of the EDC are given by Table A 94, Table A 102, and Table A 107 of the separation task 1, 2, and 3, respectively. The equipment specification and cost calculation of the SRC of the literature can be found in Table A 98, Table A 99, Table A 111, and Table A 112. The f.o.b. purchase costs of the reflux drums are given by Table A 96, Table A 104, and Table A 109 for vacuum system 1, 2, and 3, respectively. The vacuum systems costs for the liquid ring pump and steam jet ejector are given by Table A 97, Table A 105, and Table A 110 for separation system 1, 2, and 3, respectively. The results for all heat exchangers and evaporators are given in the equipment summary and cost summary by Table A 114 to Table A 116 for separation task 1, Table A 117 to Table A 119 for separation task 2 and Table A 120 to Table A 123 for separation task 3.

Summarised all assumptions and costs that contribute to the TAC have been given for the four base case designs and the separation tasks containing simulated processes using the DES and the processes of the literature. In the following chapter, the four base case designs are evaluated in terms of the TAC, and the most economical base case design is selected.

8 Selection of One Base Case Design

In the following, the base case designs are evaluated with respect to the TAC, where the tables have been given in the previous chapter. The total annual production costs are visualised for all four base cases in Figure 22.

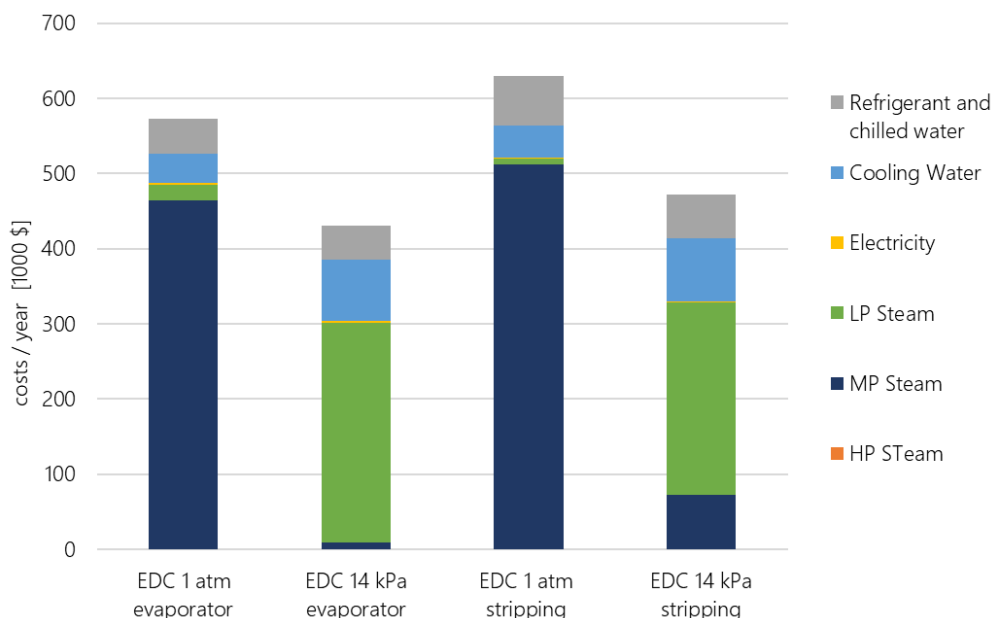


Figure 22: Total annual production costs including refrigerant, cooling water, electricity, LP, MP and HP Steam for the four different base case designs.

Comparing the production costs with each, one can say that the lower pressure cases have expectedly lower operating costs (for reasons see sensitivity analysis chapter 5.2.2). However, more cooling water is required as the temperature difference between entering and leaving cooling water is only 5°C to not violate the minimum approach temperature. Therefore, there might be room for improvement, if the EDC pressure is designed at 25 kPa instead of 14 kPa, such that still LP steam can be taken, but the cooling water difference between the leaving and entering stream amounts to 10°C.

Regarding the differences between the stripping and evaporator base case design, it is understandable that the higher capacity of the EDC - due to the additional recycle in the stripping base case - leads to higher total production costs. One might have expected that the evaporators base case has much higher costs due to the additional energy requirements of the second evaporator. However, as explained in chapter 5.3, the contribution of this energy demand to the overall energy demand is relatively small. Furthermore, one might expect that the refrigeration and chilled water costs are smaller for the stripping base case as the first evaporator is designed at higher pressures to use cooling water (see chapter B.1.4 for optimisation method). However, the stripping overhead stream is much bigger due to the stripping agent, which is why the refrigeration requirement is even higher. The higher pressure of the evaporator in the stripping base case also explains why more MP steam is needed. As these two disadvantages in the stripping base cases are both related to the operating pressure of the regeneration units, it might be a good idea to change the pressures and investigate the impact on the production costs. It might be possible to meet the constraints still when adapting the operating pressures such that:

1. Chilled water can be taken for the small evaporator overhead stream
2. LP steam can be taken for the evaporator
3. Cooling water can be taken for the stripping overhead stream.

With these modifications, the 14 kPa stripping base case has the potential of smaller operating costs than the 14 kPa evaporator base case as less LP steam is required (overhead streams of regeneration units do not need heating) and potentially less refrigerant is required. However, due to the higher capacity of the EDC, the difference is expected to be marginal.

The f.o.b. purchase costs have been given in 7.3.2, and are visualised in Figure 23.

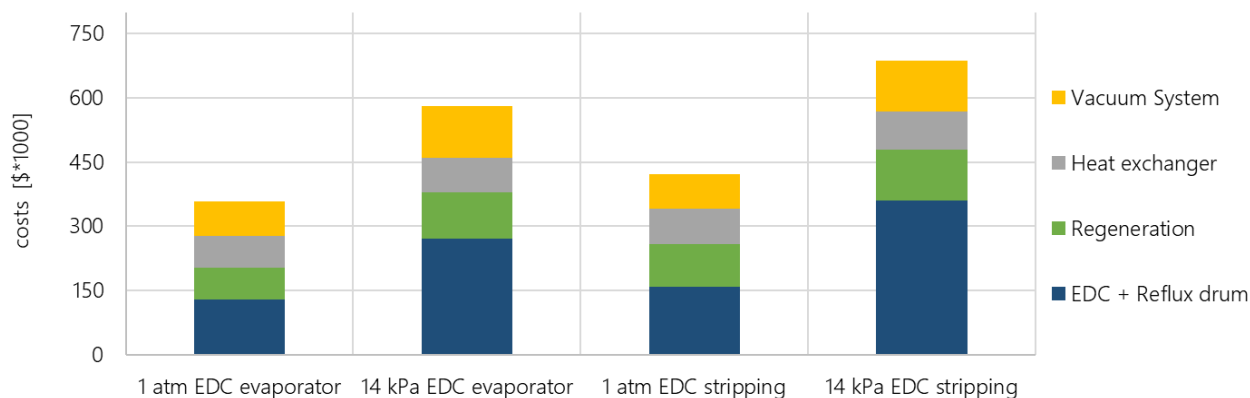


Figure 23: Equipment f.o.b. purchase costs in 10^3 \$ such as the vacuum system, heat exchanger regeneration and EDC costs for the four base case designs.

In Figure 23, it can be seen that the capital costs are expectedly higher for base cases with the EDC operating under vacuum. This has two main reasons:

1. Major effect: Addition EDC costs because of a bigger wall thickness
2. Minor effect: Costs for the liquid ring pump to create the vacuum of the EDC

When comparing the stripping column base case to the evaporators base case, one can see that the stripping base cases are more expensive. Looking in more detail reveals that the evaporator base case design has much lower costs for the EDC and the regeneration. The EDC of the stripping base case has a larger diameter and height because of the higher capacity.

A final selection for one base case design cannot be made without combining both the annual production costs as well as the total permanent investment costs, which gives the total annual costs (see chapter 7.3). The results for the total annual costs are visualised in Figure 24, in which the total capital investment times the rate of return and the annual production costs can be seen for all four base case designs.

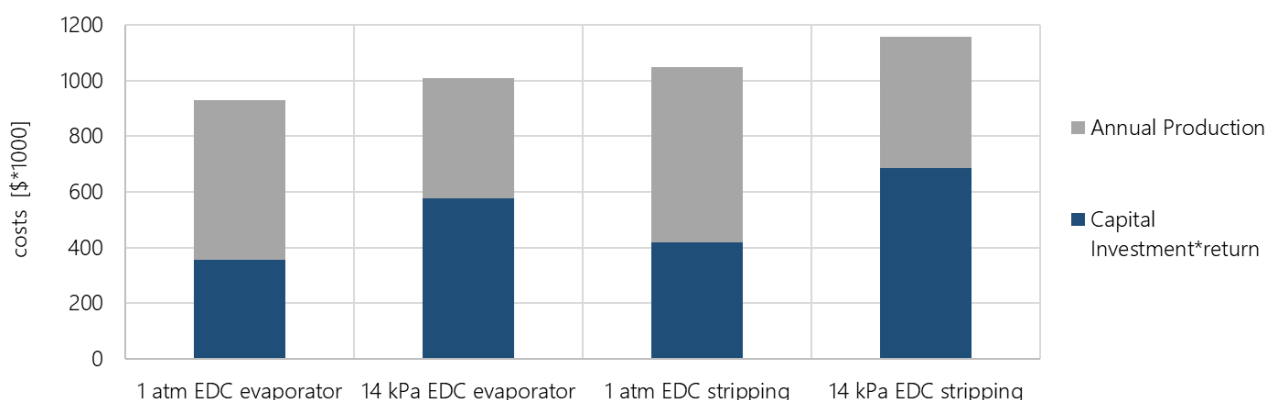


Figure 24: Total annual investment in 10^3 \$ for the four base case designs.

Concerning the base case designs of different EDC pressures, one can observe that the costs are higher for the vacuum operation. Because of the high capital investment, the ordinary vacuum distillation is usually done in only particular circumstances, for example, for thermal sensitive compounds [81]. Also, in this extractive distillation under vacuum, the added advantage of a smaller entrainer amount can still not

outweigh the disadvantages. However, it should be noted that the VLE measurements in the literature have been conducted only at atmospheric pressure. Potentially, the effect of a pressure reduction on the required entrainer amount is more significant than simulated by Aspen Plus. Moreover, as explained above, the process design of the vacuum extractive distillation can be further improved. In conclusion, the vacuum EDC base cases are rejected for this initial evaluation of the DES. Still, it should be kept in mind that in case of a significant entrainer amount reduction, it could potentially be beneficial (C 16).

Regarding the stripping column base cases, it is visible that the higher capacity makes the process disadvantageous for both capital and operating costs. Moreover, the simplicity of the evaporator base case simulation is another reason for selecting this base case design (C 15). With this decision, all separation tasks can be designed with the EDC operating at 1 atm and 2 evaporators as the DES regeneration option. It has to be mentioned that for the separation of IPA and water, the same results are obtained with the evaporators base case being less costly.

9 Process Flow Diagram & Process Stream Summary

It was decided for one process option in the previous chapter. The main goal is eventually to compare this process with the processes of the literature using a conventional solvent or an IL. For a fair comparison, for each different publication, a separation task had been established in chapter 4.1, that adapted feed flowrates and compositions, and purity and recovery constraints to the processes of the literature. Moreover, as the TAC was calculated of both, the processes of the literature, as well as the simulated processes using DESs (see chapter 7.3), heat exchangers and temperatures must match. Else, the comparability of capital and operating costs is not guaranteed. Therefore, it is essential to add certain heat exchangers in the processes of the literature, adapt temperatures and take out the implemented heat integration of the simulated processes, as the processes of the literature did not apply heat integration either. This is shown exemplarily in the following two process flow diagrams: the extractive distillation of IPA and water simulated by Ma *et al.* (2019) using the IL $[\text{Emim}]^+[\text{N}(\text{CN})_2]^-$, and the simulated process using the DES $\text{ChCl}:\text{TEG}$ (1:3) (see Figure 25 and Figure 26 on the next page) [36]. The additional benefit of heat integration is shown by further designed processes with heat integration which is shown in the appendix by Figure A 44 for this example.

As can be seen on the process of the literature in Figure 25, heat exchangers and areas of all evaporators, heat exchangers and the reboiler are added in blue. All data required for the economic assessment as described by chapter 7.3 is added if necessary and calculated with the given formulas (see chapter 7.3.2). The diameter of the column was approximated by Aspen Plus assuming the same flowrates in the column and number of stages with the DES instead of the IL. Flowrates of the vacuum system have been given by Ma *et al.* (2019) [36]. Untypically, the feed enters the EDC at 30°C and is not preheated. Also, the EDC is simplified by assuming no pressure drop. Thus, the simulated process using the DES is also designed with the exact same conditions for guaranteeing comparability, as can be seen in Figure 26.

Comparing both processes with each other, one can observe that the EDC reboiler duty is 300 kW lower for the process using DES. However, the process of the literature shows a reduced regeneration energy requirement by 150 kW. Reasons for this are given in the following chapter 10.1, where the selectivities of the different entrainers are evaluated. Overall, it can be seen that the process using DES shows lower energy requirements and entrainer amounts, both of which are discussed in chapter 10.2.

The process flow diagrams for the other processes of the literature are given by Figure A 35, Figure A 38, and Figure A 41 in the appendix for separation task 1, 2 and 3, respectively. Similarly, it is marked in blue when equipment pieces or characteristics such as heat exchangers, heat exchanger areas, pumps, duties, temperatures and diameters are added because they were missing in the literature. The matching process flow diagrams of the simulated process using DES are given by Figure A 36, Figure A 39, Figure A 43 for separation task 1, 2, and 3, respectively. Process stream summaries are given accordingly (see Table A 87, Table A 89 and Table A 91). Further, simulated heat integrated processes (Figure A 37, Figure A 40, and Figure A 44) and process stream summaries (Table A 88, Table A 90 and Table A 92) are given to state which improvement is possible through heat exchange. Exact information on how the processes have been changed compared to the base case designs and how certain characteristics are obtained for the literature processes are stated along with all process flow diagrams in the appendix (see chapter C.9.2).

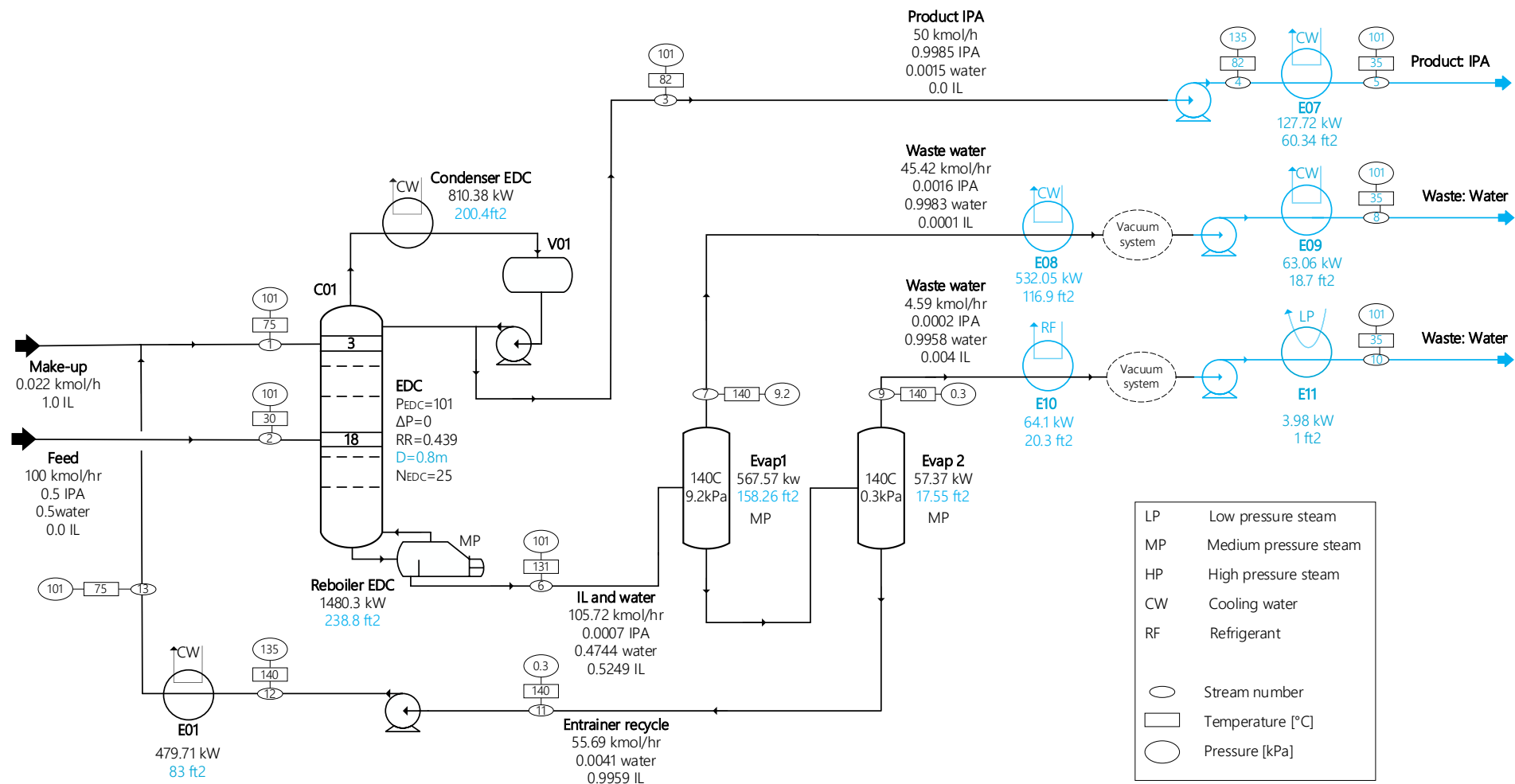


Figure 25: Extractive distillation of IPA and water with the IL $[\text{Emim}]^+[\text{N}(\text{CN})_2]^-$ taken from Ma *et al.* (2019) [36]. Added equipment or equipment characteristics necessary for the economic assessment are marked in blue

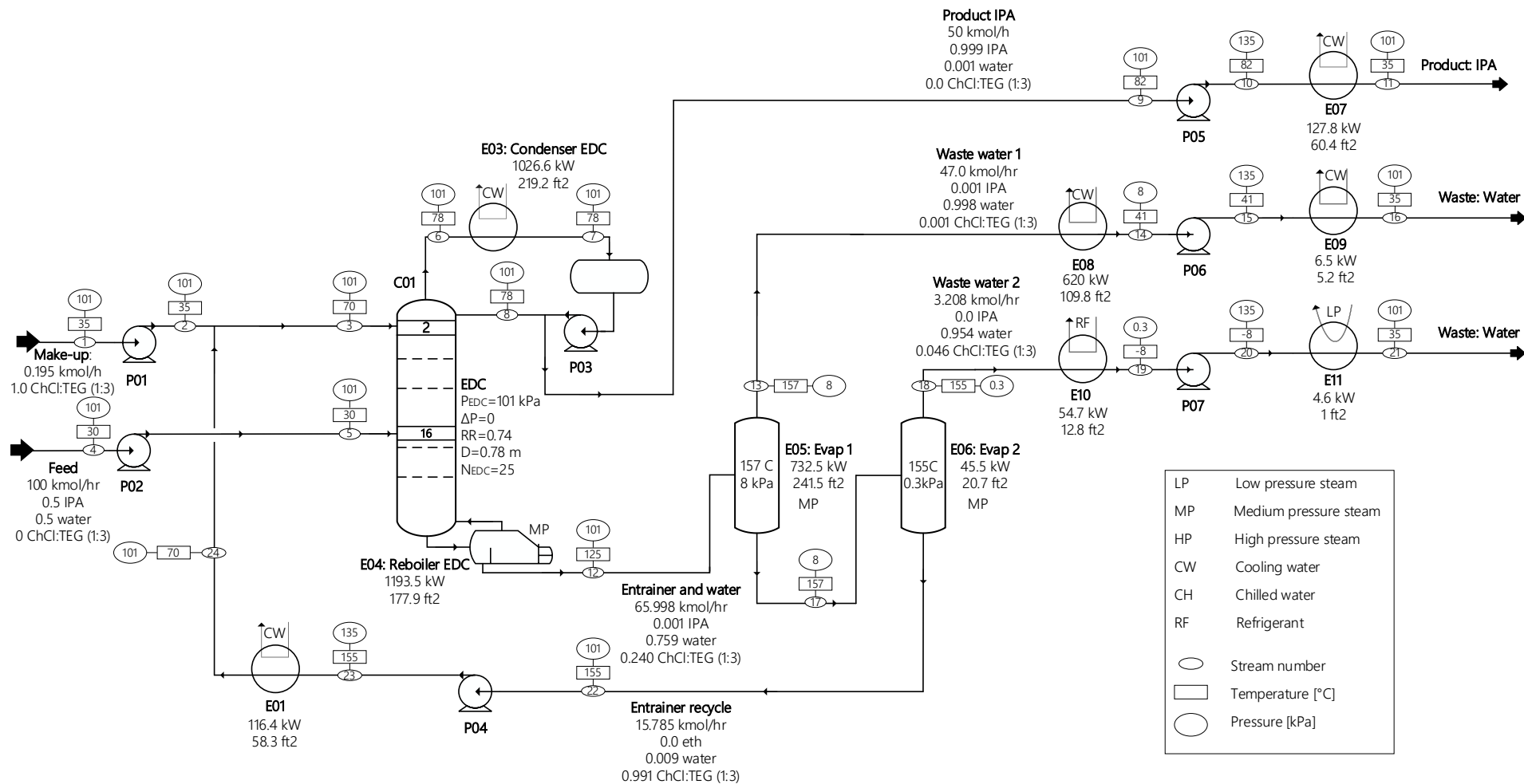


Figure 26: Process flow diagram of the extractive distillation of IPA and water using ChCl:TEG (1:3). The simulation was adapted to match the literature.

10 Evaluation of the Process using DES

As described in chapter B.2.2 in the methodology, there are certain characteristics that an entrainer should have. In this chapter, ILs, the conventional solvents and DESs are first compared in terms of these properties. Subsequently, the literature and simulated DESs processes are evaluated in terms of specific energy requirements and the total annual costs.

10.1 Properties & Characteristics

All investigated entrainers (ILs, EG, DMSO, DESs) are able to break the azeotrope and do not form new azeotropes with the considered systems. They are all heavy entrainers, simplifying the extractive distillation process. Considering the environmental and toxicity aspect, the conventional organic solvents, like EG, have been proven to cause environmental problems. EG has low toxicity, but when it is broken down, cell toxins are formed [1]. For DMSO that is generally stated as green solvent, the low toxicity has been proven [82]. ILs are also often referred to as green solvents due to their low vapour pressure, and non-flammability. However, the toxic and biodegradable aspect has also been questioned [9]. Therefore, one main reason for considering the DESs as alternative entrainer is the green and biodegradable aspect of this solvent. DESs are, in most cases obtained by renewable resources and naturally occurring components. Hence, there are mostly seen as superior green [9, 16]. Gjineci *et al.* (2015) performed a biodegradable assessment of ChCl:Ur (1:2), and ChCl:TEG (1:3), both of which were selected in this report for the two systems (ethanol and water, IPA and water) [17]. By calculating the ratio between the CBOD₅ (oxygen demand by microorganisms for the degradation of the compound within five days) and the UCBOD value (oxygen demand by microorganisms for the total degradation of the compound to CO₂ and water), the group stated that both DESs have a remarkable biodegradability ability (ChCl:Ur (1:2): ~86%, ChCl:TEG (1:3) ~51%) [17]. Thus, DESs seem promising in this aspect as compared to conventional solvents and ILs. It should be noted that the biodegradability ultimately depends on the choice of the selected constituents. A detailed life cycle assessment has to be done for each DESs [83]. Additionally, one criterion is low corrosiveness and chemical and thermal stability. However, as stated in chapter 3.2 and 7.3.2, measurements regarding these characteristics are scarce for DESs. More research has to be done to evaluate DES in terms of those properties.

The effectiveness of an entrainer in extractive distillation processes is often computed by the selectivity, which is widely accepted as the initial solvent selection criterion (see chapter B.2.2) [50]. In chapter 2.3, the most promising DES, ChCl:Ur (1:2), was accordingly selected as entrainer to separate ethanol and water. A selectivity comparison to the conventional entrainer EG and the most studied ILs, [Emim]⁺[BF₄]⁻, [Emim]⁺[N(CN)₂]⁻ and [Emim]⁺[OAc]⁻, as pointed out in chapter 2.2, is shown in Figure 27.

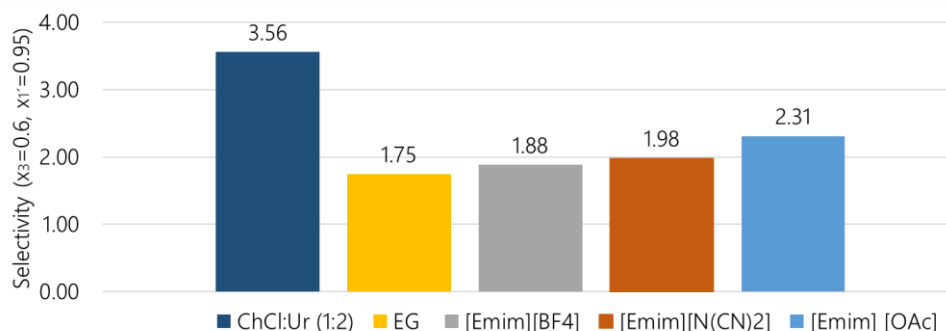


Figure 27: Selectivity at the entrainer mole fraction $x_3=0.6$ and the ethanol mole fraction on entrainer free basis $x_1=0.95$ (see chapter B.2.2.1 for choice of mole fractions). Selectivities are given for ChCl:Ur (1:2), the conventional entrainer EG and the ILs. Values were taken from an Aspen Plus simulation for EG and ChCl:Ur (1:2) and from Ge *et al.* (2008) for the ILs [40].

As can be seen, ChCl:Ur (1:2) shows much higher selectivities than the other entrainers. As explained in chapter 3.3.1, the activity coefficient of ethanol increases and that of water decreases in the presence of ChCl:Ur (1:2) resulting in high selectivity. Contrary, the literature states for ILs that the effect is cancelled out to some extent and causes only a minor increase in the selectivity [21, 40]. This is also supported by Shang *et al.* (2019) stating that the polarity and interaction with water are higher for ChCl:Ur (1:2) than for [Emim]⁺[BF4]⁻ [45].

Another important criterion is the minimum entrainer amount, which does not necessarily follow the same order as for the selectivities due to different molecular weights. One stated disadvantage of certain DESs and ILs is the high molecular weight [43]. Higher molecular weights result in a higher required entrainer amount which ultimately leads to higher viscosities and lower mass transfer rates [43]. However, ChCl:Ur (1:2) has with ~86.6 g/mol one of the lowest molecular weights and is more comparable to EG (~62 g/mol) than to the considered ILs (~170 to 200 g/mol). The minimum entrainer amounts can be found in Figure 28. It is remarkable to see that ChCl:Ur (1:2) breaks the azeotrope with only 0.1 wt%. However, as also reported by Peng *et al.* (2017), the relative volatility stays very low for small weight fractions (below 1.2 up to 10 wt%) [13]. This is the reason why still a large entrainer flowrate is used (see PFD chapter 9). Also important to note is that those results are obtained by a simulation. Experimental results have been taken by Gjineci *et al.* (2015) for a minimum of 5 wt% where the relative volatility was above one still, which prove that the DES is also experimentally the entrainer with the lowest entrainer amount [17].

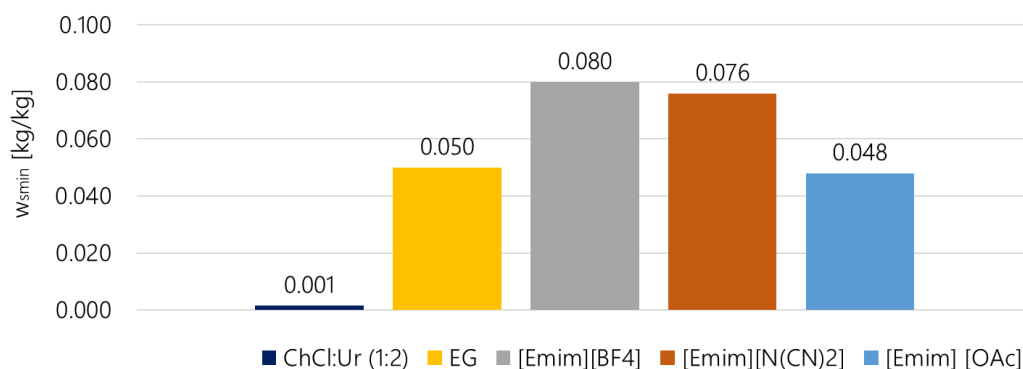


Figure 28: Minimum entrainer amounts w_{smin} for ChCl:Ur (1:2), the conventional entrainer EG and ILs. Values were taken from an Aspen Plus simulation for EG and ChCl:Ur (1:2) and from Ge *et al.* (2008) for the ILs for the boundary condition of the ethanol fraction on entrainer free basis approaching one [40].

For the IPA and water system, very similar results are obtained, in which the chosen DES ChCl:TEG (1:3) (see chapter 2.3.2) shows the highest selectivity and, at the same time the lowest minimum entrainer amount despite the high molecular weight (~147.5 g/mol). The selectivities and minimum entrainer amounts for this system can be found in Figure 29.

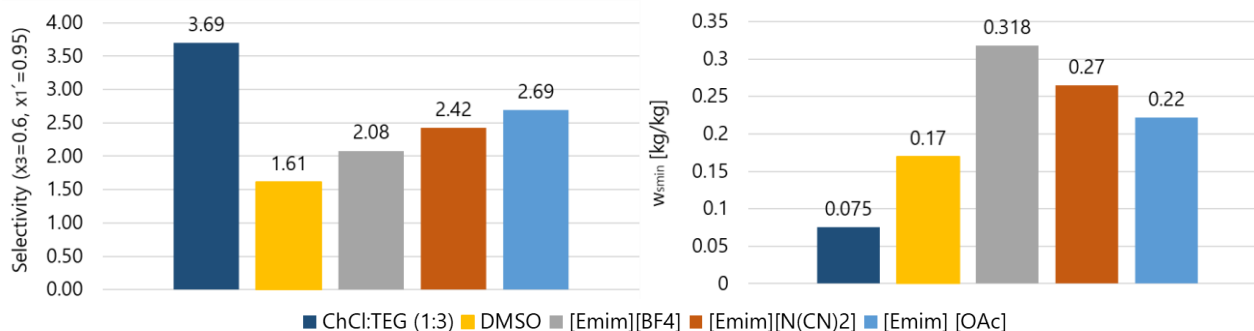


Figure 29: Selectivity (left) and minimum entrainer amount w_{smin} (right) comparison between ChCl:TEG (1:3), the conventional entrainer EG and the ILs. Values were taken from an Aspen Plus simulation for EG and ChCl:Ur (1:2) and from Zhang *et al.* (2007) for the ILs [37].

With this information, it is logical that the selected DESs result in the lowest energy requirements of the EDC. Nevertheless, the total energy requirements and TAC are also impacted by the separability of the DES and water [50]. There is an inevitable trade-off between increasing separability from ethanol and decreasing separability from water. Taking the high interaction between DES and water into consideration, it is explainable why those two components could not be separated by only one evaporator (see chapter 5.2.7) and why it was shown in chapter 9 that the energy requirements for the regeneration of the DES are higher for the separation of IPA and water. Therefore, the next chapter compares the systems in terms of total specific energy requirements and the TAC.

10.2 Specific Energy Requirements & Total Annual Costs

Next to the above-mentioned advantages of DES, it is important to evaluate the process in terms of total energy requirements and TAC. The specific energy requirements are not only decisive for the total costs but also essential for today's necessity towards more sustainable processes. As the chemical industry is significantly contributing to global energy usage and global greenhouse gas emissions, many efforts have been made to reduce the process energy requirements [84]. The specific energy requirements for the steam usage and the improvement of the processes using DES are given in Table 4 for the separation of ethanol and water. The flowsheets for the processes of the literature, the simulated processes using the DES and the heat integrated versions were already given in chapter 9 and the equipment specifications, utility summaries and total annual production costs were provided in chapter 7.

Table 4: Specific energy requirements of the processes of the literature using EG or IL and the simulated process as well as simulated heat integrated (HI) process using the DES ChCl:Ur (1:2) for the separation of ethanol and water. Shown are also the improvement of the DES process compared to the corresponding literature process.

Specific energy requirements steam [MJ / kg product]	IL literature	Aspen Plus simulation		EG literature	Aspen Plus simulation	
	Zhu <i>et al.</i> (2016) [35]	ChCl:Ur (1:2)	ChCl:Ur (1:2) HI	Bastidas <i>et al.</i> (2010) [30]	ChCl:Ur (1:2)	ChCl:Ur (1:2) HI
Reboiler + upstream	1.88	1.28	1.14	1.61	1.25	1.11
Regeneration + downstream	0.16	0.11	0.11	0.20	0.07	0.07
Total [MJ / kg product]	2.04	1.39	1.25	1.82	1.31	1.18
Improvement [%]		31.95%	38.89%		27.58%	35.10%

The specific energy requirements decrease remarkably for the process using the DES as entrainer and even further when applying heat integration (see chapter 6). With the explanation of the previous chapter, the substantial decrease in the reboiler duty is understandable. Due to the strong interaction with water, two evaporators instead of one evaporator had to be taken (see chapter 5.2.7). The expectation that the regeneration energy requirements might be higher due to the increased interaction of the DES with water would only be conditionally right if the same pressures were taken. However, lower pressures of the evaporators, as well as higher temperatures of the EDC bottoms streams, reduce the total energy requirements of the evaporators for this system.

For the IPA system, the use of chilled water after the first evaporator could be avoided by taking higher operating pressures. Hence, the energy requirements of the entrainer regeneration are higher than for the identical sequence of two evaporators used by Ma *et al.* (2019) with the IL as entrainer that showed a lower selectivity than ChCl:TEG (1:3). Very similar results as for the ethanol system are obtained of the comparison with the conventional entrainer DMSO. The potential saving of the process using DMSO as compared to the heat integrated process using the DES is 26%, as shown in Table 5.

Table 5: Specific energy requirements of the processes of the literature processes using DMSO and IL and the simulated process, as well as simulated heat integrated (HI) process using the DES ChCl:TEG (1:3) for the separation of IPA and water. Shown are also the potential savings by implementing the heat integrated process using the DES.

Specific energy requirements steam [MJ / kg product]	Literature processes		Aspen Plus Simulated processes	
	DMSO Ghuge <i>et al.</i> (2017) [31]	IL Ma <i>et al.</i> (2019) [36]	ChCl:TEG (1:3)	ChCl:TEG (1:3) HI
Reboiler + upstream	1.70	1.78	1.46	1.25
Regeneration + downstream	1.27	0.75	0.94	0.94
Total [MJ / kg product]	2.97	2.53	2.40	2.19
Savings potential [%]	26.10%	14.05%	8.57%	

Concluding, the DES as entrainer is improving the conventional process and even the ILs process in terms of specific energy requirements and therefore, also with respect to the carbon footprint. Next to the heat integration, further energetical improvements might be possible as proposed by Kiss *et al.* (2019) and Loy *et al.* (2015) through the introduction of a heat pump assisted EDC or a dividing-wall column as a measure of process intensification [5, 84–86].

It is essential to see how this energy reduction decreases the total annual production costs and how the capital costs behave to make a final conclusion. The results of the TAC for the extractive distillation of ethanol and water and IPA and water can be seen in Figure 30 (see cost tables in chapter 7.3).

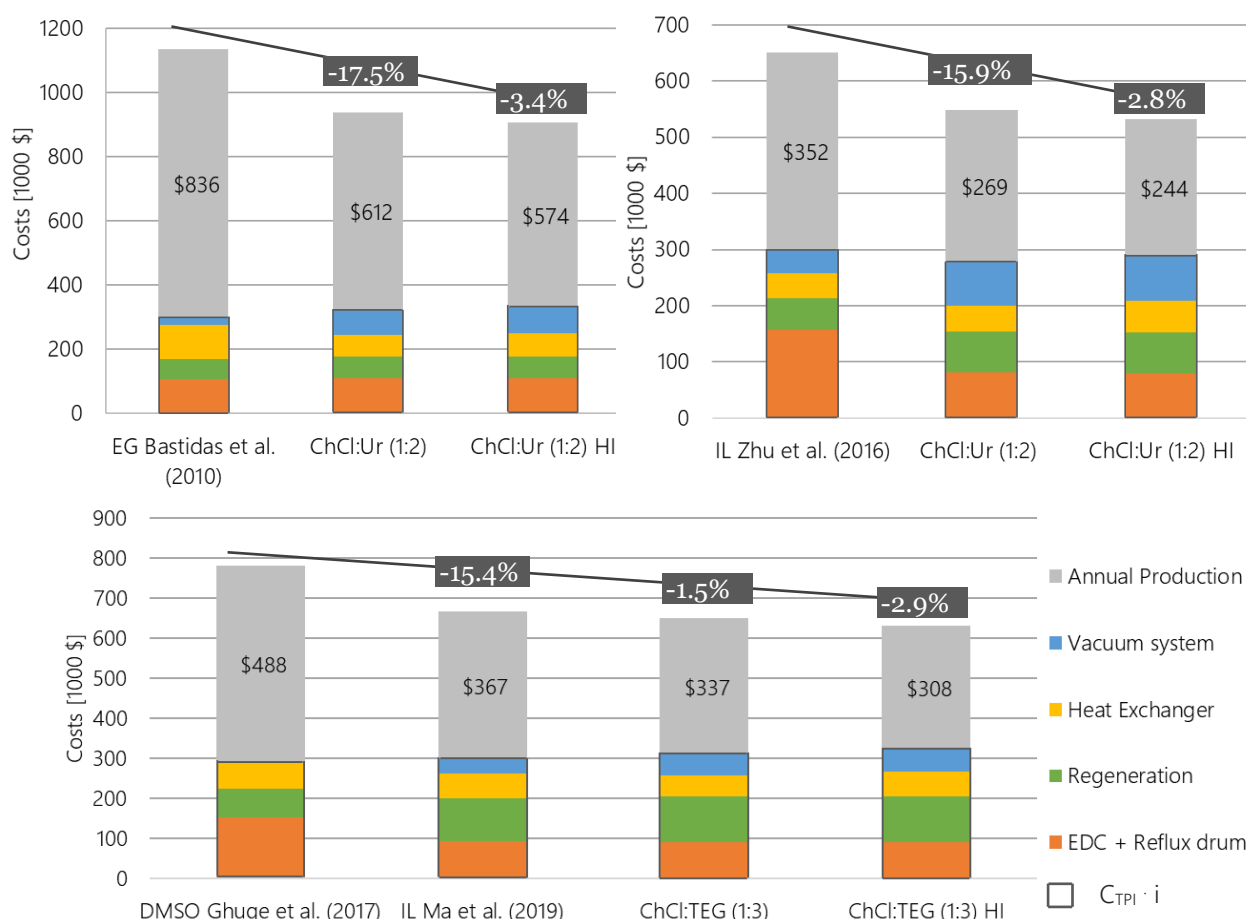


Figure 30: TAC and its relative proportions of the three separation tasks: 1: separation of ethanol and water using EG and ChCl:Ur (1:2) (top left graph) 2: separation of IPA and water using IL and ChCl:Ur (1:2) (top right graph) and 3: separation of IPA and water using, DMSO, IL and ChCl:TEG (1:3) (bottom graph) [30, 31, 35, 36]. The costs of the processes of the literature, and the simulated process, as well as the simulated heat-integrated process using DES, are shown. In the equipment costs, the lang factor (4.74), factor for the delivery of the equipment (1.05), cost index factor (607.5/500) and the return of the investment ($i=0.2$) have already been included.

For the separation of ethanol and water, it can be seen that the annual production costs are considerably lower using the DES and can be further decreased by applying heat integration. As stated above, there are two evaporators used, and the evaporators operate at a higher vacuum degree explaining the higher regeneration and vacuum system equipment costs. Presumably because of the lower separation ability, the EDC using the IL as entrainer needs 18 more stages than the process using DES, which causes the high equipment costs [35]. The separation of IPA and water shows similar results: the process using DES can significantly improve the conventional process. However, because of the explained balance between reboiler duty reductions and the increase in energy requirements of the evaporators, the improvement for the DES compared to the IL is only small. Important to mention is that for this separation of IPA and water with ChCl:TEG (1:3), MP steam was used even though LP steam could have been used according to the simulated temperatures. The reason for this is the inaccuracy of the DES implementation, which simulated the temperatures lower than the experimental data (for data validation, see chapter 3.2). Therefore, the total annual production costs are calculated for the “worst-case”, and much lower costs can be expected for the case that LP steam can indeed be used.

Summarising all possible improvements compared with the non-heat integrated process using DES and the heat integrated process using DES, Table 6 and Table 7 are obtained.

Table 6: The possible savings in the TAC of the processes using the conventional solvent or the IL when considering the process using the DES as well as the heat integrated process using the DES.

Possible TAC savings considering	TAC of the non-heat integrated process using DES		TAC of the heat integrated process using DES	
	Conventional solvent	IL	Conventional solvent	IL
Ethanol and water	17.4%	15.9%	20.2%	18.2%
IPA and water	16.6%	1.5%	19.1%	4.4%

Table 7: The possible savings in the specific energy requirements in steam of the processes using the conventional solvent or the IL when considering the process using the DES as well as the heat integrated process using the DES.

Possible energy savings considering	Specific energy requirements of the non-heat integrated process using DES		Specific energy requirements of the heat integrated process using DES	
	Conventional solvent	IL	Conventional solvent	IL
Ethanol and water	27.6%	32.0%	35.1%	38.9%
IPA and water	20.1%	6.3%	26.9%	14.2%

These summarised result of the tables above make clear that using DES as entrainers decreases the specific energy requirements and TAC compared to conventional organic solvents and ILs. Therefore, DESs are considered as a promising alternative for both conventional organic solvents and ILs.

11 Conclusions & Recommendations

11.1 Conclusions

Two conceptual process case studies were performed using Aspen Plus to investigate whether extractive distillation using DESs is promising as compared to a process using conventional entrainers and ILs. The extractive distillation processes of two systems were investigated: ethanol and water, and IPA and water (chapter 2.1). For the separation of ethanol and water, the processes using the benchmark solvent EG and the IL $[\text{Emim}]^+[\text{BF}_4]^-$ were taken from the literature [30, 35]. Similarly, for IPA and water, the processes using the conventional solvent DMSO and the IL $[\text{Emim}]^+[\text{N}(\text{CN})_2]^-$ were selected [31, 36].

It was shown that ChCl:Ur (1:2) is the best DES for the separation of ethanol and water, as the selectivity comparison showed higher values for this DES (chapter 3). For the separation of IPA and water, ChCl:TEG (1:3) was selected as per the results of a solvent screening found in the literature which determined ChCl:TEG (1:3) to be the optimal DES for this separation [47]. The conceptual design of the extractive distillation processes using DESs involved determination of the process design variables and entrainer regeneration unit through a sensitivity analysis and economic comparison (chapter 5). Interestingly, the results showed that a vacuum operation of the EDC considerably decreases entrainer amounts and, therefore, energy requirements (chapter 5.2.2). However, the comparison in terms of TAC revealed that among other investigated alternatives, the EDC operating at atmospheric pressure and the entrainer recovery consisting of two evaporators are the most economical process options (chapter 8). For a fair comparison between DESs and the organic solvents and ILs of the literature, the simulated processes using DESs and processes of the literature were adapted, and the TAC was calculated for both with equal constraints.

The evaluation of the DES showed that the specific energy requirements of the conventional process using organic solvents could be reduced by 20% and 28% for the separation of the IPA and water, and ethanol and water, respectively. When heat integration was applied, the overall reduction was shown to be even more remarkable: 27% and 35%, respectively. As the energy requirements are closely related to the CO_2 emissions, those results show that the use of DES as entrainers reduces the carbon footprint (chapter 10.2). Due to the smaller operating costs and similar values of the permanent investment costs, the heat-integrated process using DES is also outperforming the conventional process by a decrease in the TAC of 19% and 20% for the separation of the IPA and ethanol system, respectively.

It was found in the literature that the alternative entrainers, ILs, improve the overall energy efficiency [35, 36]. This can again be surpassed by the heat-integrated process using DESs, as they show an energy reduction of 14% and 39% compared to the process using ILs for the IPA and ethanol systems, respectively. Due to the smaller operating costs, the heat-integrated processes using DESs show a lower TAC by 4% and 18% for the IPA and ethanol systems, respectively.

The results of this project show that DESs are not only greener entrainers in terms of their chemical properties but also outperform organic solvents and ILs with respect to both economic attractiveness and energy demand. Overall, answering the research question, the use of a DES as an entrainer considerably reduces the specific energy requirements and TAC of the existing conventional separation processes as well as their alternative using ILs as entrainers.

In the literature, a process design and simulation of the extractive distillation of IPA and water with ChCl:TEG (1:3) and a comparison of the separation of ethanol and water with ChCl:Ur (1:2) with the conventional process cannot be found. Therefore, this work also fills a gap in the literature by confirming the economic viability of using DESs such as ChCl:Ur (1:2) and ChCl:TEG (1:3) as entrainers for extractive

distillation, and provides a template for further exploration of this type. As both separation systems improved upon use of a DES, these results suggest a general improvement of extractive distillation processes using DESs which therefore have an excellent perspective for further research and may assist in the design of more sustainable chemical processes.

11.2 Recommendations

There is an excellent perspective for further research on the topic of DESs as entrainers, not only regarding conceptual process design but also with respect to elementary research on properties. This work was limited by the small number of VLE measurements available in the literature. Related to this, the DES screening in the system of IPA and water was the only screening model that was found [47]. Furthermore, only four separation systems have been investigated, as detailed in chapter 2. It was also observed that the properties of DESs are hugely missing in the literature, as explained in chapter 3.2, where the boiling point of ChCl:TEG (1:3) had to be estimated. The decomposition temperature is a very crucial property, influencing the solvent recovery especially, and has not been reported often. Also, corrosiveness measurements of the system are important for the choice of equipment material. Hence, there is great potential for experiments improving the data collection of the DESs together with the corresponding separation systems.

Regarding the process optimisation for finding the design variable, a sensitivity analysis was sufficient for answering the research question of this project. However, there is room for improvement. In chapter 9, it was stated that the base case design with the EDC operating at 14kPa can be set to slightly higher pressures such that LP steam can still be used with an overall reduced cooling water amount. Also, for the base case design using a stripping column, it was concluded that the process might be improved by reviewing the pressure choice of the stripping column and evaporator. Those retrospective remarks can be avoided, and this process design can be further enhanced by using the multi-objective genetic algorithm, which was mentioned in chapter 4.2 as a more time-consuming but very effective undertaking to find the process design variables [4].

Concerning the process design and equipment choices, most entrainer recovery options had to be dismissed because of lacking experimental data, as explained in chapter 5. Also, a trayed column was chosen, and it was stated that this choice could be revised and confirmed by experiments (chapter 7.1.1). Furthermore, the heat transfer coefficients were approximated, and mass transfer efficiencies were not considered. Mass transfer rates can especially deviate for DES with a higher viscosity [87]. The above-mentioned choices highlight that more experimental work is necessary regarding physical and transport properties to find an optimal design which can be investigated in terms of pilot plant testing. This also aligns with the Stage-Gate Product-Development Process strategy in the book of Seider *et al.* (2006) [56]. To complete the feasibility stage, a controllability assessment has to be carried out, which can be challenging for extractive distillation processes [6]. It was shown that the process with DESs as entrainers is economically attractive, but this does not necessarily mean that it is dynamically operable [45]. Regarding sustainability, the process using DES looks promising so far, however, a complete life cycle assessment is necessary to confirm this [17]. Finally, as mentioned in chapter 10.2, the extractive distillation process using DES can be further improved in terms of energy requirements using technological inventions and process intensification [5, 84, 85, 88, 89].

Concluding, it was observed during this work that the lack of data and information is the biggest drawback of DESs, so far. For a successful industrial application of DESs, more experimental work has to be conducted, predictive models have to be developed and the process design has to enter further stages [50].

12 References

- [1] M. Ravagnani, M. H.M. Reis, R. Maciel Filho, and Wolf-Maciel, "Anhydrous ethanol production by extractive distillation: A solvent case study," *Process Safety and Environmental Protection*, vol. 88, no. 1, pp. 67–73, 2010.
- [2] A. K. Chandra, I. Patraşcu, C. S. Bîldea, and A. A. Kiss, "Eco-efficient Separation of Mono-and Dichloroacetic Acid by Thermally Coupled Extractive Distillation," *Chemical Engineering & Technology*, vol. 43, no. 12, Pages 2403–2417, 2020.
- [3] T. Mahdi, A. Ahmad, M. M. Nasef, and A. Ripin, "State-of-the-Art Technologies for Separation of Azeotropic Mixtures," *Separation & Purification Reviews*, vol. 44, no. 4, pp. 308–330, 2015.
- [4] Q. Pan, X. Shang, J. Li, S. Ma, L. Li, and L. Sun, "Energy-efficient separation process and control scheme for extractive distillation of ethanol-water using deep eutectic solvent," *Separation and Purification Technology*, vol. 219, pp. 113–126, 2019.
- [5] A. A. Kiss and R. M. Ignat, "Innovative single step bioethanol dehydration in an extractive dividing-wall column," *Separation and Purification Technology*, vol. 98, pp. 290–297, 2012.
- [6] S. Brüggemann and W. Marquardt, "Shortcut methods for nonideal multicomponent distillation: 3. Extractive distillation columns," *AIChE J.*, vol. 50, no. 6, pp. 1129–1149, 2004.
- [7] Y. Marcus, Ed., *Deep Eutectic Solvents*. Cham: Springer International Publishing, 2019.
- [8] S. Ma, Y. Hou, Y. Sun, J. Li, Y. Li, and L. Sun, "Simulation and experiment for ethanol dehydration using low transition temperature mixtures (LTTMs) as entrainers," *Chemical Engineering and Processing - Process Intensification*, vol. 121, pp. 71–80, 2017.
- [9] George Wypych, Ed., *Handbook of Solvents: Use, Health, and Environment*, 3rd ed.: ChemTech Publishing, 2019.
- [10] Z. Lei, C. Dai, J. Zhu, and B. Chen, "Extractive distillation with ionic liquids: A review," *AIChE J.*, vol. 60, no. 9, pp. 3312–3329, 2014.
- [11] Y. Zhang, J. Fang, and L. Zhang, "Isobaric Vapor–Liquid Equilibria for the Quaternary System Water + Ethanol + Ethylene Glycol + Choline Chloride and the Ternary System Water + Ethanol + Choline Chloride at 101.3 kPa," *J. Chem. Eng. Data*, vol. 64, no. 6, pp. 2894–2903, 2019.
- [12] M. Seiler, C. Jork, A. Kavarnou, W. Arlt, and R. Hirsch, "Separation of azeotropic mixtures using hyperbranched polymers or ionic liquids," *AIChE J.*, vol. 50, no. 10, pp. 2439–2454, 2004.
- [13] Y. Peng, X. Lu, B. Liu, and J. Zhu, "Separation of azeotropic mixtures (ethanol and water) enhanced by deep eutectic solvents," *Fluid Phase Equilibria*, vol. 448, pp. 128–134, 2017.
- [14] H.-J. Huang, S. Ramaswamy, U. W. Tschirner, and B. V. Ramarao, "A review of separation technologies in current and future biorefineries," *Separation and Purification Technology*, vol. 62, no. 1, pp. 1–21, 2008.
- [15] A. P. Abbott, G. Capper, D. L. Davies, R. K. Rasheed, and V. Tambyrajah, "Novel solvent properties of choline chloride/urea mixtures," *Chemical Communications*, no. 1, pp. 70–71, 2003.
- [16] F. Pena-Pereira and J. Namieśnik, "Ionic liquids and deep eutectic mixtures: sustainable solvents for extraction processes," *ChemSusChem*, vol. 7, no. 7, pp. 1784–1800, 2014.
- [17] N. Gjineci, E. Boli, A. Tzani, A. Detsi, and E. Voutsas, "Separation of the ethanol/water azeotropic mixture using ionic liquids and deep eutectic solvents," *Fluid Phase Equilibria*, vol. 424, pp. 1–7, 2015.
- [18] Aspen Technology Inc, *Aspen Plus V.8.8*.
- [19] A. Bušić *et al.*, "Bioethanol production from renewable raw materials and its separation and purification: A review," *Food technology and biotechnology*, vol. 56, no. 3, pp. 289–311, 2018.
- [20] Mordor Intelligence, *Bioethanol market*. [Online]. Available: <https://www.mordorintelligence.com/industry-reports/bio-ethanol-market> (accessed: Apr. 28 2020).
- [21] A. B. Pereiro, J.M.M. Araújo, J.M.S.S. Esperança, I. M. Marrucho, and L.P.N. Rebelo, "Ionic liquids in separations of azeotropic systems – A review," *The Journal of Chemical Thermodynamics*, vol. 46, pp. 2–28, 2012.

- [22] A. K. Frolkova and V. M. Raeva, "Bioethanol dehydration: State of the art," *Theor Found Chem Eng*, vol. 44, no. 4, pp. 545–556, 2010.
- [23] L. M. Vane, "Separation technologies for the recovery and dehydration of alcohols from fermentation broths," *Biofuels, Bioproducts and Biorefining*, vol. 2, no. 6, pp. 553–588, 2008.
- [24] A. Meirelles, S. Weiss, and H. Herfurth, "Ethanol dehydration by extractive distillation," *Journal of Chemical Technology & Biotechnology*, vol. 53, no. 2, pp. 181–188, 1992.
- [25] D. De, M. Siva Naga Sai, V. Aniya, K. Naga Jyothi, and B. Satyavathi, "Economic and environmental impact assessment of extractive distillation with renewable entrainers for reprocessing aqueous 2-Propanol," *Chemical Engineering and Processing - Process Intensification*, vol. 143, p. 107616, 2019.
- [26] S. Arifin and I.-L. Chien, "Design and Control of an Isopropyl Alcohol Dehydration Process via Extractive Distillation Using Dimethyl Sulfoxide as an Entrainer," *Ind. Eng. Chem. Res.*, vol. 47, no. 3, pp. 790–803, 2008.
- [27] N. R. Rodriguez and M. C. Kroon, "Isopropanol dehydration via extractive distillation using low transition temperature mixtures as entrainers," *The Journal of Chemical Thermodynamics*, vol. 85, pp. 216–221, 2014.
- [28] Chen, Hung-Hsing, Meng-Kai Chen, and I-Lung Chien, Ed., *Using [EMIM][OAC] as entrainer for isopropyl alcohol dehydration via extractive distillation*: IEEE, 2017.
- [29] L. Zhang, Z. Zhang, D. Shen, and M. Lan, "2-Propanol Dehydration via Extractive Distillation Using a Renewable Glycerol–Choline Chloride Deep Eutectic Solvent: Vapor–Liquid Equilibrium," *J. Chem. Eng. Data*, vol. 62, no. 2, pp. 872–877, 2017.
- [30] Paola A. Bastidas, Iván D. Gil, Gerardo Rodríguez, Ed., *Comparison of the main ethanol dehydration technologies through process simulation*, 2010.
- [31] P. D. Ghuge, N. A. Mali, and R. S. Sirsam, "Study of the Effect of Operating Parameters on the Extractive Distillation of Isopropyl Alcohol–Water Mixture Using Dimethyl Sulphoxide as an Entrainer," *Indian Chemical Engineer*, vol. 60, no. 2, pp. 141–161, 2017.
- [32] K. Haerens, S. van Deuren, E. Matthijs, and B. van der Bruggen, "Challenges for recycling ionic liquids by using pressure driven membrane processes," *Green Chem.*, vol. 12, no. 12, p. 2182, 2010.
- [33] Z. Lei, C. Li, and B. Chen, "Extractive distillation: A review," *Separation & Purification Reviews*, vol. 32, no. 2, pp. 121–213, 2003.
- [34] V. K. Verma and T. Banerjee, "Ionic liquids as entrainers for water+ethanol, water+2-propanol, and water+THF systems: A quantum chemical approach," *The Journal of Chemical Thermodynamics*, vol. 42, no. 7, pp. 909–919, 2010.
- [35] Z. Zhu, Y. Ri, M. Li, H. Jia, Y. Wang, and Y. Wang, "Extractive distillation for ethanol dehydration using imidazolium-based ionic liquids as solvents," *Chemical Engineering and Processing - Process Intensification*, vol. 109, pp. 190–198, 2016.
- [36] S. Ma, X. Shang, M. Zhu, J. Li, and L. Sun, "Design, optimization and control of extractive distillation for the separation of isopropanol-water using ionic liquids," *Separation and Purification Technology*, vol. 209, pp. 833–850, 2019.
- [37] L. Zhang, J. Han, D. Deng, and J. Ji, "Selection of ionic liquids as entrainers for separation of water and 2-propanol," *Fluid Phase Equilibria*, vol. 255, no. 2, pp. 179–185, 2007.
- [38] Q. Li, F. Xing, Z. Lei, B. Wang, and Q. Chang, "Isobaric Vapor–Liquid Equilibrium for Isopropanol + Water + 1-Ethyl-3-methylimidazolium Tetrafluoroborate," *J. Chem. Eng. Data*, vol. 53, no. 1, pp. 275–279, 2008.
- [39] J. Zhao, C.-C. Dong, C.-X. Li, H. Meng, and Z.-H. Wang, "Isobaric vapor–liquid equilibria for ethanol–water system containing different ionic liquids at atmospheric pressure," *Fluid Phase Equilibria*, vol. 242, no. 2, pp. 147–153, 2006.
- [40] Y. Ge, L. Zhang, X. Yuan, W. Geng, and J. Ji, "Selection of ionic liquids as entrainers for separation of (water+ethanol)," *The Journal of Chemical Thermodynamics*, vol. 40, no. 8, pp. 1248–1252, 2008.

- [41] G. W. Meindersma, E. Quijada-Maldonado, T. A. M. Aelmans, J. P. G. Hernandez, and A. B. de Haan, "Ionic Liquids in Extractive Distillation of Ethanol/Water: From Laboratory to Pilot Plant," vol. 1117, pp. 239–257.
- [42] H.-H. Chen, M.-K. Chen, B.-C. Chen, and I.-L. Chien, "Critical Assessment of Using an Ionic Liquid as Entrainer via Extractive Distillation," *Ind. Eng. Chem. Res.*, vol. 56, no. 27, pp. 7768–7782, 2017.
- [43] N. R. Rodríguez, A. S.B. González, P. M.A. Tijssen, and M. C. Kroon, "Low transition temperature mixtures (LTTMs) as novel entrainers in extractive distillation," *Fluid Phase Equilibria*, vol. 385, pp. 72–78, 2015.
- [44] D. Han and Y. Chen, "Combining the preconcentration column and recovery column for the extractive distillation of ethanol dehydration with low transition temperature mixtures as entrainers," *Chemical Engineering and Processing - Process Intensification*, vol. 131, pp. 203–214, 2018.
- [45] X. Shang *et al.*, "Process analysis of extractive distillation for the separation of ethanol–water using deep eutectic solvent as entrainer," *Chemical Engineering Research and Design*, vol. 148, pp. 298–311, 2019.
- [46] L. Zhang, M. Lan, X. Wu, and Y. Zhang, "Vapor–Liquid Equilibria for 2-Propanol Dehydration through Extractive Distillation Using Mixed Solvent of Ethylene Glycol and Choline Chloride," *J. Chem. Eng. Data*, vol. 63, no. 8, pp. 2825–2832, 2018.
- [47] H. Jiang, D. Xu, L. Zhang, Y. Ma, J. Gao, and Y. Wang, "Vapor–Liquid Phase Equilibrium for Separation of Isopropanol from Its Aqueous Solution by Choline Chloride-Based Deep Eutectic Solvent Selected by COSMO-SAC Model," *J. Chem. Eng. Data*, vol. 64, no. 4, pp. 1338–1348, 2019.
- [48] W. CHEN, Z. XUE, J. WANG, J. JIANG, X. ZHAO, and T. MU, "Investigation on the Thermal Stability of Deep Eutectic Solvents," *Acta Physico-Chimica Sinica*, vol. 34, no. 8, pp. 904–911, 2018.
- [49] N. Delgado-Mellado *et al.*, "Thermal stability of choline chloride deep eutectic solvents by TGA/FTIR-ATR analysis," *Journal of Molecular Liquids*, vol. 260, pp. 37–43, 2018.
- [50] J. G. Hernandez, "Extractive distillation with ionic liquids as solvents: Selection and conceptual process design," 2013.
- [51] Chemistry Libre Texts, *Organic Functional Groups: H-bond donors & H-bond acceptors*. [Online]. Available: <https://chem.libretexts.org/> (accessed: Oct. 1 2020).
- [52] Biology Libre Texts, *Functional Groups*. [Online]. Available: <https://bio.libretexts.org/> (accessed: Oct. 1 2020).
- [53] J. DeRuiter, "Carboxylic acid structure and chemistry: part 1," *Principles of Drug Action*, vol. 1, pp. 1–10, 2005.
- [54] V. Gerbaud, I. Rodriguez-Donis, L. Hegely, P. Lang, F. Denes, and X. You, "Review of extractive distillation. Process design, operation, optimization and control," *Chemical Engineering Research and Design*, vol. 141, pp. 229–271, 2019.
- [55] V. N. Kiva, E. K. Hilmen, and S. Skogestad, "Azeotropic phase equilibrium diagrams: A survey," *Chemical engineering science*, vol. 58, no. 10, pp. 1903–1953, 2003.
- [56] W. D. Seider, D. R. Lewin, J. D. Seader, S. Widagdo, R. Gani, and K. M. Ng, *Product and process design principles: Synthesis, analysis, and evaluation*, 4th ed. New York, Hoboken, NJ: Wiley, 2017.
- [57] M. T.G. Jongmans, J. Trampé, B. Schuur, and A. B. de Haan, "Solute recovery from ionic liquids: A conceptual design study for recovery of styrene monomer from [4-mebupy][BF₄]," *Chemical Engineering and Processing - Process Intensification*, vol. 70, pp. 148–161, 2013.
- [58] M. Seiler, D. Köhler, and W. Arlt, "Hyperbranched polymers: New selective solvents for extractive distillation and solvent extraction," *Separation and Purification Technology*, vol. 30, no. 2, pp. 179–197, 2003.
- [59] N. L. Mai, K. Ahn, and Y.-M. Koo, "Methods for recovery of ionic liquids—A review," *Process Biochemistry*, vol. 49, no. 5, pp. 872–881, 2014.

- [60] X. Peng, Y. Hu, Y. Liu, C. Jin, and H. Lin, "Separation of ionic liquids from dilute aqueous solutions using the method based on CO₂ hydrates," *Journal of Natural Gas Chemistry*, vol. 19, no. 1, pp. 81–85, 2010.
- [61] A. M. Scurto, S. N. V. K. Aki, and J. F. Brennecke, "Carbon dioxide induced separation of ionic liquids and water," *Chemical communications (Cambridge, England)*, no. 5, pp. 572–573, 2003.
- [62] P. Navarro *et al.*, "Stripping Columns to Regenerate Ionic Liquids and Selectively Recover Hydrocarbons Avoiding Vacuum Conditions," *Ind. Eng. Chem. Res.*, vol. 58, no. 44, pp. 20370–20380, 2019.
- [63] C. Zhu, S. Xue, R. Ikram, X. Liu, and M. He, "Experimental study on isobaric molar heat capacities of a deep eutectic solvent: choline chloride+ ethylene glycol," *J. Chem. Eng. Data*, vol. 65, no. 2, pp. 690–695, 2020.
- [64] V. R. Ferro, E. Ruiz, J. de Riva, and J. Palomar, "Introducing process simulation in ionic liquids design/selection for separation processes based on operational and economic criteria through the example of their regeneration," *Separation and Purification Technology*, vol. 97, pp. 195–204, 2012.
- [65] R. Turton, R. C. Bailie, W. B. Whiting, J. A. Shaeiwitz, and D. Bhattacharyya, *Analysis, synthesis, and design of chemical processes*, 2012.
- [66] Digital Refining, *Improving the distillation energy network*. [Online]. Available: www.digitalrefining.com (accessed: Aug. 8 2020).
- [67] I. D. Gil, Am Uyazán, J. L. Aguilar, G. Rodríguez, and La Caicedo, "Separation of ethanol and water by extractive distillation with salt and solvent as entrainer: Process simulation," *Brazilian Journal of Chemical Engineering*, vol. 25, no. 1, pp. 207–215, 2008.
- [68] M. F. Doherty and M. F. Malone, "Conceptual design of distillation systems," McGraw-Hill, 2001.
- [69] W. L. Luyben, *Principles and case studies of simultaneous design*: John Wiley & Sons, 2012.
- [70] W. L. Luyben, "Effect of Tray Pressure Drop on the Trade-off between Trays and Energy," *Ind. Eng. Chem. Res.*, vol. 51, no. 26, pp. 9186–9190, 2012.
- [71] X. You, I. Rodríguez-Donis, and V. Gerbaud, "Low pressure design for reducing energy cost of extractive distillation for separating diisopropyl ether and isopropyl alcohol," *Chemical Engineering Research and Design*, vol. 109, pp. 540–552, 2016.
- [72] A. B. de Haan and H. Bosch, *Industrial separation processes: fundamentals*: Walter de Gruyter, 2013.
- [73] I. Rodríguez-Donis, V. Gerbaud, and X. Joulia, "Thermodynamic Insights on the Feasibility of Homogeneous Batch Extractive Distillation. 1. Azeotropic Mixtures with a Heavy Entrainer," *Ind. Eng. Chem. Res.*, vol. 48, no. 7, pp. 3544–3559, 2009.
- [74] A. Gaurav, F. T.T. Ng, and G. L. Rempel, "A new green process for biodiesel production from waste oils via catalytic distillation using a solid acid catalyst – Modeling, economic and environmental analysis," *Green Energy & Environment*, vol. 1, no. 1, pp. 62–74, 2016.
- [75] Weifeng Shen, "Extension of thermodynamic insights on batch extractive distillation to continuous operation," 2012. [Online]. Available: <https://oatao.univ-toulouse.fr/8058/>
- [76] M. T.G. Jongmans, E. Hermens, M. Raijmakers, J. I.W. Maassen, B. Schuur, and A. B. de Haan, "Conceptual process design of extractive distillation processes for ethylbenzene/styrene separation," *Chemical Engineering Research and Design*, vol. 90, no. 12, pp. 2086–2100, 2012.
- [77] California State Polytechnic University, Prof. Thuan Ne Nguyen, *Thermodynamics 1 Lecture*. [Online]. Available: <https://www.cpp.edu/> (accessed: Nov. 10 2020).
- [78] Neutrium, *Pump power calculation and efficiencies*. [Online]. Available: <https://neutrium.net/> (accessed: Nov. 10 2020).
- [79] U.S. Environmental Protection Agency, *Cost Estimation: Concepts and Methodology*. [Online]. Available: www.epa.gov/ (accessed: Nov. 10 2020).
- [80] Magazine Chemical Engineering, *CE Index 2019*. [Online]. Available: <https://www.chemengonline.com/2019-chemical-engineering-plant-cost-index-annual-average/> (accessed: Nov. 16 2020).

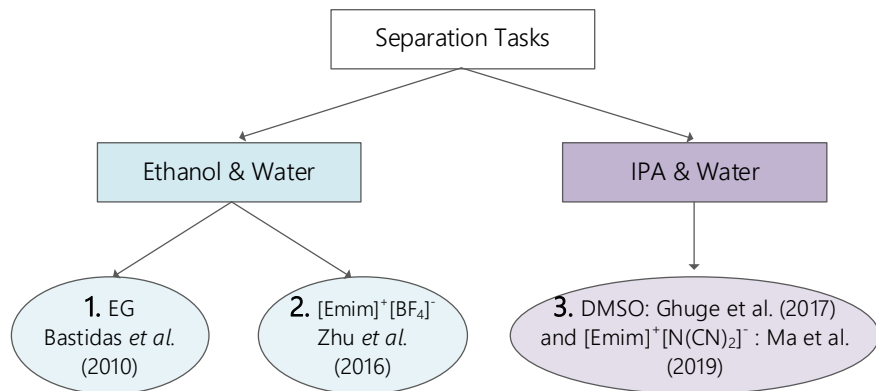
- [81] D. Greene and G. G. Vago, "Properly employ overhead condensers for vacuum columns," *Chemical engineering progress*, vol. 100, no. 2, pp. 38–43, 2004.
- [82] J. Galvao, B. Davis, M. Tilley, E. Normando, M. R. Duchon, and M. F. Cordeiro, "Unexpected low-dose toxicity of the universal solvent DMSO," *FASEB journal : official publication of the Federation of American Societies for Experimental Biology*, vol. 28, no. 3, pp. 1317–1330, 2014.
- [83] M. Francisco, A. van den Bruinhorst, and M. C. Kroon, "Low-transition-temperature mixtures (LTTMs): a new generation of designer solvents," *Angewandte Chemie (International ed. in English)*, vol. 52, no. 11, pp. 3074–3085, 2013.
- [84] A. A. Kiss, "Rethinking energy use for a sustainable chemical industry," *CHEMICAL ENGINEERING*, vol. 76, 2019.
- [85] H. Luo, C. S. Bildea, and A. A. Kiss, "Novel heat-pump-assisted extractive distillation for bioethanol purification," *Ind. Eng. Chem. Res.*, vol. 54, no. 7, pp. 2208–2213, 2015.
- [86] Y. Y. Loy, X. L. Lee, and G. P. Rangaiah, "Bioethanol recovery and purification using extractive dividing-wall column and pressure swing adsorption: An economic comparison after heat integration and optimization," *Separation and Purification Technology*, vol. 149, pp. 413–427, 2015.
- [87] E. E. Quijada-Maldonado, "On mass transfer in extractive distillation with ionic liquids," doi: 10.6100/IR760514.
- [88] S. H. Ha, N. L. Mai, and Y.-M. Koo, "Microwave-assisted separation of ionic liquids from aqueous solution of ionic liquids," *Journal of chromatography. A*, vol. 1217, no. 49, pp. 7638–7641, 2010.
- [89] M. Blahušiak, Š. Schlosser, and J. Cvengroš, "Simulation of a new regeneration process of solvents with ionic liquid by short-path distillation," *Separation and Purification Technology*, vol. 97, pp. 186–194, 2012.
- [90] A. B. Pereiro and A. Rodríguez, "Ternary (liquid+liquid) equilibria of the azeotrope (ethyl acetate+2-propanol) with different ionic liquids at T=298.15K," *The Journal of Chemical Thermodynamics*, vol. 39, no. 12, pp. 1608–1613, 2007, doi: 10.1016/j.jct.2007.04.010.
- [91] Gutiérrez Hernández, JP Juan Pablo, "Extractive distillation with ionic liquids as solvents : selection and conceptual process design,"
- [92] B. T. Safrit, A. W. Westerberg, U. Diwekar, and O. M. Wahnschafft, "Extending Continuous Conventional and Extractive Distillation Feasibility Insights to Batch Distillation," *Ind. Eng. Chem. Res.*, vol. 34, no. 10, pp. 3257–3264, 1995, doi: 10.1021/ie00037a012.
- [93] W. L. Luyben and I.-L. Chien, *Design and control of distillation systems for separating azeotropes*: John Wiley & Sons, 2011.
- [94] J. P. Barrett, "The coefficient of determination—some limitations," *The American Statistician*, vol. 28, no. 1, pp. 19–20, 1974.
- [95] Engineering Toolbox, *Utility characterisation*. [Online]. Available: www.engineeringtoolbox.com (accessed: Nov. 10 2020).
- [96] H. Jiang *et al.*, "Deep eutectic solvents effect on vapor-liquid phase equilibrium for separation of allyl alcohol from its aqueous solution," *Journal of Molecular Liquids*, vol. 279, pp. 524–529, 2019.
- [97] B. Sharma, N. Singh, T. Jain, J. P. Kushwaha, and P. Singh, "Acetonitrile Dehydration via Extractive Distillation Using Low Transition Temperature Mixtures as Entrainers," *J. Chem. Eng. Data*, vol. 63, no. 8, pp. 2921–2930, 2018.
- [98] B. Sharma, N. Singh, and J. P. Kushwaha, "Ammonium-based deep eutectic solvent as entrainer for separation of acetonitrile–water mixture by extractive distillation," *Journal of Molecular Liquids*, vol. 285, pp. 185–193, 2019.
- [99] B. Sharma, N. Singh, and J. P. Kushwaha, "Natural Deep Eutectic Solvent-Mediated Extractive Distillation for Separation of Acetonitrile + Water Azeotropic Mixture," *J. Chem. Eng. Data*, vol. 65, no. 4, pp. 1497–1505, 2020.
- [100] C. BLACK and D. E. DITSLER, "Dehydration of Aqueous Ethanol Mixtures by Extractive Distillation," vol. 115, pp. 1–15, 1974.

- [101] N. Rodriguez Rodriguez, A. van den Bruinhorst, L. J. B. M. Kollau, M. C. Kroon, and K. Binnemans, "Degradation of Deep-Eutectic Solvents Based on Choline Chloride and Carboxylic Acids," *ACS Sustainable Chem. Eng.*, vol. 7, no. 13, pp. 11521–11528, 2019.
- [102] H. Peyrovedin, R. Haghbakhsh, A. R. C. Duarte, and S. Raeissi, "A Global Model for the Estimation of Speeds of Sound in Deep Eutectic Solvents," *Molecules (Basel, Switzerland)*, vol. 25, no. 7, 2020.
- [103] F. S. Mjalli and N. M. Abdel Jabbar, "Acoustic investigation of choline chloride based ionic liquids analogs," *Fluid Phase Equilibria*, vol. 381, pp. 71–76, 2014.
- [104] M. Taherzadeh, R. Haghbakhsh, A. R. C. Duarte, and S. Raeissi, "Estimation of the heat capacities of deep eutectic solvents," *Journal of Molecular Liquids*, vol. 307, p. 112940, 2020.
- [105] F. Chemat, H. Anjum, A. M. Shariff, P. Kumar, and T. Murugesan, "Thermal and physical properties of (Choline chloride+ urea+ l-arginine) deep eutectic solvents," *Journal of Molecular Liquids*, vol. 218, pp. 301–308, 2016.
- [106] C. Florindo, F. S. Oliveira, L. P. N. Rebelo, A. M. Fernandes, and I. M. Marrucho, "Insights into the Synthesis and Properties of Deep Eutectic Solvents Based on Cholinium Chloride and Carboxylic Acids," *ACS Sustainable Chem. Eng.*, vol. 2, no. 10, pp. 2416–2425, 2014.
- [107] A. Yadav, S. Trivedi, R. Rai, and S. Pandey, "Densities and dynamic viscosities of (choline chloride+glycerol) deep eutectic solvent and its aqueous mixtures in the temperature range (283.15–363.15)K," *Fluid Phase Equilibria*, vol. 367, pp. 135–142, 2014.
- [108] F. S. Mjalli and J. Naser, "Viscosity model for choline chloride-based deep eutectic solvents," *Asia-Pac. J. Chem. Eng.*, vol. 10, no. 2, pp. 273–281, 2015.
- [109] A. R. Harifi-Mood and R. Buchner, "Density, viscosity, and conductivity of choline chloride+ ethylene glycol as a deep eutectic solvent and its binary mixtures with dimethyl sulfoxide," *Journal of Molecular Liquids*, vol. 225, pp. 689–695, 2017.
- [110] K. Shahbaz, S. Baroutian, F. S. Mjalli, M. A. Hashim, and I. M. AlNashef, "Densities of ammonium and phosphonium based deep eutectic solvents: Prediction using artificial intelligence and group contribution techniques," *Thermochimica Acta*, vol. 527, pp. 59–66, 2012.
- [111] R. B. Leron and M.-H. Li, "Molar heat capacities of choline chloride-based deep eutectic solvents and their binary mixtures with water," *Thermochimica Acta*, vol. 530, pp. 52–57, 2012.
- [112] M. T. Zafarani-Moattar, H. Shekaari, and F. Ghaffari, "The study of extent of interactions between components of natural deep eutectic solvents in the presence of water through isopiestic investigations," *Journal of Molecular Liquids*, p. 113347, 2020.
- [113] M. T. Zafarani-Moattar, H. Shekaari, and F. Ghaffari, "Vapor–Liquid Equilibria Study of the Aqueous Systems Containing {Choline Chloride + Glucose or Urea} and Their Deep Eutectic Solvents at 298.15 K and 85 kPa," *J. Chem. Eng. Data*, vol. 64, no. 11, pp. 4754–4762, 2019.
- [114] S.-H. Wu, A. R. Caparanga, R. B. Leron, and M.-H. Li, "Vapor pressure of aqueous choline chloride-based deep eutectic solvents (ethaline, glyceline, maline and reline) at 30–70°C," *Thermochimica Acta*, vol. 544, pp. 1–5, 2012.
- [115] S. Faraji, M. Mokhtarpour, E. Behboudi, A. Sadrmousavi, H. Shekaari, and M. T. Zafarani-Moattar, "Vapor–Liquid Equilibria and Computational Study for Aqueous Solutions of Novel Deep Eutectic Solvents (Amino Acid/Lactic Acid) at 298.15 K," *J. Chem. Eng. Data*, 2020.
- [116] L. A. Blanchard, Z. Gu, and J. F. Brennecke, "High-Pressure Phase Behavior of Ionic Liquid/CO₂ Systems," *J. Phys. Chem. B*, vol. 105, no. 12, pp. 2437–2444, 2001.

Appendix A Decisions & Heuristics

Table A 1: Decisions that have been made throughout the whole project and this report. Also given is the explanation and the chapter in which this decision was made.

Options and Choices		Explanation		Occurrence In chapter	Choice in chapter	Choice No.
<div>DES as entrainer</div>	Separation system					
	Acetonitrile & water	✗	<ul style="list-style-type: none">Not many VLE measurements availableNo process with the conventional entrainer available and thus no comparison possible	2		C 1
	Allyl alcohol & water	✗				
	Ethanol & water	✓	<ul style="list-style-type: none">Literature: Classic example and VLE measurements availableKnowledge gap and necessity: Not many process designs in literature	2		C 2
	<ul style="list-style-type: none">ChCl:Ur (1:2) ✓ChCl:EG (1:2) ✗ChCl:GA (1:3) ✗ChCl:TEG (1:3) ✗ChCl:LA (1:2) ✗ChCl:MA (1:1) ✗ChCl:GA (1:1) ✗	<ul style="list-style-type: none">Literature: Have shown a better separation abilityLiterature: Have not been compared to each other yet	2.3.1	2.3.1 & 3.3.3	C 3	
		<ul style="list-style-type: none">Own investigation: Smaller separation ability than ChCl:Ur and ChCl:EG	2.3.1		C 4	
		<ul style="list-style-type: none">Literature: Lower selectivity than ChCl:Ur (1:2)	2.3.1		C 5	
	IPA & water	✓	<ul style="list-style-type: none">Literature: VLE measurements availableKnowledge gap and necessity: Only one process designs in literature	2		C 6
	<ul style="list-style-type: none">ChCl:TEG (1:3) ✓	<ul style="list-style-type: none">Literature: Solvent screening was done and ChCl:TEG showed highest solvent power	2.3.2		C 7	



The results must be comparable to the processes used in industry such that the processes using DES can be evaluated. For this aim, three separation tasks (translating into three processes) had to be created (see black box diagrams *Figure A 16*, *Figure A 17* and *Figure 8*).

For *ethanol and water*, feed conditions and constraints differ in the literature. Therefore, *three* separation tasks have established that match the conditions of Bastidas *et al.* (2010) using EG [30], Pan *et al.* (2019) using ChCl:Ur (1:2) and Zhu *et al.* (2016) using an IL [35].

For *IPA and water*, the constraints and feed flowrate and concentration are the same in the literature. Therefore, *one* separation task is formulated that can be compared to the process of Ghuge *et al.* (2017) [31] using DMSO and Ma *et al.* (2019) using an IL [36].

4.1

C 8

4.1

C 9

Options and Choices	Explanation	Occurrence in chapter	Choice in chapter	Choice No.
<p>Process Options</p> <p>Regeneration Options</p> <p>Extraction</p> <p>Adsorption</p> <p>Induced phase separation</p> <p>Membrane processes</p> <p>Vacuum Distillation</p> <p>Evaporation</p> <p>Stripping</p> <p>2 Regeneration Options</p> <p>EDC 14 kPa</p> <p>EDC 101 kPa</p> <p>EDC 14 kPa</p> <p>EDC 101 kPa</p> <p>2 Pressure Cases</p> <p>Recycle-DES 99 mol%</p> <p>Recycle DES 99.5 mol%</p> <p>Recycle-DES 99 mol%</p> <p>Recycle DES 99.5 mol%</p> <p>Recycle-DES 99 mol%</p> <p>Recycle DES 99.5 mol%</p> <p>Recycle-DES 99 mol%</p> <p>Recycle DES 99.5 mol%</p> <p>2 DES Purity Cases</p>	<ul style="list-style-type: none"> Strong hydrophilia of DES might make process unfeasible Data has to be found 	5.1.2		C 10
	<ul style="list-style-type: none"> Scarce adsorption and desorption data in the literature 	5.1.2		C 11
	<ul style="list-style-type: none"> Maximum reported recovery of DES is 73% - constraints cannot be met 	5.1.2		C 12
	<ul style="list-style-type: none"> Limited purification of DES Large membrane areas 	5.1.2		C 13
	<ul style="list-style-type: none"> Simplicity: evaporation often preferred Possible decomposition 	5.1.2		C 14
	<ul style="list-style-type: none"> By far mostly applied separation techniques for non-volatile entrainer Study stated that evaporation and stripping with product EDC is best [57] 	5.1.2	8	C 15
	<ul style="list-style-type: none"> Vacuum operation base cases are less economical 	5.2.2	8	C 16
	<ul style="list-style-type: none"> It can be found that 99.5% gives slightly lower overall energy requirements 	5.2.3		C 17
Treatment of waste products are not considered in this project	Too detailed for the purpose of this project, can be considered later	5.1.2		C 18
For the two-evaporators-base-case-design, a total condenser of the EDC is chosen, and for the stripping-column-base-case-design, a partial condenser of the EDC is chosen	Total condenser is the common choice except if the product is needed as a gaseous stream (stripping agent)	5.1.3		C 19

A trayed column is chosen for the extractive distillation and stripping unit	<ul style="list-style-type: none"> At this stage sufficient Trayed columns are preferred for diameters over 0.9 m because of possible liquid maldistribution Stripping column has only 5 stages so that pressure drop is not a strong decision criteria 	7.1.1	C 20
Sieve trays are chosen	Simplest and least expensive type of tray	7.1.1	C 21
A floating tubesheet is chosen for the heat exchanger	High mechanical stress for a fixed head when the temperature difference is high	7.1.3	C 22
For areas below 100 ft ² (9.3 m ²), a double pipe heat exchanger is chosen. For areas above, a shell and tube heat exchanger is chosen. As reboiler, a kettle reboiler is chosen.	Typical choice according to heuristic H 16	7.1.3	C 23
A horizontal tube evaporator is chosen	<ul style="list-style-type: none"> At this stage sufficient and common choice Agitated film and forced circulation heat exchangers are for special systems and more expensive 	7.1.3	C 24
Valves are neglected as equipment	Too detailed process design for the purpose of this project and an only small contribution to economics	7.1.4	C 25

Table A 2: Listed heuristics and assumptions, the reasoning and application within this project. Heuristics were taken from Seider *et al.* (2006) or Turton *et al.* (2012) [56, 65].

Nr.	Heuristic / Assumption	Reasoning	Application
A 1	All streams are expected to enter and leave the system with a temperature of 35°C	To have the same temperatures for all systems (comparability). Moreover, for safety reasons, leaving streams should not be at high temperatures.	All base case design processes, final processes and processes of the literature
H 1	Separation of liquid mixtures with distillation, stripping, enhanced distillation, liquid-liquid extraction (extractive, azeotropic, reactive), crystallization, and/or adsorption.	Proven and reliable techniques applied most commonly	Choice for the entrainer regeneration unit
H 2	Near-optimal minimum temperature approaches in a heat exchanger <ul style="list-style-type: none"> • 5°C for below ambient • 10°C for ambient to 150°C • 20°C for above 150°C 	Optimum for ensuring a good driving force	Process heat exchangers
H 3	Heat exchanger pressure drops <ul style="list-style-type: none"> • 35 kPa for liquid streams without phase change • 20 kPa for vapour streams without phase change • Neglected for condensing and boiling streams 	Standard estimates and condensing or boiling streams are neglected for simplicity	Process heat exchangers
A 2	Pipeline and valve pressure drop neglected	Neglected for simplicity and purpose of this project	Pipelines, valves and pumps
H 4	Temperature change across pump for liquids neglected	Small for liquids	Process pumps
H 5	Liquid is pumped rather than gas compressed unless refrigeration is needed for additional heat exchanger [56]	Power required to compress a gas is much higher than for liquid	Additional heat exchanger used for condensing before the pump
H 6	Tray pressure drop is in the order of 0.1 psi	Typical measurement results	Distillation and stripping columns

A 3	Only heat integration solutions given by the Aspen Plus energy analyser tool of more than five years are considered	To implement only profitable heat integration solutions and it is also used as return rate in the TAC	Heat integration of the processes
H 7	Cooling water return temperatures do not exceed 40°C	Excess scaling at higher temperatures	Cooling water utility
H 8	A ton of refrigeration is the removal of 12700 kJ/h	Approximate calculation	Refrigerant requirements
H 9	Choice of refrigerants [65] <ul style="list-style-type: none"> • -18°C to -10°C: chilled brine and glycol solutions • -45°C to -10°C: ammonia, freon or butane • -100°C to -45°C: ethane or propane 	Appropriate temperature levels for the chemicals at acceptable pressure ranges	Refrigerant choice
H 10	For a three-stage steam ejector to create a vacuum of 0.26 kPa, 100 pounds of steam per pound of gas entering the vacuum are required	Approximate calculation	Steam requirements for steam jet ejector system
A 4	Pump efficiency of 80% assumed	Typical range for centrifugal pumps: 60-85%, reduced to one number for simplicity	All centrifugal pumps in the process
H 11	Sieve trays holes are 0.6 to 0.7 cm in diameter	Typical range	Sieve trays of distillation and stripping column
H 12	<ul style="list-style-type: none"> • Tray spacing is 0.5m • Space added at the top and bottom is 1.2 and 1.8m, respectively 	<ul style="list-style-type: none"> • Accessibility for cleaning and maintenance • Place for vapour derangement and liquid level and reboiler return 	For calculating the height of the distillation and stripping column
H 13	<ul style="list-style-type: none"> • Operating range is set to at 80% flooding • With the found diameter, the flooding factor should be between 0.8 and 0.4 on each tray • Active area is 90% 	<ul style="list-style-type: none"> • Safety range as a percentage of flooding velocity so that flooding does not occur • Typical range for upward vapour flow 	For calculating the diameter of the distillation and stripping column
H 14	<ul style="list-style-type: none"> • Reflux drums are in a horizontal cylindrical shape • The optimum length to diameter ratio is three 		Dimension calculation of the vapour-liquid and liquid-liquid reflux drums

H 15	<ul style="list-style-type: none"> • The reflux drum has liquid hold up of 5 minutes • The reflux drum is half-full 	Typical values and calculation procedure according to Turton <i>et al.</i> (2012) [65]	Dimensions calculation of the liquid-liquid reflux drums
A 5	<ul style="list-style-type: none"> • The HHAL of the reflux drum is 0.8 times the vessel diameter • The angle of vapour-liquid surface Θ of the reflux drum is 4.429 rad • Souders Brown parameter k_{sb} is 0.08 m/s 		Dimensions calculation of the vapour-liquid reflux drums
H 16	Heat exchange is done countercurrently in a shell-and-tube heat exchanger	For non-reacting systems, counter-current flow is the best flow condition	Heat exchangers in the process with an area above 100 ft ² (9.3 m ²).
H 17	Heat exchangers are designed as a 16-ft long tube with an outside diameter of ¾-in and a 1-in tube pitch in triangular spacing	Typical standardized design	All heat exchangers in the process
H 18	The tube side is for fouling, corrosive, scaling and high-pressure fluids while the shell side is for viscous, evaporating or condensing fluids	It is more economical to make the tubes instead of the shell in the more expensive material	All heat exchangers in the process
H 19	Countercurrent flow correction factor is 0.9 in a conservative estimate	Typical value procedure according to Turton <i>et al.</i> (2012) [65] Those values match the values proposed by Aspen Plus and taken by Ma <i>et al.</i> (2019) [18, 36]	For calculating the area of the heat exchanger
H 20	<p>The heat transfer coefficients in W/m²/°C can be taken as follows:</p> <ul style="list-style-type: none"> • water – liquid: 850 • liquid – liquid: 280 • gas – gas: 30 • reboiler: 1140 • water – water: 1140 • liquid – condensing vapour: 850 		
H 21	<ul style="list-style-type: none"> • A centrifugal pump is used for flowrates between 3 and 1135 m³/h • A rotary pump is used for small flowrates down to 0.2 m³/h 	Most economical and common solutions in practice	All pumps in the processes
H 22	<ul style="list-style-type: none"> • A liquid ring pump is used for pressures down to 2 kPa • A steam jet ejector is used for pressures down to 0.26 kPa (three stages for pressures between 0.26 and 2 kPa) 	Most economical and common solutions in practice as steam jet ejector cause high operating costs [64]	Vacuum system of the processes

A 6	Return on investment (i_{min}) is chosen to be 0.2	Seider <i>et al.</i> (2006) [56]	For the assessments in terms of TAC
A 7	The precondenser purchase and utility costs before the vacuum systems are neglected	A condenser is already included to achieve the temperature of 35°C for the exiting streams. The precondenser has only a minimal duty, and the vacuum system is not in the flowsheet	Vacuum systems costs
A 8	A plant operating factor of 0.9 is assumed (330 days of operation per year)	Seider <i>et al.</i> (2006) [56]	For the total annual production costs
A 9	The lang factor (f_{LTPi}) without working capital is assumed (4.74)	Working capital is not important for the comparison of different process options	For the f.o.b. purchase equipment costs
A 10	Material factor (F_M) equals 1 as carbon steel is assumed	Some costs equations are only given for carbon steel and not enough data in the literature on corrosiveness measurements. This project is not about the absolute numbers but about relative correlations. As this factor is assumed for all process options, the relative contributions stay correct.	For the f.o.b. purchase equipment costs
A 11	F.o.b. purchase costs of pumps are neglected	The costs are very small, and the pumps of the processes have too small powers to apply the cost equations	For the f.o.b. purchase equipment costs

Appendix B Theoretical Background & Methods

B.1 Process Modelling

The process modelling was done in Aspen Plus V8.8 [18]. The following chapter explains the thermophysical property estimation, the thermodynamic model, the used blocks for the process simulations as well as the method for determining the process design variables.

B.1.1 Thermophysical Property Estimation

DESs as relatively novel solvents are not pre-defined components in Aspen Plus, possibly due to the shortage of experimental data. Hence, the DES had to be implemented as a user-defined component creating a user-defined database [35]. The proper definition is crucial for the reliability and accuracy of the process simulation [45]. As stated in the literature, the DESs can be implemented as one non-dissociating component [12, 13].

As one input, the scalar properties of the DES are required for the simulations in Aspen Plus. Those are given in the database (see chapter 3.1 and C.3). Based on those, Aspen Plus estimated necessary missing characteristics. Furthermore, temperature-dependent properties such as density, viscosity, heat capacity, and vapour pressures are needed and influencing energy requirements. The parameters of the temperature-dependent functions available in Aspen Plus are regressed. The results of the parameter regression are given in chapter C.3.

B.1.2 Thermodynamics

For describing the VLE, the NRTL model was used. This corresponds to the procedure commonly used in the literature to simplify the calculation process [4, 26, 27, 35]. Moreover, it was found by Shang *et al.* (2019) that the NRTL model describes the VLE best for the ethanol, water, ChCl:Ur (1:2) system [45]. It should also be noted that taking the NRTL parameters of the literature does not necessarily result in the same fitness of the model. This is due to the impact of the way the DES is implemented. Dependent on the properties, parameters and molecular structures that are given to Aspen, the NRTL parameters have a different effect on the VLE because the Aspen Plus parameter estimation also yields different results for the missing parameters. Since mostly the DES implementation into Aspen is not given with respect to all necessary parameters in the considered publications, copying the NRTL parameters does not work. Hence, also the data validation has to be done within this work.

The NRTL model is based on binary interaction parameters [45]. It correlates the activity coefficients γ_i to the mole fractions, which is given by equation (5), where the parameter τ_{ji} is the dimensionless interaction parameter, R is the ideal gas constant, T is the temperature, αp_{ij} is the symmetrical non-randomness parameter, Δg_{ji} is the interaction energy parameter [90]. The parameters a_{ij} and b_{ij} are the parameter that need to be given to Aspen Plus. Those parameters are regressed by the given VLE measurements of the literature which are summarised in chapter C.3. The parameters c_{ij} and d_{ij} were set to 0.3 and 0, respectively. This is recommended for nonpolar substances with polar non-associated liquids [43]. Even though it seems acceptable to consider binary VLE data for the binary interaction parameters of the NRTL model, it can be shown that the presence of a third component alters the binary interaction due to the ionic effect that DESs have on the system [13, 43]. This was

especially considered in the first place, there are only a few DESs that were investigated in terms of a ternary VLE, and therefore there is only a reduced choice in finding the most suitable DES. The regressed parameters are given together with the data in chapter C.3, where Δg_{ji} is given in J/mole.

$$\ln(\gamma_i) = \frac{\sum_j \tau_{ji} G_{ji} x_j}{\sum_k G_{ki} x_k} + \sum_j \frac{G_{ij} x_j}{\sum_k G_{kj} x_k} \left(\tau_{ij} - \frac{\sum_m \tau_{mj} G_{mj} x_m}{\sum_k G_{kj} x_k} \right)$$

Where $G_{ij} = \exp(-\alpha p_{ij} \tau_{ji})$

$$\tau_{ji} = a_{ij} + \frac{b_{ij}}{T} + e_{ij} \ln(T) + f_{ij} T$$

$$\alpha p_{ij} = c_{ij} + d_{ij} (T - 273.15K)$$

$$\tau_{ii} = 0$$

$$G_{ii} = 1$$

$$\Delta g_{ji} = \tau_{ji} R T$$
(5)

B.1.3 Process Simulation

In Aspen Plus, the extractive distillation column and stripping column were modelled by the RadFrac model, which is commonly used [41, 76]. The evaporators were simulated with the two-outlet Flash vessels. The Newton algorithm was used for modelling the EDC and entrainer regeneration, as this is recommended for highly non-ideal systems [76].

B.1.4 Determination of Design Variables

The determination of design variables can be done in many different ways. Brüggemann and Marquardt (2004) develop a strategy based on a bifurcation analysis with pinch and composition profile maps [6]. A simultaneous iteration procedure applying the multi-objective generic algorithm is applied in the literature for finding the design variables of an extractive distillation using DES [4, 45]. A sequential quadratic programming method can also be found [25, 44]. Mostly, however, a simple sensitivity analysis and minimisation of the energy demand was applied [8, 58, 67]. For this research aim, the latter methodology is also effective enough. Still, many design variables need to be determined, all of which are dependent on each other. Hence, an iterative procedure was found, which is shown in *Figure A 1*, for the EDC, *Figure A 2* for the evaporators regeneration, and *Figure A 3* for the evaporator-stripping regeneration.

As can be seen in *Figure A 1*, one can say that the T_E and T_F are set first. Then, two different cases for the x_E are selected and in the end, evaluated in terms of energy requirements (see chapter 5.3). Similarly, the process is optimised for two different pressures and later compared in the economic analysis (see chapter 8). Subsequently, N_E , N_F , N_{th} , E/F and RR are found in this iterative process which is restarted after the optimisation of the regeneration unit. When the DESs are regenerated by two evaporators, the conditions are found in an iterative loop, as shown in *Figure A 2*. For the evaporator and stripping column sequence, the pressures are found first. The feed stage of the product recycle N_p and the temperature of the product recycle T_p are then determined. This goes in hand with adapting RR such that the purity constraint can still be met. Subsequently, the temperature of the first evaporator is found, which is adapted to minimize overall energy requirements by still meeting the constraints. The stages of the stripping column are found by investigating the impact of a one-stage increase on the purity. Finally, the product flowrate as a stripping agent is found by multiplying the minimum flowrate found through a sensitivity analysis by 1.1.

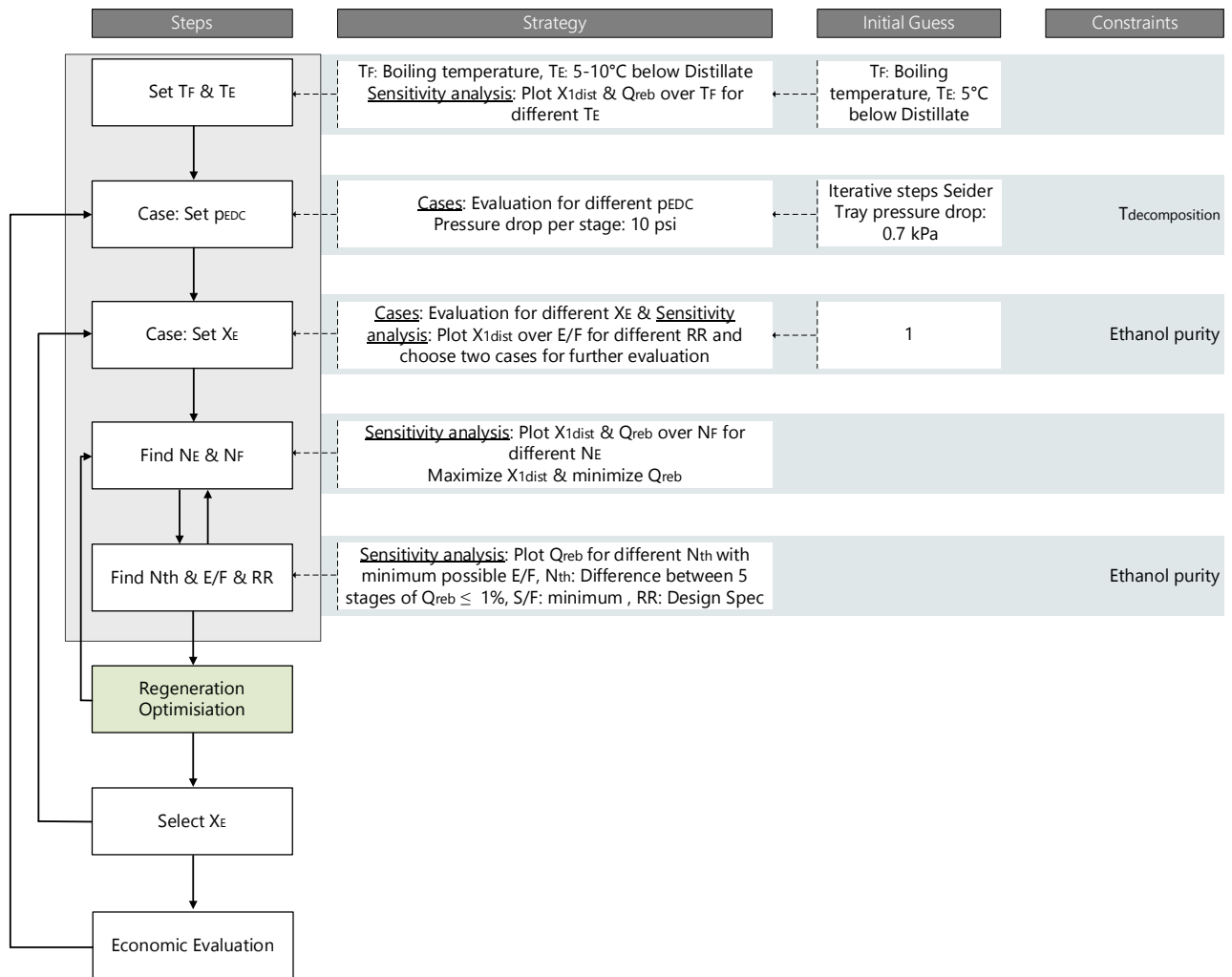


Figure A 1: Illustration of the steps in the iterative procedure to find the optimised process design variables of the EDC. Given are the steps, the strategy to find the design variables, the initial guess and the constraints that have to be met.

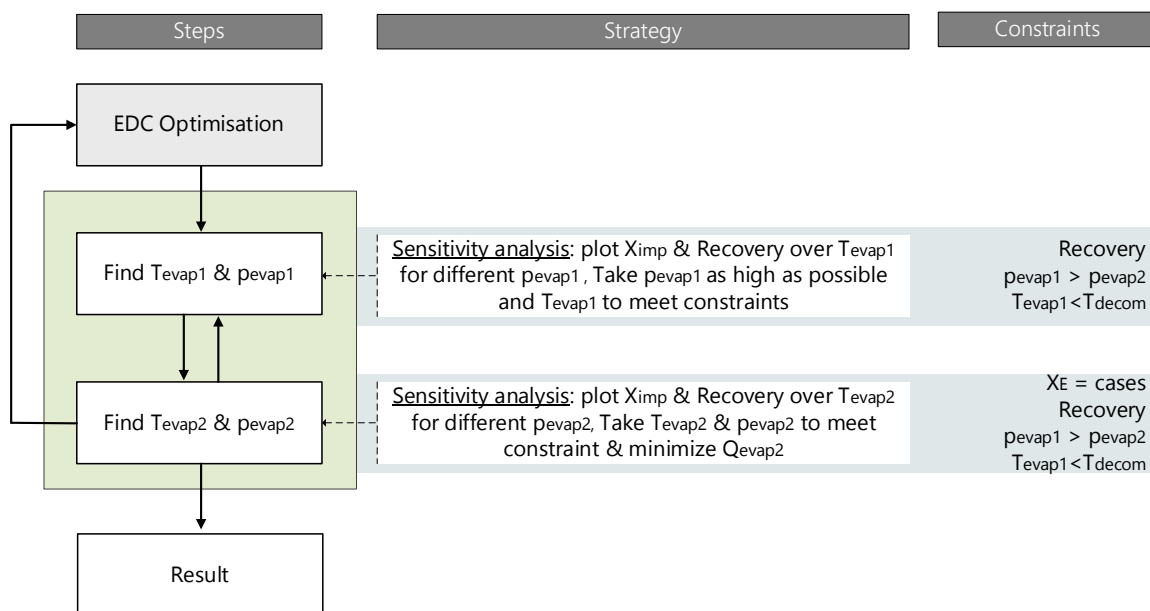


Figure A 2: Illustration of the steps in the iterative procedure to find the optimised process design variables of the evaporator regeneration unit. Given are the steps, the strategy to determine the design variables, and the initial guess.

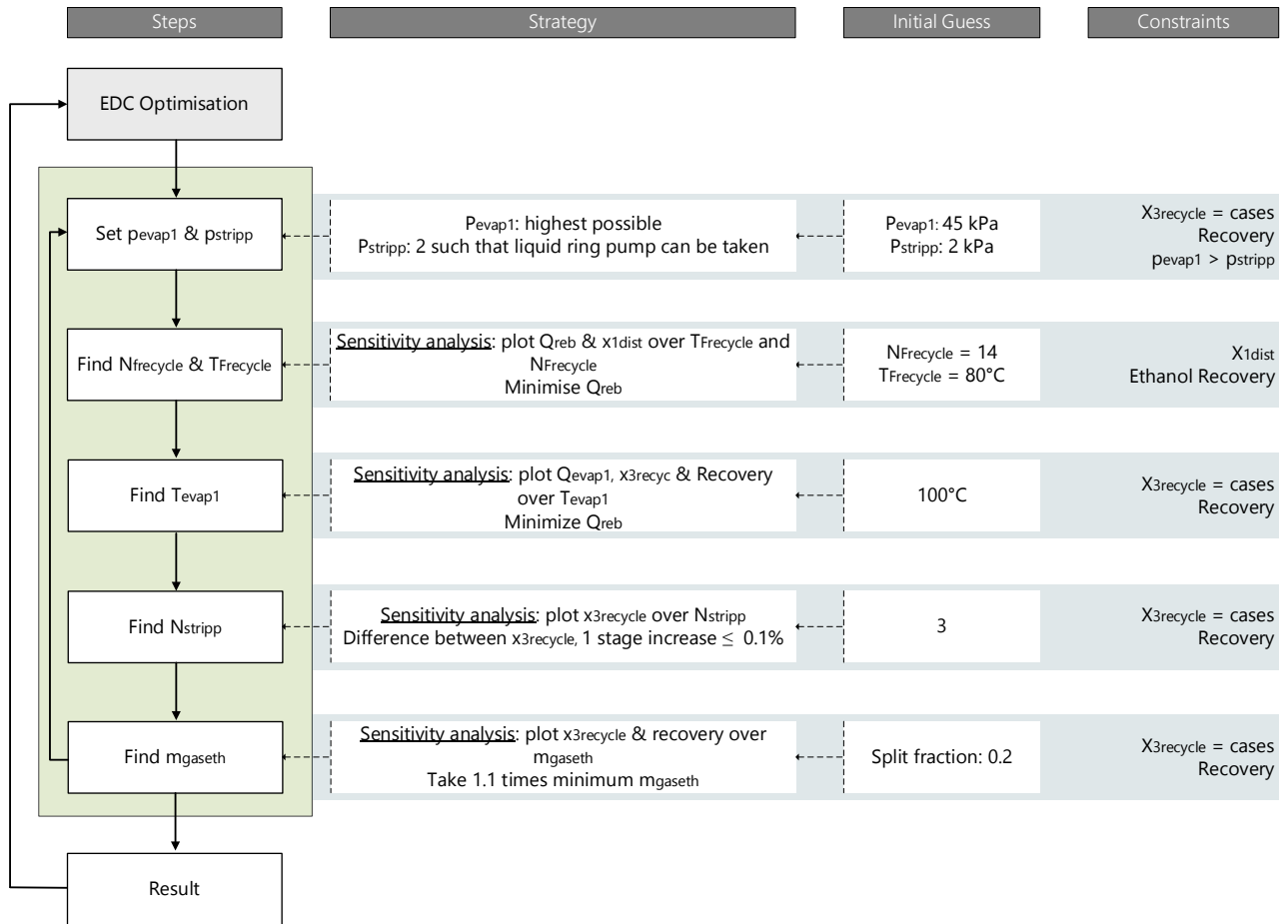


Figure A 3: Illustration of the steps in the iterative procedure to find the optimised process design variables of the evaporator and stripping base case design. Given are the steps, the strategy to determine the design variables, the initial guess and the constraints that have to be met.

B.2 Analysis

In chapter 3 and 10, different DESs, ILs and conventional entrainers are analysed. Pseudo-binary diagrams are given, and the DESs are evaluated in terms of their characteristics. Therefore, it is necessary to provide the background and methods for the calculation of those characteristics and the establishment of pseudo-binary diagrams. Moreover, statistical measures are applied to validate the simulation, which is why these equations must be given as well.

B.2.1 Pseudo-Binary Diagrams

The DESs are nonvolatile components that do not occur in the vapour phase [13]. Hence, pseudo-binary diagrams can be created by expressing the liquid phase on an entrainer free basis, according to equation (6) [13]:

$$\begin{aligned}x_1' &= \frac{x_1}{1 - x_3} \\x_2' &= 1 - x_1'\end{aligned}\quad (6)$$

In publications, the VLE is often given in terms of the mole fraction on entrainer free basis x_1' , and the weight fraction of the entrainer (w_3). By a mass balance and the molecular weights (see chapter C.3), the mole fraction x_1 can be calculated as follows:

$$x_1 = \frac{x_1'}{x_1' + x_2' + \frac{w_3}{1-w_3} \frac{x_1' M_1 + x_2' M_2}{M_3}} \quad (7)$$

With this equation, the VLE can be given in terms of x_1 , x_2 , and x_3 , as given in chapter C.3.3.

B.2.2 Characteristics of Entrainers

In this work, many characteristics of the DESs as entrainers are considered. Generally, there are certain properties that are desired [54, 91]:

- Entrainers should not form new azeotropes with the components to be separated. Also, heavy entrainers, with boiling points 30-40 degrees higher than the components to be separated are preferred.
- The separation of the mixture of entrainer and the other component should be easy
- Moreover, the entrainer must be chemically and thermally stable such that it does not degrade or react under the high temperatures of the EDC.
- To reduce costs of the equipment materials, the entrainer should be non-corrosive
- Entrainers should be environmentally friendly and non-toxic
- Entrainer should increase the relative volatility between the components to be separated above one at least
- Entrainers should not form a miscibility gap with the components to be separated

B.2.2.1 Selectivity, Relative Volatility & Capacity

The latter two points translate into the selectivity and capacity towards the components to be separated, both of which are often the main criteria for solvent selection. In the literature, the entrainer with the highest selectivity is often stated to result in the lowest TAC [50]. The selectivity can be expressed as follows [54]:

$$S_{1,2} = \frac{\gamma_{1,3}}{\gamma_{2,3}} \quad (8)$$

With this equation, it is trivial that selectivities of potential entrainers can only be compared at a consistent entrainer concentration (index 3) [50]. For the evaluation of different DES, the graph of selectivity over entrainer mole fraction is shown. For the final comparison with EG, DMSO and ILs, the selectivities were taken for an entrainer mole fraction of 0.63, even though usually an infinite entrainer solution is assumed. This has three reasons:

1. The literature provides measured values for the relative volatilities only for a narrow range and not for high entrainer mole fractions (maximum $x_3=0.7$). Moreover, the literature gives these experimental values for $x_1=0.95$, which was therefore taken [37, 40].
2. The selectivity of the given systems IPA, water and DES, and ethanol, water and DES shows a maximum instead of the typical linear increase of selectivity by entrainer mole fractions as was shown in chapter 3.3. This is in agreement with the results of Zhang *et al.* (2019) [11]
3. The exact entrainer mole fraction of 0.63 was chosen as this corresponds to the mole fraction of the extractive section in the simulated process.

Closely related to this, relative volatilities are calculated in this project by equation (9).

$$\alpha_{1,2} = \frac{\gamma_1/x_1}{\gamma_2/x_2} \quad (9)$$

A capacity value high enough to avoid liquid phase demixing is also essential, as it complicated extractive distillation processes. As there is no miscibility gap for the considered DES, the capacity is not evaluated in this work.

B.2.2.2 Residue Curve Maps & Minimum Entrainer Amounts

A residue curve map (RCM) is the liquid composition profile in a column operating under total reflux ratio and with an infinite number of trays. Each point of the residual curve reflects a different distillation time. As residue curves are solutions to a gradient system in terms of boiling temperatures, the direction of the residue curve corresponds to rising temperatures and times [45, 54]. Hence, the stable node and unstable node of the ternary diagram are the components with the highest and lowest boiling points, respectively. The saddle point represents the component with the intermediate boiling point [54]. In order to identify distillation processes and to establish separation classes and configurations to separate ternary mixtures, the topological Serafimov's classification of 26 ternary diagrams is commonly applied [92]. With DESs as the heavy entrainer, the minimum boiling azeotropes and the direct split to get ethanol or IPA at the distillate, the considered ternary systems belong to the class 1.0-1a.

Often, the feasibility of extractive distillation processes is evaluated by an analysis of the ternary RCMs [35, 55]. The general feasibility criterion states that a "*homogeneous extractive distillation of a A–B mixture with entrainer E feeding is feasible if: (1) A or B is the most volatile (respectively the least volatile) component of the mixture ABE in a region where (2) there exists a residue curve connecting E to A or E to B following a decreasing (respectively increasing) temperature direction towards the A or B apex*" ^{1 citation Gerbaud *et al.* (2019)} [54].

The location where the isovolatility line ($\alpha_{1,2} = 1$) intercepts one edge of the ternary diagram, reflects the minimum entrainer composition for a feasible separation [44]. Mostly, there is a strong correlation between relative volatility and selectivity enhancement and minimum molar entrainer amounts. However, the lowest minimum entrainer amount does not always result in the highest

selectivities at each entrainer concentration, as the selectivity can also increase non-linearly with the entrainer amount [54]. This was shown by Luyben and Chien (2010) and is also the case for the DESs systems, which show the above-mentioned maximum [93]. Also, as explained in chapter 10.1, for the system of ethanol and water, a very small ChCl:Ur (1:2) amount is required, even though relative volatilities stay very low for entrainer weight fraction below 10%.

The minimum entrainer amount is an important assessment criterion, as smaller entrainer amounts decrease energy consumption (see chapter 5.2.5). Moreover, with smaller entrainer amounts, the liquid load of the column is reduced, such that the dimensions can be designed smaller, leading to decreased costs. Furthermore, a smaller entrainer amount simplifies the implementation and operation [31, 91].

B.2.3 Data Validation

Statistical measures are applied to validate the simulation (see chapter 3.2). The root mean square deviation (RMSD) is typically used and given by the following equation, where n is the number of data points \hat{y}_i is the data point, both of which are given by the literature [45]. The symbol y_i corresponds to the simulated point.

$$\text{RMSD} = \sqrt{\frac{1}{n} \sum_{i=1}^n (y_i - \hat{y}_i)^2} \quad (10)$$

For the coefficient of determination R^2 , which was used to validate the simulation of the VLE, the mean of the experimental data \bar{y} is calculated according to equation (11) [94].

$$\bar{y} = \frac{1}{n} \sum_{i=1}^n y_i \quad (11)$$

Subsequently, R^2 can be calculated as follows [94].

$$R^2 = 1 - \frac{\sum_{i=1}^n (\hat{y}_i - y_i)^2}{\sum_{i=1}^n (\hat{y}_i - \bar{y})^2} \quad (12)$$

In the best case, R^2 is equal to 1, when the data matches the simulation exactly.

B.3 Utility Requirements and Classifications

The pump power (Q_{hp}) and heat exchanger loads (Q_{HE}) were directly taken from Aspen Plus or calculated as follows [65, 78]:

$$\dot{Q}_{HE} = \dot{m} \cdot c_p \cdot \Delta T \quad (13)$$

$$\dot{Q}_{hp} = Q \cdot \Delta p \quad (14)$$

where \dot{m} is the mass flowrate, c_p is the heat capacity, ΔT is the temperature difference, Q is the volume flow rate, and Δp is the pressure difference.

For pumps, the calculation of the electric power accounts for inefficiencies in the power transmissions from the shaft to the fluid and inefficiencies converting the electric energy in kinetic energy. The final formula can be seen in the following, where the efficiency η is assumed according to A 4 [78].

$$P_m = \dot{Q}_{hp} / \eta \quad (15)$$

For supplying the heat exchanger duties, LP, MP and HP steam, cooling water, or a refrigerant are used. The three different steam classifications are based on Seider *et al.* (2006), expect for medium pressure steam that is taken from Turton *et al.* (2012) [56, 65]. The different steam classes and the characteristics can be seen below.

Table A 3: Steam classes that are taken as utilities for this project, the absolute pressure, temperature and evaporation enthalpy [95].

Conditions			Steam class		
			High Pressure (HP)	Medium Pressure (MP)	Low Pressure (LP)
p	[Bara]	:	30	11.5	3.6
T	[°C]	:	233.8	186	139.9
h_e	[kJ/kg]	:	1794	1991	2144

Steam is assumed to enter the heat exchanger as saturated vapour and leave the heat exchanger as a saturated liquid [56]. The amount of steam is calculated according to equation (16), where \dot{m}_s is the steam mass flow rate, and h_e is the evaporation energy of the steam [95].

$$\dot{m}_s = \dot{Q}_{HE} / h_e \quad (16)$$

For three-stage steam jet ejector, equation (17) is used to calculate the amount of MP steam [56] (see heuristic H 10).

$$\begin{aligned} \dot{m}_s &= 10 \dot{m}_g \\ \dot{m}_g &\text{ in lb /hr} \end{aligned} \quad (17)$$

The cooling water amount is calculated according to equation (18), where c_{pw} is the heat capacity of water, and ΔT_w the temperature difference of the cooling water [95].

$$\dot{m}_w = \dot{Q}_{HE} / c_{pw} \cdot \Delta T_w \quad (18)$$

The characteristics of cooling water are shown in *Figure A 4*.

Table A 4: Characteristics of cooling water that is taken as utility in this project [95].

Water	T [°C]		C _{pw}
	In	out	
Cooling	20 ⁽¹⁾	40 ⁽²⁾	4.2
Chilled	5	10	4.21
Remarks	(1) Design value (2) Maximum allowed (3) At ground level		

For supplying a refrigerant, most commonly a vapour compression cycle is employed [56, 77]. Only the evaporation step is considered in this project. The duty of the condenser and the work of the pump is not considered in this work. The refrigerant mass flowrate m_R and refrigeration capacity Q_R is calculated by equation (19) and (20) where h_v is the saturated vapour enthalpy and h_L the saturated liquid enthalpy [77].

$$m_R = \dot{Q}_{HE} / (h_v - h_L) \quad (19)$$

$$Q_R = \dot{Q}_{HE} \cdot 3600 \frac{s}{h} \cdot 12700 \frac{\text{tonne}}{\frac{kJ}{h}} \quad (20)$$

The necessary characteristics of the used refrigerant ammonia are shown below.

Table A 5: Characteristics of the refrigerant ammonia that is taken as a utility in this project [95].

Ammonia	T [°C]	p [Bara]	h _L [kJ/kg]	h _v [kJ/kg]
Cooling	-13	2.68	1430.5	126.2
Remarks	Enters as saturated vapour and leaves as saturated liquid			

B.4 Purchase Costs of the Equipment

The cost equations for calculating the f.o.b. purchase costs are given in the following for each equipment that was used in the processes. Pumps have been neglected (A 17).

Table A 6: F.o.b. purchase cost calculation of the towers; formulas and meaning. For this calculation, the head thickness is assumed to be equal to the shell thickness [56]

Meaning	Formula
Costs of the empty vessel	$C_v = \exp\{7.2756 + 0.18255 [\ln(W)] + 0.02297 [\ln(W)]^2\}$ W in lb (21)
Cost of platforms and ladders	$C_{PL} = 300.9 (D)^{0.63316} (L)^{0.80161}$ D and L in ft (22)
Base costs for sieve trays	$C_{BT} = 468 \exp(0.1739 D)$ D in ft (23)
Costs for installed trays	$C_T = N_T F_{TT} F_M C_{BT}$ with F_{TT} and $F_M = 1$ (24)
Purchase cost	$C_P = F_M C_V + C_{PL} + C_T$ with $F_M = 1$ (25)

Table A 7: F.o.b. purchase cost calculation for the reflux drums [56].

Meaning	Formula
Costs of an empty vessel	$C_v = \exp\{8.9552 - 0.2330 [\ln(W)] + 0.04333 [\ln(W)]^2\}$ W in lb, for $1000 \leq W \leq 920000$ (26)
Cost of platforms and ladders	$C_{PL} = 2005 (D)^{0.20294}$ D in ft (27)
Purchase cost	$C_P = F_M C_v + C_{PL}$ with $F_M = 1$ (28)

Table A 8: F.o.b. purchase cost calculation for heat exchangers [56].

Meaning	Formula
Heat load	$Q = c_p \dot{m} \Delta T$
Logarithmic mean	$\Delta T_{LM} = \frac{\Delta T_1 - \Delta T_2}{\ln\left(\frac{\Delta T_1}{\Delta T_2}\right)}$ (29)
Heat transfer coefficient	$U = \text{Heuristics book}$
Correction factor	$F = 0.9$ (heuristic)
Area	$A = \frac{Q}{U \Delta T_{LM} F}$ (30)
Base costs	Shell and tube: $C_b = \exp(11.0545 - 0.9228 \ln(A) + 0.09861 \ln(A)^2)$ Double pipe: $C_b = \exp(7.1460 + 0.16 \ln(A))$ Kettle reboiler: $C_b = \exp(11.967 - 0.8709 \ln(A) + 0.09005 \ln(A)^2)$ A in ft^2 (31)
Purchase costs	Shell and tube $C_p = F_M F_L C_b$ Double pipe and kettle reboiler: $C_p = F_M C_b$ with $F_M = 1$ and $F_L = 1.05$ (32)

Table A 9: F.o.b. purchase cost calculation for evaporators [56].

Meaning	Formula
Heat load	$Q = c_p \dot{m} \Delta T$
Logarithmic mean	$\Delta T_{LM} = \frac{\Delta T_1 - \Delta T_2}{\ln\left(\frac{\Delta T_1}{\Delta T_2}\right)}$
Heat transfer coefficient	$U = \text{Heuristics book}$
Correction factor	$F = 0.9(\text{heuristic})$
Area	$A = \frac{Q}{U \Delta T_{LM} F}$
Purchase costs	$C_P = 4060 A^{0.53}$ A in ft^2 (33)

Table A 10: F.o.b. purchase cost calculation for the liquid ring pump and steam jet ejector [56].

Meaning		Formula	
Operating pressure	p	from Aspen Plus process simulation	
Volume equipment	V	from Aspen Plus process simulation	
Air leakage	W_{air}	$W_{\text{air}} = 5 + V^{0.66} \cdot (0.0298 + 0.03088 \ln(p)^2)$	(34)
Temperature precondenser	T_{cond}	from Aspen Plus process simulation	
Product	W_{product}	from Aspen Plus: flash calculation	
Flow to vacuum	W_{vacuum}	$W_{\text{vacuum}} = W_{\text{air}} + W_{\text{product}}$	(35)
Size factor – Steam Jet ejector	S_{steamjet}	$S_{\text{steamjet}} = \frac{W_{\text{vacuum}}}{P}$ $6.1 \leq S \leq 100$ W_{vacuum} in lb/hr, P in torr	(36)
Size factor – liquid ring pump	S_{liquid}	$S_{\text{liquid}} = W_{\text{vacuum}}$ with W in ft^3/min	(37)
Factor stages	F_{stages}	$F_{\text{stages}} = 2.1$	
Purchase costs steamjet	$C_{P,\text{steamjet}}$	$C_{P,\text{steamjet}} = 1690 S^{0.41} F_{\text{stages}}$ with $F_{\text{stages}} = 2.1$	(38)
Purchase costs liquid	$C_{P,\text{liquid}}$	$C_{P,\text{liquid}} = 8250 \cdot S^{0.35}$ for $0 \leq S \leq 100$	(39)
Compressor power	P_{comp}	from Aspen Plus process simulation	
MP steam requirement		$W_{\text{steam}} = W_{\text{vacuum}} \cdot 10$	(40)

Appendix C Supplement to the Main Text

C.1 Innovation Map

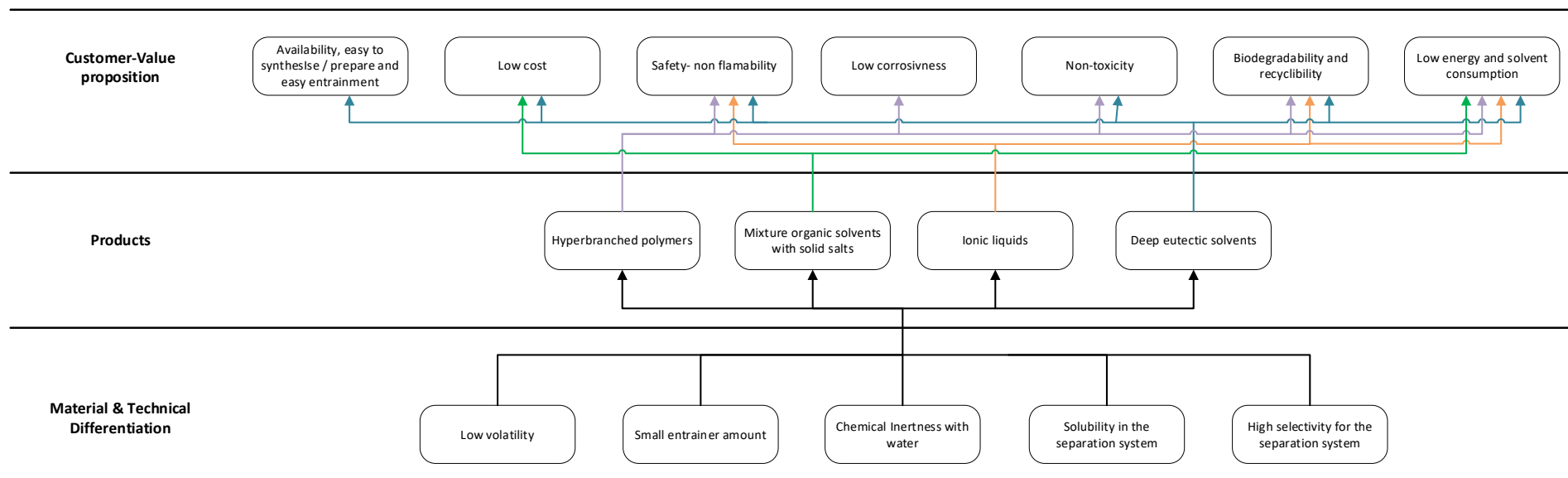


Figure A 4: Innovation map of hyperbranched polymers, a mixture of organic solvents and solid salts, and deep eutectic solvents.

C.2 Literature Review

Table A 11: Advantages and disadvantages of alternative entrainers to organic solvents for the use in extractive distillations [4, 8, 10, 12].

Entrainer	Advantages	Disadvantages
Mixture of dissolved salt + organic solvent	<ul style="list-style-type: none"> • High production capacity • Low energy consumption 	<ul style="list-style-type: none"> • Potential dissolution, recycle and transport problems • Possible corrosion to the equipment • Possible contaminant of the overhead product by organic solvent
Hyperbranched polymers	<ul style="list-style-type: none"> • High selectivity and separation efficiency • No contamination of the overhead product • Properties can be tuned 	<ul style="list-style-type: none"> • High price • Difficulty in finding raw material
Ionic liquids	<ul style="list-style-type: none"> • No contamination of the overhead product • Properties can be tuned • High selectivity • Low energy consumption 	<ul style="list-style-type: none"> • High price • Complex synthetic process • Toxicity of pyridinium and imidazolium-based ILs

C.2.1 List of Publications: DESs as Entrainer in Extractive Distillation

Table A 12: Literature review showing the main publications about the use of DES as entrainer in extractive distillation processes. Shown are the components to be separated, the used DES, the publication and the topic of the application being divided in either the measurement of the VLE or the process design.

Components	DES (HBA : HBD)	VLE	Process design	Breaks AP*
Ethanol & Water	Choline chloride : Malic acid (1:1)	[43]		
	Choline chloride : Lactic acid (1:2)	[43]		x
	Choline chloride : Glycolic acid (1:1) & (1:3)	[43]	[8]	x
	Choline chloride : Urea (1:2)	[13, 17]	[4, 36, 44]	x
	Choline chloride : Triethylene glycol	[17]		x
	Choline chloride : Ethylene glycol	[11]		x
Isopropanol & Water	Choline chloride : Lactic acid	[27]		
	Choline chloride : Glycolic acid	[27]		
	Choline chloride : Glycerol	[29]	[25]	x
	Choline chloride : Ethylene glycol	[46]		x

	Choline chloride : Triethylene glycol	[47]		x
Allyl alcohol & Water	Choline chloride : Urea	[96]		x
	Choline chloride : Glycerol	[96]		x
Acetonitrile & Water	Choline chloride : Glycolic acid	[97]		x
	Tetramethylammonium chloride : Glycolic acid	[98]		x
	Choline chloride : Malic acid	[99]		

C.2.2 Process Details of Investigated Publications

Table A 13: Details of the publications about the process design and simulation of the extractive distillation of ethanol and water using the conventional solvent ethylene glycol as entrainer (EG). *in case of mismatching units or lacking energy consumption / kg ethanol data has been changed or calculated

	Kiss <i>et al.</i> (2012) [5]	Bastidas <i>et al.</i> (2010) [30]	Black <i>et al.</i> (1974) [100]
Entrainer	EG	EG	EG
Feed flowrate [kmol/h]	319.4	245	283
Feed composition (x_{ET}) [mol/mol]	0.85	0.885	0.86
Ethanol purity	0.995	0.997	0.998
$N_{T\ EDC}$	17	21	46
$N_{T\ SRC}$	16	12	9
E/F	1.66	0.8	4.09
Energy consumption [MJ/kg of ethanol]	2.03	1.63	2.87

Table A 14: Details of the publications about the process design and simulation of the extractive distillation of ethanol and water using DESs as entrainer (ChCl:Ur (1:2) and ChCl:GC (1:3)). *in case of mismatching units or lacking energy consumption/kg ethanol data has been changed or calculated

	Pan <i>et al.</i> (2019) [4]	Han <i>et al.</i> (2018) [44]	Ma <i>et al.</i> (2017) [8]
Entrainer	ChCl:Ur (1:2)	ChCl:Ur (1:2)	ChCl:GA (1:3)
Feed flowrate [kmol/h]	100	105	100
Feed composition (x_{ET}) [mol/mol]	0.8	0.37	0.85
Ethanol purity [mol/mol]	0.995	0.998	0.9994
$N_{T\ EDC}$	17	25	22
$N_{T\ SRC}$		6	
E/F	0.305	0.38	0.3
Energy consumption [MJ/kg of ethanol]	1.39	3.47	1.91

Table A 15: Details of the publications about the process design and simulation of the extractive distillation of ethanol and water using the ILs as entrainer ([Emim]⁺[BF₄]⁻ and [Emim]⁺[N(CN)₂]⁻). *in case of mismatching units or lacking energy consumption/kg ethanol data has been changed or calculated

	Zhu <i>et al.</i> (2016) [35]	Jork <i>et al.</i> (2004) [12]	Meindersma <i>et al.</i> (2012) [41]
Entrainer	[Emim] ⁺ [BF ₄] ⁻	[Emim] ⁺ [BF ₄] ⁻	[Emim] ⁺ [N(CN) ₂] ⁻
Feed flowrate [kmol/h]	100	200	200
Feed composition (x _{ET}) [mol/mol]	0.85	0.7	0.8
Ethanol purity [mol/mol]	0.9993	0.998	0.998
N _{T EDC}	40	28	30
N _{T SRC}	15		
E/F [mol/mol]	0.32	0.5	0.54
Energy consumption [MJ/kg of ethanol]	2.27	1.77	1.72

Table A 16: Details of the publications about the process design and simulation of the extractive distillation of IPA and water using the conventional entrainer DMSO. *in case of mismatching units or lacking energy consumption/kg ethanol data has been changed or calculated

	Airfin <i>et al.</i> (2008) [26]	Ghughe <i>et al.</i> (2017) [31]
Entrainer	DMSO	DMSO
Feed flowrate [kmol/h]	100	100
Feed composition (x _{ET}) [mol/mol]	0.5	0.5
Ethanol purity [mol/mol]	0.9999	0.9999
N _{T EDC}	41	41
N _{T SRC}	24	20
E/F [mol/mol]	1.02	1
Energy consumption [MJ/kg of IPA]	3.04	2.97
TAC [10 ³ USD]	8009	

Table A 17: Details of the publications about the process design and simulation of the extractive distillation of IPA and water using the DES ChCl:TEG (1:2) as entrainer. *in case of mismatching units or lacking energy consumption/kg ethanol data has been changed or calculated

	De <i>et al.</i> (2019) [25]
Entrainer	ChCl:GLY (1:2)
Feed flowrate [kmol/h]	100
Feed composition (x _{ET}) [mol/mol]	0.67
Ethanol purity [mol/mol]	0.999
N _{T EDC}	23
N _{T SRC}	10
E/F [mol/mol]	0.5
Energy consumption [MJ/kg of IPA]	2.01
TAC [*10 ³ USD]	928.1

Table A 18: Details of the publications about the process design and simulation of the extractive distillation of IPA and water using the ILs as entrainer ($[\text{Emim}]^+[\text{N}(\text{CN})_2]^-$ and $[\text{Emim}]^+[\text{OAc}]^-$). *in case of mismatching units or lacking energy consumption/kg ethanol data has been changed or calculated

	Ma <i>et al.</i> (2019) [36]	Chen <i>et al.</i> (2017) [28]
Entrainer	$[\text{Emim}]^+[\text{N}(\text{CN})_2]^-$	$[\text{Emim}]^+[\text{OAc}]^-$
Feed flowrate [kmol/h]	100	76.9
Feed composition (x_{ET}) [mol/mol]	0.5	0.65
Ethanol purity [mol/mol]	0.998	0.9999
$N_{\text{T EDC}}$	25	49
$N_{\text{T SRC}}$		
E/F [mol/mol]	0.55	0.26
Energy consumption [MJ/kg of IPA]	2.52	1.33
TAC [$\cdot 10^3$ USD]	771.5	532.12

C.2.3 Extractive Distillation with ILs as Entrainers

For the ethanol and water system, the following main results for ILs as entrainers have been found in the literature.

Table A 19: Different studies about the use of ILs as entrainer in the extractive distillation of ethanol and water. Shown are the ILs, the essential findings, and the publication about the VLE measurement or process design.

IL	Remarks / Results	VLE	Process design
$[\text{Emim}]^+[\text{BF}_4]^-$, $[\text{Bmim}]^+[\text{BF}_4]^-$	<ul style="list-style-type: none"> $[\text{Emim}]^+[\text{BF}_4]^-$ is superior to conventional entrainers [12, 35] Heat integration does not have a strong effect 		[12, 35]
$[\text{Emim}]^+[\text{N}(\text{CN})_2]^-$	<ul style="list-style-type: none"> Pilote plant has been established Without heat integration, the process shows a similar energy demand as the conventional process 		[41]
$[\text{Mmim}]^+[\text{DMP}]^-$, $[\text{Bmim}]^+[\text{DEP}]^-$, $[\text{Bmim}]^+[\text{Br}]^-$, $[\text{Bmim}]^+[\text{Cl}]^-$, $[\text{Bmim}]^+[\text{PF}_6]^-$	<ul style="list-style-type: none"> $[\text{Bmim}]^+[\text{PF}_6]^-$ limited water solubility Salting out effect: $[\text{Bmim}]^+[\text{Cl}]^- > [\text{Bmim}]^+[\text{Br}]^- > [\text{Bmim}]^+[\text{PF}_6]^-$ Salting out effect: $[\text{Bmim}]^+[\text{DMP}]^- > [\text{Emim}]^+[\text{DEP}]^-$ 	[39]	
$[\text{Bmim}]^+[\text{BF}_4]^-$, $[\text{Emim}]^+[\text{BF}_4]^-$, $[\text{Bmim}]^+[\text{N}(\text{CN})_2]^-$, $[\text{Emim}]^+[\text{N}(\text{CN})_2]^-$, $[\text{Bmim}]^+[\text{Cl}]^-$, $[\text{Emim}]^+[\text{Cl}]^-$, $[\text{Bmim}]^+[\text{OAc}]^-$, $[\text{Emim}]^+[\text{OAc}]^-$	<ul style="list-style-type: none"> $[\text{Emim}]^+[\text{Cl}]^-$ has the strongest effect on VLE $[\text{Emim}]^+[\text{OAc}]^-$ is the most promising $[\text{Bmim}]^+[\text{Cl}]^-$ & $[\text{Emim}]^+[\text{Cl}]^-$ have high T_m & viscosities 	[40]	

Regarding the anion, most researchers came to the same conclusion. The ILs with the anion chloride $[\text{Cl}]^-$, acetate $[\text{OAc}]^-$, and bromide $[\text{Br}]^-$ gave the highest relative volatilities [34]. Among them, the chloride anion ($[\text{Cl}]^-$) proves to show the strongest salting-out effect. However, they also have a high viscosity (η) which complicates the process as the rate of heat- and mass-transport processes are slowed down affecting mixing, pumping, and agitation operations [21, 34, 35, 39, 40]. That is why some researchers considered $[\text{OAc}]^-$ as most promising, while others state that its low decomposition temperature (T_d) is a considerable disadvantage for the regeneration unit [10, 21, 35, 40]. Hence, researchers investigated also ILs that have a weaker salting-out effect.

Concerning the cation, the researcher's opinions aligned as well. According to Verma *et al.* (2010), imidazolium-based ionic liquids are showing the best performance in a solvent screening [34]. Among those, 1-ethyl-3-methylimidazolium ($[\text{Emim}]^+$) and 1-butyl-3-methylimidazolium ($[\text{Bmim}]^+$) have been studied the most. Since $[\text{Emim}]^+$ has a shorter chain length compared to $[\text{Bmim}]^+$ it has a higher selectivity and exhibits better ability for the elimination of the azeotrope [35].

Regarding the IPA-water system, similar results can be found which are listed in Table A 20. The anions $[\text{OAc}]^-$ and $[\text{Cl}]^-$, and the cation $[\text{Emim}]^+$ have the most significant effect on the relative volatility [21, 34, 36].

Table A 20: Different studies about the use of ILs as entrainer in the extractive distillation of IPA and water. Shown are the ILs, the essential findings, and the publication about the VLE measurement or process design.

IL	Remarks / Results	VLE	Process design
$[\text{Bmim}]^+[\text{BF}_4]^-$, $[\text{Emim}]^+[\text{BF}_4]^-$, $[\text{Bmim}]^+[\text{N}(\text{CN})_2]^-$, $[\text{Emim}]^+[\text{N}(\text{CN})_2]^-$, $[\text{Bmim}]^+[\text{OAc}]^-$, $[\text{Emim}]^+[\text{OAc}]^-$, $[\text{Bmim}]^+[\text{Cl}]^-$	<ul style="list-style-type: none"> $[\text{Cl}]^- \approx [\text{OAc}]^- > [\text{N}(\text{CN})_2]^- > [\text{BF}_4]^-$ [21] $[\text{Emim}]^+[\text{BF}_4]^-$ - Unstable in aqueous conditions [21] 	[37] [38]	
$[\text{Emim}]^+[\text{N}(\text{CN})_2]^-$			[36]
$[\text{Emim}]^+[\text{OAc}]^-$	<ul style="list-style-type: none"> No significant improvement compared to DMSO 		[42]

C.3 Process & Property Data Collection

C.3.1 Pure Component Properties

Table A 21: Physical and chemical properties and safety and toxicity data of ethanol, water and IPA.

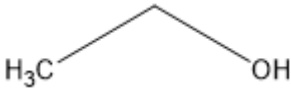
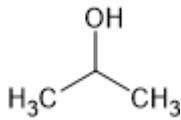
	Ethanol	Water	Isopropanol
IUPAC name	Ethanol	Water	Propan-2-ol
Chemical formula	C ₂ H ₆ O	H ₂ O	C ₃ H ₈ O
Structural formula			
Mw [g/mol]	46.07	18.015	60.096
T _m [°C]	-114.5	0	-89
T _b [°C]	78.32	99.98	82.6
ρ [g/mL] (20°C)	0.7893	0.997	1.1255
Water solubility	Soluble		Soluble
Hazard statements	Highly flammable, causes eye irritation		Highly flammable, causes eye irritation, causes drowsiness or dizziness
LD50 [mg/kg]	7060		5045

Table A 22: Physical and chemical properties and safety and toxicity data of ChCl, Ur, and GA.

	Choline chloride	Urea	Glycolic acid
IUPAC name	2-Hydroxy-N,N,N-trimethylethanaminium chloride	Carbonyl diamide	2-Hydroxyethanoic acid
Type	HBA, quaternary ammonium salt and an alcohol	HBD, amide	HBD, hydroxy acid

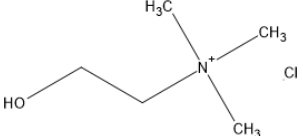
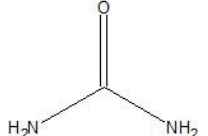
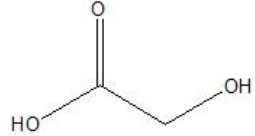


Natural source / Production	Naturally produced by organisms	Deamination of amino acids	sugarcane, sugar beets, pineapple, cantaloupe and unripe grapes
Chemical formula	$C_5H_{14}ClNO$	CH_4N_2O	$C_2H_4O_3$
Structural formula			
Mw [g/mol]	139.62	60.06	76.05
T _m [°C]	302	133-135	75
T _b [°C]	-	-	-
ρ [g/mL] (20°C)		1.32	1.49
Water solubility	Soluble	Soluble	Soluble
Hazard statements	Causes eye irritation	-	severe skin burns and eye damage, causes respiratory irritation
LD50 [mg/kg]	3400	8471	2040

Table A 23: Physical and chemical properties and safety and toxicity data of EG and TEG.

	Ethylene Glycol	Triethylene Glycol
IUPAC name	ethane-1,2-diol	2,2'-[Ethane-1,2-diylbis(oxy)]di(ethan-1-ol)
Type	HBD	HBD
Chemical formula	$(CH_2OH)_2$	$C_6H_{14}O_4$
Structural formula		
Mw [g/mol]	62.068	150.174
T _m [°C]	-12.9	-7
T _b [°C]	197.3	285
ρ [g/mL] (20°C)	1.1132	1.1255
Water solubility	Soluble	Soluble

Harmful if swallowed, cause damage to organs 4700	May cause eye and skin irritation 15000
--	--

Table A 24: Physical and chemical properties and safety and toxicity data of ChCl:Ur (1:2) and ChCl:GA (1:3).

	Choline chloride Urea (1:2)	Choline chloride Glycolic acid (1:3)
M_w [g/mol]	86.58 [44]	91.94 [8]
T_m [°C]	12 [7]	-16 (Tg) [8]
T_b [°C]	172.45 [44]	218 [101]
T_c [°C]	371.27 [44]	
P_c [bar]	49.35 [44]	19.7157 [8]
V_c [cm ³ /kmol]	254.37 [44]	1002.06 [8]
ω	0.23 [44]	0.13121 [8]

Table A 25: Physical and chemical properties and safety and toxicity data of ChCl:EG (1:2) and ChCl:TEG (1:3).

	Choline chloride Ethylene Glycol (1:2)	Choline chloride Triethylene glycol (1:3)
M_w [g/mol]	87.92 [102]	147.535
T_m [°C]	-66.85 [103]	-19.8 [7]
T_b [°C]	165.85 [102]	
T_c [°C]	328.85 [102]	437.52 [104]
P_c [bar]	40.39 [102]	27.36 [104]
V_c [cm ³ /kmol]	259.67 [102]	441.205 [104]
ω	0.952 [102]	1.0138 [104]

C.3.2 Temperature-Dependent Properties

Table A 26: Density measurements for different temperatures of ChCl:Ur (1:2) [105], ChCl:GA (1:3) [106], ChCl:EG (1:2) [107] and ChCl:TEG (1:3) at 1 atm [108].

T [K]	ρ ChCl:Ur (1:2) [g/cm ³]	ρ ChCl:GA (1:3) [g/cm ³]	ρ ChCl:EG (1:2) [g/cm ³]	ρ ChCl:TEG (1:3) [g/cm ³]
293.15		1.191		
298.15	1.1979	1.188		
303.15	1.1952	1.185	1.1114	1.1254
308.15	1.1926	1.182		
313.15	1.1900	1.179	1.1057	1.1189
318.15	1.1874	1.176		
323.15	1.1848	1.173	1.1001	1.1125
328.15	1.1822	1.170		
333.15	1.1796	1.167	1.0947	1.1062
338.15	1.1770	1.164		
343.15	1.1744	1.161	1.0887	1.0998
348.15	1.1718	1.158		
353.15	1.1692	1.155	1.0819	1.0935
363.15			1.0744	

Table A 27: Viscosity measurements for different temperatures of ChCl:Ur (1:2) [105], ChCl:GA (1:3) [106] and ChCl:EG (1:2) at 1 atm [109].

T [K]	η ChCl:Ur (1:2) [mN-sec/m ²]	η ChCl:GA (1:3) [mN-sec/m ²]	η ChCl:EG (1:2) [mN-sec/m ²]
293.15		779.4	
298.15	748	547.9	
303.15	512	394.8	
308.15	352	290.6	309
313.15	243	218.6	258
318.15	170	167.0	219
323.15	120	130.1	188
328.15	86	102.9	162
333.15	63	82.82	142
338.15	48	67.03	125
343.15	37	55.25	110
348.15	30	45.93	87.9
353.15		38.91	71.1

Table A 28: Vapor pressure (p_{vap}) for different temperatures for the component ChCl:Ur (1:2) [110]. This vapor pressure measurement is taken for each DESs.

T [K]	p_{vap} [Pa]
343.15	0.3357
353.15	0.6130
363.15	0.8976
373.15	1.3319
383.15	1.8760
393.15	2.9406

C.3.3 Vapor-Liquid Equilibrium

Table A 29: Heat capacity measurements for different temperatures of ChCl:Ur (1:2) [111], ChCl:TEG (1:3) [108] and ChCl:EG (1:2) at 1 atm [63].

ChCl:EG (1:2)		ChCl:TEG (1:3)		ChCl:Ur (1:2)	
T [K]	C_p [J/mol/K]	T [K]	C_p [J/mol/K]	T [K]	C_p [J/mol/K]
313.25	184.8	298.15	299.0	303.15	181.4
313.29	184.5	300.65	300.3	308.15	182.2
313.35	184.4	303.15	301.5	313.15	183.2
313.39	184.4	305.65	302.8	318.15	183.5
313.50	184.3	308.15	303.7	323.15	184.5
313.57	184.3	310.65	304.5	328.15	185.3
323.37	188.1	313.15	304.7	333.15	186.4
323.44	188.0	315.65	304.6	338.15	187.4
323.46	187.9	318.15	304.6	343.15	188.5
323.49	188.0	320.65	304.3	348.15	189.5
323.56	187.9	323.15	304.3	353.15	190.8
323.60	187.9	325.65	304.9		
333.25	191.8	328.15	305.8		
333.31	191.4	330.65	306.7		
333.34	191.5	333.15	307.4		
333.37	191.4	335.65	308.6		
333.39	191.5	338.15	309.4		
333.41	191.2	340.65	309.9		

343.27	194.6	343.15	310.0
343.32	194.5	345.65	311.8
343.36	194.4	348.15	312.2
343.39	194.4	350.65	312.4
343.43	194.4	353.15	314.6
343.45	194.4		

Table A 30: VLE data for the ternary system IPA (1), Water (2) and ChCl:TEG (1:3) (3) for different weight fractions of ChCl:TEG (1:3) at 1 atm [47].

T [K]	x ₁	x ₂	x ₃	y ₁	y ₂
w ₃ =3 %wt					
354.77	0.083	0.905	0.012	0.104	0.896
354.25	0.163	0.826	0.011	0.187	0.813
353.73	0.248	0.742	0.011	0.278	0.722
353.54	0.366	0.624	0.010	0.337	0.663
354.62	0.710	0.283	0.006	0.457	0.543
356.29	0.812	0.182	0.006	0.477	0.523
357.24	0.837	0.158	0.005	0.497	0.503
360.41	0.889	0.106	0.005	0.526	0.474
364.12	0.936	0.059	0.004	0.602	0.398
368.87	0.958	0.038	0.004	0.705	0.295
371.71	0.977	0.019	0.004	0.815	0.185
372.73	0.990	0.006	0.004	0.936	0.065
w ₃ =5 %wt					
355.50	0.100	0.880	0.020	0.128	0.872
354.78	0.149	0.833	0.019	0.178	0.822
353.88	0.316	0.667	0.017	0.297	0.703
353.62	0.370	0.614	0.016	0.327	0.673
354.57	0.562	0.426	0.013	0.385	0.615
354.96	0.594	0.394	0.012	0.395	0.605

355.31	0.623	0.365	0.012	0.404	0.596
356.84	0.695	0.294	0.011	0.423	0.577
358.41	0.768	0.222	0.010	0.458	0.543
360.21	0.838	0.153	0.009	0.501	0.499
362.11	0.878	0.114	0.008	0.536	0.464
364.76	0.930	0.063	0.008	0.612	0.388
369.03	0.964	0.029	0.007	0.764	0.236

$w_3=10\text{ \%wt}$

356.91	0.027	0.930	0.043	0.024	0.976
354.62	0.143	0.818	0.040	0.108	0.892
356.21	0.553	0.421	0.027	0.329	0.671
358.03	0.663	0.314	0.023	0.395	0.605
360.32	0.714	0.264	0.022	0.425	0.575
360.98	0.724	0.252	0.024	0.439	0.561
362.56	0.757	0.222	0.020	0.457	0.543
364.32	0.790	0.190	0.020	0.480	0.520
367.11	0.850	0.132	0.018	0.534	0.466
371.21	0.937	0.048	0.015	0.741	0.259
373.25	0.976	0.010	0.014	0.934	0.066

$w_3=15\text{ \%wt}$

357.34	0.012	0.921	0.067	0.008	0.992
356.32	0.059	0.877	0.064	0.037	0.963
356.23	0.386	0.565	0.049	0.200	0.800
361.78	0.627	0.336	0.038	0.322	0.679
366.72	0.753	0.215	0.032	0.436	0.564
368.34	0.803	0.167	0.030	0.498	0.502
370.46	0.843	0.130	0.027	0.562	0.438
372.01	0.905	0.070	0.025	0.699	0.301
373.67	0.960	0.018	0.022	0.899	0.102

374.59	0.969	0.010	0.022	0.939	0.061
--------	-------	-------	-------	-------	-------

Table A 31: VLE data for the ternary system Ethanol (1), Water (2) and ChCl:Ur (1:2) (3) for different weight fractions of ChCl:Ur (1:2) at 1 atm [13].

T [K]	x ₁	x ₂	y ₁	y ₂
w ₃ =30 wt%				
354.34	0.794	0.024	0.982	0.018
354.34	0.77	0.053	0.965	0.035
354.1	0.728	0.104	0.93	0.07
354.1	0.652	0.184	0.896	0.104
354.05	0.566	0.282	0.832	0.168
354.3	0.434	0.429	0.776	0.224
355.2	0.276	0.608	0.694	0.306
356.16	0.218	0.673	0.642	0.358
358.29	0.133	0.769	0.567	0.433
361.51	0.075	0.833	0.484	0.516
363.5	0.054	0.859	0.416	0.584
364.65	0.047	0.864	0.391	0.609
368.98	0.023	0.892	0.25	0.75
w ₃ =20 wt%				
353.53	0.788	0.101	0.928	0.072
353.42	0.728	0.172	0.877	0.123
353.5	0.621	0.28	0.829	0.171
353.61	0.523	0.388	0.764	0.236
353.94	0.446	0.471	0.739	0.261
354.62	0.33	0.595	0.668	0.332
355.32	0.267	0.663	0.638	0.362
356.02	0.215	0.719	0.6	0.4

359.67	0.096	0.845	0.496	0.504
363.64	0.051	0.897	0.382	0.618
365.62	0.035	0.912	0.322	0.678
367.05	0.03	0.918	0.281	0.719
368.63	0.023	0.925	0.227	0.773
370.26	0.015	0.935	0.151	0.849
372.45	0.008	0.942	0.08	0.92
352.46	0.887	0.059	0.948	0.052
$w_3=10$ wt%				
352.46	0.858	0.089	0.923	0.077
352.46	0.839	0.109	0.909	0.091
352.46	0.766	0.184	0.853	0.147
352.66	0.672	0.281	0.796	0.204
353.07	0.57	0.387	0.74	0.26
353.68	0.45	0.511	0.695	0.305
354.49	0.343	0.622	0.651	0.349
355.52	0.242	0.727	0.607	0.393
356.42	0.197	0.773	0.576	0.424
356.94	0.163	0.809	0.56	0.44
357.54	0.153	0.819	0.538	0.462
361.53	0.07	0.905	0.416	0.584
364.03	0.043	0.933	0.334	0.666
366.52	0.028	0.948	0.261	0.739
370.09	0.015	0.962	0.137	0.863
372.03	0.006	0.972	0.057	0.943

Table A 32: VLE data for the ternary system Ethanol (1), Water (2) and ChCl:EG (1:2) (3) at 1 atm [11]

T [K]	x_1	x_2	y_1	y_2
378.11	0.0959	0.3852	0.6502	0.3498
369.36	0.1227	0.4915	0.6414	0.3586

364.34	0.1425	0.569	0.6253	0.3747
361.08	0.1582	0.6298	0.6293	0.3707
359.27	0.1689	0.679	0.5888	0.4112
357.99	0.1797	0.7168	0.5801	0.4199
357.24	0.1869	0.7501	0.5621	0.4379
356.61	0.195	0.7759	0.5582	0.4418

Table A 33: VLE data for the ternary system Ethanol (1), Water (2) and ChCl:GA (1:3) (3) at 1 atm [43].

T [K]	x ₁	x ₂	y ₁	y ₂
365.31	0.025	0.775	0.22	0.7799
361.86	0.05	0.75	0.308	0.6919
357.62	0.1	0.7	0.463	0.5369
355.9	0.125	0.675	0.5	0.4999
354.72	0.15	0.65	0.529	0.4709
353.57	0.2	0.6	0.59	0.4099
353.03	0.25	0.55	0.64	0.3599
352.25	0.3	0.5	0.67	0.3299
351.8	0.35	0.45	0.71	0.2899
351.22	0.4	0.4	0.744	0.2559
351.12	0.502	0.298	0.816	0.1839
351.14	0.601	0.199	0.844	0.1559
351.01	0.651	0.149	0.89	0.1099
351.01	0.701	0.099	0.919	0.0809
351.02	0.75	0.05	0.949	0.0509
351.04	0.775	0.025	0.983	0.0169

C.3.4 Aspen Parameters

Table A 34: Parameters of the NRTL model for the four systems at 1 atm.

	Δg_{12} [J/mol]	Δg_{21} [J/mol]	α_{NRTL}
--	-------------------------	-------------------------	------------------------

ChCl:GA (1:3) (1) + Water (2)	-2.496	120474.3	0.47
ChCl:GA (1:3) (1) + Ethanol (2)	-8.32	83.2	0.3
Water (1) + ChCl:Ur (1:2) (2)	1212.996	-5593.98	0.3
Ethanol (1) + ChCl:Ur (1:2) (2)	64003	4179	0.3
ChCl:EG (1:2) (1) + Water (2)	-4992.03	74880.43	0.3
ChCl:EG (1:2) (1) + Ethanol (2)	-8.32	83.3	0.3
IPA (1) + ChCl:TEG (1:3) (2)	2494.2	-7101.82	0.3
Water (1) + ChCl:TEG (1:3) (2)	35589.33	-12379.79	0.3

Table A 35: Chosen property function in Aspen for the temperature-dependent properties and the regressed parameters.

DES Parameter No	1	2	3	4	5
CPIG [kJ / kmol / K]					
ChCl:GA (1:3)	177.5821	0.127726	-0.00017	7.76E-06	3.01E-09
ChCl:EG (1:2)	170.3794	0.305985	0.001745	-1.60E-05	-1.87E-08
ChCl:Ur (1:2)	177.5821	0.127726	-0.00017	7.76E-06	3.01E-09
ChCl:TEG (1:3)	212.5733	0.016783	-0.0002	9.49E-06	1.37E-08
CPLIKC [kJ / kmol / K]					
ChCl:GA (1:3)	0	0.28085	1.68E-12		
ChCl:EG (1:2)	0	0.28085	1.68E-12		
ChCl:Ur (1:2)	0	0.28085	1.68E-12		
ChCl:TEG (1:3)	0	0.00028	0		
VLPO [cm ³ /mol]					
ChCl:GA (1:3)	76.37343081	0.038811717	2.48E-05		
ChCl:EG (1:2)	68.4221366	0.026012872	2.96E-05		
ChCl:Ur (1:2)	62.5322576	0.02587313	2.21E-05		
ChCl:TEG (1:3)	129.2830332	0.056856012	0.0001782		
MULAND [10 ⁻³ Pa s]					

ChCl:GA (1:3)	-113.3708477	10000	15.113186		
ChCl:EG (1:2)	444.6619793	-49321.2969	0		
ChCl:Ur (1:2)	444.6619793	-49321.2969	0		
ChCl:TEG (1:3)	444.6619793	-49321.2969	0		

C.4 Aspen Implementation of the DES

C.4.1 Data Validation

When considering only a binary system, more DESs have been investigated, as shown in Table A 36.

Table A 36: Publications with binary VLE measurements of water and DES. Listed are several HBDs that form a DES with ChCl as HBA.

HBD (HBA:ChCl)	
Water + DES	Sucrose [112], Fructose [112], Glucose [113], Glycercol [114], Lactic Acid [115], Alanine [115], Glycine [115], Histidine [115], Malonic acid [114], Ethylene Glycol [114], Urea [113, 114]

C.4.1.1 Residue Mean Square Deviations

Table A 37: RMSD of the regression of the heat capacity, the density, the viscosity and the vapor pressure for the four DESs ChCl:Ur (1:2), ChCl:EG (1:2), ChCl:GA (1:3) and ChCl:TEG (1:3)

	RMSD _{cp} [J/mol/K]	RMSD _p [g/cm ³]	RMSD _η [mN-sec/m ²]	RMSD _{p_{vap}} [Pa]
ChCl:Ur (1:2)	0.123	0.109	3.054	2.187
ChCl:EG (1:2)	0.108	0.094	4.225	2.187
ChCl:GA (1:3)	0.240	0.034	3.02	2.187
ChCl:TEG (1:3)	0.398	0.041	3.02	2.187

C.4.1.2 Simulated VLE Curves with Data Points

In Figure A 5, the simulation results and experimental measurements for 30 wt% of ChCl:Ur (1:2) are plotted in a diagram of the vapour mole fraction (y_1) (left), temperature (T) (middle) and relative volatility (α) (right) over the liquid mole fraction of ethanol on entrainer free basis (x_1).

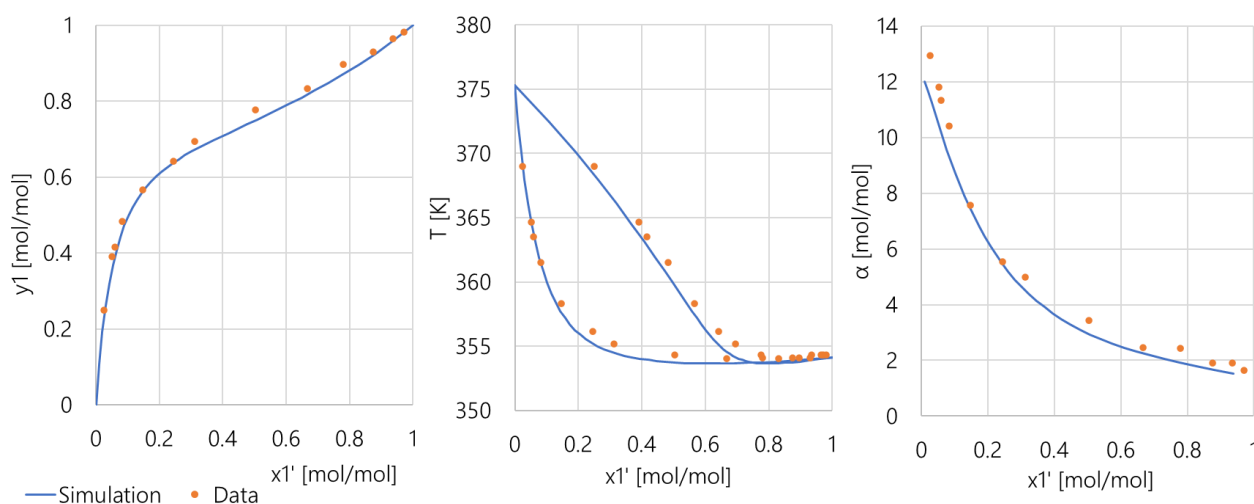


Figure A 5: Simulation results and experimental measurements for 30 wt% of ChCl:Ur (1:2) plotted in a vapour mole fraction (y_1) over the liquid mole fraction of ethanol (x_1) diagram (left), the temperature over x_1 diagram (middle), and the relative volatility (α) over x_1 diagram (right) [13].

In Figure A 5, it can be seen that the data lies closely around the simulation curves, which was already indicated by the statistical fitness parameters in Table 1. Thus, it can be concluded that the NRTL model predicts the data very well, which would give a reliable start for the process simulation.

In Figure A 6, the simulation results and experimental measurements for 15 wt% of ChCl:TEG (1:3) are plotted in a diagram of the vapour mole fraction (y_1) (left), temperature (T) (middle) and relative volatility (α) (right) over the liquid mole fraction of ethanol on entrainer free basis (x_1) [47].

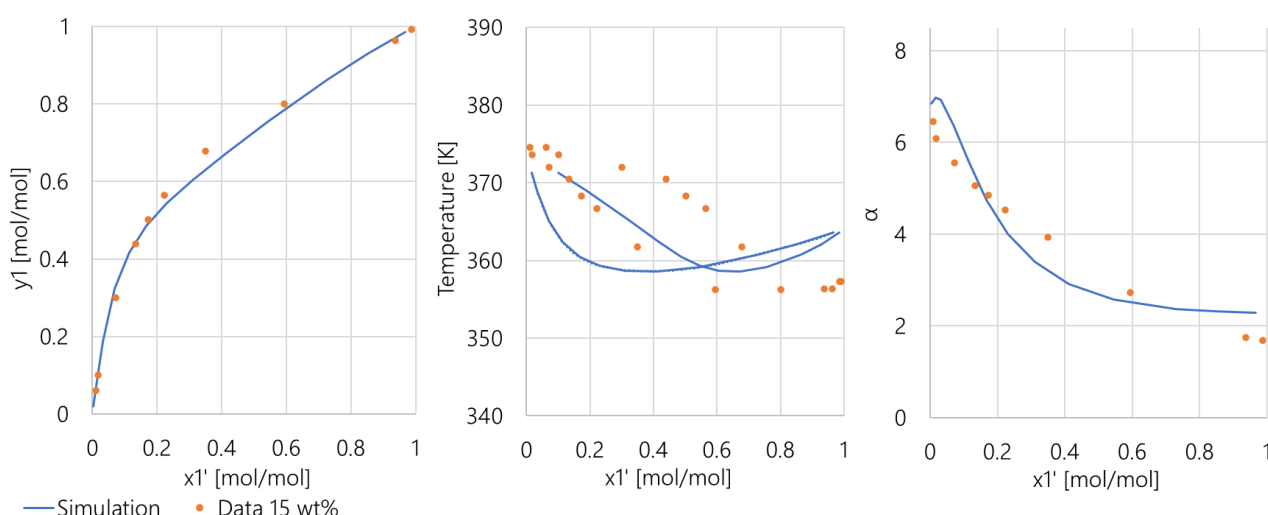


Figure A 6: Simulation results and experimental measurements for 15 wt% of ChCl:TEG (1:3) plotted in a vapour mole fraction (y_1) over the liquid mole fraction of ethanol (x_1) diagram (left), the temperature over x_1 diagram (middle), and the relative volatility (α) over x_1 diagram (right) [47].

As can be seen in Figure A 6, the temperature simulation is not very accurate and also the relative volatility is predicted less good than for the other systems. The NRTL regression for this system involving IPA was particularly tricky, which was most likely also the case for other research groups. For instance,

Rodriguez *et al.* (2014) give for each different weight fractions of the DES a different set of NRTL parameters [27]. Zhang *et al.* (2017) split the DES into the HBD and HBA component for the Aspen implantation and give the NRTL parameters for the four-component system [29]. Plugging in the parameters given by Jiang *et al.* (2019) results in a miscibility gap even though this should not occur for the soluble DESs [47]. The group does not report about any miscibility gap and also does not show the temperature fit for their regression, which would have been interesting. The difficulty of the simulation of the system might be related to its complex inverse behaviour: For small ethanol liquid mole fractions, the relative volatility shows an increasing trend by increasing the DES amounts while for higher ethanol mole fractions, the relative volatility is higher for higher DES amounts. Another difficulty lies in the negligible vapour pressure of the DES. The vapour fraction of the DES is assumed to be zero in the data set so that the relative error in the Aspen regression is very high, and the regression frequently fails to converge. Indeed, for this system, the regression function in Aspen always resulted in an error, which is why NRTL parameters from Jiang *et al.* (2019) were taken and adapted manually until the best fit was achieved and until the miscibility gap vanished [47].

In Figure A 7, the simulation results and experimental measurements for 20 mole% of ChCl:GA (1:3) are plotted in a diagram of the vapour mole fraction (y_1) (left), temperature (T) (middle) and relative volatility (α) (right) over the liquid mole fraction of ethanol on entrainer free basis (x_1') [43]. There were no other mole fractions of ChCl:GA (1:3) found in the literature.

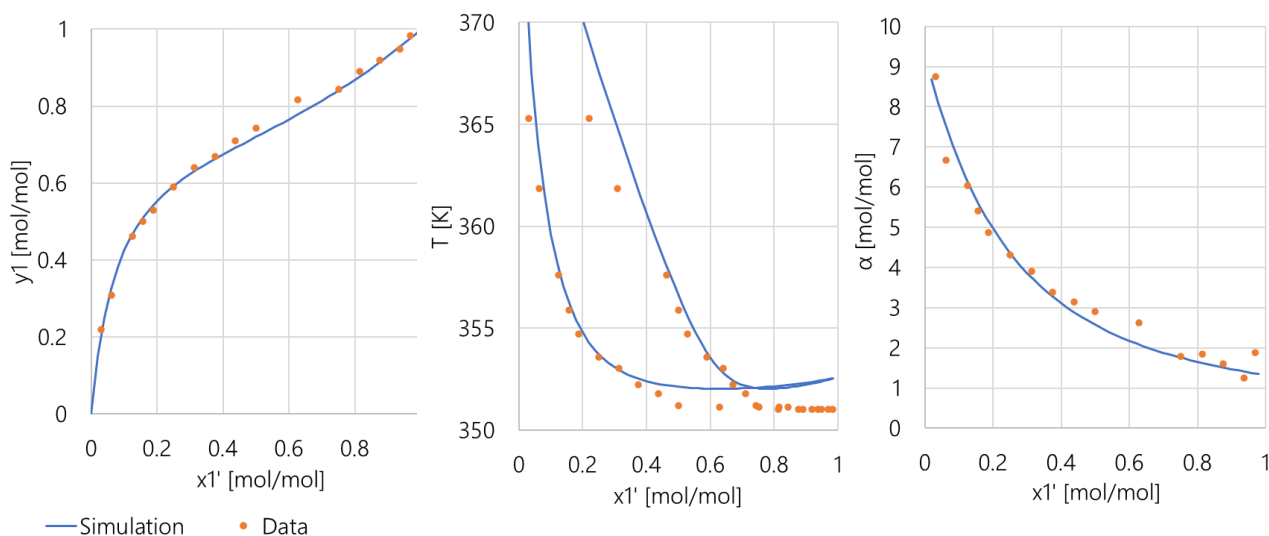


Figure A 7: Simulation results and experimental measurements for 20 mole% of ChCl:GA (1:3) plotted in a vapor mole fraction (y_1) over the liquid mole fraction of ethanol (x_1') diagram (left), the temperature over x_1' diagram (middle), and the relative volatility (α) over x_1' diagram (right) [43].

In Figure A 7, it can be seen that the vapour fraction of ethanol and the relative volatility are predicted very well. However, the temperature prediction is less accurate, especially for smaller amounts of ethanol and for the vapour composition curve. Unfortunately, the data fit in the literature was not shown in the temperature over the composition diagram. The simulation curve shown in the y-x diagram in the literature seems to deviate from the measurements more than in this simulation [43]. Since the vapour composition and relative volatility are predicted very well and have a more significant effect on the process design parameters, and the RMSD is below 5 K, the NRTL model considered to be accurate enough.

In Figure A 8, the simulation results and experimental measurements for ChCl:EG (1:2) are plotted in a diagram of the vapor mole fraction (y_1) (left), temperature (T) (middle) and relative volatility (α) (right) over the liquid mole fraction of ChCl:EG (1:2)) [46].

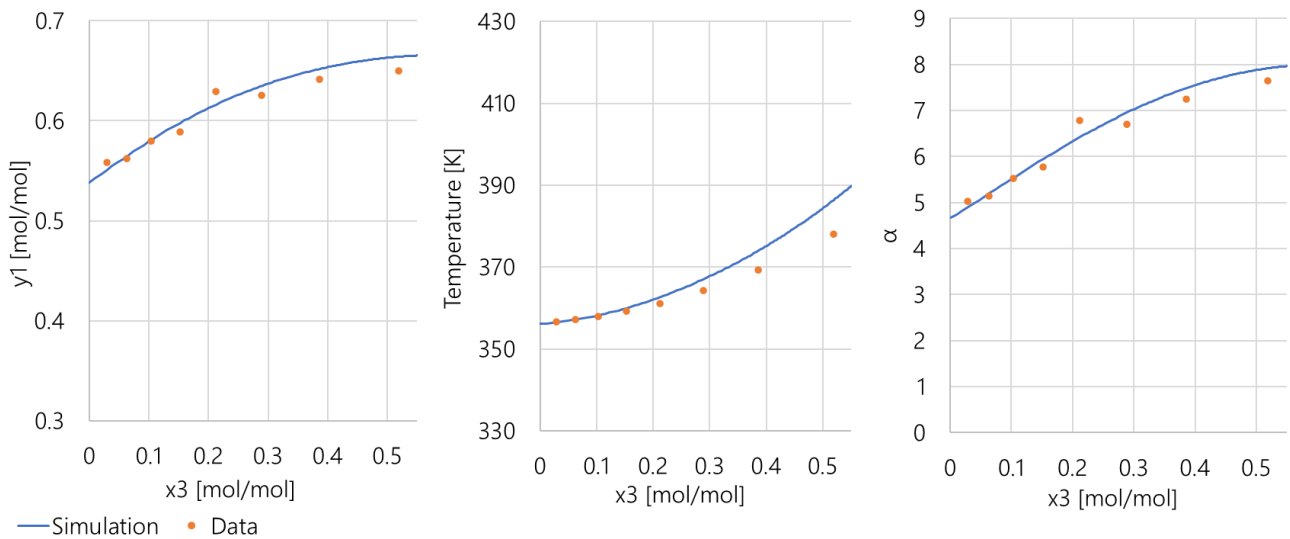


Figure A 8: Simulation results and experimental measurements for 20 mole% of ethanol on entrainer free basis plotted in a diagram of the vapour mole fraction (y_1), the temperature and the relative volatility (α) over the mole fraction of ChCl:EG (1:2) [46].

Contrary to the other systems, in this publication the entrainer free mole fraction of ethanol has been kept constant to 0.2 and the ChCl:EG (1:2) mole fraction was varied. It can be overserved that there are no strong deviations, and the NRTL model is considered to describe the VLE well.

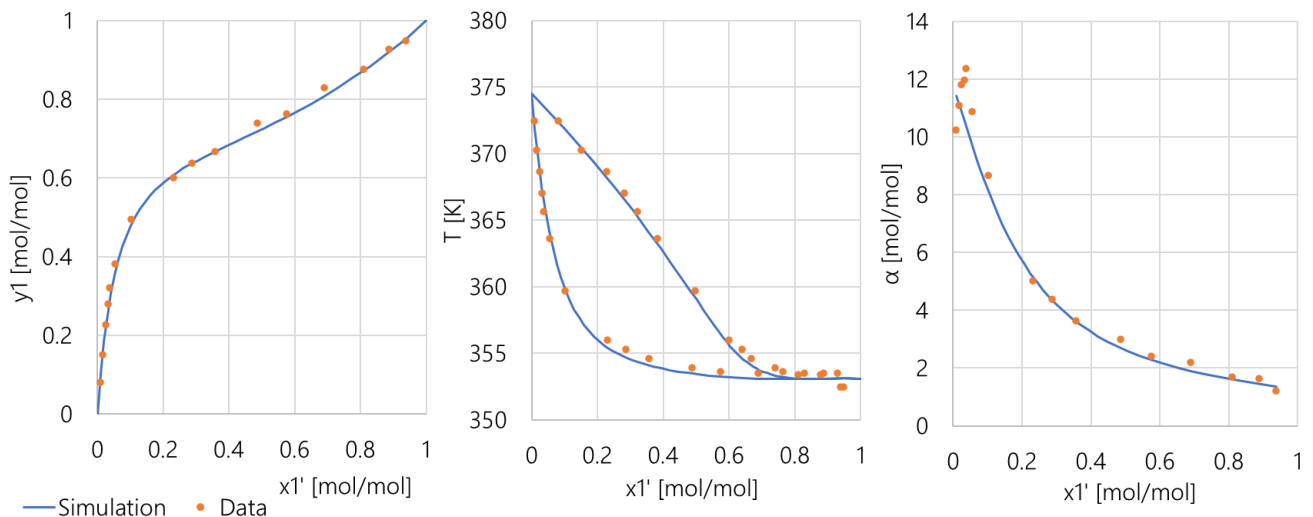


Figure A 9: Simulation results and experimental measurements for 20 wt% of ChCl:Ur (1:3) plotted in a vapor mole fraction (y_1) over the liquid mole fraction of ethanol (x_1') diagram (left), the temperature over x_1' diagram (middle), and the relative volatility (α) over x_1' diagram (right) [13].

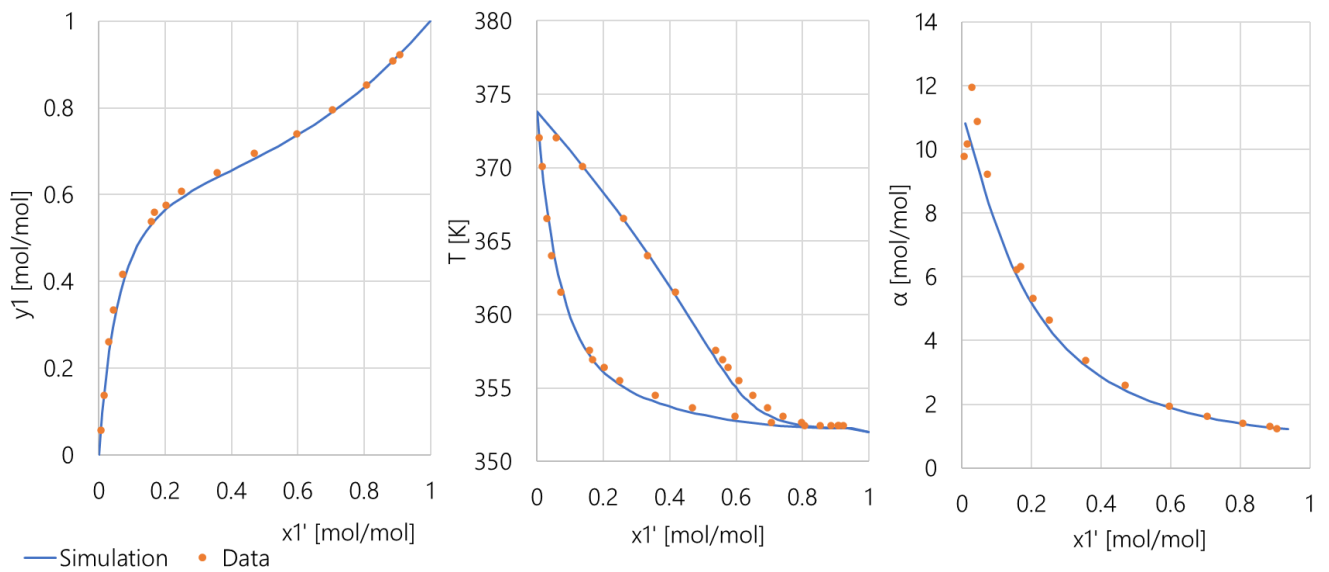


Figure A 10: Simulation results and experimental measurements for 10 wt% of ChCl:Ur (1:3) plotted in a vapor mole fraction (y_1) over the liquid mole fraction of ethanol (x_1') diagram (left), the temperature over x_1' diagram (middle), and the relative volatility (α) over x_1' diagram (right) [13].

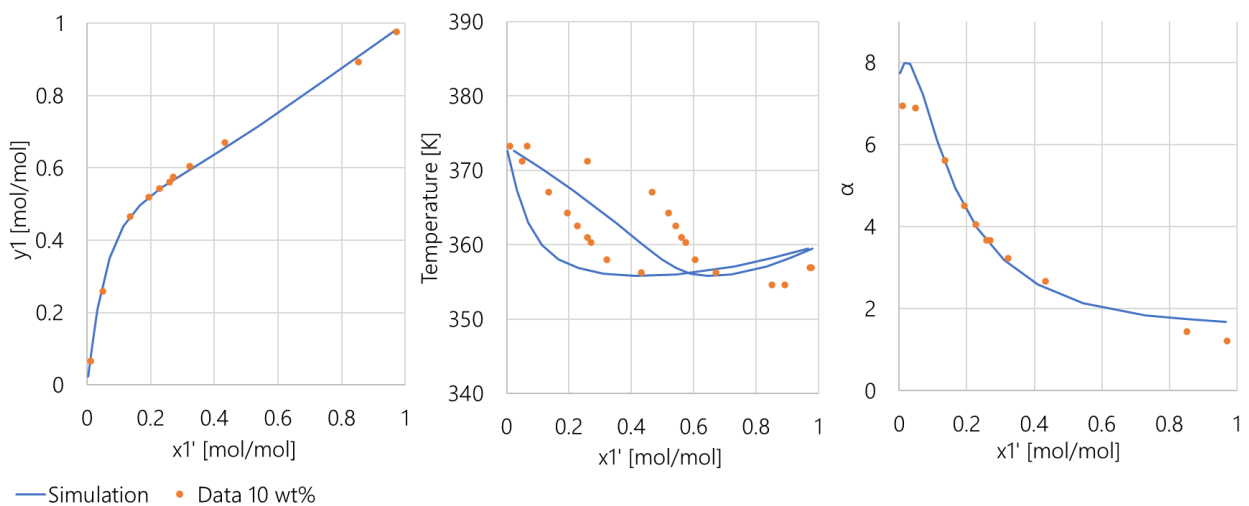


Figure A 11: Simulation results and experimental measurements for 10 wt% of ChCl:TEG (1:3) plotted in a vapor mole fraction (y_1) over the liquid mole fraction of ethanol (x_1') diagram (left), the temperature over x_1' diagram (middle), and the relative volatility (α) over x_1' diagram (right) [47].

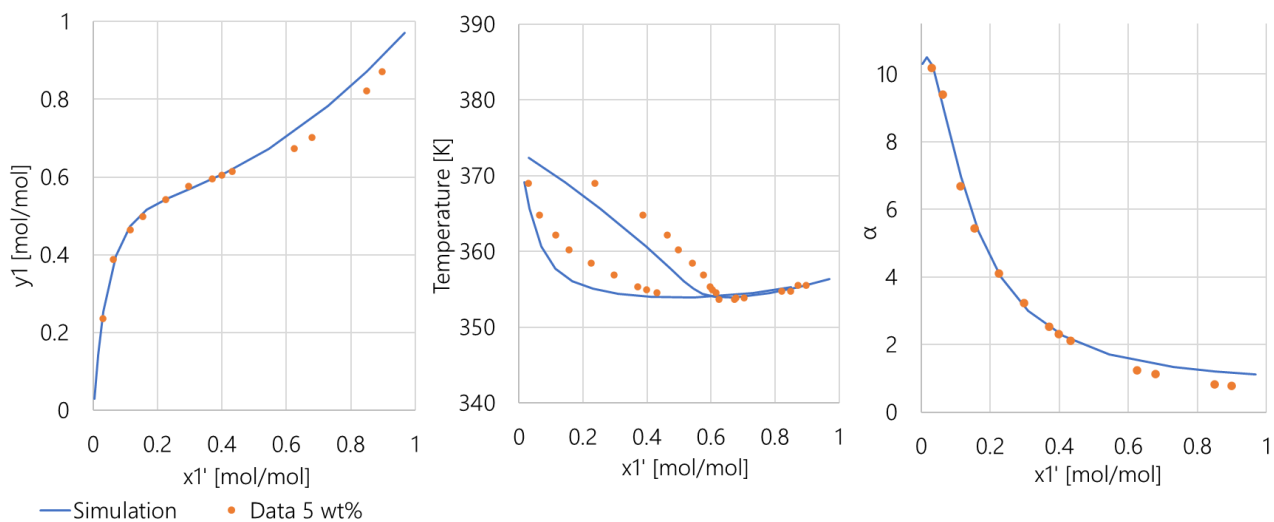


Figure A 12: Simulation results and experimental measurements for 5 wt% of ChCl:TEG (1:3) plotted in a vapor mole fraction (y_1) over the liquid mole fraction of ethanol (x_1') diagram (left), the temperature over x_1' diagram (middle), and the relative volatility (α) over x_1' diagram (right) [47].

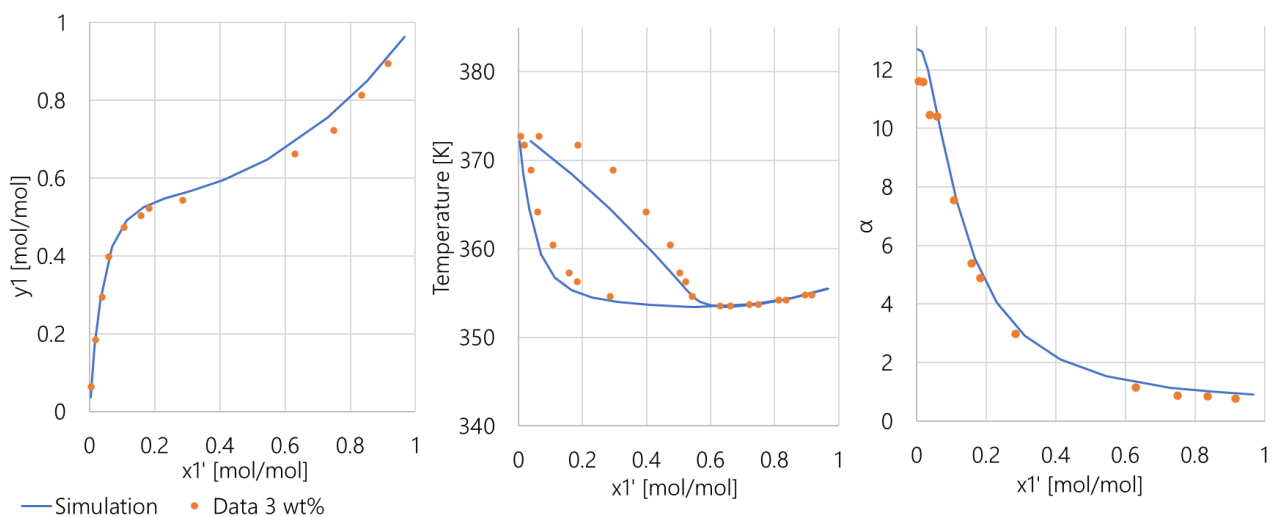


Figure A 13: Simulation results and experimental measurements for 3 wt% of ChCl:TEG (1:3) plotted in a vapor mole fraction (y_1) over the liquid mole fraction of ethanol (x_1') diagram (left), the temperature over x_1' diagram (middle), and the relative volatility (α) over x_1' diagram (right) [47].

C.4.2 Analysis of the Activity Coefficients

Ethanol and water:

To understand the underlying mechanism of the addition of the DES, the activity coefficient of ethanol (γ_1) and water (γ_2) are plotted over the mole fraction of ChCl:EG (1:2) for two different ethanol mole fractions on DES free basis (x_1). Similar plots were obtained for the other DESs ChCl:Ur (1:2) and ChCl:GA (1:3).

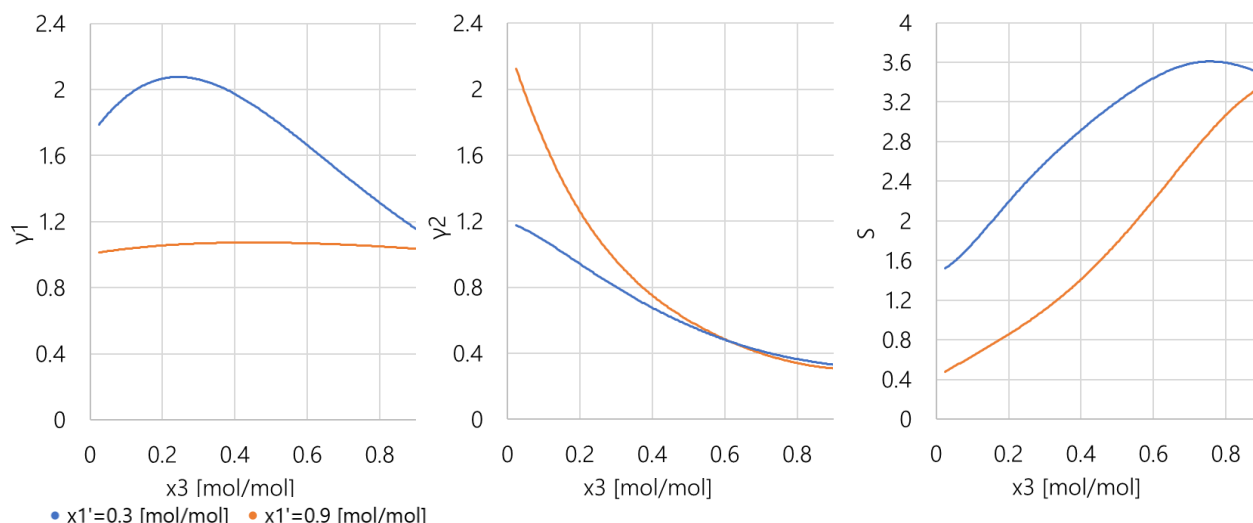


Figure A 14: Simulation results of the activity coefficient of ethanol (γ_1) (left) and water (γ_2) (middle) and the selectivity (right) as defined in Chapter B.2.2.1 plotted over the mole fraction of ChCl:EG (1:2) for two different ethanol mole fractions on entrainer free basis.

From these plots, it can be observed that γ_1 is always greater than one, which means a positive deviation from the ideality due to weaker attractive forces between the three-component system. In contrast, the activity coefficient of water also decreases below one, indicating negative deviations due to stronger attractive forces. This is in agreement with the publication of Rodriguez *et al.* (2015) and Zhang *et al.* (2018) [43, 46]. According to Shang *et al.* (2018), water and the DES have both a high hydrogen bond donor and acceptor ability. As the selectivity represents the ratio between the two activity coefficients, the opposite effects of the DES on ethanol/water enhance the selectivity, which can be seen on the right graph. Thus, the addition of the DES benefits the goal of obtaining the most volatile compound.

Water and the DES have both a high hydrogen bond donor and acceptor ability. This was investigated by Shang *et al.* (2018), who explained this with respect to the σ -profiles [46]. The σ -profiles is divided into the HBD, nonpolar and HBA region. According to his group, the peak at -0.017 e-/Å² for ChCl/Urea (1:2) in the hydrogen bond donor region can result in a preferred interaction with the peak of water in the hydrogen bond acceptor region (0.015 e-/Å²) [45]. Thus, the hydrogen bonding between the DES and water might be stronger than the water-water interaction. In contrast, ethanol shows a peak in the non-polar region and is less likely than water to form hydrogen bonds with the DESs. The forces between ethanol molecules are stronger than the hydrogen bonding to the DES [45]. In this sense, it is also clear why a higher ethanol concentration ($x_1' = 0.9$) would increase the activity coefficient of water but decrease the activity coefficient of ethanol.

IPA and water (see Figure 7):

Since the interaction between IPA and the DES is the strongest, higher IPA concentrations result in lower activity coefficients of IPA. However, for the activity coefficient of water, an inversion of behaviour can be observed. For high IPA concentrations and low DES concentrations, the interactions of water are the weakest, while increasing the DES concentration leads to the stronger interaction between water and its neighbouring molecules. This behaviour of the shifting interactions eventually leads to the inversions of the VLE curves shown in Figure 6. At high water concentrations, a smaller DES concentration leads to a better distribution to separate IPA and water. However, as the IPA concentration increases, the DES has a positive effect on the separation due to the strong hydrogen bonding interaction with IPA. The inversion of the behaviour reminds of the behaviour when two phases are formed as investigated by Zhao *et al.* (2006) [39]. The selectivity in the right plot reaches a stationary point because of the asymptote of the activity coefficients.

C.4.3 Residue Curve Maps

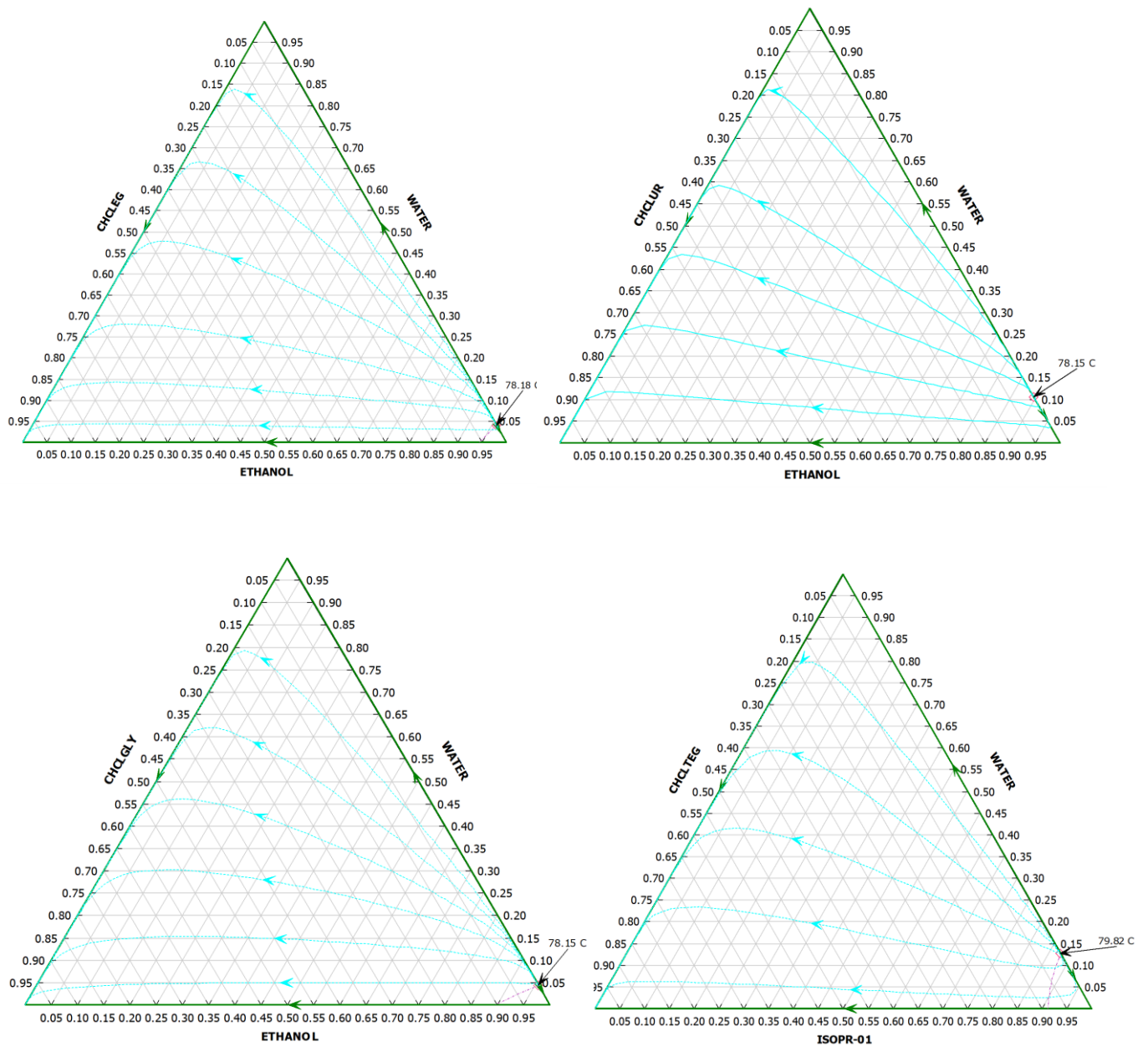


Figure A 15: Residue curve maps for the system ethanol and water with the DES ChCl:EG (1:2) (top left), ChCl:Ur (1:2) (top right), and ChCl:GA (1:3) (bottom left) and for the system IPA and water with ChCl:TEG (1:3) (bottom right) on mass basis. The isovolatility curve and azeotropic point is also shown.

C.5 Preliminary Process Synthesis: Black-Box Diagrams

1. A feed of 245 kmol/h consisting of 88.5 mol% ethanol and 11.5 mol% water is to be separated in such a way that the ethanol purity of the distillate amounts to 99.7 mol%, and the recovery of ethanol and the DES equals a minimum 99.9% and 99%, respectively. This process is compared to the process of Bastidas *et al.* (2010) using EG (see Table A 13) [30].

Given in the main text (chapter 4.1)

2. A feed of 100 kmol/h consisting of 85 mol% ethanol and 15 mol% water is to be separated in such a way that the ethanol purity of the distillate amounts to 99.9 mol%, and the recovery of ethanol and the DES equals a minimum 99.9% and 99%, respectively. This process is compared to the process of Zhu *et al.* (2016) using $[\text{Emim}]^+[\text{BF}_4]^-$ (see Table A 15) [35].

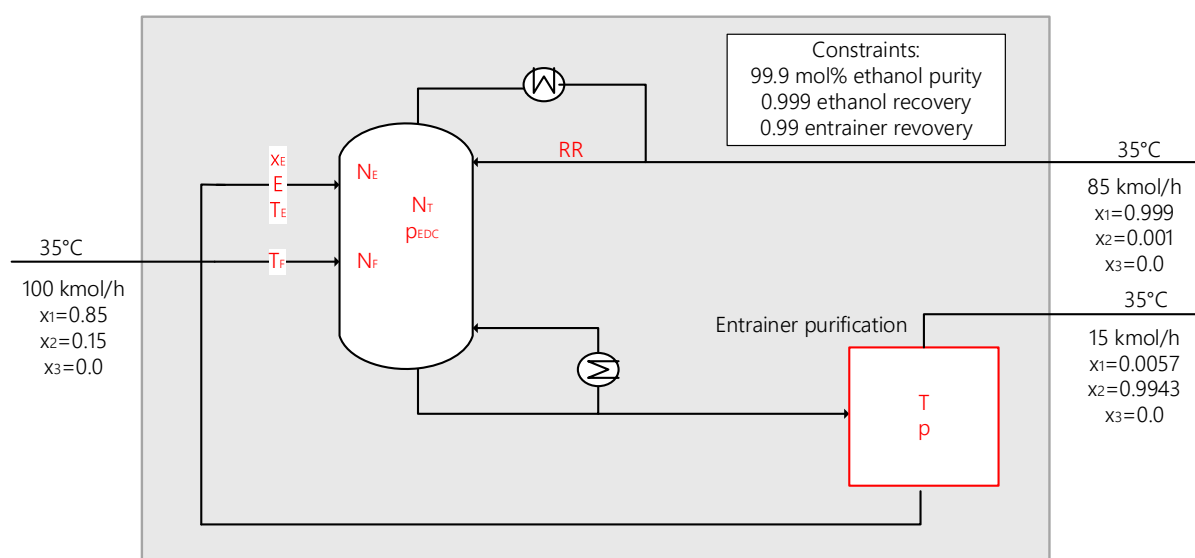


Figure A 16: Black box diagram for the separation of ethanol (1) and water (2) using the process details of Zhu *et al.* (2019) [35]. The constraints (in box) and the design variables and unknowns (in red) are given as well. However, for this diagram, the separation efficiency of the entrainer and water has been assumed to be 100%.

3. A feed of 100 kmol/h consisting of 50 mol% IPA and 50 mol% water is to be separated in such a way that the IPA purity of the distillate amounts to 99.9 mol%, and the recovery of IPA and the DES equals a minimum of 99.9% and 99%, respectively. This process is compared to the process with DMSO and $[\text{Emim}]^+[\text{N}(\text{CN})_2]^-$ (see Table A 17, and Table A 18) [25, 31, 36].

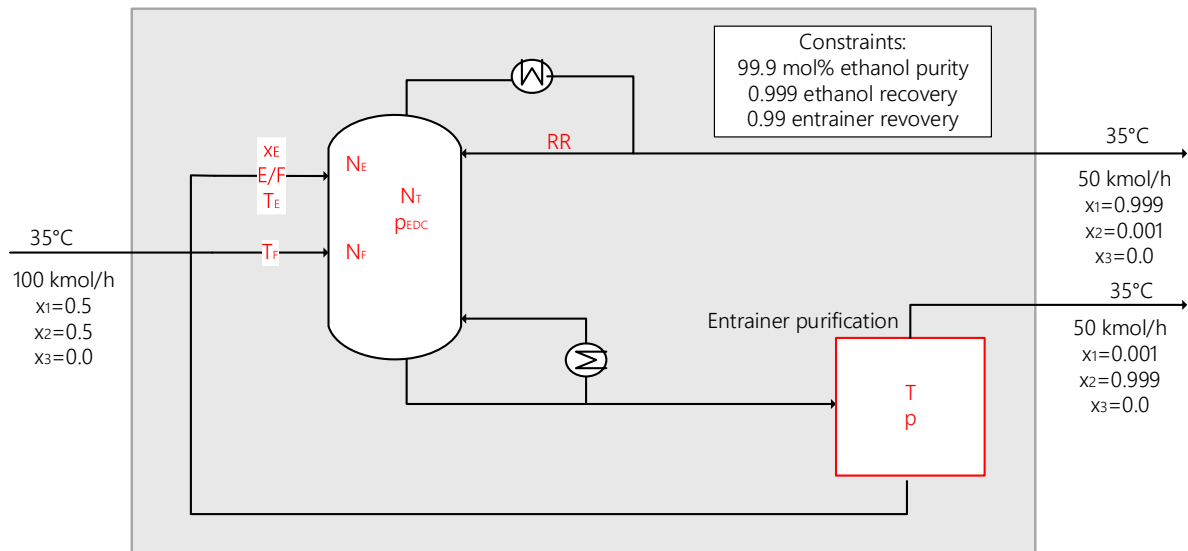


Figure A 17: Black box diagram for the separation of IPA (1) and water (2). The constraints (in box) and the design variables and unknowns (in red) are given as well. However, for this diagram, the separation efficiency of the entrainer and water has been assumed to be 100%.

C.6 Base Case Design: Entrainer Regeneration Options

Table A 38: The different regeneration technologies, and their application in the literature, advantages and disadvantages.

Regeneration technology	Remarks and processes in literature	Advantage	Disadvantage
Extraction with solvent	<ul style="list-style-type: none"> Not possible due to high water solubility of DES [116] Equilibrium data missing 	<ul style="list-style-type: none"> Simple No complex equipment Controlled recovery Moderate conditions 	<ul style="list-style-type: none"> Not efficient Loss of compounds Pre-concentration step required Potentially diminishes the "green" aspects
Extraction with $scCO_2$	<ul style="list-style-type: none"> Equilibria data missing Difficult for hydrophilic DES [61] 	<ul style="list-style-type: none"> Green Efficient Moderate conditions 	<ul style="list-style-type: none"> High costs
Induced phase separation by CO_2	<ul style="list-style-type: none"> Equilibria data missing Difficult for hydrophilic DES [60] 	<ul style="list-style-type: none"> Green Efficient Simple Moderate conditions 	<ul style="list-style-type: none"> High costs
Nanofiltration	<ul style="list-style-type: none"> DES study [32]: permeate cannot be reused DES study [32]: only small purification possible 	<ul style="list-style-type: none"> Solvent-less operation Low energy demand Simple Moderate conditions 	<ul style="list-style-type: none"> Relatively low flux and retention

Reverse Osmosis	<ul style="list-style-type: none"> • DES study [32]: only small purification possible 	<ul style="list-style-type: none"> • Solvent-less operation • Low energy demand • Moderate conditions 	<ul style="list-style-type: none"> • Relatively low flux and retention • Limited by osmotic pressure • Require pre-treatment of mixture
Pervaporation	<ul style="list-style-type: none"> • DES study [32]: only small purification possible 	<ul style="list-style-type: none"> • Solvent-less operation • Low energy demand • Moderate conditions 	<ul style="list-style-type: none"> • Require large membrane area
Adsorption	<ul style="list-style-type: none"> • Require equilibrium adsorption, desorption data • Work needed to find good adsorbent 	<ul style="list-style-type: none"> • Robust • Moderate conditions • Easy operation 	<ul style="list-style-type: none"> • Difficulty in finding suitable adsorbent for purity requirements
Vacuum distillation	<ul style="list-style-type: none"> • De <i>et al.</i> (2019) [25] • Han <i>et al.</i> (2018) [44] 	<ul style="list-style-type: none"> • Robust 	<ul style="list-style-type: none"> • High energy consumption [88] • Potential partial decomposition
Evaporation	<ul style="list-style-type: none"> • Pan <i>et al.</i> (2019) [4] • Meindersma <i>et al.</i> (2012) [41] • Zhu <i>et al.</i> (2016) [35] • Ma <i>et al.</i> (2017) [8] • Ma <i>et al.</i> (2019) [36] • Jongmans <i>et al.</i> (2012) [76] • Chen <i>et al.</i> (2017) [28] 	<ul style="list-style-type: none"> • Simple • Mostly applied • Thermally gentler than distillation column 	<ul style="list-style-type: none"> • Potential partial decomposition • High energy consumption • Not as effective as a distillation column
Stripping	<ul style="list-style-type: none"> • Seiler <i>et al.</i> (2004) [12] • Chen <i>et al.</i> (2017) [42] 	<ul style="list-style-type: none"> • Moderate conditions 	<ul style="list-style-type: none"> • Not as effective as distillation column • Requirement of refrigerant

C.7 Process Simulation

C.7.1 Sensitivity Analysis

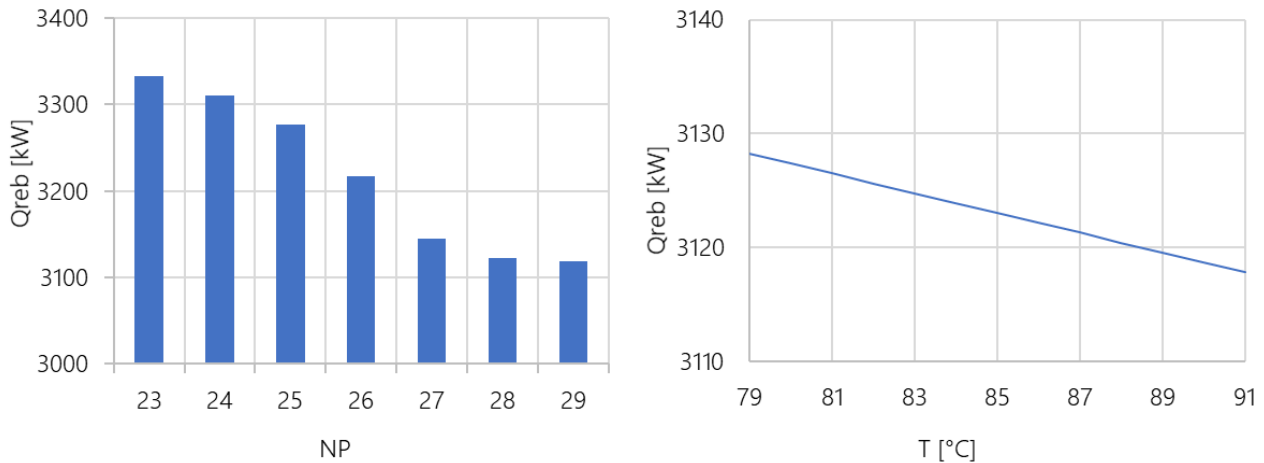


Figure A 18: Reboiler duty (Q_{reb}) for different stripping agent recycle stages (N_P) and temperatures. The purity is always adapted by RR to meet the constraint of 99.7 mol% ethanol.

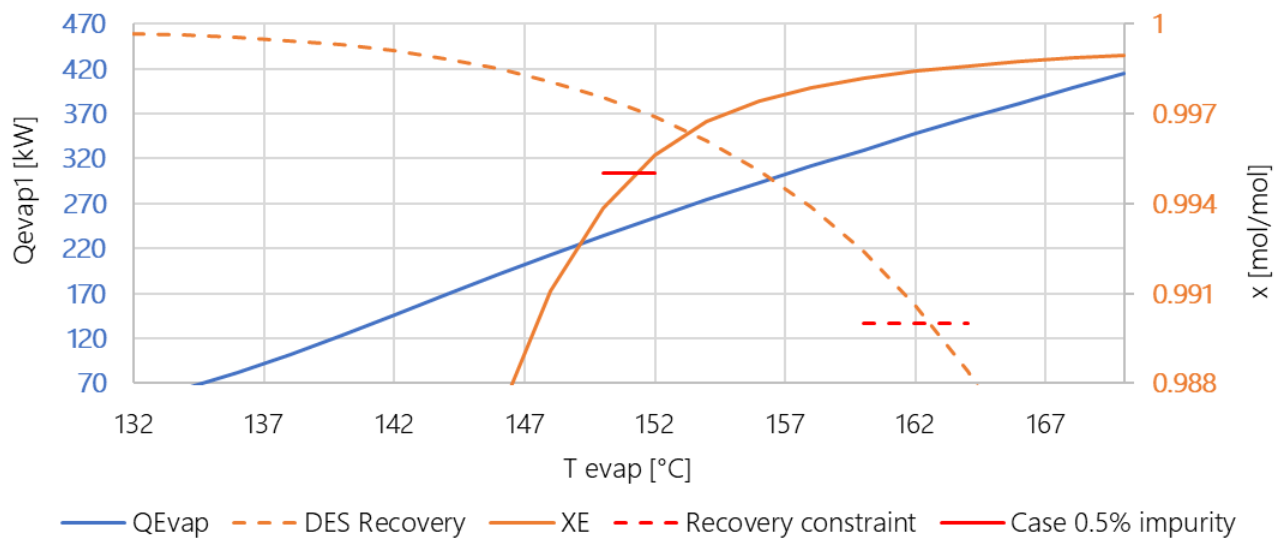


Figure A 19: Energy requirements of the evaporator (Q_{evap}) in the evaporator and stripping process and purity (x_E) and recovery of the entrainer of the recycle stream. Shown are also the purity and recovery constraints.

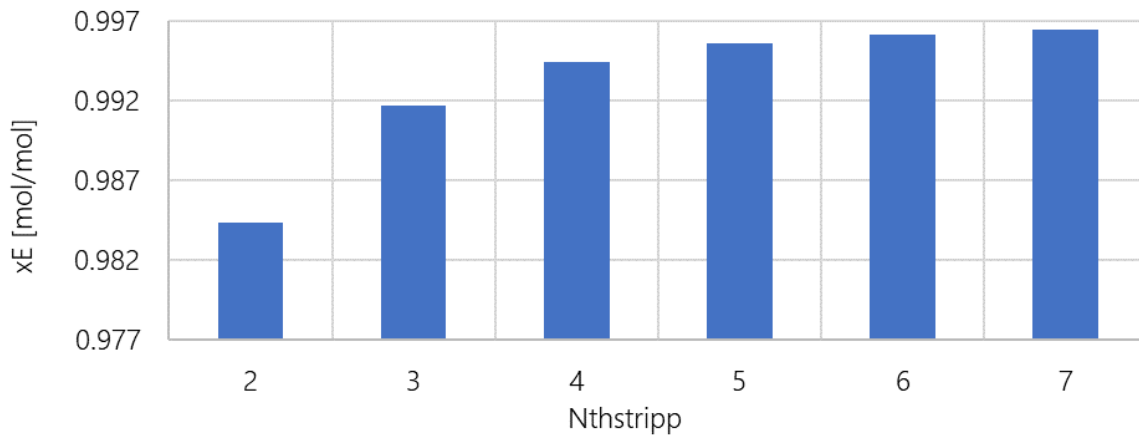


Figure A 20: Purity of the entrainer recycle stream for different total number of stages of the stripping column.

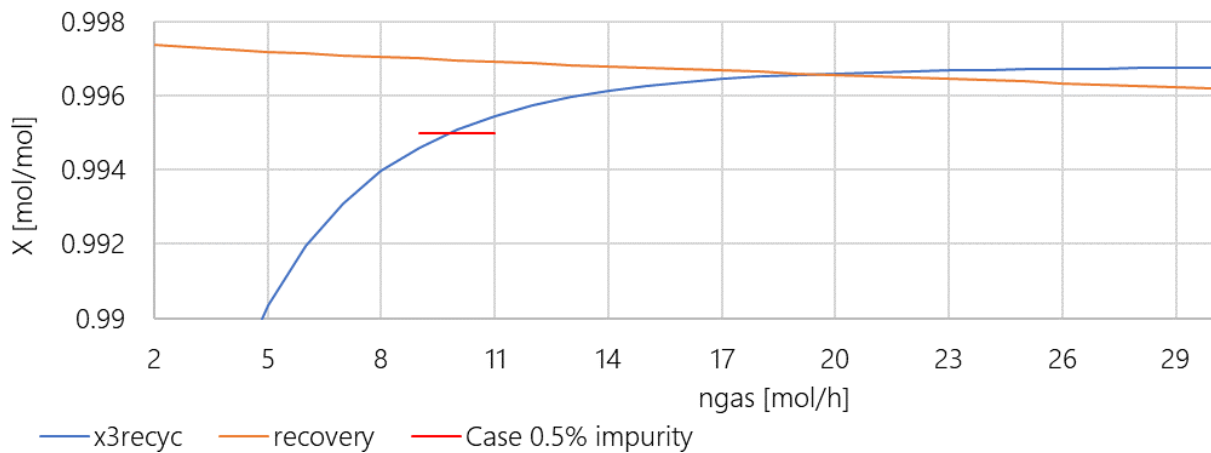


Figure A 21: Recovery and purity of the entrainer recycle stream over the stripping agent flowrate (n_{gas}). Shown is also the purity constraint.

C.8 Base Case Designs

C.8.1 Aspen Flow Sheets before Heat Integration

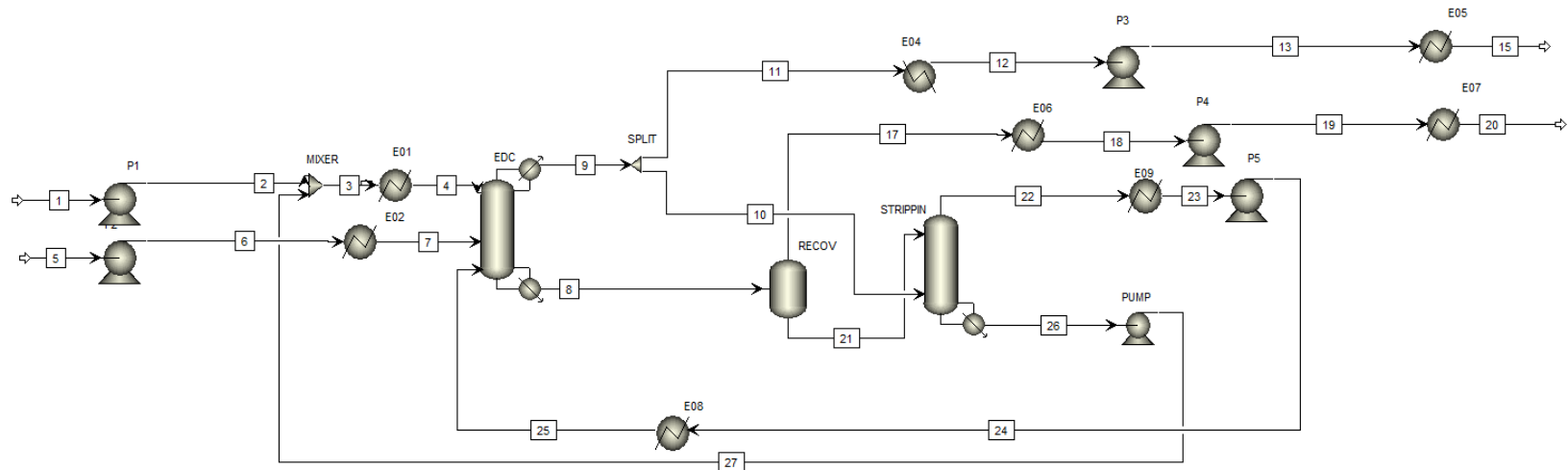


Figure A 22: Aspen Plus flowsheet of the base case design with the EDC operating at 1 atm and using a stripping column as entrainer regeneration option [18].

Table A 39: Process stream summary of the base case design with the EDC operating at 1 atm and using a stripping column as entrainer regeneration option.

Stream No	1	2	3	4	5	6	7	8	9	10	11	12	13
Temperature [°C]	35	35.1	87.8	73	35	35.1	83	154.4	78.3	78.3	78.3	78.3	78.3
Pressure [kPa]	101.3	160	160	125	101.3	160	125	124.8	101.3	101.3	101.3	101.3	135
Negative enthalpy flow [kW]	1.9	1.9	1220.2	1276.4	18864	18864	18438	4772.7	14600	642.42	13957	16322	16322
Vapor fraction	0	0	0	0	0	0	0	0	1	1	1	0	0
Mole Flow [kmol/hr]	0.10	0.10	72.04	72.04	245.00	245.00	245.00	121.43	227.26	10.00	217.26	217.26	217.26
Mole Frac													
CHCLUR	1	1	0.991	0.991	0	0	0	0.589	0	0	0	0	0
WATER	0	0	0.005	0.005	0.115	0.115	0.115	0.409	0.003	0.003	0.003	0.003	0.003
ETHANOL	0	0	0.003	0.003	0.885	0.885	0.885	0.002	0.997	0.997	0.997	0.997	0.997

Stream No	15	17	18	19	20	21	22	23	24	25	26	27
Temperature [°C]	35	150	76.9	76.9	35	150	100	-4.9	-4.7	86	87.6	87.8
Pressure [kPa]	101.3	45	45	135	101.3	45	2	1	160	125	2	160
Negative enthalpy flow [kW]	16675.0	1829.6	2172.9	2172.8	2198	2646.5	2069.9	2502.7	2502.5	2427.3	1219	1218.3
Vapor fraction	0	1	0	0	0	0	1	0	0	0	0	0
Mole Flow [kmol/hr]	217.26	27.84	27.84	27.84	27.84	93.60	31.66	31.66	31.66	31.66	71.94	71.94
Mole Frac												
CHCLUR	0	0.004	0.004	0.004	0.004	0.763	0.004	0.004	0.004	0.004	0.991	0.991
WATER	0.003	0.989	0.989	0.989	0.989	0.237	0.688	0.688	0.688	0.688	0.005	0.005
ETHANOL	0.997	0.008	0.008	0.008	0.008	0	0.308	0.308	0.308	0.308	0.003	0.003

The Flowsheet is given in the main text (see Figure 19)

Table A 41: Process stream summary of the base case design with the EDC operating at 1 atm and using only evaporators as entrainer regeneration option.

Stream No	1	2	3	5	6	7	8	9	10	11	12	13	
Temperature [°C]	35	35.1	120.9	35	35.1	83	78.3	78.3	78.3	78.3	78.3	35	
Pressure [kPa]	101	160	160	101.3	160	125	101	101	101	101.3	135	101.3	
Negative enthalpy flow [kW]	11.9	11.9	978.33	18864	18864	18438	16137	18872	2550	16322	16322	16675	
Vapor fraction	0	0	0	0	0	0	1	0	0	0	0	0	
Mole Flow [kmol/hr]	0.6	0.6	65.6	245.0	245.0	245.0	251.2	251.2	33.9	217.3	217.3	217.3	
<i>Mole Frac</i>													
CHCLUR	1	1	0.995	0	0	0	0	0	0	0	0	0	
WATER	0	0	0.005	0.115	0.115	0.115	0.003	0.003	0.003	0.003	0.003	0.003	
ETHANOL	0	0	0	0.885	0.885	0.885	0.997	0.997	0.997	0.997	0.997	0.997	
Stream No	14	15	16	17	18	19	20	21	22	23	24	25	26
Temperature [°C]	168.8	106	15.2	9.9	35	106	121.5	-6.7	-6.6	35	121.5	121.7	73
Pressure [kPa]	121.3	2	2	135	101.3	2	0.3	0.3	135	101.3	0.3	160	125
Negative enthalpy flow [kW]	2935.6	1585.6	1906.8	1906.7	1894.1	1334.3	253.86	320.76	320.74	315.86	967.15	966.42	1148.4
Vapor fraction	0	1	0	0	0	0	1	0	0	0	0	0	0
Mole Flow [kmol/hr]	93.3	24.0	24.0	24.0	24.0	69.3	4.3	4.3	4.3	4.3	65.0	65.0	65.6
<i>Mole Frac</i>													
CHCLUR	0.699	0.006	0.006	0.006	0.006	0.94	0.112	0.112	0.112	0.112	0.995	0.995	0.995
WATER	0.298	0.985	0.985	0.985	0.985	0.06	0.888	0.888	0.888	0.888	0.005	0.005	0.005
ETHANOL	0.002	0.009	0.009	0.009	0.009	0	0	0	0	0	0	0	0

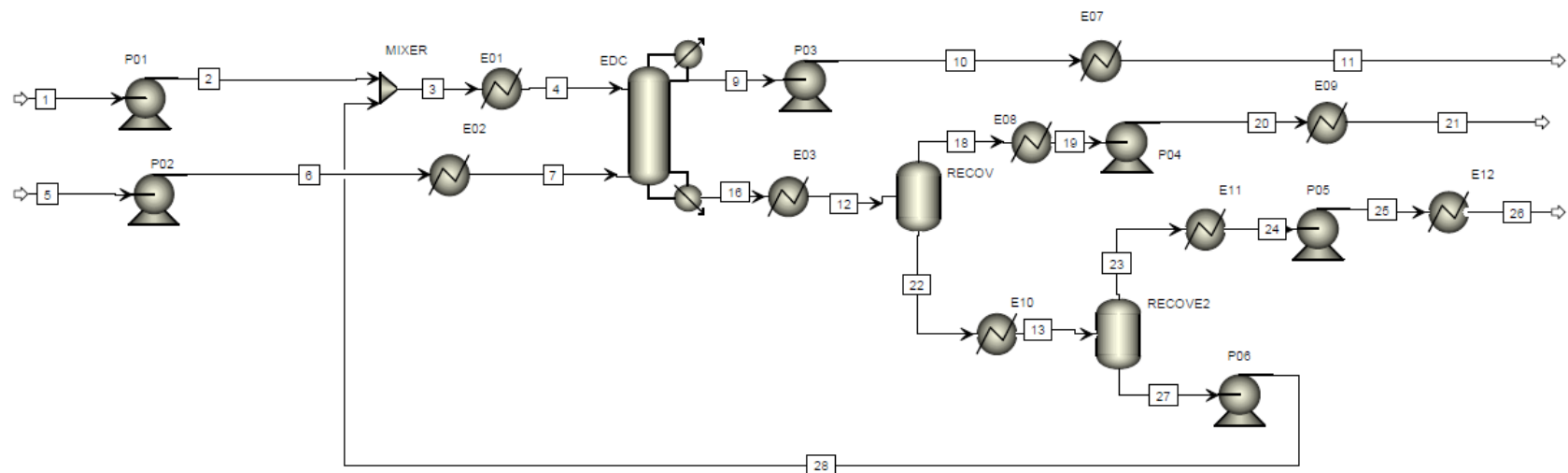


Figure A 24: Aspen Plus flowsheet of the base case design with the EDC operating at 14kPa and using only evaporators as entrainer regeneration option [18].

Table A 42: Process stream summary of the base case design with the EDC operating at 14kPa and using only evaporators as entrainer regeneration option [18].

Stream No	1	2	3	4	5	6	7	9	10	11	16
Temperature [°C]	35	35.1	120.9	35	35	35.1	78	35.2	35.3	35	118.4
Pressure [kPa]	101.3	160	160	101.3	101.3	160	101.3	14	135	101.3	34
Negative enthalpy flow [kW]	10.0	10.0	790.93	1031.9	18864	18864	18486	16674	16673	16675	2974.0
Vapor fraction	0	0	0	0	0	0	0	0	0	0	0
Mole Flow [kmol/hr]	0.5	0.5	53.0	53.0	245.0	245.0	245.0	217.3	217.3	217.3	80.8
Mole Frac											
CHCLUR	1	1	0.995	0.995	0	0	0	0	0	0	0.653
WATER	0	0	0.005	0.005	0.115	0.115	0.115	0.003	0.003	0.003	0.344
ETHANOL	0	0	0	0	0.885	0.885	0.885	0.997	0.997	0.997	0.003
Stream No	18	19	20	21	22	23	24	25	26	27	28
Temperature [°C]	107.7	15.2	10	35	107.7	121.5	-6.7	-6.6	35	121.5	121.7
Pressure [kPa]	2	2	135	101.3	2	0.3	0.3	101.3	101.3	0.3	160
Negative enthalpy flow [kW]	1648.0	1982.8	1982.7	1969.6	1056.3	191.4	241.84	241.83	238.14	781.55	780.91
Vapor fraction	1	0	0	0	0	1	0	0	0	0	0
Mole Flow [kmol/hr]	25.0	25.0	25.0	25.0	55.8	3.3	3.3	3.3	3.3	52.5	52.5
Mole Frac											
CHCLUR	0.006	0.006	0.006	0.006	0.943	0.112	0.112	0.112	0.112	0.995	0.995
WATER	0.985	0.985	0.985	0.985	0.057	0.888	0.888	0.888	0.888	0.005	0.005
ETHANOL	0.009	0.009	0.009	0.009	0	0	0	0	0	0	0

C.8.2 Process Design Variables

Table A 43: Optimised design parameters of the EDC operating at 1 atm, and the evaporators.

Design Parameter	EDC	Evaporator 1	Evaporator 2
N_{th}	30		
N_F	22		
T_F [°C]	83		
N_E	3		
T_E [°C]	73		
Mole RR	0.156		
E/F	0.26		
Tops rate [kmol/h]	217.26	24	4
Duty [kW]	3064	297	33
Pressure [kPa]	101 (Condenser)	2	0.3
Temperature [°C]		106	121.5

Table A 44: Optimised design parameters of the EDC operating at 14 kPa, and the evaporators.

Design Parameter	EDC	Evaporator 1	Evaporator 2
N_{th}	30		
N_F	22		
T_F [°C]	83		
N_E	3		
T_E [°C]	30		
Mole RR	0.152		
E/F	0.21		
Tops rate [kmol/h]	217.26	25	3
Duty [kW]	2758	308	26
Pressure [kPa]	14 (Condenser)	2	0.3
Temperature [°C]		107.7	121.5

Table A 45: Optimised design parameters of the EDC operating at 1 atm, the evaporators, and the stripping column.

Design Parameter	EDC	Evaporator 1	Stripping Column
N_{th}	35		
N_F	22		
T_F [°C]	83		
N_E	3		
T_E [°C]	73		
Mole RR	0.14		
E/F	0.29		
Tops rate [kmol/h]	217.26	28	32
Duty [kW]	3127	321	
Pressure [kPa]	101 (Condenser)	45	2
Temperature [°C]		150	100 – top / 88 – bottom
n_{gas} [kmol/h]			10
N_P	32		
T_P [°C]	86		

Table A 46: Optimised design parameters of the EDC operating at 1 atm, the evaporators, and the stripping column.

Design Parameter	EDC	Evaporator 1	Stripping Column
N_{th}	35		5
N_F	22		
T_F [°C]	78		
N_E	3		
T_E [°C]	30		
Mole RR	0.148		
E/F	0.23		
Tops rate [kmol/h]	217.26	28	27
Duty [kW]	2889	321	
Pressure [kPa]	14 (Condenser)	45	2
Temperature [°C]		149	97 – top / 81 – bottom
n_{gas} [kmol/h]			10
N_P	32		
T_P [°C]	80		

C.8.3 Heat integration

Base case design: EDC 1 atm evaporators

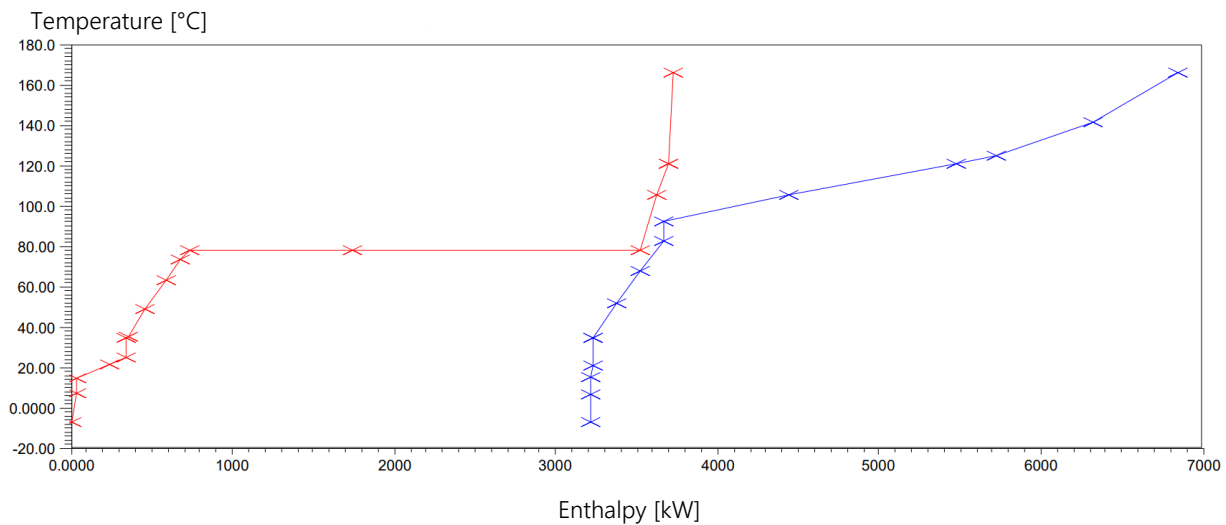


Figure A 25: Hot (red) and cold (blue) composite curve for the 1 atm EDC base case with two evaporators [18].

Table A 47: Solutions for heat integration found by the Aspen Plus Energy Analyser for the process shown in Figure 19 using two evaporators and the EDC at 1atm [18]. Each solution shows the energy saving in percent, the payback in years, and the heat exchanger locations. Implemented solutions and rejected solutions are marked in green and red, respectively.

Solution No.	Energy savings [%]	Payback [y]	Hot fluid side	Cold fluid side
1	6.98	1.71	Upstream to E07	Upstream to E02
2	4.21	1.83	Upstream to E01	Upstream to E02
3	0.63	6.34	Upstream to E11	Upstream to E09

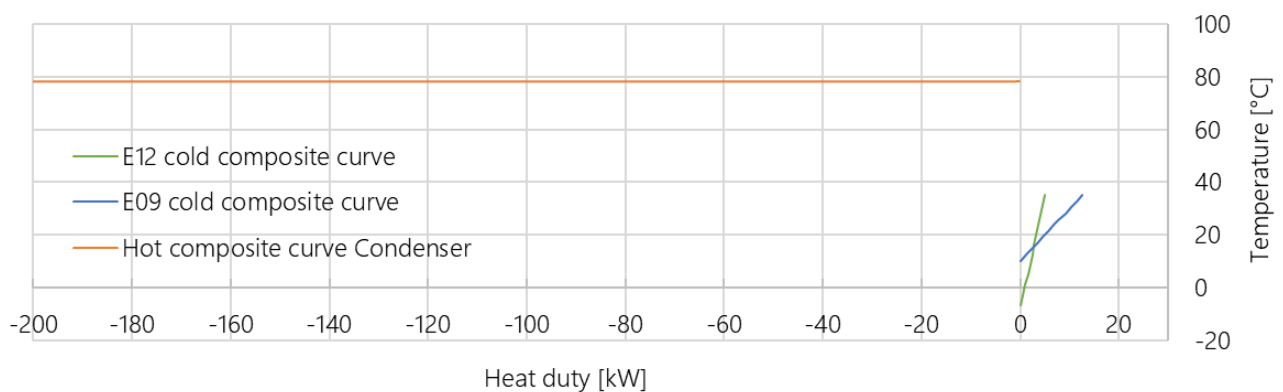


Figure A 26: Composite curves of the remaining to heaters using utilities (green and blue) and the condenser of the EDC for the process using two evaporators and the EDC at 1 atm. The potentially saved energy requirements are too small for profitable process heat integration and are therefore rejected.

Base case design: EDC 14 kPa evaporators

Table A 48: Solutions for heat integration found by the Aspen Plus Energy Analyser for the process shown in Figure A 24 for the process using 2 evaporators and the EDC at 14 kPa [18]. Each solution shows the energy saving in percent, the payback in years, and the heat exchanger locations. Implemented solutions and rejected solutions are marked in green and red, respectively.

Solution No.	Energy-saving [%]	Payback [y]	Hot fluid side	Cold fluid side
1	5.92	1.63	Upstream to E01	Upstream to E02
2	0.35	7.28	Upstream to E06	Upstream to E03
3	0.34	8.03	Upstream to E06	Upstream to E02

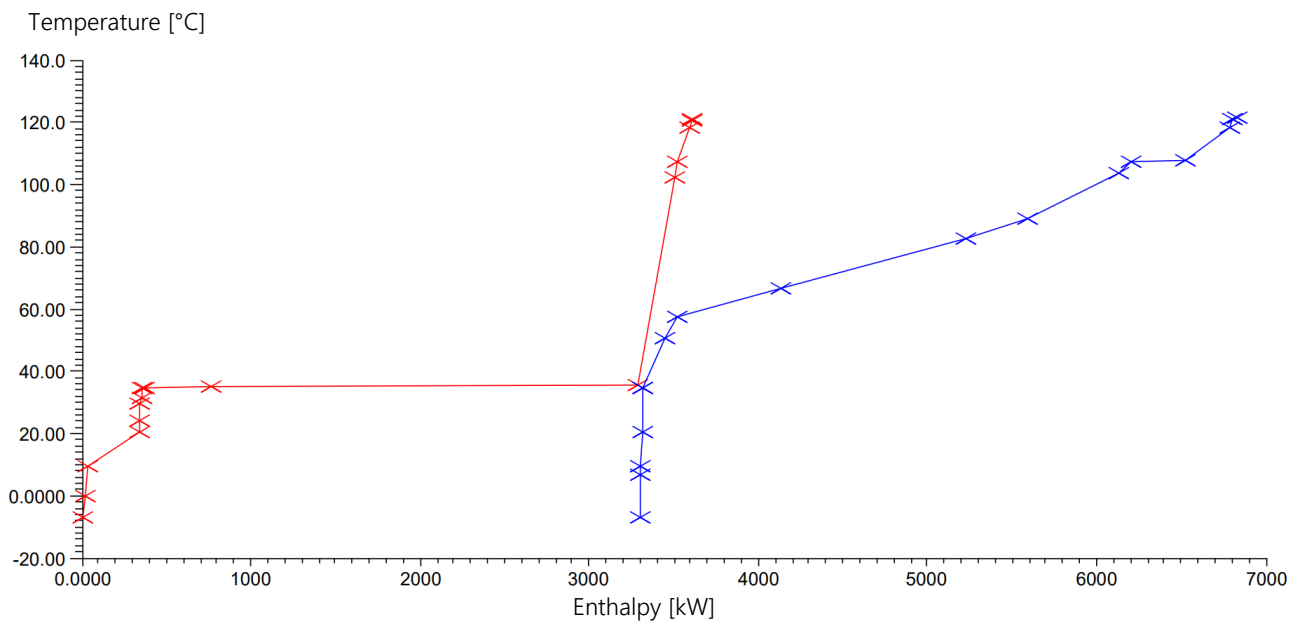


Figure A 27: Hot (red) and cold (blue) composite curve of the process using 2 evaporators and the EDC operating at 14 kPa. Less energy savings are possible than for the 1atm process [18].

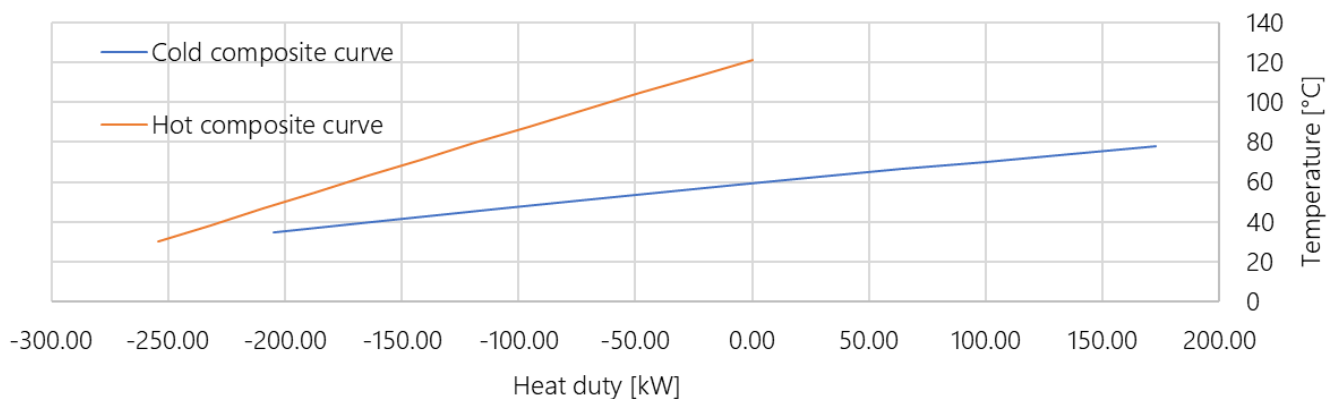


Figure A 28: Composite curves of the integrated process part for the process using 2 evaporators and the EDC at 14 kPa. The hot composite curve (orange) is the entrainer recycle cooling (E01), and the cold composite curve is the main feed (E02).

Base case design: EDC 1 atm stripping

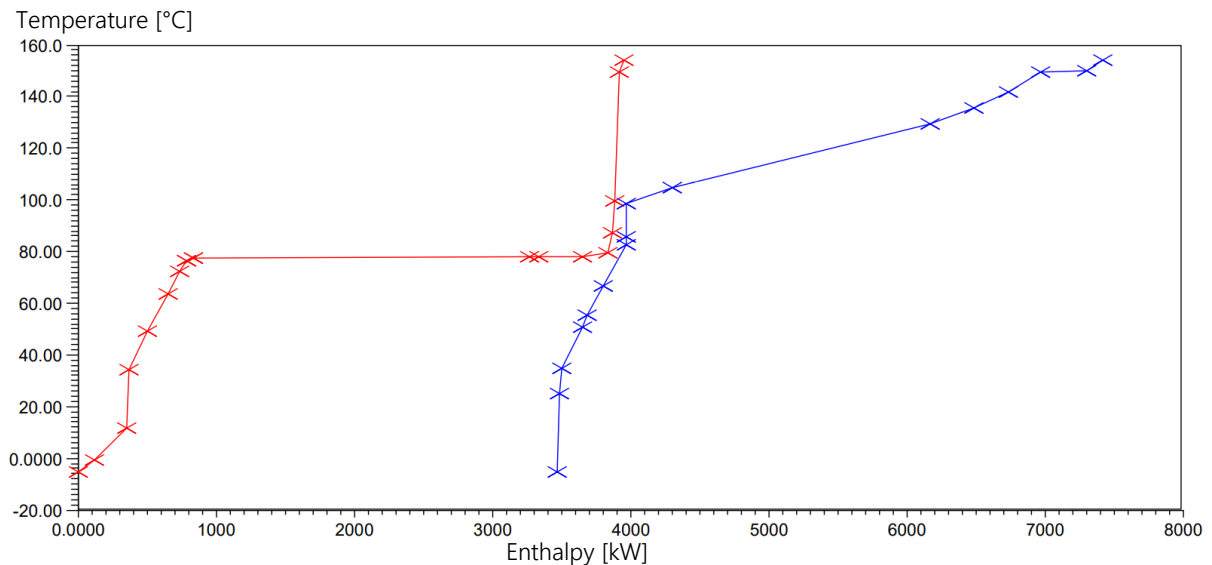


Figure A 29: Hot (red) and cold (blue) composite curve in a diagram of the temperature over the enthalpy for the process using a stripping column and the EDC at 101 kPa [18].

Less heat integration is possible than for the evaporator 1 atm EDC base case. The reason for this is that the entrainer recycle that leaves the stripping column is closer to the target temperature than for the evaporator cases (E01: ~55kW). Moreover, since the evaporator operates at a much higher temperature, the cooler E03 before that heat exchanger has a small duty.

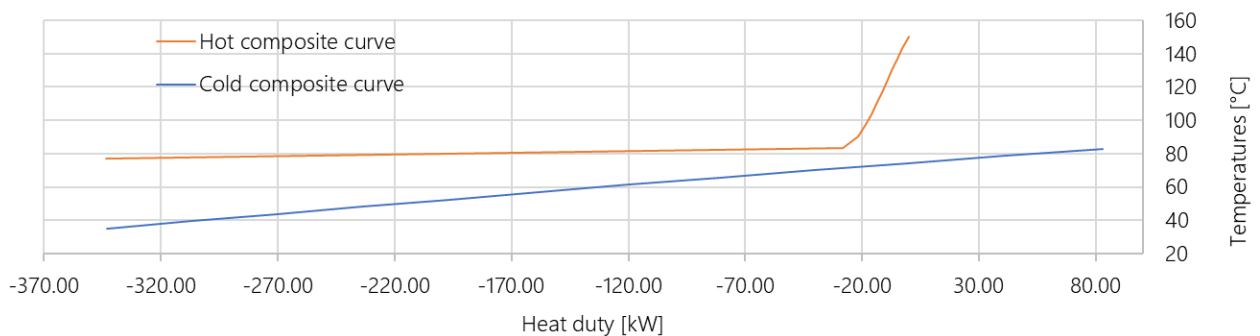


Figure A 30: Composite curves of the integrated process part for the process using a stripping column and the EDC at 101 kPa. The hot composite curve (orange) is the vapour that needs cooling after the evaporator (E06), and the cold composite curve (blue) is the main feed (E02).

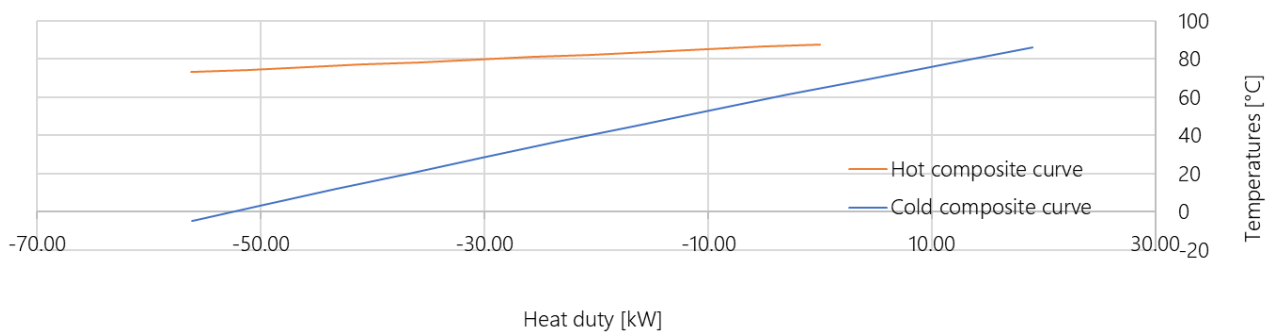


Figure A 31: Composite curves of the integrated process part for the process using a stripping column and the EDC at 101 kPa. The hot composite curve (orange) is the entrainer recycle cooling (E01), and the cold composite curve (blue) is the ethanol and water mixture coming from the stripping column as recycle to the EDC.

C.8.4 Heat-Integrated Aspen Flow Sheets & Process Stream Summaries

The process flow sheet is given in the main text in Figure 21

Table A 49: Process stream summary of the heat-integrated base case design with the EDC operating at 101 kPa and using only evaporators as entrainer regeneration option

Stream No	1	2	3	4	5	6	7	8	9	10	11	12	13	14
Temperature [°C]	35	35.1	73	35	35.1	66.5	83.2	154.4	78.3	78.3	78.3	78.3	45.9	35
Pressure [kPa]	101	160	125	101.3	190	160	125	124.8	101.3	101.3	101.3	170	135	101.3
Negative enthalpy flow [kW]	11.3	11.3	1067.9	18864	18863	18593	18435	4772.7	14600	642.42	16322	16322	16592	16675
Vapor fraction	0	0	0	0	0	0	0	0	1	1	0	0	0	0
Mole Flow [kmol/hr]	0.6	0.6	61.0	245.0	245.0	245.0	245.0	121.43	227.26	10.00	217.3	217.3	217.3	217.3
<i>Mole Frac</i>														
CHCLUR	1	1	0.995	0	0	0	0	0.589	0	0	0	0	0	0
WATER	0	0	0.005	0.115	0.115	0.115	0.115	0.409	0.003	0.003	0.003	0.003	0.003	0.003
ETHANOL	0	0	0	0.885	0.885	0.885	0.885	0.002	0.997	0.997	0.997	0.997	0.997	0.997
Stream No	15	16	17	18	19	20	21	22	23	24	25	26	27	
Temperature [°C]	166.6	106	25.2	9.9	35	106	121.5	-6.7	-6.6	35	121.5	121.7	73.4	
Pressure [kPa]	121.3	2	2	135	100	2	0.3	0.3	135	101.3	0.3	160	125	
Negative enthalpy flow [kW]	2897	1603.5	1928.2	1928.2	1915.4	1240.8	236.11	298.34	298.32	293.78	899.31	898.61	1056.6	
Vapor fraction	0	1	0	0	0	0	1	0	0	0	0	0	0	
Mole Flow [kmol/hr]	89.4	24.3	24.3	24.3	24.3	64.5	4.0	4.0	4.0	4.0	60.4	60.4	60.4	
<i>Mole Frac</i>														
CHCLUR	0.686	0.006	0.006	0.006	0.006	0.94	0.112	0.112	0.112	0.112	0.995	0.995	0.995	
WATER	0.311	0.986	0.986	0.986	0.986	0.06	0.888	0.888	0.888	0.888	0.005	0.005	0.005	
ETHANOL	0.002	0.009	0.009	0.009	0.009	0	0	0	0	0	0	0	0	



Stream No	1	2	3	4	5	6	7	8	12	13	14	20
Temperature [°C]	35	35	47.7	30	35	35.1	59.2	78	35.2	35.3	58.4	107.7
Pressure [kPa]	100	135	135	101.3	101.3	170	135	101.3	14	101.3	34	2
Negative enthalpy flow [kW]	10.0	10.0	989.35	1036.5	18864	18864	18659	18486	16674	16673	19264	1649.6
Vapor fraction	0	0	0	0	0	0	0	0	0	0	0	1
Mole Flow [kmol/hr]	0.5	0.5	52.6	52.6	245.0	245.0	245.0	245.0	217.3	217.3	285.4	25.0
Mole Frac												
CHCLUR	1	1	0.995	0.995	0	0	0	0	0	0	0.184	0.006
WATER	0	0	0.005	0.005	0.115	0.115	0.115	0.115	0.003	0.003	0.698	0.986
ETHANOL	0	0	0	0	0.885	0.885	0.885	0.885	0.997	0.997	0.118	0.008
Stream No	21	22	23	24	26	27	28	29	30	31	32	26
Temperature [°C]	15.4	10.1	35	107.7	121.5	-6.6	-6.5	35	121.5	121.7	47.8	121.5
Pressure [kPa]	2	135	101.3	2	0.3	0.3	135	101.3	0.3	170	135	0.3
Negative enthalpy flow [kW]	1984.5	1984.5	1971.4	1047.6	189.92	239.96	239.95	236.3	774.99	774.32	979.32	189.92
Vapor fraction	0	0	0	0	1	0	0	0	0	0	0	1
Mole Flow [kmol/hr]	25.0	25.0	25.0	55.3	3.2	3.2	3.2	3.2	52.1	52.1	52.1	3.2
Mole Frac												
CHCLUR	0.006	0.006	0.006	0.943	0.112	0.112	0.112	0.112	0.995	0.995	0.995	0.112
WATER	0.986	0.986	0.986	0.057	0.888	0.888	0.888	0.888	0.005	0.005	0.005	0.888
ETHANOL	0.008	0.008	0.008	0	0	0	0	0	0	0	0	0

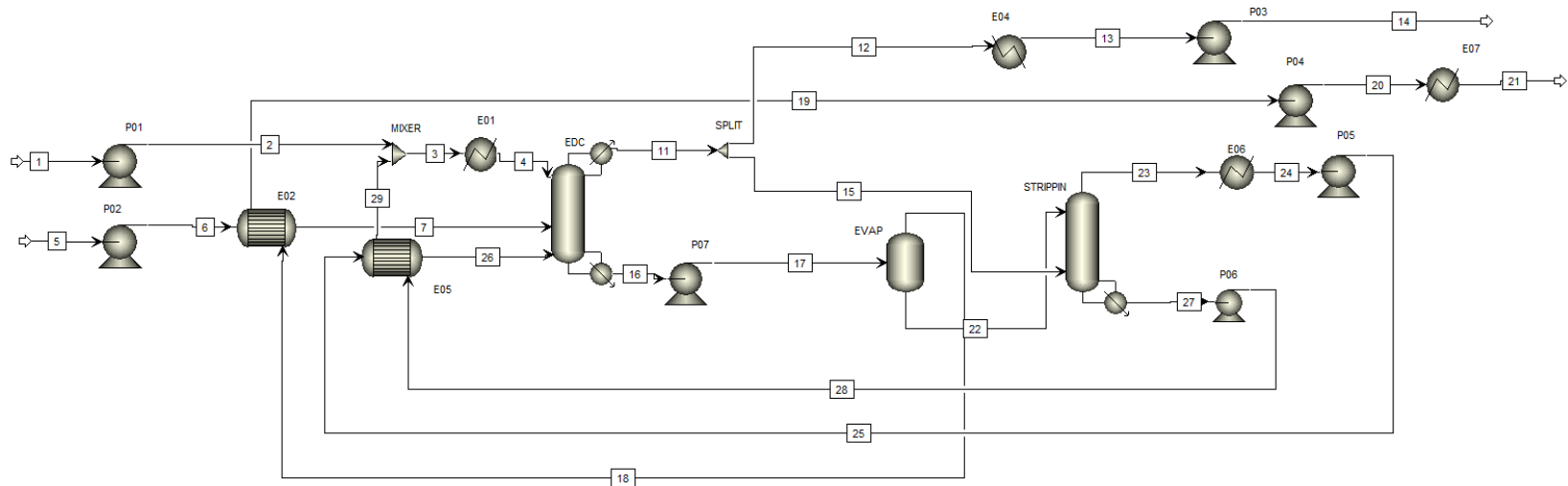


Figure A 33: Aspen Plus flowsheet of the heat-integrated base case design with the EDC operating at 14 kPa and the stripping column as entrainer regeneration option [18].

Table A 51: Process stream summary of the heat-integrated base case design with the EDC operating at 14 kPa and the stripping column as entrainer regeneration option.

Stream No	1	2	3	4	5	6	7	11	12	13	14	15	16
Temperature [°C]	35	35	63.1	30	35	35	74.3	35.2	35.2	35.2	35.3	35.2	110.9
Pressure [kPa]	101.3	135	135	101.3	101.3	135	101.3	14	14	14	101.3	14	37.4
Negative enthalpy flow [kW]	1.9	1.9	1023.7	1118.3	18864	18864	18521	14791	14140	16674	16673	650.83	4418
Vapor fraction	0	0	0	0	0	0	0	1	1	0	0	1	0
Mole Flow [kmol/hr]	0.1	0.1	56.1	56.1	245.0	245.0	245.0	227.3	217.3	217.3	217.3	10.0	101.2
Mole Frac													
CHCLUR	0.978	0.978	0.991	0.991	0	0	0	0	0	0	0	0	0.55
WATER	0.014	0.014	0.005	0.005	0.115	0.115	0.115	0.003	0.003	0.003	0.003	0.003	0.448
ETHANOL	0.009	0.009	0.004	0.004	0.885	0.885	0.885	0.997	0.997	0.997	0.997	0.997	0.002
Stream No	17	18	19	20	21	22	23	24	25	26	27	28	29
Temperature [°C]	110.9	149	76.9	77	35	149	97.4	-5.1	-4.9	71.1	81.7	81.9	63.2
Pressure [kPa]	101.3	45	45	135	101.3	45	2	1	135	101.3	2	160	135
Negative enthalpy flow [kW]	4417.6	1830.0	2172.9	2172.8	2198.1	2102.6	1786	2159.7	2159.6	2104.6	967.45	966.81	1021.8
Vapor fraction	0	1	0	0	0	0	1	0	0	0	0	0	0
Mole Flow [kmol/hr]	101.2	27.8	27.8	27.8	27.8	73.3	27.3	27.3	27.3	27.3	56.0	56.0	56.0
Mole Frac													
CHCLUR	0.55	0.003	0.003	0.003	0.003	0.758	0.003	0.003	0.003	0.003	0.991	0.991	0.991
WATER	0.448	0.989	0.989	0.989	0.989	0.242	0.64	0.64	0.64	0.64	0.005	0.005	0.005
ETHANOL	0.002	0.007	0.007	0.007	0.007	0	0.357	0.357	0.357	0.357	0.004	0.004	0.004

C.8.5 Utility Summary

Table A 53: Summary of all utilities used for each equipment for the base case design with the 1 atm EDC and two evaporators. The equipment numbering equals the flowsheet shown in Figure 21. Additionally to this flowsheet, there is the steam jet ejector for creating the vacuum of the second evaporator, and the liquid ring pumps for creating the vacuum of the first evaporator.

SUMMARY OF UTILITIES														
EQUIPMENT		UTILITIES												
Nr.	Type	Heating					Cooling				Power			
		Load	Consumption (t/h)				Load	Consumption (t/h)			Actual Load	Consumption		
			Steam			Hot		Cooling water	Chilled water	Refrig.		Steam (t/h)		Electr.
			LP	MP	HP	Oil						kW	HP	MP
	Condenser EDC						2747.79	236.98						
	Reboiler EDC	3077.4		5.50										
E07	Cooler						83.26	7.18						
E08	Cooler						318.4		54.68					
E09	Heater	12.77	0.02											
E11	Cooler						66.94			0.19				
E12	Cooler	4.55	0.01											
Evap 1	Evaporator 1	40.92	0.07											
Evap 2	Evaporator 2	106.52	0.18											
P01	Pump										0.001			0.001
P02	Pump										0.70			0.70
P03	Pump										0.56			0.56
P04	Pump										0.06			0.06
P05	Pump										0.01			0.01
P06	Pump										0.73			0.73
	Vacuum 1 - steam jet ejector												0.11	
	Vacuum 2 – liquid ring pump													1.93
TOTAL		3242.2	0.28	5.5			3216.4	244.2	54.7	0.19	2.1		0.1	3.99

Table A 54: Summary of all utilities used for each equipment for the base case design with the 14 kPa EDC and two evaporators. The equipment numbering equals the Aspen flowsheet shown in Figure A 32. Additionally, there is the steam jet ejector for creating the vacuum of the second evaporator, and the liquid ring pumps for creating the vacuum of the EDC and the first evaporator.

SUMMARY OF UTILITIES														
EQUIPMENT		UTILITIES												
Nr.	Type	Heating					Cooling				Power			
		Load	Consumption (t/h)				Load	Consumption (t/h)			Actual Load	Consumption		
			Steam			Hot		Cooling water	Chilled water	Refrig.		Steam (t/h)		Electr.
			LP	MP	HP	Oil						kW	HP	MP
	Condenser EDC						2924.92	504.40						
E01	Cooler						47.13	8.13						
E02	Heater	172.51	0.29											
	Reboiler EDC	2805.6	4.71											
E06	Cooler						331		56.99					
E07	Heater	13.07	0.02											
E08	Cooler						50.05			0.14				
E09	Heater	3.65	0.01											
Evap 1	Evaporator 1	270.5	0.45											
Evap 2	Evaporator 2	82.82	0.14											
P01	Pump										0.0001			0.0001
P02	Pump										0.55			0.55
P03	Pump										0.68			0.68
P04	Pump										0.06			0.06
P05	Pump										0.01			0.01
P06	Pump										0.67			0.67
	Vacuum1-steam jet ejector												0.11	
	Vacuum2 - liquid ring pumps										3.19			
TOTAL		3348.15	5.62	0.11			3353.1	512.53	56.99	0.14	5.16			1.97

Table A 55: Summary of all utilities used for each equipment for the base case design with the 1atm EDC and the stripping column. The equipment numbering equals the Aspen flowsheet shown in Figure A 33. Additionally, there are the liquid ring pumps for creating the vacuum of the evaporator and the stripping column.

SUMMARY OF UTILITIES														
EQUIPMENT		UTILITIES												
Nr.	Type	Heating					Cooling				Power			
		Load	Consumption (t/h)			Load	Consumption (t/h)			Actual Load	Consumption		Electr. kWh	
			Steam				Hot	Cooling water	Air		Refrig.	Steam (t/h)		
			kW	LP	MP		HP					Oil		kW
E02	Heater	82.29	0.14											
E04	Cooler						2364.99	203.97						
E05	Cooler						353.31	30.47						
E07	Cooler						25.27	2.18						
E08	Cooler						425.79			1.30				
	Reboiler EDC	3136.49		5.67										
	Condenser EDC						359.62	31.02						
Evap	Evaporator	289.6		0.52										
P01	Pump										0.0002			0.0002
P02	Pump										0.70			0.70
P03	Pump										0.27			0.27
P04	Pump										0.05			0.05
P05	Pump										0.14			0.14
P06	Pump										0.74			0.74
	Vacuum - liquid ring pumps										1.36			
TOTAL		3508.38	0.14	6.19			3558.99	270.23		1.30	3.26			1.90

Table A 56: Summary of all utilities used for each equipment for the base case design with the 14kPa EDC and the stripping column. The equipment numbering equals the Aspen flowsheet shown in Figure A 33. Additionally, there are the liquid ring pumps for creating the vacuum of the EDC, the evaporator and the stripping column.

SUMMARY OF UTILITIES														
EQUIPMENT		UTILITIES												
Nr.	Name	Heating					Cooling				Power			
		Load	Consumption (t/h)				Load	Consumption (t/h)			Actual Load	Consumption		Electr.
			Steam			Hot		Cooling water	Air	Refrig.		Steam (t/h)		
			LP	MP	HP	Oil						kW	HP	
E01	Cooler						94.60	16.31						
E04	Cooler						2533.79	436.95						
E06	Heater						373.66			1.03				
E07	Heater						25.26	4.36						
	Reboiler EDC	2931.1	4.92											
	Condenser EDC						395.82	68.26						
Evap	Evaporator	484.99		0.87										
P01	Pump										0.0002			0.0002
P02	Pump										0.27			0.27
P03	Pump										0.68			0.68
P04	Pump										0.05			0.05
P05	Pump										0.11			0.11
P06	Pump										0.64			0.64
P07	Pump										0.30			0.30
	Vacuum - liquid ring pumps										2.59			
TOTAL		3416.1	4.92	0.87			3423.13	525.88		1.03	4.64			2.02

C.8.6 Equipment List & Economic Assessment

C.8.6.1 Equipment Sizing & Purchase Costs

Table A 57: Equipment sizing of the EDC columns with all required characteristics for the four base case designs.

Meaning	Formulas	Results				Units
		Base case designs				
		14 kpa EDC Evaporators	14 kpa EDC Stripping	1 atm EDC Evaporators	1 atm EDC Stripping	
Number of trays : N	Aspen Process Optimisation	30	35	30	35	
Height : H	$H = 0.5 N + 3$	18 / 59.06 / 708.66	20.5 /67.26 /807.09	18 / 59.06 / 708.66	20.5 /67.26/807.09	m/ft/in
Tangent-to-tangent length : L	$L = 0.5 N$	15 / 49.21 / 590.55	17.5 /57.41 /688.98	15 / 49.21 / 590.55	17.5 /57.41 /688.98	m/ft/in
Diameter : D	Aspen tray sizing and rating	2.23 / 7.32 / 87.80	2.28 / 7.48 / 89.76	1.26 / 4.13 / 49.61	1.28 / 4.2 / 50.39	m/ft/in
Lowest pressure : P _o	Aspen Plus Process Simulation	14 / 2.03	14 / 2.03	101 / 14.65	101 / 14.65	kPa/psig
Design Pressure : P _d	$\begin{array}{l} P_d = 10 \\ \text{For } P_o \text{ between 0 and 5} \\ P_d = \exp \{0.60608 + 0.91615[\ln(P_o)] \\ \quad + 0.0015655[\ln(P_o)]^2\} \\ \text{For } P_o \text{ between 10 and 1000 psig} \end{array}$	10	10	21.69	21.69	psig
Highest temperature : T _o	Aspen Plus Process Simulation	60 / 140	65 / 149	94 / 201.20	103 / 217.40	°C / °F
Design temperature : T _d	$T_d = T_o + 50 \text{ }^{\circ}\text{F}$	190	199	251.2	267.40	°F
Modulus of elasticity : E _M	Seider <i>et al.</i> (2006) book p.575	29500000	29500000			psi
Wall thickness : t _E	$t_E = 1.3 D \left(\frac{P_d L}{E_M D} \right)^{0.4} \quad \text{for } \frac{t_E}{D} \leq 0.05$ L and D in inches	0.632 / 16.05	0.681 / 17.30			in / cm
Correction : t _{EC}	$t_{EC} = L(0.18D_i - 2.2) \times 10^{-5} - 0.19$ if $t_{EC} \geq 0$	-0.110 / -2.79	-0.094 / -2.38			in / cm
Maximum allowable stress : S	Seider <i>et al.</i> (2006) book p.575			15000	15000	
Necessary wall thickness : t _W	$t_{W,vacuum} = t_E + t_{EC}$ $t_{W,atm} = \frac{0.22 (D + 18) L^2}{S D^2} \quad \text{L and D in inches}$	0.632 / 16.05	0.681 / 17.30	0.141 / 3.57	0.188 / 4.76	in / cm
Corrosive allowance : t _c	Seider <i>et al.</i> (2006) book p.575	0.125 / 3.17	0.125 / 3.17	0.125 / 3.17	0.125 / 3.17	in / cm
Actual wall thickness : t _s	$t_s = t_W + t_c$	0.757 / 19.22	0.806 / 20.47	0.266 / 6.74	0.313 / 7.94	in / cm
Weight of shell and two heads : W	$W = \pi (D + t_s) (L + 0.8 D) t_s \rho_{carbon}$ L and D in inches , $\rho_{carbon} = 0.284 \text{ lb/in}^3$	39491.87 /17913.23	49526.62/2246 4.92	7442.5 / 2275.8	20305.3 / 4674.4	lb / kg

Table A 58: Purchase costs calculation of the EDC column for the four base case designs

Meaning	Formula	Results			
		Base case designs			
		14 kpa EDC Evaporators	14 kpa EDC Stripping	1 atm EDC Evaporators	1 atm EDC Stripping
Costs of empty vessel	$C_v = \exp\{7.2756 + 0.18255 [\ln(W)] + 0.02297 [\ln(W)]^2\}$ W in lb	\$ 130,709.49	\$ 152,257.82	\$ 45,642.69	\$ 55,477.83
Cost of platforms and ladders	$C_{PL} = 300.9 (D)^{0.63316} (L)^{0.80161}$ D and L in ft	\$ 24,101.35	\$ 27,656.92	\$ 16,790.33	\$ 19,189.11
Base costs for sieve trays	$C_{BT} = 468 \exp(0.1739 D)$ D in ft	\$ 1,670.32	\$ 1,718.65	\$ 960.40	\$ 971.42
Costs for installed trays	$C_T = N_T F_{TT} F_M C_{BT}$ with F_{TT} and $F_M = 1$	\$ 50,109.48	\$ 60,152.79	\$ 28,811.90	\$ 33,999.64
Purchase cost	$C_P = F_M C_V + C_{PL} + C_T$	\$ 204,920.32	\$ 240,067.53	\$ 91,244.92	\$ 108,666.57

Table A 59: Equipment sizing of the stripping columns with all required characteristics for the stripping base cases.

Meaning	Formulas	Results		Units
		Base Case Designs		
		14 kpa EDC Stripping	1 atm EDC Stripping	
Number of trays : N	Aspen Process Optimisation	5	5	
Height : H	H = 0.5 N + 3	5.5 / 18.04 / 216.54	5.5 / 18.04 / 216.54	m/ft/in
Tangent-to-tangent length : L	L = 0.5 N	2.5 / 8.2 / 98.43	2.5 / 8.2 / 98.43	m/ft/in
Diameter : D	Aspen tray sizing and rating	0.95 / 3.12 / 37.40	0.98 / 3.22 / 38.58	m/ft/in
Lowest pressure : P _o	Process	2 / 0.29	2 / 0.29	kPa/psi g
Design Pressure : P _d	P _d = 10 For P _o between 0 and 5	10	10	psig
Highest temperature : T _o	Process	97 / 206.6	100 / 212	°C / °F
Design temperature : T _d	T _d = T _o + 50 °F	256.6	262	°F
Modulus of elasticity : E _M	Seider <i>et al.</i> (2006) book p.575	29500000	29500000	psi
Wall thickness : t _E	$t_E = 1.3 D \left(\frac{P_d L}{E_M D} \right)^{0.4}$ for $\frac{t_E}{D} \leq 0.05$	0.185 / 4.70	0.188 / 4.79	in / cm

		L and D in inches			
Correction	: t_{EC}	$t_{EC} = L(0.18D_i - 2.2) \times 10^{-5} - 0.19$ if $t_{EC} \geq 0$	-0.186 / -4.71	-0.184 / -4.7	in / cm
Necessary wall thickness	: t_W	$t_W = t_E + t_{EC}$	0.185 / 4.70	0.188 / 4.79	in / cm
Corrosive allowance	: t_c	Seider <i>et al.</i> (2006) book p.575	0.125 / 3.17	0.125 / 3.17	in / cm
Actual wall thickness	: t_s	$t_s = t_W + t_c$	0.310 / 7.87	0.313 / 7.96	in / cm
Weight of shell and two heads	: W	$W = \pi (D + t_s) (L + 0.8 D) t_s \rho_{\text{carbon}}$ L and D in inches, $\rho_{\text{carbon}} = 0.284 \text{ lb/in}^3$	1337.7 / 606.77	1405.5 / 637.52	lb / kg

Table A 60: Purchase costs calculation of the stripping column for the stripping base case designs

Meaning	Formula	Results	
		14 kpa EDC Stripping	1 atm EDC Stripping
Costs of an empty vessel	$C_v = \exp\{7.2756 + 0.18255 [\ln(W)] + 0.02297 [\ln(W)]^2\}$ W in lb	\$ 17677.76	\$ 18,133.06
Cost of platforms and ladders	$C_{PL} = 300.9 (D)^{0.63316} (L)^{0.80161}$ D and L in ft	\$ 3339.11	\$ 3,405.49
Base costs for sieve trays	$C_{BT} = 468 \exp(0.1739 D)$ D in ft	\$ 804.71	\$ 818.60
Costs for installed trays	$C_T = N_T F_{TT} F_M C_{BT}$ with F_{TT} and $F_M = 1$	\$4023.54	\$ 4,093.00
Purchase cost	$C_P = F_M C_V + C_{PL} + C_T$	\$ 25,040.41	\$ 25,631.55

Table A 61 Equipment sizing of the reflux drums of the two evaporator base cases designs.

Necessary characteristics for economic analysis				
Meaning	Formulas	Results		Units
		14 kpa EDC evaporator	1 atm EDC evaporator	
Liquid flowrate	\dot{V}_L	0.0041	0.0044	m ³ /s
Holdup volume	$V_{ho} = t_{ho} \cdot \dot{V}_L$ with $t_{ho} = 300$ (heuristic)	1.22	1.32	m ³
Volume vessel	$V_{ves} = \frac{V_{ho}}{0.5}$	2.44	2.64	m ³
Diameter vessel	$D_{ves} = \sqrt[3]{\frac{4 V_{ves}}{3 \pi}}$	1.01/3.32/39.84	1.04/3.41/40.88	m/ft/in
Length vessel	$L_{ves} = 3 D_{des}$ (heuristic)	3.04/9.96/119.51	3.12/10.22/122.65	m/ft/in
Lowest pressure	Aspen Plus Process Simulation	14/2.03	101/14.65	kPa/psig
Design pressue	$P_d = \exp \{0.60608 + 0.91615[\ln(P_o)] + 0.0015655[\ln(P_o)]^2\}$ For operating pressure between 10 and 1000 psig $P_d = 10$ For operating pressure between 0 and 5 psig	10	21.69	psig
Highest temperature	Aspen Plus Process Simulation	35/145	78/172.40	°C/°F
Design Temperature	$T_d = T_{highest} + 50$ °F	145.0	222.4	°F
Maximum allowable stress	$S(T_d) = \text{Seider } et al. (2006) \text{ book Table p. 575}$		15000	Psi
Fractional weld Efficiency	$E(\text{Material}) = \text{Seider } et al. (2006) \text{ p. 575}$		0.85	
Modulus of elasticity	$E_M(T_d) = \text{Seider } et al. (2006) \text{ Table p. 576}$	29500000		Psi
Wall thickness for vacuum	$t_{E,vacuum} = 1.3 D \left(\frac{P_d L}{E_M D} \right)^{0.4}$ for $\frac{t_E}{D} \leq 0.05$ L and D in inches	0.53/0.208		cm/in
Correction for vacuum	$t_{EC,vacuum} = L(0.18D_i - 2.2) \times 10^{-5} - 0.19$ if $t_{EC} \geq 0$	-0.47/-0.184		cm/in
Necessary wall thickness	$t_{W,vacuum} = t_{E,vacuum} + t_{EC,vacuum}$ $t_{W,atm} = \frac{P_d D}{2 S E - 1.2 P_d}$	0.53/0.208	0.8/0.035	cm/in
Corrosive allowance	$t_c = 0.125$	0.32/0.125	0.32/0.125	cm/in
Actual wall thickness	$t_s = t_w + t_c$	0.85/0.333	0.41/0.160	cm/in
Weight of shell and two heads	$W = \pi (D + t_s) (L + 0.8 D) t_s \rho_{carbon}$ L and D in inches, $\rho_{carbon} = 0.284 \text{ lb/in}^3$	817.9/1803.3	412.17/908.69	kg/lb

Table A 62: Equipment sizing of the reflux drums of the stripping column base cases designs.

Meaning	Formulas	Results		Units
		14 kpa EDC stripping	1 atm EDC stripping	
Density liquid	ρ_l	786.79	733.63	kg/m ³
Density gas	ρ_g	0.263	1.605	kg/m ³
Cross-sectional area	$A_z = \frac{D_{ves}^2}{8} (2\pi - \theta - \sin\theta)$ $= 0.3518 D_{ves}^2$			m ²
Volumetric gas flowrate	\dot{v}_g	11.56	1.82	m ³ /s
Maximum vapour velocity	$u_{gmax} = k_{SB} \sqrt{\frac{\rho_l - \rho_g}{\rho_g}} = \frac{\dot{v}_g}{A_z}$	4.43	1.71	m/s
Diameter vessel	$D_{ves} = \sqrt{\frac{\dot{v}_g}{0.3518 u_{gmax}}}$	2.74 / 8.99 / 107.93	1.74 / 5.71 / 68.56	m/ft/in
Length vessel	$L_{ves} = 3D_{des}$	8.22 / 26.98 / 323.79	5.22 / 17.14 / 205.67	m/ft/in
Volume vessel	$V_{ves} = \frac{\pi}{4} D_{ves}^2 L_{ves}$	48.54	12.44	m ³
Lowest pressure	Aspen Plus Process Simulation	14 2.03	101/14.65	kPa/psig
Design Pressure vacuum	$P_d = \exp \{0.60608 + 0.91615[\ln(P_o)] + 0.0015655[\ln(P_o)]^2\}$ For operating pressure between 10 and 1000 psig $P_d = 10$ For operating pressure between 0 and 5 psig	10	21.69	psig
Highest temperature	Aspen Plus Process Simulation	35/145.0	78 /222.40	°C/°F
Design Temperature	$T_d = T_{highest} + 50 \text{ }^\circ\text{F}$	145.0	222.4	°F
Maximum allowable stress	$S(T_d) = \text{Seider et al. (2006) Table p. 575}$		15000	Psi
Modulus of elasticity	$E_M(T_d) = \text{Seider et al. (2006) Table p. 576}$	29500000		psi
Fractional weld Efficiency	$E(\text{Material}) = \text{Seider et al. (2006) p. 575}$		0.85	
Wall thickness for vacuum	$t_{E,vacuum} = 1.3 D \left(\frac{P_d L}{E_M D} \right)^{0.4}$ for $\frac{t_E}{D} \leq 0.05$ L and D in inches	0.370/0.94		in/cm
Correction for vacuum	$t_{EC,vacuum} = L(0.18D_i - 2.2) \times 10^{-5} - 0.19$ if $t_{EC} \geq 0$	-0.19/-0.48		in/cm
Necessary wall thickness	$t_{W,vacuum} = t_{E,vacuum} + t_{EC}$ $t_{W,atm} = \frac{P_d D}{2 S E - 1.2 P_d}$ L and D in inches	0.370/0.94	0.058/0.15	in/cm
Corrosive allowance	$t_c = 0.125$	0.125/0.32	0.125/0.32	in/cm
Actual wall thickness	$t_s = t_W + t_c$	0.495/1.26	0.183/0.47	in/cm
Weight of shell and two heads	$W = \pi (D + t_s) (L + 0.8 D) t_s \rho_{carbon}$ L and D in inches, $\rho_{carbon} = 0.284 \text{ lb/in}^3$	19627.88/8903.07	2928.06/1328.15	lb/kg

Table A 63: Purchase cost calculation of the reflux drums for the four base case designs

Meaning	Formula	Results			
		Base case designs			
		14 kpa EDC Evaporators	14 kpa EDC Stripping	1 atm EDC Evaporators	1 atm EDC Stripping
Costs of an empty vessel	$C_v = \exp\{8.9552 - 0.2330 [\ln(W)] + 0.04333 [\ln(W)]^2\}$ W in lb, for $1000 \leq W \leq 920000$	\$ 15,427.57	\$ 53,408.54	\$ 11,833.16	\$ 19,074.21
Cost of platforms and ladders	$C_{PL} = 2005 (D)^{0.20294}$ D in ft	\$ 2,557.79	\$ 3,131.20	\$ 2,571.30	\$ 2,855.69
Purchase cost	$C_P = F_M C_V + C_{PL}$ with $F_M = 1$	\$ 17,985.36	\$ 56,539.75	\$ 14,404.47	\$ 21,929.91

Table A 64: Equipment specification and purchase cost calculation for the vacuum systems of the base case design with the 14 kPa EDC and evaporators.

Meaning		Formulas	EDC + reflux drum	Vacuum Evap 1	Vacuum Evap 2	Units
			Liquid ring pump	Liquid ring pump	Steam jet ejector	
Operating pressure	p	from Aspen Plus process simulation	105.0	15.0	2.25	torr
Volume equipment	V	from Aspen Plus process simulation	2568.87	122.17	7.06	ft ³
Air leakage	W _{air}	W _{air} = 5 + V ^{0.66} . (0.0298 + 0.03088 ln(p) ²)	33.68	7.60	5.20	lb/hr
Temperature precondenser	T _{cond}	from Aspen Plus process simulation	0	9	-8	°C
Product	W _{product}	from Aspen Plus: flash calculation	6.42	10.54	18.03	lb/hr
Flow to vacuum	W _{vacuum}	W _{vacuum} = W _{air} + W _{product}	53.13	234.55	23.23	ft ³ /min n lb/hr
Size factor – Steam Jet ejector	S _{steamjet}	S _{steamjet} = $\frac{W_{vacuum}}{P}$ 6.1 ≤ S ≤ 100 W _{vacuum} in lb/hr, P in torr			10.32	
Size factor – liquid ring pump	S _{liquid}	S _{liquid} = W _{vacuum} with W in ft ³ /min	53.13	234.55		ft ³ /min n
Factor stages	F _{stages}	F _{stages} = 2.1			2.1	
Purchase costs steamjet	C _{P,steamjet}	C _{P,steamjet} = 1690 . S ^{0.41} . F _{stages}			\$9 242.23	

		with $F_{\text{stages}} = 2.1$				
Purchase costs liquid	$C_{P,\text{liquid}}$	$C_{P,\text{liquid}} = 8250 \cdot S^{0.35}$ for $0 \leq S \leq 100$	\$33 137.19	\$55 723.32		
Compressor power	P_{comp}	from Aspen Plus process simulation	1.24	1.952		kW
MP steam requirement		$W_{\text{steam}} = W_{\text{vacuum}} \cdot 10$			232.3	lb/hr

Table A 65: Equipment specification and purchase cost calculation for the vacuum systems of the base case design with the 1 atm EDC and evaporators.

Meaning		Formulas	Vacuum Evap 1	Vacuum Evap 2	Units
			Liquid ring pump	Steam jet ejector	
Operating pressure	p	from Aspen Plus process simulation	15.0	2.25	torr
Volume equipment	V	from Aspen Plus process simulation	114.44	7.06	ft ³
Air leakage	W_{air}	$W_{\text{air}} = 5 + V^{0.66} \cdot (0.0298 + 0.03088 \ln(p)^2)$	7.49	5.20	lb/hr
Temperature precondenser	T_{cond}	from Aspen Plus process simulation	9	-8	°C
Product	W_{product}	from Aspen Plus: flash calculation	10.59	19.50	lb/hr
Flow to vacuum	W_{vacuum}	$W_{\text{vacuum}} = W_{\text{air}} + W_{\text{product}}$	233.327	24.702	ft ³ /min / lb/hr
Size factor – Steam Jet ejector	S_{steamjet}	$S_{\text{steamjet}} = \frac{W_{\text{vacuum}}}{p}$ $6.1 \leq S \leq 100$ W_{vacuum} in lb/hr, p in torr		10.98	
Size factor – liquid ring pump	S_{liquid}	$S_{\text{liquid}} = W_{\text{vacuum}}$ with W in ft ³ /min	233.33		ft ³ /min
Factor stages	F_{stages}	$F_{\text{stages}} = 2.1$		2.1	
Purchase costs steamjet	$C_{P,\text{steamjet}}$	$C_{P,\text{steamjet}} = 1690 \cdot S^{0.41} \cdot F_{\text{stages}}$ with $F_{\text{stages}} = 2.1$		\$9 478.00	
Purchase costs liquid	$C_{P,\text{liquid}}$	$C_{P,\text{liquid}} = 8250 \cdot S^{0.35}$ for $0 \leq S \leq 100$	\$55 621.37		
Compressor power	P_{comp}	from Aspen Plus process simulation	1.938		kW
MP steam requirement		$W_{\text{steam}} = W_{\text{vacuum}} \cdot 10$		247.02	lb/hr

Table A 66: Equipment specification and purchase cost calculation for the vacuum systems of the base case design with the 14 kPa EDC and a stripping column.

Meaning	Formulas	EDC + reflux drum	Vacuum Evap 1	Vacuum Evap 2	Units
		Liquid ring pump	Liquid ring pump	Liquid ring pump	
Operating pressure p	from Aspen Plus process simulation	105.0	337.5	15.00	torr
Volume equipment V	from Aspen Plus process simulation	4670.08	13.12	137.67	ft ³
Air leakage W_{air}	$W_{air} = 5 + V^{0.66} \cdot (0.0298 + 0.03088 \ln(p)^2)$	47.54	6.04	7.82	lb/hr
Temperature precondenser T_{cond}	from Aspen Plus process simulation	0	60	-8	°C
Product $W_{product}$	from Aspen Plus: flash calculation	9.15	3.04	6.41	lb/hr
Flow to vacuum W_{vacuum}	$W_{vacuum} = W_{air} + W_{product}$	75.67	6.042	131.765	ft ³ /min
Size factor – liquid ring pump S_{liquid}	$S_{liquid} = W_{vacuum}$ with W in ft ³ /min	75.67	6.04	131.77	ft ³ /min
Factor stages F_{stages}	$F_{stages} = 2.1$			2.1	
Purchase costs - liquid ring pump $C_{P,liquid}$	$C_{P,liquid} = 8250 \cdot S^{0.35}$ for $0 \leq S \leq 100$	\$37 504.35	\$15 483.43	\$45 539.05	
Compressor power P_{comp}	from Aspen Plus process simulation	1.24	1.952		kW

Table A 67: Equipment specification and purchase cost calculation for the vacuum systems of the base case design with the 1 atm EDC and a stripping column.

Meaning	Formulas	Vacuum Evap 1	Vacuum Evap 2	Units
		Liquid ring pump	Liquid ring pump	
Operating pressure p	from Aspen Plus process simulation	337.5	15.00	torr
Volume equipment V	from Aspen Plus process simulation	13.23	146.51	ft ³
Air leakage W_{air}	$W_{air} = 5 + V^{0.66} \cdot (0.0298 + 0.03088 \ln(p)^2)$	6.05	7.94	lb/hr
Temperature precondenser T_{cond}	from Aspen Plus process simulation	70	-8	°C
Product $W_{product}$	from Aspen Plus: flash calculation	17.90	6.33	lb/hr

Flow to vacuum	W_{vacuum}	$W_{\text{vacuum}} = W_{\text{air}} + W_{\text{product}}$	13.475	132.705	ft ³ /min
Size factor – liquid ring pump	S_{liquid}	$S_{\text{liquid}} = W_{\text{vacuum}}$ with W in ft ³ /min	13.48	132.71	ft ³ /min
Factor stages	F_{stages}	$F_{\text{stages}} = 2.1$		2.1	
Purchase costs liquid	$C_{\text{P,liquid}}$	$C_{\text{P,liquid}} = 8250 S^{0.35}$ for $0 \leq S \leq 100$	\$20 501.66	\$45 652.49	
Compressor power	P_{comp}	from Aspen Plus process simulation	1.938		kW

C.8.6.2 Equipment Summary & Costs

Table A 68: Summary of the equipment, the important equipment characteristics and the costs for each equipment for the 1 atm EDC evaporators base case. The total equipment costs for the year 2019 and the total permanent investment are also given. The corresponding flowsheet can be found in Figure 21.

Exchangers	Type	Area [ft ²]				Cp
E08	Double pipe	62.41				\$2,410.44
E07	Double pipe	76.08				\$2,494.60
E02	Shell and Tube	313.52				\$8,432.34
E12	Double pipe	1.00				\$1,247.38
E01	Shell and Tube	335.36				\$8,556.76
E09	Double pipe	1.52				\$1,333.28
Reboiler EDC	Kettle reboiler	710.23				\$25,104.67
E11	Double pipe	15.34				\$1,925.62
Condenser EDC	Shell and tube	739.70				\$10,866.42
Evap 1	Horizontal tube	17.37				\$18,433.31
Evap 2	Horizontal tube	26.52				\$42,747.29
					Total HE	\$123,552.11
Towers	Type	Diameter [ft]	Height [ft]	Volume [ft ³]	Pressure [psig]	Cp
EDC	Vertical, sieve trays	4.13	59.06	792.61	14.65	\$91,244.92
					Total Towers	\$91,244.92
Vessels	Type	Diameter [ft]	Length [ft]	Volume [ft ³]	Pressure [psig]	Cp
Reflux drum EDC	Horizontal	3.41	10.22	93.13	14.65	\$14,404.47
					Total Vessels	\$14,404.47
Vacuum System	Type	Volume [ft ³]	Temperature [°C]	Flow [lb/h] or [ft ³ /min]	Pressure [torr]	Cp
Evap 1	Liquid ring pump	114.44	9	233.33	15.00	\$55,621.37
Evap 2	Steam jet ejector	7.06	-8	24.70	2.25	\$9,478.00
					Total Vacuum	\$65,099.37
					TOTAL 2019	\$357,575.56
					CTPI	\$1,779,653.55

Table A 69: Summary of the equipment, the important equipment characteristics and the costs for each equipment for the 14 kPa EDC evaporators base case. The total equipment costs for the year 2019 and the total permanent investment are also given. The corresponding flowsheet can be found in Figure A 32.

Exchangers	Type	Area [ft2]				Cp
E08	Double pipe	12.94				\$1,873.88
Reboiler EDC	Kettle reboiler	663.0				\$24,583.01
Condenser EDC	Shell and tube	3150.18				\$23,129.64
E07	Double pipe	1.58				\$1,351.80
E02	Double pipe	34.45				\$2,213.74
E06	Double pipe	69.78				\$2,453.86
E01	Double pipe	42.80				\$2,275.29
E05	Shell and tube	279.37				\$8,240.64
E09	Double pipe	1.00				\$1,256.54
Evap 1	Horizontal tube	121.0				\$51,575.56
Evap 2	Horizontal tube	66.0				\$37,409.49
					Total HE	\$156,363.45
Towers	Type	Diameter [ft]	Height [ft]	Volume [ft3]	Pressure [psig]	Cp
EDC	Vertical, sieve trays	7.32	59.06	2482.72	2.03	\$204,920.32
					Total Towers	\$204,920.32
Vessels	Type	Diameter [ft]	Length [ft]	Volume [ft3]	Pressure [psig]	Cp
Reflux drum EDC	Horizontal	3.32	9.96	86.15	2.03	\$17,985.36
					Total Vessels	\$ 17,985.36
Vacuum System	Type	Volume [ft3]	Temperature [°C]	Flow [lb/h] or [ft3/min]	Pressure [torr]	Cp
Vacuum EDC	Liquid ring pump	2568.87	0	53.13	105.01	\$33,137.19
Vacuum Evap 1	Liquid ring pump	122.17	9	234.55	15.00	\$55,723.32
Vacuum Evap 2	Steam jet ejector	7.06	-8	23.23	2.25	\$ 9,242.23
					Total Vacuum	\$98,102.74
					TOTAL 2019	\$580,006.82
					CTPI	\$2,886,693.95

Table A 70: Summary of the equipment, the important equipment characteristics and the costs for each equipment for the 1atm EDC stripping base case. The total equipment costs for the year 2019 and the total permanent investment are also given. The corresponding flowsheet can be found in Figure A 34.

Exchangers	Type	Area [ft2]				Cp
E08	Shell and tube	352.03				\$8,802.38
E04	Shell and tube	628.92				\$10,420.80
E07	Double pipe	9.45				\$1,817.83
E02	Double pipe	19.09				\$2,034.20
E06	Double pipe	83.76				\$2,577.24
Reboiler EDC	Kettle reboiler	726.94				\$25,288.49
E01	Double pipe	84.53				\$2,581.03
E05	Shell and tube	174.50				\$7,843.01
Condenser EDC	Shell and tube	150.00				\$7,748.27
Evap	Horizontal tube	139.8				\$55,671.10
					Total HE	\$124,784.35
Towers	Type	Diameter [ft]	Height [ft]	Volume [ft3]	Pressure [psig]	Cp
EDC	Vertical, sieve trays	4.20	67.26	931.58	14.65	\$108,666.57
Stripping column	Vertical, sieve trays	3.22	18.04	146.51	0.29	\$ 25,631.55
					Total Towers	\$134,298.13
Vessels	Type	Diameter [ft]	Length [ft]	Volume [ft3]	Pressure [psig]	Cp
Reflux drum EDC	Horizontal	5.71	17.14	439.33	14.65	\$21,929.91
					Total Vessels	\$21,929.91
Vacuum System	Type	Volume [ft3]	Temperature [°C]	Flow [lb/h] or [ft3/min]	Pressure [torr]	Cp
Evap 1	Liquid ring pump	13.23	70	13.48	337.53	\$20,501.66
stripping	Liquid ring pump	146.51	-8	132.71	15.00	\$45,652.49
					Total Vacuum	\$ 66,154.15
					TOTAL 2019	\$421,807.35
					CTPI	\$2,099,335.16

Table A 71: Summary of the equipment, the important equipment characteristics and the costs for each equipment for the 14 kPa EDC stripping base case. The total equipment costs for the year 2019 and the total permanent investment are also given. The corresponding flowsheet can be found in Figure A 33.

Exchangers	Type	Area [ft ²]				Cp
E04	Shell and tube	2890.59				\$22,289.29
E07	Double pipe	8.90				\$1,800.46
E02	Double pipe	84.44				\$2,580.59
E06	Double pipe	408.50				\$9,133.67
Reboiler EDC	Kettle reboiler	631.31				\$24,230.36
E01	Double pipe	63.34				\$2,464.52
E05	Double pipe	24.44				\$2,116.28
Condenser EDC	Shell and tube	426.19				\$9,237.69
Evap	Horizontal tube	226.34				\$71,870.52
					Total HE	\$145,723.38
Towers	Type	Diameter [ft]	Height [ft]	Volume [ft ³]	Pressure [psig]	Cp
EDC	Vertical, sieve trays	7.48	67.26	2955.76	2.03	\$240,067.53
Stripping column	Vertical, sieve trays	3.12	18.04	137.67	0.29	\$25,040.41
					Total Towers	\$265,107.94
Vessels	Type	Diameter [ft]	Length [ft]	Volume [ft ³]	Pressure [psig]	Cp
Reflux drum EDC	Horizontal	8.99	26.98	1714.33	2.03	\$ 56,539.75
					Total Vessels	\$56,539.75
Vacuum System	Type	Volume [ft ³]	Temperature [°C]	Flow [lb/h] or [ft ³ /min]	Pressure [torr]	Cp
Vacuum EDC	Liquid ring pump	4670.08	0	75.67	105.01	\$37,504.35
Evap 1	Liquid ring pump	13.12	60	6.04	337.53	\$15,483.43
Stripping column	Liquid ring pump	137.67	-8	131.77	15.00	\$ 45,539.05
					Total Vacuum	\$ 98,526.83
					TOTAL 2019	\$687,565.95
					CTPI	\$3,422,015.73

C.8.6.3 Total Annual Production Costs

Table A 72: Utility consumption, and prices, and annual costs of the utilities of the base case design with the 1 atm EDC and two evaporators.

Bill of Materials			Product Production: 78702 ton/year		
Utilities	Consumption (unit/kg product)	Price (\$/unit utility)	Cost (\$/kg product)	Consumption (unit/year)	Annual Costs (\$/year)
HP Steam [ton/yr]	0.00	\$14.50	\$0.00	0.00	\$0.00
MP Steam [ton/yr]	562.26	\$10.50	\$5,903.75	44251.43	\$464,639.99
LP Steam [ton/yr]	40.23	\$6.60	\$265.50	3166.03	\$20,895.80
Electricity [kWh/yr]	400.50	\$0.06	\$24.03	31520.36	\$1,891.22
Cooling water [m ³ /yr]	24532.60	\$0.02	\$490.65	1930775.55	\$38,615.51
Chilled water [GJ/yr]	114.82	\$4.00	\$459.30	9036.96	\$36,147.82
Refrigerant [GJ/yr]	24.14	\$5.50	\$132.77	1899.92	\$10,449.58
Total Variable Costs					\$572,639.93

Table A 73: Utility consumption, and prices, and annual costs of the utilities of the base case design with the 14kPa EDC and two evaporators.

Bill of Materials			Product Production: 78702 ton/year		
Utilities	Consumption (unit/kg product)	Price (\$/unit utility)	Cost (\$/kg product)	Consumption (unit/year)	Annual Costs (\$/year)
HP Steam [ton/yr]	0.00	\$14.50	\$0.00	0.00	\$0.00
MP Steam [ton/yr]	10.56	\$10.50	\$110.86	830.97	\$8,725.22
LP Steam [ton/yr]	563.17	\$6.60	\$3,716.91	44322.67	\$292,529.61
Electricity [kWh/yr]	516.01	\$0.06	\$30.96	40610.95	\$2,436.66
Cooling water [m ³ /yr]	51496.77	\$0.02	\$1,029.94	4052922.00	\$81,058.44
Chilled water [GJ/yr]	119.37	\$4.00	\$477.47	9394.57	\$37,578.30
Refrigerant [GJ/yr]	18.05	\$5.50	\$99.27	1420.45	\$7,812.46
Total Variable Costs					\$430,140.68

Table A 74: Utility consumption, and prices, and annual costs of the utilities of the base case design with the 1 atm EDC and the stripping column.

Bill of Materials			Product Production: 78702 ton/year		
Utilities	Consumption (unit/kg product)	Price (\$/unit utility)	Cost (\$/kg product)	Consumption (unit/year)	Annual Costs (\$/year)
HP Steam [ton/yr]	0.00	\$14.50	\$0.00	0.00	\$0.00
MP Steam [ton/yr]	619.93	\$10.50	\$6,509.24	48789.84	\$512,293.34
LP Steam [ton/yr]	13.84	\$6.60	\$91.36	1089.42	\$7,190.16
Electricity [kWh/yr]	327.48	\$0.06	\$19.65	25773.80	\$1,546.43
Cooling water [m ³ /yr]	26890.86	\$0.02	\$537.82	2116376.48	\$42,327.53
Refrigerant [GJ/yr]	153.55	\$5.50	\$844.55	12085.08	\$66,467.96
Total Variable Costs					\$629,825.41

Table A 75: Utility consumption, and prices, and annual costs of the utilities of the base case design with the 14kPa EDC and the stripping column.

Bill of Materials	Product Production: 78702 ton/year				
Utilities	Consumption (unit/kg product)	Price (\$/unit utility)	Cost (\$/kg product)	Consumption (unit/year)	Annual Costs (\$/year)
HP Steam [ton/yr]	0.00	\$14.50	\$0.00	0.00	\$0.00
MP Steam [ton/yr]	86.84	\$10.50	\$911.85	6834.75	\$71,764.84
LP Steam [ton/yr]	493.05	\$6.60	\$3,254.12	38804.17	\$256,107.51
Electricity [kWh/yr]	463.78	\$0.06	\$27.83	36500.87	\$2,190.05
Cooling water [m ³ /yr]	52838.05	\$0.02	\$1,056.76	4158484.42	\$83,169.69
Refrigerant [GJ/yr]	134.75	\$5.50	\$741.15	10605.46	\$58,330.01
Total Variable Costs					\$471,562.11

C.8.6.4 Total Annual Costs

Table A 76: TAC calculation for the extractive distillation of ethanol and using ChCl:Ur (1:2) for the four base case designs.

	1 atm EDC evaporator	14 kPa EDC evaporator	1 atm EDC stripping	14 kPa EDC stripping
EDC + Reflux drum	\$ 105,649.39	\$ 222,905.68	\$ 130,596.48	\$ 296,607.28
Regeneration	\$ 61,180.60	\$ 88,985.05	\$ 81,302.66	\$ 96,910.92
Heat Exchanger	\$ 62,371.51	\$ 67,378.39	\$ 69,113.25	\$ 73,852.85
Vacuum system	\$ 65,099.37	\$ 98,102.74	\$ 66,154.15	\$ 98,526.83
total equipment 2019	\$ 357,575.56	\$ 580,006.81	\$ 421,807.35	\$ 687,565.93
C _{TPI}	\$ 1,779,653.54	\$ 2,886,693.90	\$ 2,099,335.17	\$ 3,422,015.65
C _{TPI} * i _{min}	\$ 355,930.71	\$ 577,338.78	\$ 419,867.03	\$ 684,403.13
C _{AP}	\$ 572,639.93	\$ 430,140.68	\$ 629,825.41	\$ 471,562.11
TAC	\$ 928,570.64	\$ 1,007,479.46	\$ 1,049,692.45	\$ 1,155,965.24

C.9 Final DES Processes & Literature Comparison

C.9.1 Utility Summary

C.9.1.1 Separation Task 1

Table A 77: Summary of utilities for the process separating ethanol and water using EG in the literature of Bastidas *et al.* (2010) [30]. The equipment numbering equals the process flowsheet shown by Figure A 35.

SUMMARY OF UTILITIES														
EQUIPMENT		UTILITIES												
Nr.	Type	Heating					Cooling				Power			
		Load	Consumption (t/h)				Load	Consumption (t/h)			Actual Load	Consumption		
			Steam			Hot		Cooling water	Chilled water	Refrig.		Steam (t/h)		Electr.
			kW	LP	MP	HP						Oil	kW	HP
E01	Cooler						689.55	56.07						
E02	Heater	153.25	0.64											
E07	Cooler						353.00	30.49						
E08	Cooler						18.15	1.57						
Condenser EDC	Cooler						3531.00	304.40						
Condenser SRC	Cooler						650.44	56.07						
Reboiler EDC	Kettle	4316.82		7.81										
Reboiler SRC	Kettle	566.88		1.02										
Vacuum system	Liquid ring pump										1.27			
Total		5036.95	0.64	8.83			5242.14	448.60			1.27			

Table A 78: Summary of utilities of the non-heat integrated process for the extractive distillation of ethanol and water with ChCl:Ur (1:2). The equipment numbering equals the process flowsheet shown by Figure A 36.

SUMMARY OF UTILITIES														
EQUIPMENT		UTILITIES												
Nr.	Type	Heating					Cooling				Power			
		Load	Consumption (t/h)			Hot	Load	Consumption (t/h)			Actual Load	Consumption		Electr.
			Steam					Cooling water	Chilled water	Refrig.		Steam (t/h)		
			kW	LP	MP							HP	Oil	
E01	Cooler						168.60	14.44						
E02	Heater	378.99	0.64											
E03	Condenser EDC						2750.53	237.22						
E04	Reboiler EDC	3088.70		5.58										
E05	Evap 1	53.63	0.09											
E06	Evap 2	111.57	0.19											
E07	Cooler						353.26	30.47						
E08	Cooler						319.12		54.80					
E09	Heater	9.90												
E10	Cooler						66.94			0.05				
E11	Heater	4.81	0.01											
Vacuum system	Steam jet ejector			0.11										
Vacuum system	Liquid ring pump										1.20			
Total		3647.96	0.92	5.69			3658.45	282.13	54.80	0.05	1.20			

Table A 79: Summary of utilities of the heat integrated process for extractive distillation of ethanol and water with ChCl:Ur (1:2), the. The equipment numbering equals the process flowsheet shown by Figure A 37.

SUMMARY OF UTILITIES														
EQUIPMENT		UTILITIES												
Nr.	Type	Heating					Cooling				Power			
		Load	Consumption (t/h)			Load	Consumption (t/h)			Actual Load	Consumption		Electr.	
			Steam				Hot	Cooling water	Chilled water		Refrig.	Steam (t/h)		
		kW	LP	MP	HP	Oil	kW			HP		MP	kWh	
E03	Condenser EDC						2750.53	237.22						
E04	Reboiler EDC	3088.55		5.58										
E05	Evap 1	53.63	0.09											
E06	Evap 2	111.57	0.19											
E07	Cooler						142.27	12.27						
E08	Cooler						319.12		54.80					
E09	Heater	9.89	0.02											
E10	Cooler						66.94			0.19				
E11	Heater	4.82	0.01											
Vacuum system	Steam jet ejector			0.11										
Vacuum system	Liquid ring pump										1.20			
Total		3268.81	0.30	5.70			3278.86	249.49	54.80	0.19	1.20			

C.9.1.2 Separation Task 2

Table A 80: Summary of utilities for the process separating ethanol and water using the IL [Emim]⁺[BF₄]⁻ in the literature of Zhu *et al.* (2016) [35]. The equipment numbering equals the process flowsheet shown by Figure A 38.

SUMMARY OF UTILITIES														
EQUIPMENT		UTILITIES												
Nr.	Type	Heating					Cooling				Power			
		Load	Consumption (t/h)			Load	Consumption (t/h)			Actual Load	Consumption			
			Steam				Hot	Cooling water	Chilled water		Refrig.	Steam (t/h)		Electr.
			kW	LP	MP		HP					Oil	kW	HP
E02	Heater													
E07	Cooler						137.24	11.82						
E08	Cooler						188.73	16.28						
E09	Cooler						3.42	0.59						
Evap 1	Flash	170.41	0.29											
Reboiler	Heater	2047.80		3.70										
Condenser							1851.60	160.10						
Vacuum system	Liquid ring pump										1.27			
Total		2218.2	0.29	3.70			2180.99	188.79			1.27			

Table A 81: Summary of utilities of the non-heat integrated process for the extractive distillation of ethanol and water with ChCl:Ur (1:2). The equipment numbering equals the process flowsheet shown by Figure A 39.

SUMMARY OF UTILITIES														
EQUIPMENT		UTILITIES												
Nr.	Type	Heating					Cooling				Power			
		Load	Consumption (t/h)			Load	Consumption (t/h)			Actual Load	Consumption			
			Steam				Hot	Cooling water	Chilled water		Refrig.	Steam (t/h)		Electr.
			kW	LP	MP		HP					Oil	kW	HP
E03	Condenser EDC						1163.32	100.33						
E04	Reboiler EDC	1393.55		2.52										
E05	Evap 1	66.01	0.11											
E06	Evap 2	42.54	0.07											
E07	Cooler						138.34	11.93						
E08	Cooler						187.70		32.23					
E09	Heater	5.59	0.01											
E10	Cooler						26.81			0.07				
E11	Heater	1.88	0.00											
Vacuum system				0.07										
Vacuum system	Liquid ring pump										1.70			
Total		1509.57	0.19	2.59			1516.17	112.26	32.23	0.07	1.70			

Table A 82: Summary of utilities of the heat integrated process for the extractive distillation of ethanol and water with ChCl:Ur (1:2). The equipment numbering equals the process flowsheet shown by Figure A 40.

SUMMARY OF UTILITIES														
EQUIPMENT		UTILITIES												
Nr.	Type	Heating					Cooling				Power			
		Load	Consumption (t/h)			Load	Consumption (t/h)			Actual Load	Consumption			
			Steam				Hot	Cooling water	Chilled water		Refrig.	Steam (t/h)		Electr.
		kW	LP	MP	HP	Oil	kW			Cooling water		Chilled water	Refrig.	kW
E03	Condenser EDC						1051.49	90.69						
E04	Reboiler EDC	1239.58		2.24										
E05	Evap 1	66.01	0.11											
E06	Evap 2	42.54	0.07											
E07	Cooler						96.53	8.33						
E08	Cooler						187.70		32.23					
E09	Heater	5.59	0.01											
E10	Cooler						26.81			0.07				
E11	Heater	1.88	0.00											
Vacuum system				0.07										
Vacuum system	Liquid ring pump										1.70			
Total		1355.60	0.19	2.32			1362.53	99.01	32.23	0.07	1.70			

C.9.1.3 Separation Task 3

Table A 83: Summary of utilities for the process separating IPA and water using DMSO in the literature of Ghuge *et al.* (2017) [31]. The equipment numbering equals the process flowsheet shown by Figure A 41.

SUMMARY OF UTILITIES														
EQUIPMENT		UTILITIES												
Nr.	Type	Heating					Cooling				Power			
		Load	Consumption (t/h)			Load	Consumption (t/h)			Actual Load	Consumption			
			Steam				Hot	Cooling water	Chilled water		Refrig.	Steam (t/h)		Electr
			kW	LP	MP		HP					Oil	kW	HP
E01	Cooler						510.10	43.72						
E07	Cooler						127.77	11.02						
E08	Cooler						70.54	6.08						
Condenser EDC	Cooler						883.47	75.73						
Condenser SRC	Cooler						830.00	71.14						
Reboiler EDC	Kettle	1412.80		2.55										
Reboiler SRC	Horizontal tube	1061.10			2.13									
Total		2473.90		2.55	2.13		2421.88	207.69						

Table A 84: Summary of utilities for the process separating IPA and water using the IL [Emim]⁺[N(CN)₂]⁻ in the literature of Ma *et al.* (2019) [36]. The equipment numbering equals the process flowsheet shown by Figure A 42.

SUMMARY OF UTILITIES														
EQUIPMENT		UTILITIES												
Nr.	Type	Heating					Cooling				Power			
		Load	Consumption (t/h)			Load	Consumption (t/h)			Actual Load	Consumption			
			Steam				Hot	Cooling water	Chilled water		Refrig.	Steam (t/h)		Electr.
			kW	LP	MP		HP					Oil	kW	HP
E01	Cooler						479.70	82.23						
E07	Cooler						127.72	11.02						
E08	Cooler						532.05	45.89						
E09	Cooler						63.06	5438.37						
E10	Cooler						64.09			0.18				
E11	Heater	3.98	0.01											
Reboiler	Kettle	1480.30		2.68										
Evap 1	Horizontal tube	567.57		1.03										
Evap 2	Horizontal tube	57.37		0.10										
Condenser	Cooler						810.38	69.46						
Vacuum system	Liquid ring pump										0.38			
Vacuum system	Steam jet ejector			0.09										
Total		2109.22	0.01	3.90			2077.00	5646.97		0.18	0.38			

Table A 85: Summary of utilities of the non-heat integrated process for the extractive distillation of IPA and water with ChCl:TEG (1:3). The equipment numbering equals the process flowsheet shown by Figure A 43.

SUMMARY OF UTILITIES														
EQUIPMENT		UTILITIES												
Nr.	Type	Heating					Cooling				Power			
		Load	Consumption (t/h)			Load	Consumption (t/h)			Actual Load	Consumption		Electr.	
			Steam				Hot	Cooling water	Chilled water		Refrig.	Steam (t/h)		
			kW	LP	MP		HP					Oil		kW
E01	Cooler						116.40	10.04						
E03	Condenser EDC						1026.55	88.53						
E04	Reboiler EDC	1193.50		2.16										
E05	Evap 1	732.54		1.32										
E06	Evap 2	45.51		0.08										
E07	Cooler						127.78	11.02						
E08	Cooler						620.37	53.50						
E09	Cooler						6.49	0.56						
E10	Cooler						54.68			0.15				
E11	Heater	4.56	0.01											
Vacuum system	Steam jet ejector			0.06										
Vacuum system	Liquid ring pump										1.52			
Total		1976.12	0.01	3.62			1952.27	163.66	0.00	0.15	1.52			

Table A 86: Summary of utilities of the heat integrated process for the extractive distillation of IPA and water with ChCl:TEG (1:3). The equipment numbering equals the process flowsheet shown by Figure A 44.

SUMMARY OF UTILITIES														
EQUIPMENT		UTILITIES												
Nr.	Type	Heating					Cooling				Power			
		Load	Consumption (t/h)			Load	Consumption (t/h)			Actual Load	Consumption			
			Steam				Hot	Cooling water	Chilled water		Refrig.	Steam (t/h)		Electr.
			kW	LP	MP		HP					Oil	kW	HP
E03	Condenser EDC						1025.95							
E04	Reboiler EDC	1026.40		1.86										
E05	Evap 1	732.54		1.32										
E06	Evap 2	45.51		0.08										
E07	Cooler						77.78	6.71						
E08	Cooler						620.37	53.50						
E09	Cooler						6.49	0.56						
E10	Cooler						54.68			0.15				
E11	Heater	4.56	0.01											
Vacuum system	Steam jet ejector			0.06										
Vacuum system	Liquid ring pump										1.52			
Total		1809.02	0.01	3.32			1785.27	60.77		0.15	1.52			

C.9.2 Flowsheets & Process Stream Summary

The flowsheets of the simulated non-heat-integrated DES processes, the simulated heat-integrated DES processes and the literature processes are shown. The literature processes do not include heat integration, which is why for comparability the DES process is also simulated without heat integration. Eventually, heat integration is applied to show a further improvement of the DES process. For the literature processes, heat exchangers and information had to be added in case it was missing in the literature and is shown in blue in the flowsheets. Heat exchanger duties and areas are calculated as usual. For the evaporators of the literature processes, the logarithmic mean temperature difference is approximated by $\Delta T_{LM} = \Delta T_1 - \Delta T_2$. For the literature processes, only information and stream numbering is shown that it is necessary for the economic assessment and given in the units required for the cost equations. For each stream is numbered and complete stream summaries are given. Compared to the base case designs, changes had to be made for the comparability. For example, the pressure drop of the columns is zero, which is why also a total number of stages changes compared to the base case designs. More details can be found below the flowsheets.

C.9.2.1 Separation Task 1

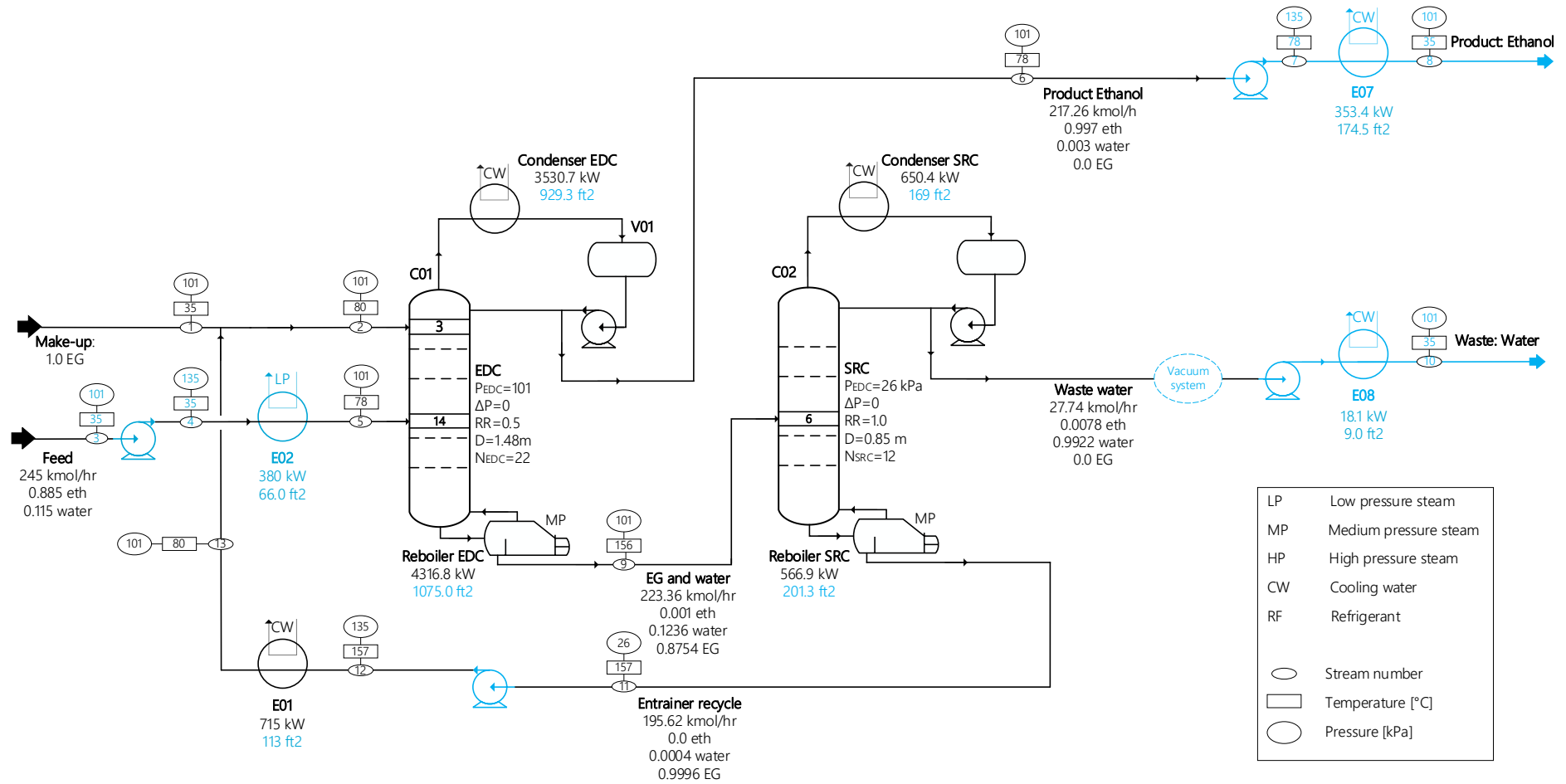


Figure A 35: Literature process of the separation of ethanol and water with the conventional solvent EG taken from Bastidas *et al.* (2010) [30]. Added equipment or equipment characteristics necessary for the economic assessment are marked in blue.

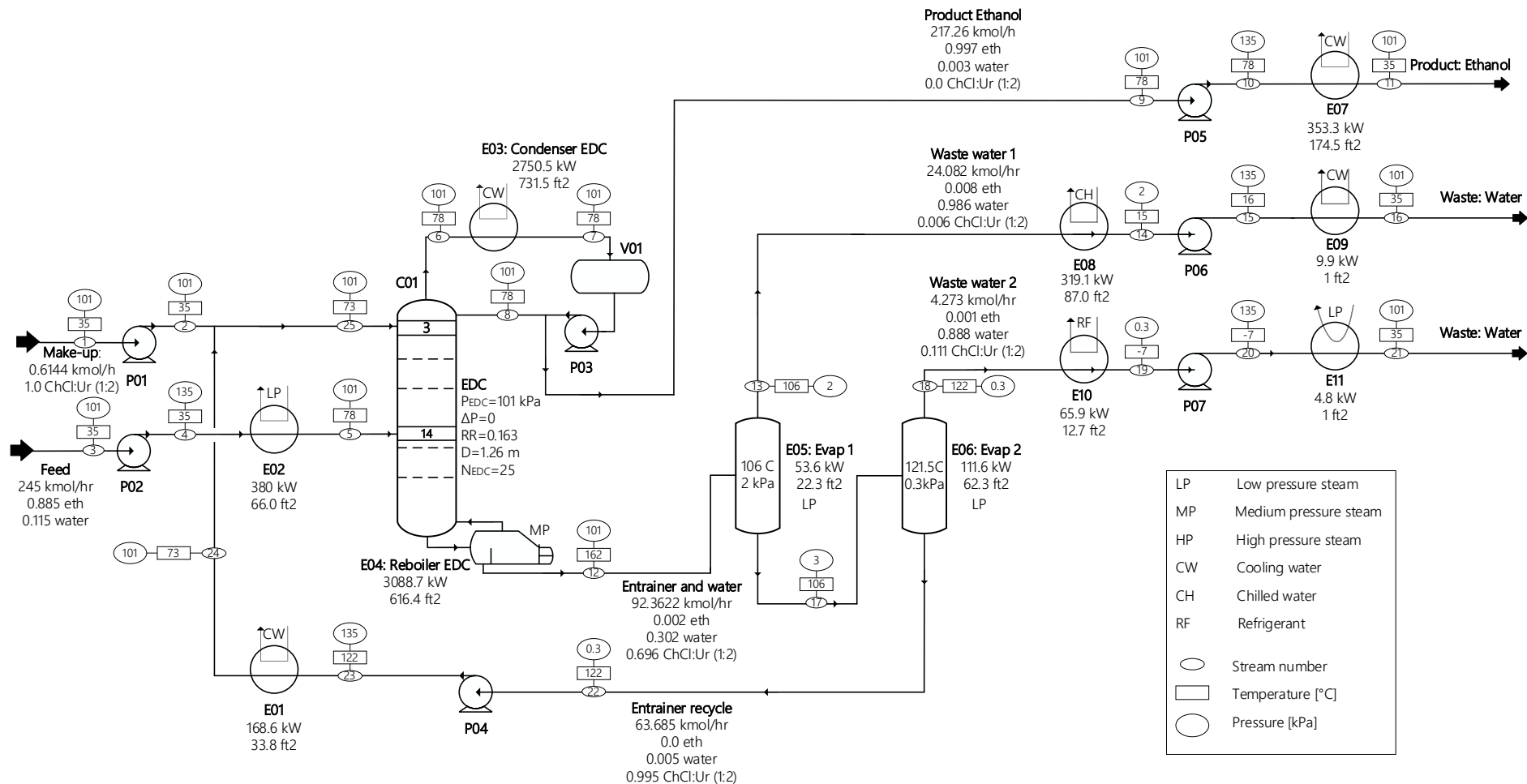


Figure A 36: Process flowsheet for the separation of ethanol and water using ChCl:Ur (1:2). This process is compared with the conventional process using EG.

Table A 87: Process stream summary for the separation of ethanol and water using ChCl:Ur (1:2). This process is compared with the conventional process using EG.

Process Stream Summary																	
STREAM	Nr.	1		2		3		4		5		6		7		8	
COMP	MW	kg/s	mol/s	kg/s	mol/s	kg/s	mol/s	kg/s	mol/s	kg/s	mol/s	kg/s	mol/s	kg/s	mol/s	kg/s	mol/s
ChCl:Ur (1:2)	86.58	0.015	0.173	0.015	0.173	0.000	0.000	0.000	0.000	0.000	0.000	0.000	0.000	0.000	0.000	0.000	0.000
Water	18.02	0.000	0.000	0.000	0.000	0.141	7.826	0.141	7.826	0.141	7.826	0.004	0.206	0.004	0.206	0.001	0.029

Ethanol	46.07	0.000	0.000	0.000	0.000	2.775	60.229	2.775	60.229	2.775	60.229	3.224	69.981	3.224	69.981	0.452	9.808
Total		0.015	0.173	0.015	0.173	2.916	68.056	2.916	68.056	2.916	68.056	3.228	70.187	3.228	70.187	0.452	9.837
Enthalpy flow	kW		12		12		18864		18864		18485		16232		18983		2661
Vapor frac			0		0		0		0		0		1		0		0
Press.	kPa		101.0		101.0		101.3		135.0		101.3		101.3		101.3		101.3
Temp	°C		35		35.1		35		35.1		78.1		78.3		78.3		78.3
STREAM	Nr.	9		10		11		12		13		14		15		16	
COMP	MW	kg/s	mol/s	kg/s	mol/s	kg/s	mol/s	kg/s	mol/s	kg/s	mol/s	kg/s	mol/s	kg/s	mol/s	kg/s	mol/s
ChCl:Ur (1:2)	86.58	0.000	0.000	0.000	0.000	0.000	0.000	1.546	17.861	0.003	0.038	0.003	0.038	0.003	0.038	0.003	0.038
Water	18.02	0.003	0.177	0.003	0.177	0.003	0.177	0.139	7.738	0.119	6.595	0.119	6.595	0.119	6.595	0.119	6.595
Ethanol	46.07	2.772	60.173	2.772	60.173	2.772	60.173	0.003	0.057	0.003	0.056	0.003	0.056	0.003	0.056	0.003	0.056
Total		2.775	60.350	2.775	60.350	2.775	60.350	1.688	25.656	0.125	6.689	0.125	6.689	0.125	6.689	0.125	6.689
Enthalpy flow	kW		16322		16322		16675		2957		1589		1908		1908		1899
Vapor frac			0		0		0		0		1		0		0		0
Press.	kPa		101.3		135.0		101.3		101.3		2.0		2.0		135.0		100.0
Temp	°C		78.3		78.3		35		161.8		106		15.4		15.5		35
STREAM	Nr.	17		18		19		20		21		22		23		24	
COMP	MW	kg/s	mol/s	kg/s	mol/s	kg/s	mol/s	kg/s	mol/s	kg/s	mol/s	kg/s	mol/s	kg/s	mol/s	kg/s	mol/s
ChCl:Ur (1:2)	86.58	1.543	17.823	0.011	0.133	0.011	0.133	0.011	0.133	0.011	0.133	1.532	17.690	1.532	17.690	1.532	17.690
Water	18.02	0.021	1.143	0.019	1.054	0.019	1.054	0.019	1.054	0.019	1.054	0.002	0.089	0.002	0.089	0.002	0.089
Ethanol	46.07	0.000	0.000	0.000	0.000	0.000	0.000	0.000	0.000	0.000	0.000	0.000	0.000	0.000	0.000	0.000	0.000
Total		1.564	18.966	0.030	1.187	0.030	1.187	0.030	1.187	0.030	1.187	1.533	17.779	1.533	17.779	1.533	17.779
Enthalpy flow	kW		1315		250		316		316		311		953		952		1121
Vapor frac			0		1		0		0		0		0		0		0
Press.	kPa		2.0		0.3		0.3		135.0		101.3		0.3		135.0		101.3
Temp	°C		106		121.5		-6.6		-6.5		35		121.5		121.7		73
STREAM	Nr.	25															
COMP	MW	kg/s	mol/s	kg/s	mol/s	kg/s	mol/s	kg/s	mol/s	kg/s	mol/s	kg/s	mol/s	kg/s	mol/s	kg/s	mol/s
ChCl:Ur (1:2)	86.58	1.546	17.861														
Water	18.02	0.002	0.089														
Ethanol	46.07	0.000	0.000														
Total		1.548	17.951														
Enthalpy flow	kW		1132														
Vapor frac			0														
Press.	kPa		101.3														
Temp	°C		72.6														

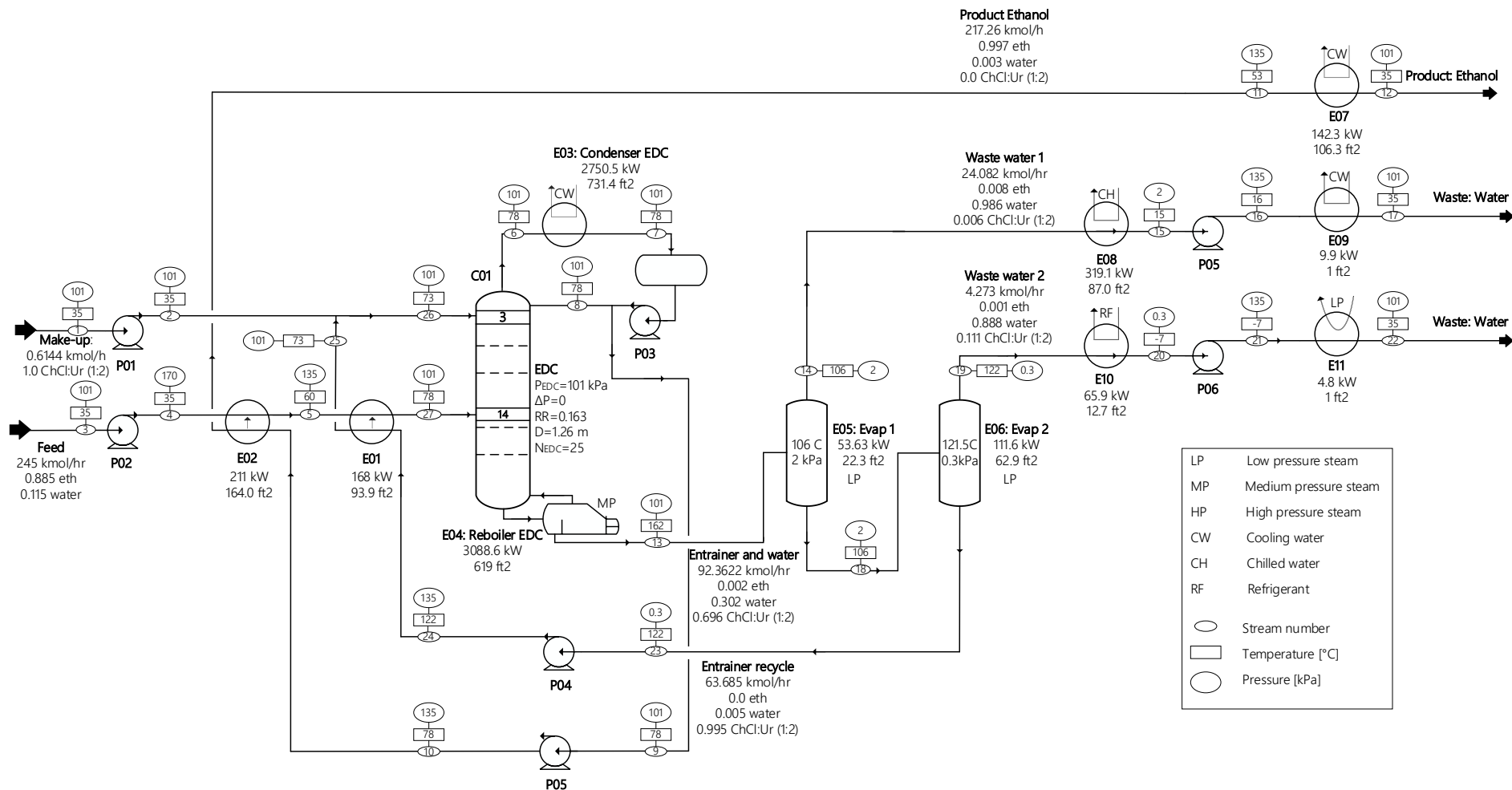


Figure A 37: Process flowsheet for the separation of ethanol and water using ChCl:Ur (1:2) using heat integration.

Table A 88: Process stream summary for the separation of ethanol and water using ChCl:Ur (1:2) using heat integration.

Process Stream Summary															
STREAM	Nr.	1		2		3		4		5		6		7	
COMP	MW	kg/s	mol/s	kg/s	mol/s	kg/s	mol/s	kg/s	mol/s	kg/s	mol/s	kg/s	mol/s	kg/s	mol/s
ChCl:Ur (1:2)	86.58	0.015	0.173	0.015	0.173	0.000	0.000	0.000	0.000	0.000	0.000	0.000	0.000	0.000	0.000

Water	18.02	0.000	0.000	0.000	0.000	0.141	7.826	0.141	7.826	0.141	7.826	0.004	0.206	0.004	0.206	0.000	0.006
Ethanol	46.07	0.000	0.000	0.000	0.000	2.775	60.229	2.775	60.229	2.775	60.229	3.224	69.981	3.224	69.981	0.312	2.125
Total		0.015	0.173	0.015	0.173	2.916	68.056	2.916	68.056	2.916	68.056	3.228	70.187	3.228	70.187	0.312	2.131
Enthalpy flow	kW		12		12		18864		18864		18653		16232		18983		576
Vapor frac			0		0		0		0		0		1		0		0
Press.	kPa		101.0		101.0		101.3		170.0		135.0		135.0		135.0		135.0
Temp	°C		35		35.1		35		35.1		59.9		78.3		78.3		78.3
STREAM	Nr.	9		10		11		12		13		14		15		16	
COMP	MW	kg/s	mol/s	kg/s	mol/s	kg/s	mol/s	kg/s	mol/s	kg/s	mol/s	kg/s	mol/s	kg/s	mol/s	kg/s	mol/s
ChCl:Ur (1:2)	86.58	0.000	0.000	0.000	0.000	0.000	0.000	0.000	0.000	1.546	17.861	0.003	0.038	0.003	0.038	0.003	0.038
Water	18.02	0.003	0.177	0.003	0.177	0.003	0.177	0.003	0.177	0.139	7.738	0.119	6.595	0.119	6.595	0.119	6.595
Ethanol	46.07	2.772	60.173	2.772	60.173	2.772	60.173	2.772	60.173	0.003	0.057	0.003	0.056	0.003	0.056	0.003	0.056
Total		2.775	60.350	2.775	60.350	2.775	60.350	2.775	60.350	1.688	25.656	0.125	6.689	0.125	6.689	0.125	6.689
Enthalpy flow	kW		16322		16322		16533		16675		2957		1589		1908		1908
Vapor frac			0		0		0		0		0		1		0		0
Press.	kPa		101.3		135.0		135.0		101.3		101.3		2.0		2.0		135.0
Temp	°C		78.3		78.3		53.3		35		161.7		106		15.4		15.5
STREAM	Nr.	17		18		19		20		21		22		23		24	
COMP	MW	kg/s	mol/s	kg/s	mol/s	kg/s	mol/s	kg/s	mol/s	kg/s	mol/s	kg/s	mol/s	kg/s	mol/s	kg/s	mol/s
ChCl:Ur (1:2)	86.58	0.003	0.038	1.543	17.823	0.011	0.133	0.011	0.133	0.011	0.133	0.011	0.133	1.532	17.690	1.532	17.690
Water	18.02	0.119	6.595	0.021	1.143	0.019	1.054	0.019	1.054	0.019	1.054	0.019	1.054	0.002	0.089	0.002	0.089
Ethanol	46.07	0.003	0.056	0.000	0.000	0.000	0.000	0.000	0.000	0.000	0.000	0.000	0.000	0.000	0.000	0.000	0.000
Total		0.125	6.689	1.564	18.966	0.030	1.187	0.030	1.187	0.030	1.187	0.030	1.187	1.533	17.779	1.533	17.779
Enthalpy flow	kW		1899		1315		250		316		316		311		953		952
Vapor frac			0		0		1		0		0		0		0		0
Press.	kPa		101.3		2.0		0.3		0.3		135.0		101.3		0.3		135.0
Temp	°C		35		106		121.5		-6.6		-6.5		35		121.5		121.7
STREAM	Nr.	25		26		27											
COMP	MW	kg/s	mol/s	kg/s	mol/s	kg/s	mol/s	kg/s	mol/s	kg/s	mol/s	kg/s	mol/s	kg/s	mol/s	kg/s	mol/s
ChCl:Ur (1:2)	86.58	1.532	17.690	1.546	17.861	0.000	0.000										
Water	18.02	0.002	0.089	0.000	0.089	0.141	7.826										
Ethanol	46.07	0.000	0.000	0.000	0.000	2.775	60.229										
Total		1.533	17.779	1.546	17.951	2.916	68.056										
Enthalpy flow	kW		1.12E+03		1132		18485										
Vapor frac			0		0		0										
Press.	kPa		101.3		101.3		101.3										
Temp	°C		73.2		72.6		78.1										

C.9.2.2 Separation Task 2

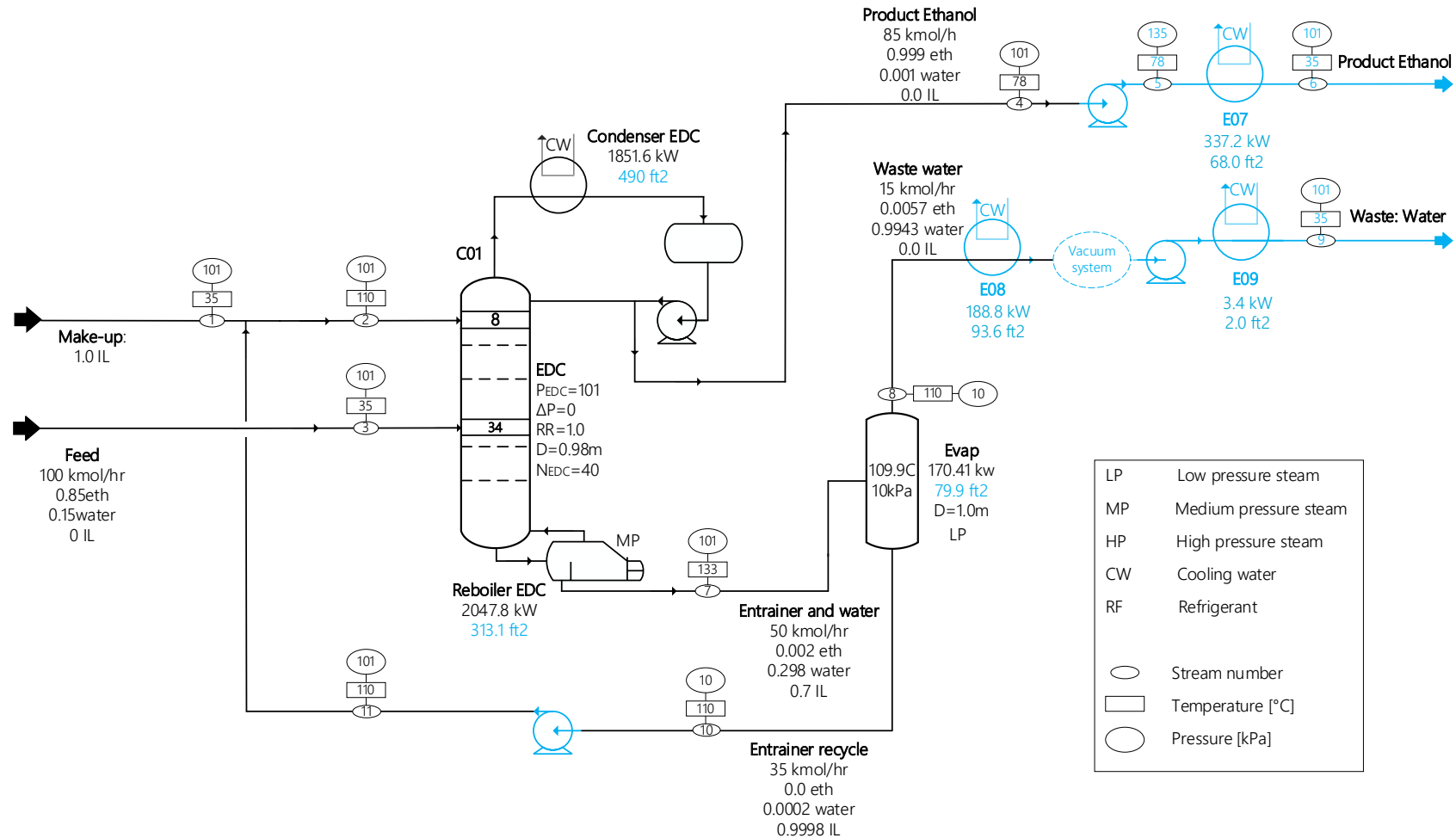


Figure A 38: Literature process of the separation of ethanol and water with the IL [Emim]⁺[BF₄]⁻ taken from Zhu *et al.* (2016) [35]. Added equipment or equipment characteristics necessary for the economic assessment are marked in blue. No IL recovery constraint can be found.

Untypically, the entrainer is not cooled down, and the feed is not heated up. Hence, the same counts for the simulated DES process, which is shown in the following figure.

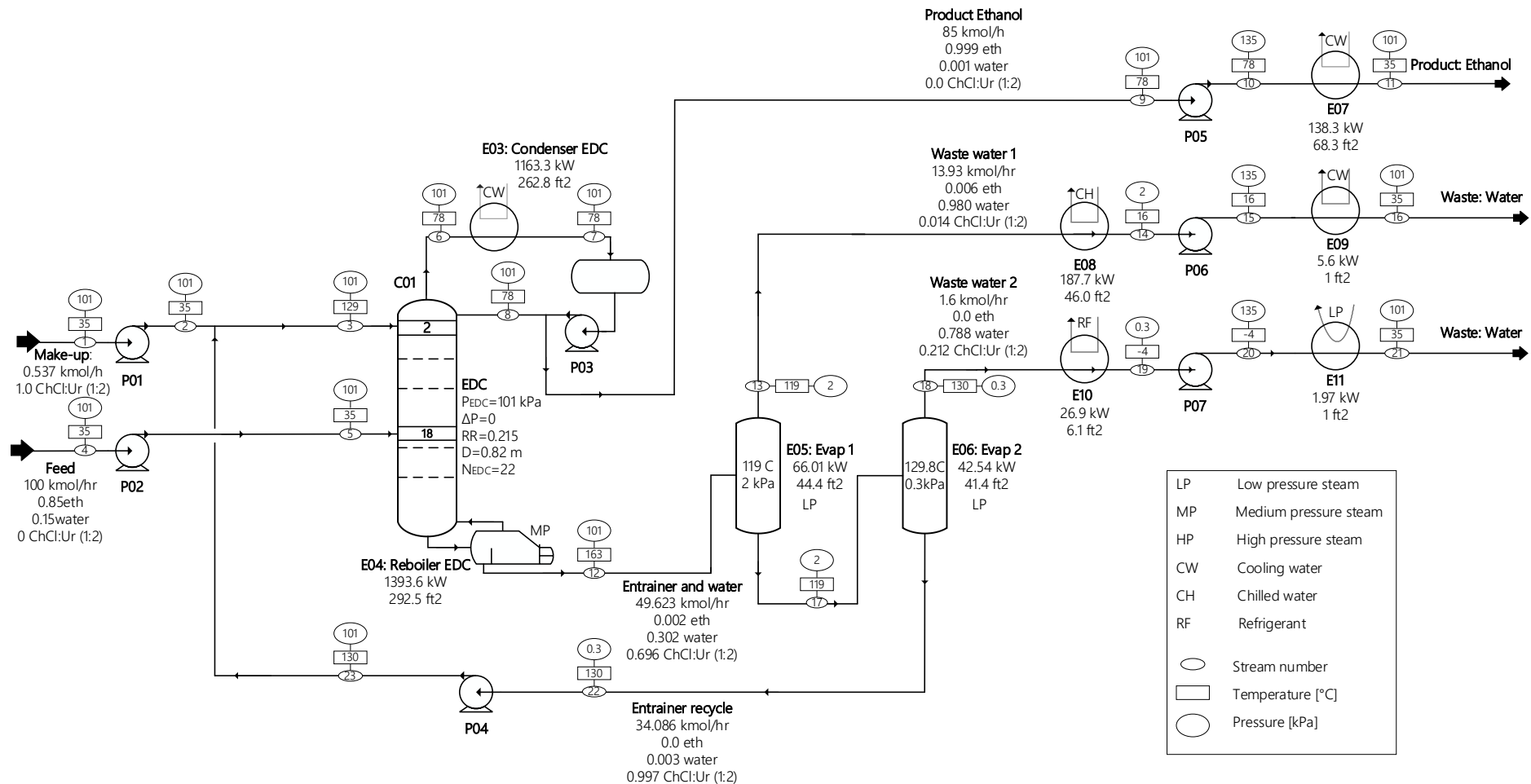


Figure A 39: Process flowsheet for the separation of ethanol and water using ChCl:Ur (1:2). This process is compared with the process using the IL.

Table A 89: Process stream summary for the separation of ethanol and water using ChCl:Ur (1:2). This process is compared with the process using the IL.

Process Stream Summary																	
STREAM	Nr.	1		2		3		4		5		6		7		8	
COMP	MW	kg/s	mol/s	kg/s	mol/s	kg/s	mol/s	kg/s	mol/s	kg/s	mol/s	kg/s	mol/s	kg/s	mol/s	kg/s	mol/s
ChCl:Ur (1:2)	86.58	0.013	0.149	0.013	0.149	0.830	9.589	0.000	0.000	0.000	0.000	0.000	0.000	0.000	0.000	0.000	0.000

Water	18.02	0.000	0.000	0.000	0.000	0.001	0.029	0.075	4.167	0.075	4.167	0.000	0.027	0.000	0.027	0.000	0.015
Ethanol	46.07	0.000	0.000	0.000	0.000	0.000	0.000	1.088	23.611	1.088	23.611	1.320	28.659	1.320	28.659	0.233	5.061
Total		0.013	0.149	0.013	0.149	0.831	9.618	1.163	27.778	1.163	27.778	1.321	28.688	1.321	28.688	0.234	5.076
Enthalpy flow	kW		10		10		497		7707		7707		6595		7758		1373
Vapor frac			0		0		0		0		0		1		0		0
Press.	kPa		101.0		101.3		101.3		101.3		101.3		101.3		101.3		101.3
Temp	°C		35		35		128.6		35		35		78.3		78.3		78.3
STREAM	Nr.		9		10		11		12		13		14		15		16
COMP	MW		kg/s mol/s		kg/s mol/s		kg/s mol/s		kg/s mol/s		kg/s mol/s		kg/s mol/s		kg/s mol/s		kg/s mol/s
ChCl:Ur (1:2)	86.58	0.000	0.001	0.000	0.001	0.000	0.001	0.830	9.588	0.005	0.053	0.005	0.053	0.005	0.053	0.005	0.053
Water	18.02	0.000	0.022	0.000	0.022	0.000	0.022	0.075	4.173	0.068	3.792	0.068	3.792	0.068	3.792	0.068	3.792
Ethanol	46.07	1.087	23.588	1.087	23.588	1.087	23.588	0.001	0.023	0.001	0.023	0.001	0.023	0.001	0.023	0.001	0.023
Total		1.087	23.611	1.087	23.611	1.087	23.611	0.906	13.784	0.074	3.869	0.074	3.869	0.074	3.869	0.074	3.869
Enthalpy flow	kW		6385		6385		6524		1588		910		1098		1097		1092
Vapor frac			0		0		0		0		1		0		0		0
Press.	kPa		101.3		135.0		101.3		101.3		2.0		2.0		135.0		101.3
Temp	°C		78.3		78.3		35		162.7		119		16.1		16.2		35
STREAM	Nr.		17		18		19		20		21		22		23		
COMP	MW		kg/s mol/s		kg/s mol/s		kg/s mol/s		kg/s mol/s		kg/s mol/s		kg/s mol/s		kg/s mol/s		kg/s mol/s
ChCl:Ur (1:2)	86.58	0.825	9.534	0.008	0.095	0.008	0.095	0.008	0.095	0.008	0.095	0.817	9.440	0.817	9.440		
Water	18.02	0.007	0.381	0.006	0.352	0.006	0.352	0.006	0.352	0.006	0.352	0.001	0.029	0.001	0.029		
Ethanol	46.07	0.000	0.000	0.000	0.000	0.000	0.000	0.000	0.000	0.000	0.000	0.000	0.000	0.000	0.000		
Total		0.832	9.915	0.015	0.447	0.015	0.447	0.015	0.447	0.015	0.447	0.818	9.468	0.818	9.468		
Enthalpy flow	kW		612		83		110		110		108		487		487		
Vapor frac			0		1		0		0		0		0		0		
Press.	kPa		2.0		0.3		0.3		135.0		101.3		0.3		101.3		
Temp	°C		119		129.8		-3.9		-3.8		35		129.8		129.9		

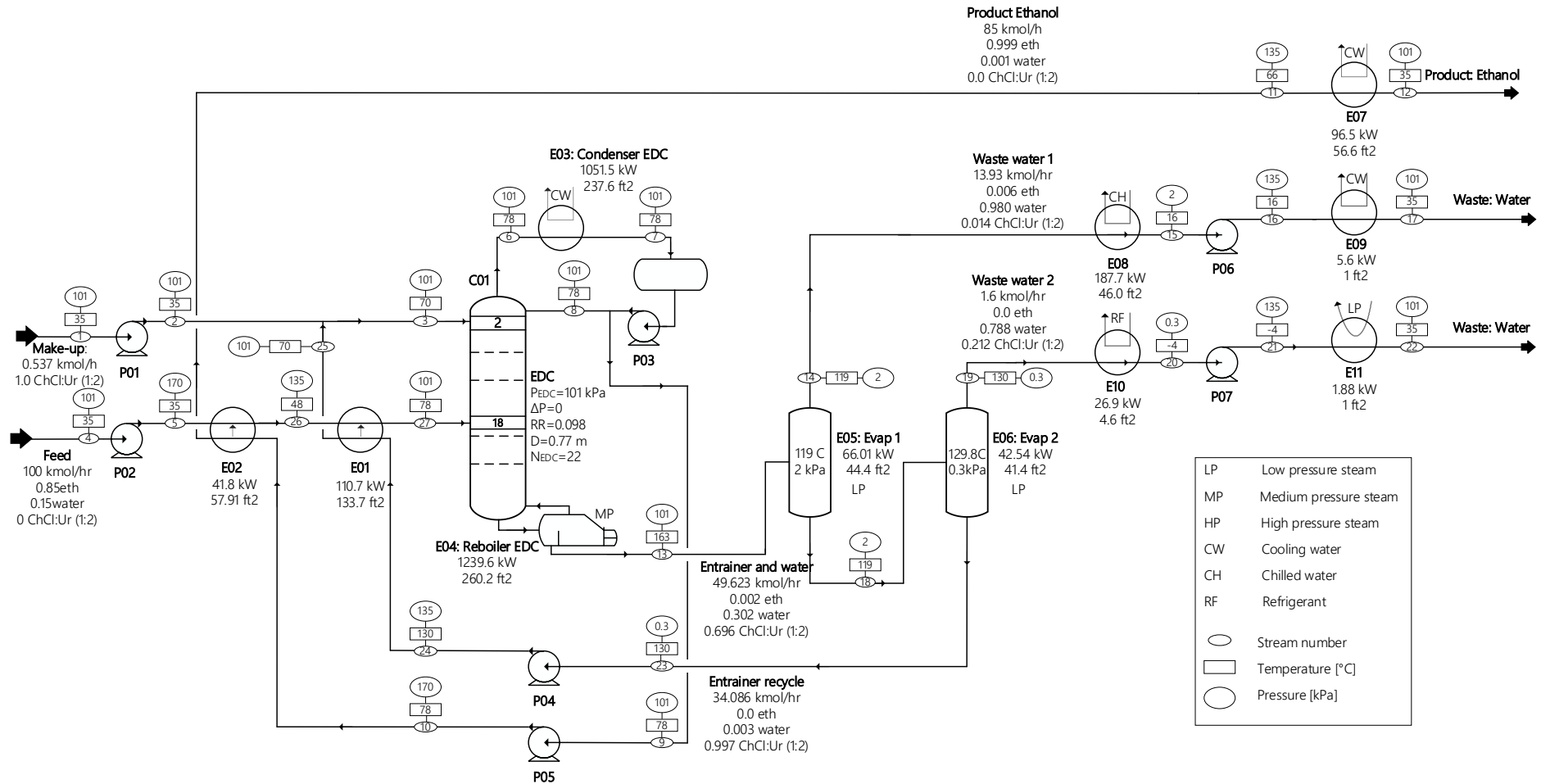


Figure A 40: Process flowsheet for the separation of ethanol and water using ChCl:Ur (1:2) using heat integration. This process is compared with the process using the IL.

Table A 90: Process stream summary for the separation of ethanol and water using ChCl:Ur (1:2) using heat integration.

Process Stream Summary																	
STREAM	Nr.	1		2		3		4		5		6		7		8	
COMP	MW	kg/s	mol/s	kg/s	mol/s	kg/s	mol/s	kg/s	mol/s	kg/s	mol/s	kg/s	mol/s	kg/s	mol/s	kg/s	mol/s
ChCl:Ur (1:2)	86.58	0.013	0.149	0.013	0.149	0.830	9.589	0.000	0.000	0.000	0.000	0.000	0.000	0.000	0.000	0.000	0.000
Water	18.02	0.000	0.000	0.000	0.000	0.001	0.029	0.075	4.167	0.075	4.167	0.000	0.027	0.000	0.027	0.000	0.015

Ethanol	46.07	0.000	0.000	0.000	0.000	0.000	0.000	1.088	23.611	1.088	23.611	1.320	28.659	1.320	28.659	0.233	5.061
Total		0.013	0.149	0.013	0.149	0.831	9.618	1.163	27.778	1.163	27.778	1.321	28.688	1.321	28.688	0.234	5.076
Enthalpy	kW		10		10		608		7707		7707		6595		7758		1373
Vapor frac			0		0		0		0		0		1		0		0
Press.	kPa		101.0		160.0		101.3		101.3		170.0		170.0		170.0		170.0
Temp	°C		35		35.1		69.5		35		35.1		78.3		78.3		78.3
STREAM	Nr.	9		10		11		12		13		14		15		16	
COMP	MW	kg/s	mol/s	kg/s	mol/s	kg/s	mol/s	kg/s	mol/s	kg/s	mol/s	kg/s	mol/s	kg/s	mol/s	kg/s	mol/s
ChCl:Ur	86.58	0.000	0.001	0.000	0.001	0.000	0.001	0.000	0.001	0.830	9.588	0.825	9.534	0.005	0.053	0.005	0.053
Water	18.02	0.000	0.022	0.000	0.022	0.000	0.022	0.000	0.022	0.075	4.173	0.007	0.381	0.068	3.793	0.068	3.793
Ethanol	46.07	1.087	23.588	1.087	23.59	1.087	23.588	1.087	23.588	0.001	0.023	0.000	0.000	0.001	0.023	0.001	0.023
Total		1.087	23.611	1.087	23.611	1.087	23.611	1.087	23.611	0.906	13.784	0.832	9.915	0.074	3.869	0.074	3.869
Enthalpy	kW		6385		6385		6427		6524		1588		612		1098		1097
Vapor frac			0		0		0		0		0		0		0		0
Press.	kPa		101.3		170.0		170.0		101.3		101.3		2.0		2.0		135.0
Temp	°C		78.3		78.4		66.1		35		162.8		119		16.1		16.2
STREAM	Nr.	17		18		19		20		21		22		23		24	
COMP	MW	kg/s	mol/s	kg/s	mol/s	kg/s	mol/s	kg/s	mol/s	kg/s	mol/s	kg/s	mol/s	kg/s	mol/s	kg/s	mol/s
ChCl:Ur	86.58	0.005	0.053	0.005	0.053	0.008	0.095	0.008	0.095	0.008	0.095	0.008	0.095	0.817	9.440	0.817	9.440
Water	18.02	0.068	3.793	0.068	3.793	0.006	0.352	0.006	0.352	0.006	0.352	0.006	0.352	0.001	0.029	0.001	0.029
Ethanol	46.07	0.001	0.023	0.001	0.023	0.000	0.000	0.000	0.000	0.000	0.000	0.000	0.000	0.000	0.000	0.000	0.000
Total		0.074	3.869	0.074	3.869	0.015	0.447	0.015	0.447	0.015	0.447	0.015	0.447	0.818	9.468	0.818	9.468
Enthalpy	kW		1092		910		83		110		110		108		487		487
Vapor frac			0		1		1		0		0		0		0		0
Press.	kPa		100.0		2.0		0.3		0.3		135.0		101.3		0.3		170.0
Temp	°C		35		119		129.8		-3.9		-3.8		35		129.8		130
STREAM	Nr.	25		26		27											
COMP	MW	kg/s	mol/s	kg/s	mol/s	kg/s	mol/s	kg/s	mol/s	kg/s	mol/s	kg/s	mol/s	kg/s	mol/s	kg/s	mol/s
ChCl:Ur	86.58	0.817	9.440	0.000	0.000	0.000	0.000										
Water	18.02	0.001	0.029	0.075	4.167	1.088	4.167										
Ethanol	46.07	0.000	0.000	1.088	23.611	1.088	23.611										
Total		0.818	9.468	1.163	27.778	2.175	27.778										
Enthalpy	kW		597		7.67E+03		7554										
Vapor frac			0		0		0										
Press.	kPa		170.0		136.8		101.3										
Temp	°C		70.4		47.6		78.2										

C.9.2.3 Separation Task 3

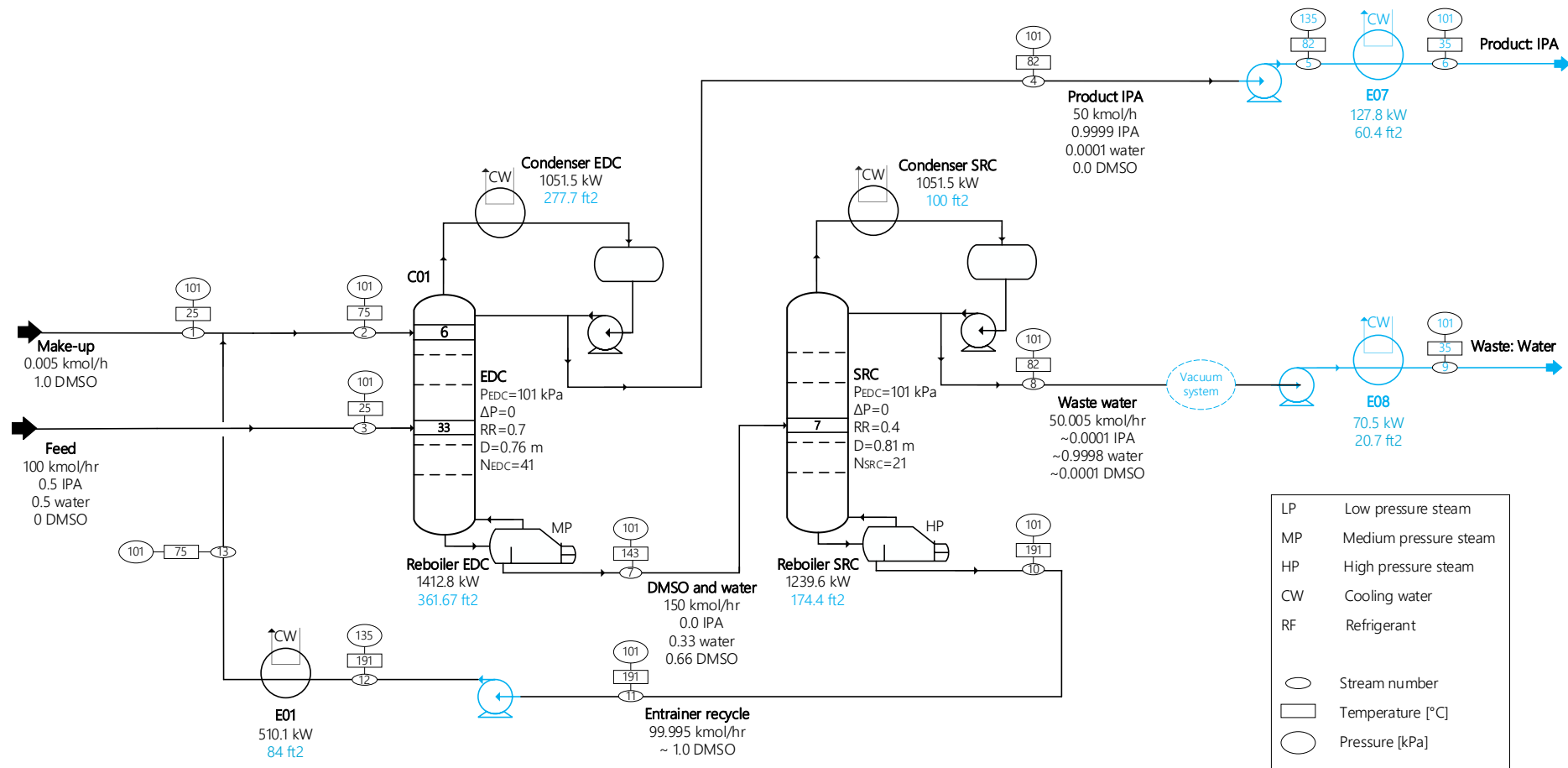


Figure A 41: Literature process of the separation of IPA and water with the conventional entrainer DMSO taken from Ghuge *et al.* (2019) [31]. Added equipment or equipment characteristics necessary for the economic assessment are marked in blue.

Untypically, the entrainer is cooled down to 25 °C instead of the temperature proposed by Doherty and Malone (2001) [68]. Also, the feed is not heated up. Thus, the simulated DES process is also designed like that for better comparability. Areas were given by Ghuge *et al.* (2019) but were adapted by taking the exact same heat transfer coefficients as described by *H* 2.

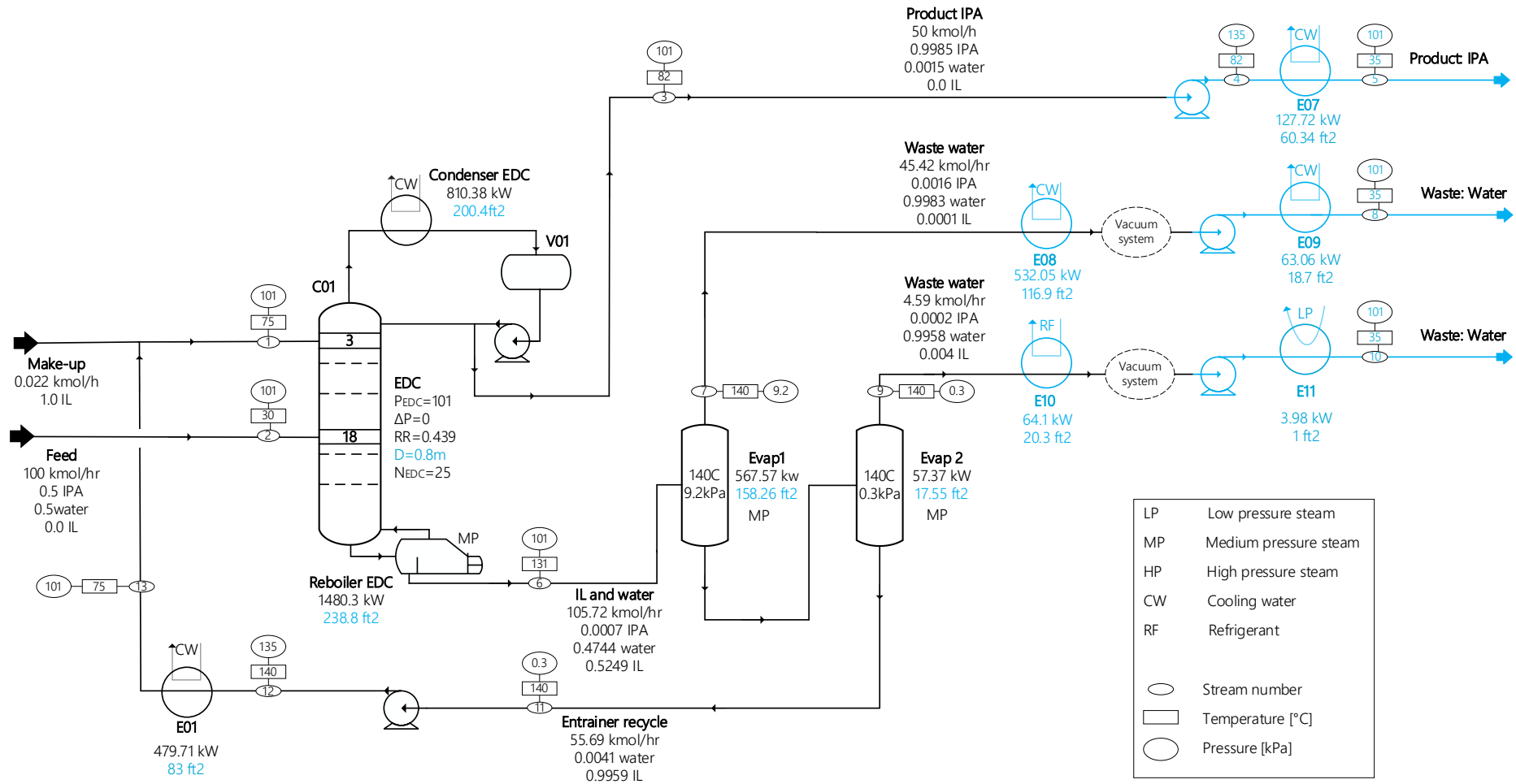


Figure A 42: Literature process of the separation of IPA and water with the IL $[\text{Emim}]^+[\text{N}(\text{CN})_2]^-$ taken from Ma *et al.* (2019) [36]. Added equipment or equipment characteristics necessary for the economic assessment are marked in blue.

The diameter of the column was approximated by Aspen Plus assuming the same flowrates in the column and number of stages with the DES instead of the IL. Unlike the other literature process, flowrates of the vacuum system have been given by Ma *et al.* (2019) [36].

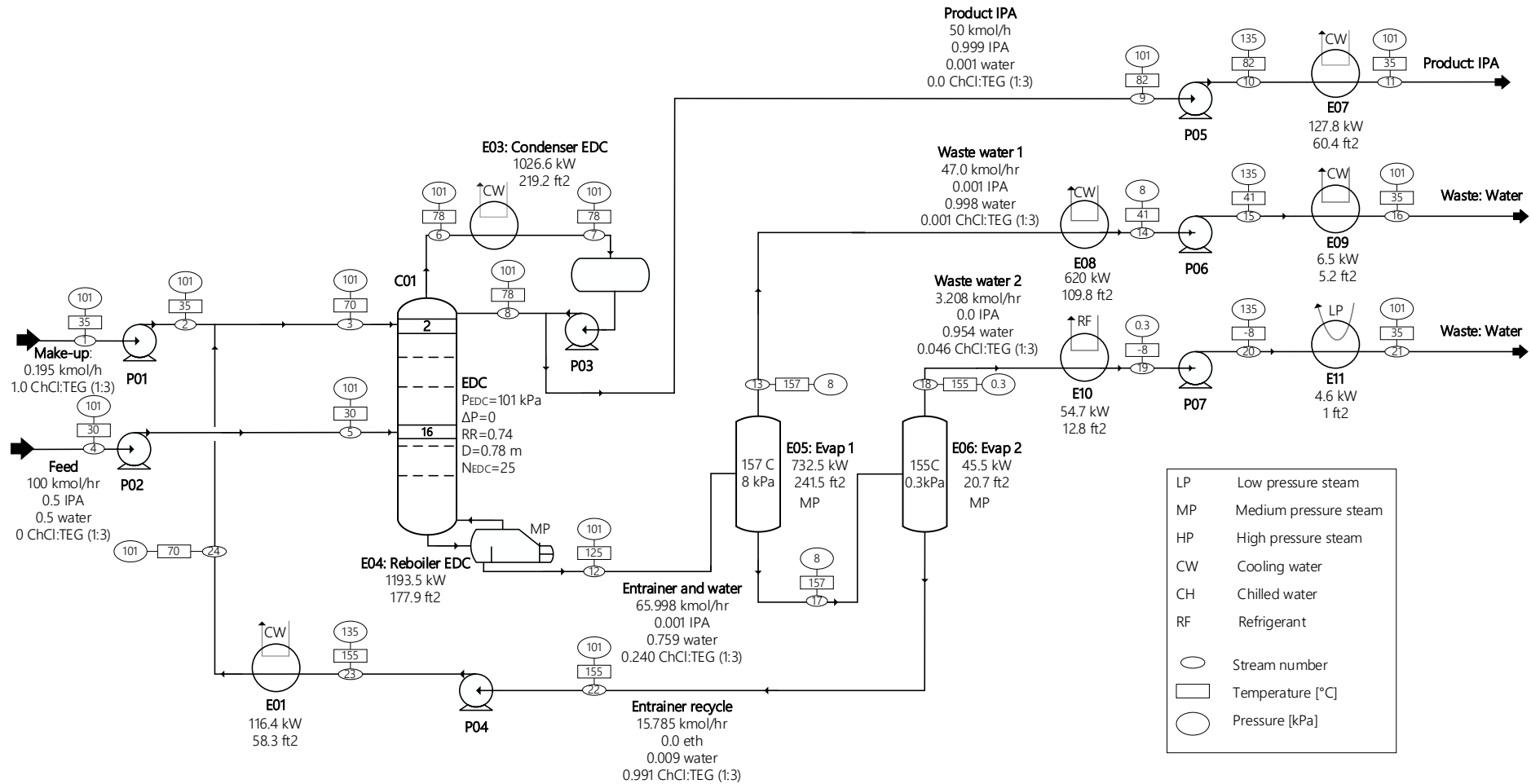


Figure A 43: Process flow diagram of the extractive distillation of IPA and water using ChCl:TEG (1:3). The simulation was adapted to match the literature.

Table A 91: Process stream summary for the separation of IPA and water using ChCl:TEG (1:3).

Process Stream Summary																	
STREAM	Nr. Name	1		2		3		4		5		6		7		8	
COMP	MW	kg/s	mol/s	kg/s	mol/s	kg/s	mol/s	kg/s	mol/s	kg/s	mol/s	kg/s	mol/s	kg/s	mol/s	kg/s	mol/s
ChCl:TEG (1:3)	147.5	0.009	0.059	0.009	0.059	0.65	4.405	0.000	0.000	0.009	0.059	0.009	0.059	0.65	4.405	0.000	0.000
Water	18.02	0.000	0.000	0.000	0.000	0.001	0.039	0.250	13.889	0.000	0.000	0.000	0.000	0.001	0.039	0.250	13.889
Ethanol	60.1	0.000	0.000	0.000	0.000	0.000	0.000	0.835	13.889	0.000	0.000	0.000	0.000	0.000	0.000	0.835	13.889
Total		0.009	0.059	0.009	0.059	0.651	4.444	1.085	27.778	0.009	0.059	0.009	0.059	0.651	4.444	1.085	27.778
Enthalpy flow	kW	29		29		2126		8384		8384		7300		8468		4202	
Vapor frac		0		0		0		0		0		1		0		0	
Press.	kPa	101.3		150.0		101.3		101.3		150.0		150.0		150.0		150.0	
Temp	°C	35		35.1		74.5		30		30.1		78.3		78.3		78.3	
STREAM	Nr. Name	9		10		11		12		13		14		15		16	
COMP	MW	kg/s	mol/s	kg/s	mol/s	kg/s	mol/s	kg/s	mol/s	kg/s	mol/s	kg/s	mol/s	kg/s	mol/s	kg/s	mol/s
ChCl:TEG (1:3)	147.5	0.000	0.000	0.000	0.000	0.000	0.000	0.650	4.405	0.003	0.018	0.003	0.018	0.003	0.018	0.003	0.018
Water	18.02	0.000	0.014	0.000	0.014	0.000	0.014	0.251	13.914	0.235	13.025	0.235	13.025	0.235	13.025	0.235	13.025
Ethanol	60.1	0.834	13.875	0.834	13.875	0.834	13.875	0.001	0.014	0.001	0.014	0.001	0.014	0.001	0.014	0.001	0.014
Total		0.834	13.889	0.834	13.889	0.834	13.889	0.901	18.333	0.238	13.057	0.238	13.057	0.238	13.057	0.238	13.057
Enthalpy flow	kW	4266		4266		4394		6077		3101.6		3722		3722		3728	
Vapor frac		0		0		0		0		1		0		0		0	
Press.	kPa	101.3		135.0		101.3		101.3		8.0		8.0		135.0		101.3	
Temp	°C	82		82.1		35		124.9		157		41.3		41.4		35	
STREAM	Nr. Name	17		18		19		20		21		22		23		24	
COMP	MW	kg/s	mol/s	kg/s	mol/s	kg/s	mol/s	kg/s	mol/s	kg/s	mol/s	kg/s	mol/s	kg/s	mol/s	kg/s	mol/s
ChCl:TEG (1:3)	147.5	0.647	4.387	0.006	0.041	0.006	0.041	0.006	0.041	0.006	0.041	0.641	4.346	0.641	4.346	0.641	4.346
Water	18.02	0.016	0.889	0.015	0.850	0.015	0.850	0.015	0.850	0.015	0.850	0.001	0.039	0.001	0.039	0.001	0.039
Ethanol	60.1	0.000	0.000	0.000	0.000	0.000	0.000	0.000	0.000	0.000	0.000	0.000	0.000	0.000	0.000	0.000	0.000
Total		0.663	5.276	0.021	0.891	0.021	0.891	0.021	0.891	0.021	0.891	0.642	4.385	0.642	4.385	0.642	4.385
Enthalpy flow	kW	2243		217		272		272		267		1980		1980		2103	
Vapor frac		0		1		0		0		0		0		0		0	
Press.	kPa	8.0		0.3		0.3		135.0		101.3		0.3		135.0		101.3	
Temp	°C	157		155		-8.4		-8.3		35		155		155.2		70	

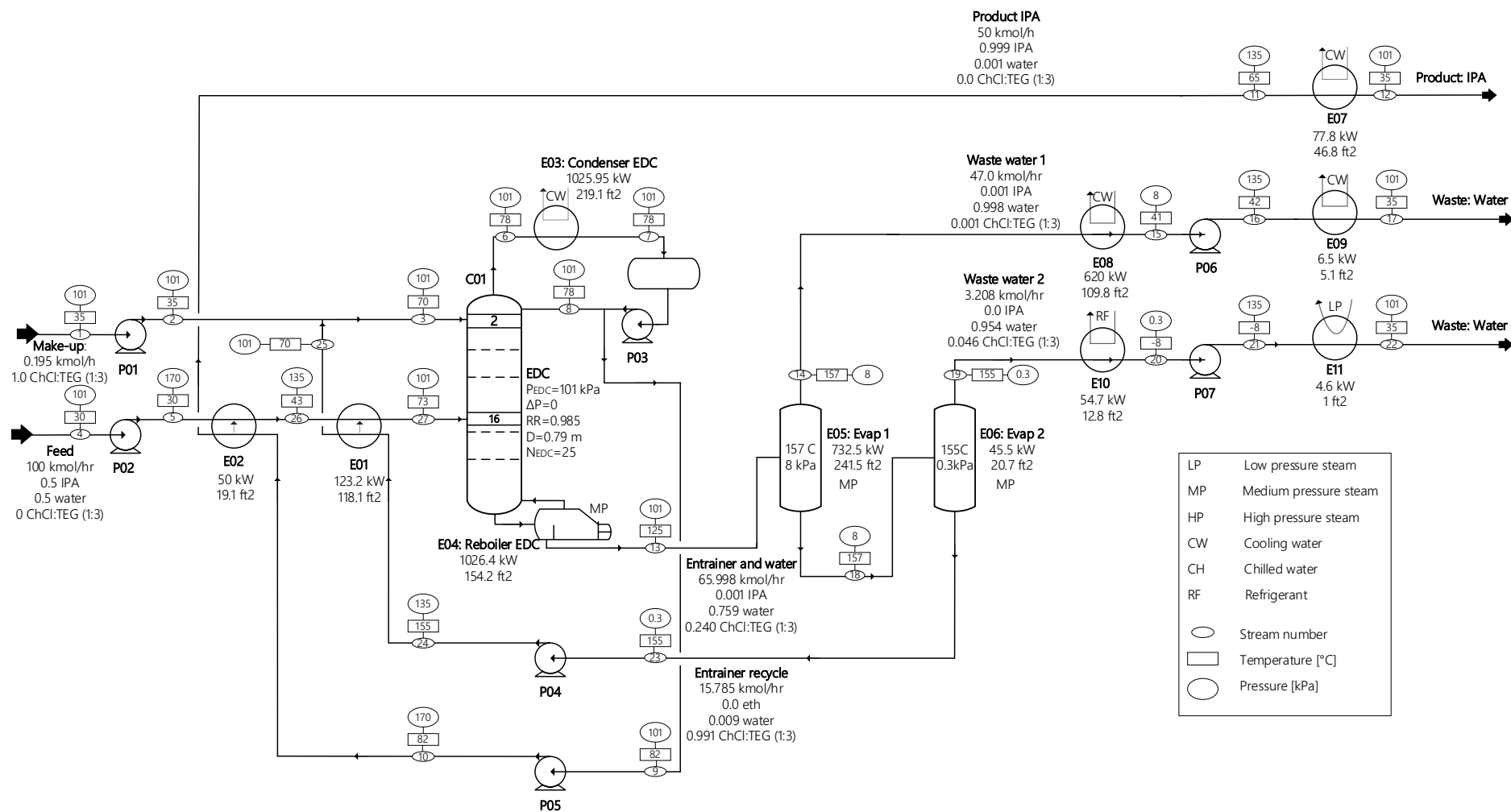


Figure A 44: Process flowsheet for the separation of IPA and water using ChCl:TEG (1:3) and applying heat integration.

Table A 92: Process stream summary for the separation of IPA and water using ChCl:TEG (1:3) and applying heat integration.

Process Stream Summary																	
STREAM	Nr.	1		2		3		4		5		6		7		8	
COMP	MW	kg/s	mol/s	kg/s	mol/s	kg/s	mol/s	kg/s	mol/s	kg/s	mol/s	kg/s	mol/s	kg/s	mol/s	kg/s	mol/s
ChCl:TEG (1:3)	147.5	0.009	0.059	0.009	0.059	0.65	4.405	0.000	0.000	0.000	0.000	0.00	0.000	0.000	0.000	0.000	0.000
Water	18.02	0.000	0.000	0.000	0.000	0.001	0.039	0.250	13.889	0.250	13.889	0.00	0.027	0.000	0.027	0.001	0.040

Ethanol	60.1	0.000	0.000	0.000	0.000	0.00	0.000	0.835	13.889	0.835	13.889	1.655	27.542	1.655	27.542	0.821	13.640
Total		0.009	0.059	0.009	0.059	0.651	4.444	1.085	27.778	1.085	27.778	1.656	27.569	1.656	27.569	0.822	13.681
Enthalpy flow	kW		29		29		2132		8384		8384		7300		8468		4202
Vapor frac			0		0		0		0		0		1		0		0
Press.	kPa		101.3		101.3		101.3		101.3		170.0		170.0		170.0		170.0
Temp	°C		35		35		69.5		30		30.1		78.3		78.3		78.3
STREAM	Nr.		9		10		11		12		13		14		15		16
COMP	MW	kg/s	mol/s	kg/s	mol/s	kg/s	mol/s	kg/s	mol/s	kg/s	mol/s	kg/s	mol/s	kg/s	mol/s	kg/s	mol/s
ChCl:TEG (1:3)	147.5	0.000	0.000	0.000	0.000	0.000	0.000	0.000	0.000	0.650	4.405	0.003	0.018	0.003	0.018	0.003	0.018
Water	18.02	0.000	0.014	0.000	0.014	0.000	0.014	0.000	0.014	0.251	13.914	0.235	13.03	0.235	13.03	0.235	13.03
Ethanol	60.1	0.834	13.875	0.834	13.875	0.834	13.88	0.834	13.88	0.001	0.014	0.001	0.014	0.001	0.014	0.001	0.014
Total		0.834	13.889	0.834	13.889	0.834	13.89	0.834	13.89	0.901	18.33	0.238	13.06	0.238	13.057	0.238	13.057
Enthalpy flow	kW		4266		4266		4315.8		4394		6077		3102		3722		3722
Vapor frac			0		0		0		0		0		1		0		0
Press.	kPa		101.3		135.0		135.0		101.3		101.3		8.0		8.0		135.0
Temp	°C		82		82.1		64.5		35		124.9		157		41.3		41.5
STREAM	Nr.		17		18		19		20		21		22		23		24
COMP	MW	kg/s	mol/s	kg/s	mol/s	kg/s	mol/s	kg/s	mol/s	kg/s	mol/s	kg/s	mol/s	kg/s	mol/s	kg/s	mol/s
ChCl:TEG (1:3)	147.5	0.003	0.018	0.647	4.387	0.006	0.041	0.006	0.041	0.006	0.041	0.006	0.041	0.641	4.346	0.641	4.346
Water	18.02	0.235	13.03	0.016	0.889	0.015	0.850	0.015	0.850	0.015	0.850	0.015	0.850	0.001	0.039	0.001	0.039
Ethanol	60.1	0.001	0.014	0.000	0.000	0.000	0.000	0.000	0.000	0.000	0.000	0.000	0.000	0.000	0.000	0.000	0.000
Total		0.238	13.06	0.663	5.276	0.021	0.891	0.021	0.891	0.021	0.891	0.021	0.891	0.642	4.385	0.642	4.385
Enthalpy flow	kW		3728		2243		217		272		272		267		1980		1980
Vapor frac			0		0		1		0		0		0		0		0
Press.	kPa		101.3		8.0		0.3		0.3		135.0		101.3		0.3		152.0
Temp	°C		35		157		155		-8.4		-8.3		35		155		155.2
STREAM	Nr.		25		26		27										
COMP	MW	kg/s	mol/s	kg/s	mol/s	kg/s	mol/s	kg/s	mol/s	kg/s	mol/s	kg/s	mol/s	kg/s	mol/s	kg/s	mol/s
ChCl:TEG (1:3)	147.5	0.641	4.346	0.00	0.000	0.000	0.000										
Water	18.02	0.001	0.039	0.25	13.889	0.835	13.889										
Ethanol	60.1	0.000	0.000	0.84	13.889	0.835	13.889										
Total		0.642	4.385	1.085	27.778	1.669	27.778										
Enthalpy flow	kW		2103		8.33E+03		8211										
Vapor frac			0		0		0										
Press.	kPa		152.0		170.0		170.0										
Temp	°C		70		42.8		73.1										

C.9.3 Equipment Specification & Economic Assessment

The equipment specification must be done for both literature and simulated DES processes in order to perform the economic assessment. Therefore, the required characteristics that were missing in the literature are determined as well. The characteristics that were given by the literature are marked in green. The simulated process, including heat integration, is only given in case of varying parameters compared to the non-heat integrated process.

C.9.3.1 Equipment Sizing & Purchase Costs

C.9.3.1.1 Separation Task 1

Table A 93: Equipment specification of the EDC of the simulated process using ChCl:Ur (1:2) and the literature process using EG [30]. Data given by the literature is marked in green.

Meaning	Formulas	Results		Units
		EG Bastidas <i>et al.</i> (2010) [30]	Aspen Plus simulation ChCl:Ur (1:2)	
Number of trays : N	Aspen Process Optimisation / Literature	22	25	
Height : H	$H = 0.5 N + 3$	14 / 45.93/551.18	15.5 / 50.85	m/ft/in
Tangent-to-tangent length : L	$L = 0.5 N$	11 / 36.09/ 433.07	12.5 / 41.01	m/ft/in
Diameter : D	Aspen tray sizing and rating / Literature	1.48/ 4.86/ 58.27	1.26 / 4.13	m/ft/in
Lowest pressure : P_o	Aspen Plus Process Simulation / Literature	101 / 14.65	101 / 14.65	kPa/psig
Design Pressure : P_d	$P_d = \exp \{0.60608 + 0.91615[\ln(P_o)] + 0.0015655[\ln(P_o)]^2\}$ For P_o between 10 and 1000 psig	21.69	21.69	psig
Highest temperature : T_o	Aspen Plus Process Simulation	156 / 312.8	120 / 248	°C / °F
Design temperature : T_d	$T_d = T_o + 50 \text{ }^\circ\text{F}$	362.8	298	°F
Maximum allowable stress : S	Seider <i>et al.</i> (2006) book p.575	15000	15000	psi
Necessary wall thickness : t_w	$t_{w,vacuum} = t_E + t_{EC}$ $t_{w,atm} = \frac{0.22 (D + 18) L^2}{S D^2}$ L and D in inches	0.00157 / 0.062	0.00248/ 0.098	cm / in
Corrosive allowance : t_c	Seider <i>et al.</i> (2006) book p.575	0.0032 / 0.125	0.0032/ 0.125	cm / in
Actual wall thickness : t_s	$t_s = t_w + t_c$	0.00474 / 0.187	0.00565/ 0.223	cm / in
Weight of shell and two heads : W	$W = \pi (D + t_s) (L + 0.8 D) t_s \rho_{carbon}$ L and D in inches , $\rho_{carbon} = 0.284 \text{ lb/in}^3$	2118.59 /4670.70	2385.92/5260.00	kg/ lb

Table A 94: Equipment f.o.b. purchase costs of the EDC of the simulated process using ChCl:Ur (1:2) and the literature process using EG [30].

Meaning	Formula	Results	
		EG Bastidas <i>et al.</i> (2010) [30]	Aspen Plus simulation ChCl:Ur (1:2)
Costs of empty vessel	$C_v = \exp\{7.2756 + 0.18255 [\ln(W)] + 0.02297 [\ln(W)]^2\}$ W in lb	\$34 812.38	\$37 267.23
Cost of platforms and ladders	$C_{PL} = 300.9 (D)^{0.63316} (L)^{0.80161}$ D and L in ft	\$14 498.92	\$14 507.30
Base costs for sieve trays	$C_{BT} = 468 \exp(0.1739 D)$ D in ft	\$1 088.84	\$960.40
Costs for installed trays	$C_T = N_T F_{TT} F_M C_{BT}$ with F_{TT} and $F_M = 1$	\$23 954.40	\$24 009.91
Purchase cost	$C_P = F_M C_V + C_{PL} + C_T$	\$73265.70	\$75 784.45

Table A 95: Equipment specification of the reflux drum of the simulated process using ChCl:Ur (1:2) and the literature process using EG [30].

Necessary characteristics for economic analysis				
Meaning	Formulas	Results		Units
		EG Bastidas <i>et al.</i> (2010) [30]	Aspen Plus simulation ChCl:Ur (1:2)	
Liquid flowrate	Aspen Plus simulation / $\dot{V}_L = \frac{\dot{m}_{ethanol}}{(1 - RR) \rho_L}$	0.0056	0.0044	m ³ /s
Holdup volume	$V_{ho} = t_{ho} \cdot \dot{V}_L$ with $t_{ho} = 300$ (heuristic)	1.691	1.320	m ³
Volume vessel	$V_{ves} = \frac{V_{ho}}{0.5}$	3.381	2.640	m ³
Diameter vessel	$D_{ves} = \sqrt[3]{\frac{4 V_{ves}}{3 \pi}}$	1.128 / 3.70 / 44.42	1.039/3.41/ 40.90	m/ft/in
Length vessel	$L_{ves} = 3 D_{des}$ (heuristic)	3.384 / 11.10 /133.25	3.116/ 10.22/ 122.69	m/ft/in
Lowest pressure	Aspen Plus Process Simulation	101 / 14.65	101 / 14.65	kPa/psig
Design pressue	$P_d = \exp \{0.60608 + 0.91615[\ln(P_o)] + 0.0015655[\ln(P_o)]^2\}$	21.69	21.69	psig

	For operating pressure between 10 and 1000 psig $P_d = 10$ For operating pressure between 0 and 5 psig			
Highest temperature	Aspen Plus Process Simulation	78 / 172.40	78 /172.40	°C/°F
Design Temperature	$T_d = T_{\text{highest}} + 50 \text{ }^{\circ}\text{F}$			°F
Maximum allowable stress	$S(T_d) = \text{Seider } et al. (2006) \text{ Table p. 575}$	15000.00	15000.00	Psi
Fractional weld Efficiency	$E(\text{Material}) = \text{Seider } et al. (2006) \text{ p. 575}$	0.85	0.85	
Necessary wall thickness	$t_{w,atm} = \frac{P_d D}{2 S E - 1.2 P_d}$	0.00096/ 0.038	0.00088 / 0.035	cm/in
Corrosive allowance	$t_c = 0.125$	0.0032 /0.125	0.0032/ 0.125	cm/in
Actual wall thickness	$t_s = t_w + t_c$	0.00414 / 0.163	0.00406/ 0.160	cm/in
Weight of shell and two heads	$W = \pi (D + t_s) (L + 0.8 D) t_s \rho_{\text{carbon}}$ L and D in inches, $\rho_{\text{carbon}} = 0.284 \text{ lb/in}^3$	495.50 / 1092.38	412.48/ 909.37	kg/lb

Table A 96: Equipment purchase costs of the reflux drum of the simulated process using ChCl:Ur (1:2) and the literature process using EG [30].

Meaning	Formula	Results	
		EG Bastidas <i>et al.</i> (2010) [30]	Aspen Plus simulation ChCl:Ur (1:2)
Costs of an empty vessel	$C_v = \exp\{8.9552 - 0.2330 [\ln(W)] + 0.04333 [\ln(W)]^2\}$ W in lb, for $1000 \leq W \leq 920000$	\$12 656.42	\$11 836.34
Cost of platforms and ladders	$C_{PL} = 2005 (D)^{0.20294}$ D in ft	\$ 2 614.91	\$2 571.48
Purchase cost	$C_P = F_M C_V + C_{PL}$ with $F_M = 1$	\$15 271.33	\$14 407.82

Table A 97: Equipment specification and f.o.b. purchase costs of the vacuum system of the simulated process using ChCl:Ur (1:2) and the literature process using EG [30]. Data given by the literature is marked in green.

Meaning	Formulas	EG Bastidas <i>et al.</i> (2010) [30]	Aspen Plus simulation ChCl:Ur (1:2)		Units
		Vacuum SRC Liquid ring pump	Vacuum Evap 1 Liquid ring pump	Vacuum Evap 2 Steam jet ejector	

Operating pressure	p	from Aspen Plus process simulation	195.0	15.0	2.25	torr
Volume equipment	V	from Aspen Plus process simulation	180.35	96.24	39.85	ft ³
Air leakage	W _{air}	$W_{air} = 5 + V^{0.66} \cdot (0.0298 + 0.03088 \ln(p)^2)$	10.45	7.22	5.62	lb/hr
Temperature precondenser	T _{cond}	from Aspen Plus process simulation	35	10	-8.00	°C
Product	W _{product}	from Aspen Plus: flash calculation	1.31	12.15	19.38	lb/hr
Flow to vacuum	W _{vacuum}	$W_{vacuum} = W_{air} + W_{product}$	11.63	255.81	25.00	ft ³ /min lb/hr
Size factor – Steam Jet ejector	S _{steamjet}	$S_{steamjet} = \frac{W_{vacuum}}{P}$ 6.1 ≤ S ≤ 100 W _{vacuum} in lb/hr, P in torr			11.11	
Size factor – liquid ring pump	S _{liquid}	S _{liquid} = W _{vacuum} with W in ft ³ /min	11.63	255.81		ft ³ /min
Factor stages	F _{stages}	F _{stages} = 2.1			2.10	
Purchase costs steamjet	C _{P,steamjet}	C _{P,steamjet} = 1690 S ^{0.41} F _{stages} with F _{stages} = 2.1			\$9524.40	
Purchase costs liquid	C _{P,liquid}	C _{P,liquid} = 8250 S ^{0.35} for 0 ≤ S ≤ 100	\$19 471.83	\$57 441.49		
Compressor power	P _{comp}	from Aspen Plus process simulation	0.33	0.33		kW
MP steam requirement	W _{steam}	W _{steam} = W _{vacuum} 10			249.98	lb/hr

Table A 98: Equipment specification of the SRC used for the solvent recovery of EG by Bastidas *et al.* (2010) [30]. Data given by the literature is marked in green.

Meaning	Formulas	Results	Units
		EG Bastidas <i>et al.</i> (2010)	
Number of trays : N		12.00	
Height : H	H = 0.5 N + 3	9.00/ 29.53/ 254.33	m/ft/in
Tangent-to-tangent length : L	L = 0.5 N	6.00/ 19.69/ 236.22	m/ft/in
Diameter : D		0.85/ 2.79/ 33.46	m/ft/in
Lowest pressure : P _o	Process	26.00/3.77	kPa/psig
Design Pressure : P _{d,vacuum}	P _d = 10 For P _o between 0 and 5	10.00	psig
Design Pressure : P _{d,atmospheric}	P _d = exp {0.60608 + 0.91615[ln(P _o)] + 0.0015655[ln(P _o)] ² } For P _o between 10 and 1000 psig		psig

Highest temperature	: T_o	Process	155/ 311	°C / °F
Design temperature	: T_d	$T_d = T_o + 50\text{ °F}$	361	°F
Modulus of elasticity	: E_M	Seider <i>et al.</i> (2006) book p.575	28300000	psi
Wall thickness	: t_E	$t_E = 1.3 D \left(\frac{P_d L}{E_M D} \right)^{0.4}$ for $\frac{t_E}{D} \leq 0.05$ L and D in inches	0.0063/ 0.2496	cm / in
Correction	: t_{EC}	$t_{EC} = L(0.18D_i - 2.2) \times 10^{-5} - 0.19$ if $t_{EC} \geq 0$	-0.0046/ -0.1810	cm / in
Maximum allowable stress	: S	Seider <i>et al.</i> (2006) book p.575		
Necessary wall thickness	: $t_{W,vacuum}$	$t_W = t_E + t_{EC}$	0.0063/0.2496	cm / in
Necessary wall thickness	: $t_{W,atmospheric}$	$t_W = \frac{0.22 (D + 18) L^2}{S D^2}$ L and D in inches		cm / in
Corrosive allowance	: t_c	Seider <i>et al.</i> (2006) book p.575	0.0032/ 0.1250	cm / in
Actual wall thickness	: t_s	$t_s = t_W + t_c$	0.0095/ 0.3746	cm / in
Weight of shell and two heads	: W	$W = \pi (D + t_s) (L + 0.8 D) t_s \rho_{carbon}$ L and D in inches , $\rho_{carbon} = 0.284\text{ lb/in}^3$	1348.61/ 2973.18	kg / lb

Table A 99: Equipment purchase costs of the SRC used for the solvent recovery of EG by Bastidas *et al.* (2010) [30]

Meaning	Formula	Results
		EG Bastidas <i>et al.</i> (2010)
Costs of empty vessel	$C_v = \exp\{7.2756 + 0.18255 [\ln(W)] + 0.02297 [\ln(W)]^2\}$ W in lb	\$27 028.37
Cost of platforms and ladders	$C_{PL} = 300.9 (D)^{0.63316} (L)^{0.80161}$ D and L in ft	\$6 278.08
Base costs for sieve trays	$C_{BT} = 468 \exp(0.1739 D)$ D in ft	\$760.08
Costs for installed trays	$C_T = N_T F_{TT} F_M C_{BT}$ with F_{TT} and $F_M = 1$	\$9 120.98
Purchase cost	$C_P = F_M C_V + C_{PL} + C_T$	\$42 427.43

Table A 100: Equipment purchase costs of the reflux drum of the SRC used for the solvent recovery of EG by Bastidas *et al.* (2010) [30]

Meaning	Formula	Results
		EG Bastidas <i>et al.</i> (2010)
Costs of an empty vessel	$C_v = \exp\{8.9552 - 0.2330 [\ln(W)] + 0.04333 [\ln(W)]^2\}$ W in lb, for $1000 \leq W \leq 920000$	\$ 7,591.18
Cost of platforms and ladders	$C_{PL} = 2005 (D)^{0.20294}$ D in ft	\$ 2,139.62
Purchase cost	$C_P = F_M C_V + C_{PL}$ with $F_M = 1$	\$ 9,730.80

C.9.3.1.2 Separation Task 2

Table A 101: Equipment specification of the EDC of the simulated process using ChCl:Ur (1:2) and the literature process using the IL [EMIM]⁺[BF₄]⁻ for the ethanol and water system [35]. Data given by the literature is marked in green.

Meaning	Formulas	Results		Units
		IL Zhu <i>et al.</i> (2016) [35]	ChCl:Ur (1:2)	
Number of trays : N	Aspen Process Optimisation / Literature	40	22	
Height : H	$H = 0.5 N + 3$	23/ 75.46 / 905.51	14/ 45.93/ 551.18	m/ft/in
Tangent-to-tangent length : L	$L = 0.5 N$	20/ 65.62/ 787.40	11/ 36.09/ 433.07	m/ft/in
Diameter : D	Aspen tray sizing and rating / Literature	0.98/ 3.22/ 38.58	0.8207/ 2.69/ 32.31	m/ft/in
Lowest pressure : P _o	Aspen Plus Process Simulation	101/ 14.65	101/ 14.65	kPa/psig
Design Pressure : P _d	$P_d = \exp \{0.60608 + 0.91615[\ln(P_o)] + 0.0015655[\ln(P_o)]^2\}$ For P _o between 10 and 1000 psig	21.69	21.69	psig
Highest temperature : T _o	Aspen Plus Process Simulation	133 / 271.40	100/212.00	°C / °F
Design temperature : T _d	$T_d = T_o + 50 \text{ }^\circ\text{F}$	321.40	262.00	°F
Maximum allowable stress : S	Seider <i>et al.</i> (2006) book p.575	15000.00	15000.00	psi
Necessary wall thickness : t _w	$t_{w,vacuum} = t_E + t_{EC}$ $t_{w,atm} = \frac{0.22 (D + 18) L^2}{S D^2}$ L and D in inches	0.00878/ 0.346	0.00337/ 0.133	cm / in
Corrosive allowance : t _c	Seider <i>et al.</i> (2006) book p.575	0.0032/ 0.125	0.0032/ 0.125	cm / in
Actual wall thickness : t _s	$t_s = t_w + t_c$	0.01195/ 0.471	0.00654/ 0.258	cm / in

Weight of shell and two heads	: W	$W = \pi (D + t_s) (L + 0.8 D) t_s \rho_{\text{carbon}}$ L and D in inches, $\rho_{\text{carbon}} = 0.284 \text{ lb/in}^3$	6083.54/ 13411.90	1557.14/ 3432.90	kg/ lb
-------------------------------	-----	---	-------------------	------------------	--------

Table A 102: Equipment f.o.b. purchase costs of the EDC of the simulated process using ChCl:Ur (1:2) and the literature process using the IL [EMIM]⁺[BF₄]⁻ for the ethanol and water system [35].

Meaning	Formula	Results	
		IL Zhu <i>et al.</i> (2016) [35]	ChCl:Ur (1:2)
Costs of empty vessel	$C_v = \exp\{7.2756 + 0.18255 [\ln(W)] + 0.02297 [\ln(W)]^2\}$ W in lb	\$65 204.24	\$29 266.15
Cost of platforms and ladders	$C_{PL} = 300.9 (D)^{0.63316} (L)^{0.80161}$ D and L in ft	\$18 034.55	\$9 981.55
Base costs for sieve trays	$C_{BT} = 468 \exp(0.1739 D)$ D in ft	\$818.60	\$747.48
Costs for installed trays	$C_T = N_T F_{TT} F_M C_{BT}$ with F_{TT} and $F_M = 1$	\$32 744.00	\$16 444.58
Purchase cost	$C_P = F_M C_V + C_{PL} + C_T$	\$115 982.79	\$55 692.28

Table A 103: Equipment specification of the reflux drum of the simulated process using ChCl:Ur (1:2) and the literature process using the IL [EMIM]⁺[BF₄]⁻ for the ethanol and water system [35].

Necessary characteristics for economic analysis				
Meaning	Formulas	Results		Units
		IL Zhu <i>et al.</i> (2016) [35]	ChCl:Ur (1:2)	
Liquid flowrate	Aspen Plus simulation / $\dot{V}_L = \frac{\dot{m}_{\text{ethanol}}}{(1 - RR) \rho_L}$	0.0030	0.0016	m ³ /s
Holdup volume	$V_{ho} = t_{ho} \cdot \dot{V}_L$ with $t_{ho} = 300$ (heuristic)	0.890	0.488	m ³
Volume vessel	$V_{ves} = \frac{V_{ho}}{0.5}$	1.779	0.976	m ³
Diameter vessel	$D_{ves} = \sqrt[3]{\frac{4 V_{ves}}{3 \pi}}$	0.911/ 2.99/ 35.86	0.746/ 2.45/ 29.36	m/ft/in
Length vessel	$L_{ves} = 3 D_{des}$ (heuristic)	2.732/ 8.96/ 107.57	2.237/ 7.34/ 88.07	m/ft/in
Lowest pressure	Aspen Plus Process Simulation	101/ 14.65	101/ 14.65	kPa/psig

Design pressure	$P_d = \exp \{0.60608 + 0.91615[\ln(P_o)] + 0.0015655[\ln(P_o)]^2\}$ For operating pressure between 10 and 1000 psig	21.69	21.69	psig
Highest temperature	Aspen Plus Process Simulation	78/ 172.40	78/ 172.40	°C/°F
Design Temperature	$T_d = T_{\text{highest}} + 50 \text{ }^\circ\text{F}$	222.40	222.40	°F
Maximum allowable stress	$S(T_d) = \text{Seider } et \text{ al. (2006) Table p. 575}$	15000.00	15000.00	Psi
Fractional weld Efficiency	$E(\text{Material}) = \text{Seider } et \text{ al. (2006) p. 575}$	0.85	0.85	
Necessary wall thickness	$t_{w,atm} = \frac{P_d D}{2 S E - 1.2 P_d}$	0.00078/ 0.031	0.00063/ 0.025	cm/in
Corrosive allowance	$t_c = 0.125$	0.0032/ 0.125	0.0032/ 0.125	cm/in
Actual wall thickness	$t_s = t_w + t_c$	0.00395/ 0.156	0.00381/ 0.150	cm/in
Weight of shell and two heads	$W = \pi (D + t_s) (L + 0.8 D) t_s \rho_{\text{carbon}}$ L and D in inches, $\rho_{\text{carbon}} = 0.284 \text{ lb/in}^3$	308.69/ 680.55	199.70/ 440.27	kg/lb

Table A 104: Equipment purchase costs of the reflux drum of the simulated process using ChCl:Ur (1:2) and the literature process using the IL [EMIM]⁺[BF₄]⁻ for the ethanol and water system [35].

Meaning	Formula	Results	
		IL Zhu <i>et al.</i> (2016) [35]	ChCl:Ur (1:2)
Costs of an empty vessel	$C_v = \exp\{8.9552 - 0.2330 [\ln(W)] + 0.04333 [\ln(W)]^2\}$ W in lb, for $1000 \leq W \leq 920000$	\$10 710.52	\$9 343.99
Cost of platforms and ladders	$C_{PL} = 2005 (D)^{0.20294}$ D in ft	\$2 503.75	\$2 404.15
Purchase cost	$C_P = F_M C_V + C_{PL}$ with $F_M = 1$	\$13 214.27	\$11 748.14

Table A 105: Equipment specification and f.o.b. purchase costs of the vacuum system of the simulated process using ChCl:Ur (1:2) and the literature process using the IL [EMIM]⁺[BF₄]⁻ for the ethanol and water system [35].

Meaning	Formulas	IL Zhu <i>et al.</i> (2016)	ChCl:Ur (1:2)		Units	
		Vacuum Evap 1 Liquid ring pump	Vacuum Evap 1 Liquid ring pump	Vacuum Evap 2 Steam jet ejector		
Operating pressure	p	from Aspen Plus process simulation	75.0	15.0	2.03	torr
Volume equipment	V	from Aspen Plus process simulation	284.02	44.41	11.99	ft³
Air leakage	W _{air}	W _{air} = 5 + V ^{0.66} . (0.0298 + 0.03088 ln(p) ²)	11.34	6.34	5.26	lb/hr
Temperature precondenser	T _{cond}	from Aspen Plus process simulation	9	10	-8	°C
Product	W _{product}	from Aspen Plus: flash calculation	9.00	8.79	11.05	lb/hr
Flow to vacuum	W _{vacuum}	W _{vacuum} = W _{air} + W _{product}	61.05	255.811	16.31428	ft³/min lb/hr
Size factor – Steam Jet ejector	S _{steamjet}	S _{steamjet} = $\frac{W_{vacuum}}{P}$ 6.1 ≤ S ≤ 100 W _{vacuum} in lb/hr, P in torr			8.06	
Size factor – liquid ring pump	S _{liquid}	S _{liquid} = W _{vacuum} with W in ft³/min	61.05	255.81		ft³/min
Factor stages	F _{stages}	F _{stages} = 2.1			2.1	
Purchase costs steamjet	C _{P,steamjet}	C _{P,steamjet} = 1690 . S ^{0.41} . F _{stages} with F _{stages} = 2.1			\$8 348.53	
Purchase costs liquid	C _{P,liquid}	C _{P,liquid} = 8250 . S ^{0.35} for 0 ≤ S ≤ 100	\$34 789.16	\$57 441.49		
Compressor power	P _{comp}	from Aspen Plus process simulation	1.27	1.7		kW
MP steam requirement	W _{steam}	W _{steam} = W _{vacuum} . 10			163.1428	lb/hr

C.9.3.1.3 Separation Task 3

Table A 106: Equipment specification of the EDC separating IPA and water of the simulated process using ChCl:TEG (1:3) and the literature process using the conventional solvent DMSO and the IL [Emim]⁺[N(CN)₂]⁻ [31, 36]. Data given by the literature is marked in green.

Meaning	Formulas	Results			Units
		DMSO Ghuge <i>et al.</i> (2017) [31]	IL Ma <i>et al.</i> (2019) [36]	ChCl: TEG (1:3)	
Number of trays : N	Aspen Process Optimisation	41	25	25	
Height : H	$H = 0.5 N + 3$	23.5/ 77.10/ 925.20	15.5/ 50.85/ 610.24	15.5/ 50.85/ 610.24	m/ft/in
Tangent-to-tangent length : L	$L = 0.5 N$	20.5/ 67.26/ 807.09	12.5/ 41.01/ 492.13	12.5/ 41.01/ 492.13	m/ft/in
Diameter : D	Aspen tray sizing and rating	0.70/ 2.30/ 27.56	0.80/ 2.63/ 31.59	0.79/ 2.59/ 31.09	m/ft/in
Lowest pressure : P _o	Aspen Plus Process Simulation	101/ 14.65	101/ 14.65	101/ 14.65	kPa/psig
Design Pressure : P _d	$P_d = \exp \{0.60608 + 0.91615[\ln(P_o)] + 0.0015655[\ln(P_o)]^2\}$ For P _o between 10 and 1000 psig	21.69	21.69	21.69	psig
Highest temperature : T _o	Aspen Plus Process Simulation	143.5/ 290.3	130.8/ 267.44	100/ 212	°C / °F
Design temperature : T _d	$T_d = T_o + 50 \text{ }^\circ\text{F}$	340.3	317.44	262	°F
Maximum allowable stress : S	Seider <i>et al.</i> (2006) book p.575	15000.00	15000.00	15000.00	psi
Necessary wall thickness : t _w	$t_{w,vacuum} = t_E + t_{EC}$ $t_{w,atm} = \frac{0.22 (D + 18) L^2}{S D^2}$ L and D in inches	0.01456/ 0.573	0.00448/ 0.177	0.00458/ 0.180	cm / in
Corrosive allowance : t _c	Seider <i>et al.</i> (2006) book p.575	0.0032/ 0.125	0.0032/ 0.125	0.0032/0.125	cm / in
Actual wall thickness : t _s	$t_s = t_w + t_c$	0.01773/ 0.698	0.00766/ 0.302	0.00776/ 0.305	cm / in
Weight of shell and two heads : W	$W = \pi (D + t_s) (L + 0.8 D) t_s \rho_{carbon}$ L and D in inches , $\rho_{carbon} = 0.284 \text{ lb/in}^3$	6615.69/ 14585.1	2012.38/ 4436.5	2005.14/ 4420.6	kg/ lb

Table A 107: Equipment f.o.b. purchase costs of the EDC separating IPA and water of the simulated process using ChCl:TEG (1:3) and the literature process using the conventional solvent DMSO and the IL [Emim]⁺[N(CN)₂]⁻ [31, 36].

Meaning	Formula	Results		
		DMSO Ghuge <i>et al.</i> (2017) [31]	IL Ma <i>et al.</i> (2019) [36]	ChCl: TEG (1:3)
Costs of empty vessel	$C_v = \exp\{7.2756 + 0.18255 [\ln(W)] + 0.02297 [\ln(W)]^2\}$ W in lb	\$ 68 690.24	\$ 33 807.45	\$ 33 738.20
Cost of platforms and ladders	$C_{PL} = 300.9 (D)^{0.63316} (L)^{0.80161}$ D and L in ft	\$ 14 865.49	\$ 10 900.98	\$ 10 792.56
Base costs for sieve trays	$C_{BT} = 468 \exp(0.1739 D)$ D in ft	\$ 697.74	\$ 739.67	\$ 734.39
Costs for installed trays	$C_T = N_T F_{TT} F_M C_{BT}$ with F_{TT} and $F_M = 1$	\$ 28 607.29	\$ 18 491.86	\$ 18 359.76
Purchase cost	$C_P = F_M C_V + C_{PL} + C_T$	<u>\$ 112 163.03</u>	<u>\$ 63 200.28</u>	<u>\$ 62 890.52</u>

Table A 108: Equipment specification of the reflux drum of the simulated process using ChCl:TEG (1:3) and the literature process using the conventional solvent DMSO and the IL [Emim]⁺[N(CN)₂]⁻ for the IPA and water system [31, 36].

Necessary characteristics for economic analysis						
Meaning	Formulas	Results				Units
		DMSO Ghuge <i>et al.</i> (2017) [31]	IL Ma <i>et al.</i> (2019) [36]	ChCl: TEG (1:3)	ChCl: TEG (1:3) HI	
Liquid flowrate	Aspen Plus simulation / $\dot{V}_L = \frac{\dot{m}_{ethanol}}{(1 - RR) \rho_L}$	0.0039	0.0035	0.0023	0.0021	m ³ /s
Holdup volume	$V_{ho} = t_{ho} \cdot \dot{V}_L$ with $t_{ho} = 300$ (heuristic)	1.156	1.051	0.688	0.616	m ³
Volume vessel	$V_{ves} = \frac{V_{ho}}{0.5}$	2.312	2.102	1.376	1.231	m ³
Diameter vessel	$D_{ves} = \sqrt[3]{\frac{4 V_{ves}}{3 \pi}}$	0.994/ 3.26/ 39.13	0.963/ 3.16/ 37.90	0.836/ 2.74/ 32.91	0.806/ 2.64/ 31.72	m/ft/in
Length vessel	$L_{ves} = 3 D_{des}$ (heuristic)	2.982/ 9.78/ 117.39	2.888/ 9.48/ 113.71	2.508/ 8.23/ 98.74	2.417/ 7.93/ 95.15	m/ft/in
Lowest pressure	Aspen Plus Process Simulation	101/ 14.65	101/ 14.65	101/ 14.65	101/ 14.65	kPa/psig
Design pressure	$P_d = \exp \{0.60608 + 0.91615[\ln(P_o)] + 0.0015655[\ln(P_o)]^2\}$	21.69	21.69	21.69	21.69	psig

	For operating pressure between 10 and 1000 psig					
Highest temperature	Aspen Plus Process Simulation	82/ 179.60	78/ 172.40	124.91/ 256.84	78/ 172.40	°C/°F
Design Temperature	$T_d = T_{\text{highest}} + 50\text{ °F}$	229.60	222.40	306.84	222.40	°F
Maximum allowable stress	$S(T_d) = \text{Seider } et\ al. (2006) \text{ book Table p. 575}$	15000.00	15000.00	15000.00	15000.00	Psi
Fractional weld Efficiency	$E(\text{Material}) = \text{Seider } et\ al. (2006) \text{ p. 575}$	0.85	0.85	0.85	0.85	
Necessary wall thickness	$t_{w,atm} = \frac{P_d D}{2 S E - 1.2 P_d}$	0.00085/ 0.033	0.00082/ 0.032	0.00071/ 0.028	0.00069/ 0.027	cm/in
Corrosive allowance	$t_c = 0.125$	0.0032/ 0.125	0.0032/ 0.125	0.0032/ 0.125	0.0032/ 0.125	cm/in
Actual wall thickness	$t_s = t_w + t_c$	0.00402/ 0.158	0.00399/ 0.157	0.00389/ 0.153	0.00386/ 0.152	cm/in
Weight of shell and two heads	$W = \pi (D + t_s) (L + 0.8 D) t_s \rho_{\text{carbon}}$ L and D in inches , $\rho_{\text{carbon}} = 0.284 \text{ lb/in}^3$	374.06/ 824.66	348.76/ 768.88	255.98/ 564.33	236.17/ 520.66	kg/lb

Table A 109: F.o.b. purchase costs of the reflux drum of the simulated process using ChCl:TEG (1:3) and the literature process using the conventional solvent DMSO and the IL [Emim]⁺[N(CN)₂]⁻ for the IPA and water system [31, 36].

Meaning	Formula	Results			
		DMSO Ghuge <i>et al.</i> (2017) [31]	IL Ma <i>et al.</i> (2019) [36]	ChCl: TEG (1:3)	ChCl: TEG (1:3) HI
Costs of an empty vessel	$C_v = \exp\{8.9552 - 0.2330 [\ln(W)] + 0.04333 [\ln(W)]^2\}$ W in lb, for $1000 \leq W \leq 920000$	\$ 11 434.60	\$ 11 160.92	\$ 10 079.69	\$ 9 829.12
Cost of platforms and ladders	$C_{PL} = 2005 (D)^{0.20294}$ D in ft	\$ 2 548.51	\$ 2 532.13	\$ 2 460.60	\$ 2 442.19
Purchase cost	$C_P = F_M C_v + C_{PL}$ with $F_M = 1$	\$ 13 983.11	\$ 13 693.05	\$ 12 540.29	\$ 12 271.31

Table A 110: Equipment specification and f.o.b. purchase costs of the vacuum system of the simulated process using ChCl:TEG (1:3) and the literature process using the IL [Emim]⁺[N(CN)₂]⁻ for the IPA and water system [36]. Data given by the literature is marked in green.

Meaning		Formulas	IL Ma <i>et al.</i> (2019) [36]		ChCl: TEG (1:3)		Units
			Vacuum Evap 1 Liquid ring pump	Vacuum Evap 2 Steam jet ejector	Vacuum SRC Liquid ring pump	Vacuum Evap 2 Steam jet ejector	
Operating pressure	p	from Aspen Plus process simulation/ Literature	68.8	2.62	60.0	2.025	torr
Volume equipment	V	from Aspen Plus process simulation			97.52	24.18	ft³
Air leakage	W _{air}	W _{air} = 5 + V ^{0.66} . (0.0298 + 0.03088 ln(p)²)	5.11	5.11	8.01	5.42	lb/hr
Temperature precondenser	T _{cond}	from Aspen Plus process simulation / Literature	25	-10	35	-15	°C
Product	W _{product}	from Aspen Plus: flash calculation / Literature	1.51	15.35	12.98	6.73	lb/hr
Flow to vacuum	W _{vacuum}	W _{vacuum} = W _{air} + W _{product} / Literature	18.78	20.46	82.36	12.15	ft³/min lb/hr
Size factor – Steam Jet ejector	S _{steamjet}	S _{steamjet} = $\frac{W_{vacuum}}{P}$ 6.1 ≤ S ≤ 100 W _{vacuum} in lb/hr, P in torr		7.82		6.00	
Size factor – liquid ring pump	S _{liquid}	S _{liquid} = W _{vacuum} with W in ft³/min	18.78		82.36		ft³/min
Factor stages	F _{stages}	F _{stages} = 2.1		2.1		2.1	
Purchase costs steam jet	C _{P,steamjet}	C _{P,steamjet} = 1690 . S ^{0.41} . F _{stages} with F _{stages} = 2.1		\$ 8 246.39		\$ 7 398.61	
Purchase costs liquid	C _{P,liquid}	C _{P,liquid} = 8250 . S ^{0.35} for 0 ≤ S ≤ 100	\$ 23 027.53		\$ 38 633.10		
Compressor power	P _{comp}	from Aspen Plus process simulation	0.38		1.52		kW
MP steam requirement	W _{steam}	W _{steam} = W _{vacuum} . 10		204.64		121.5114	lb/hr

Table A 111: Equipment specification of the SRC used for the solvent recovery of DMSO by Ghuge *et al.* (2010) [31]. Data given by the literature is marked in green.

Meaning	Formulas	Results	Units
		DMSO Ghuge <i>et al.</i> (2017)	
Number of trays : N		20	
Height : H	$H = 0.5 N + 3$	13/ 42.65/ 511.81	m/ft/in
Tangent-to-tangent length : L	$L = 0.5 N$	10/ 32.81/ 393.70	m/ft/in
Diameter : D		0.81/ 2.66/ 31.89	m/ft/in
Lowest pressure : P_o		101/ 14.65	kPa/psig
Design Pressure : $P_{d,atmospheric}$	$P_d = \exp \{0.60608 + 0.91615[\ln(P_o)] + 0.0015655[\ln(P_o)]^2\}$ For P_o between 10 and 1000 psig	21.69	psig
Highest temperature : T_o	Process	155/311	°C / °F
Design temperature : T_d	$T_d = T_o + 50$ °F	361	°F
Modulus of elasticity : E_M	Seider <i>et al.</i> (2006) book p.575		psi
Wall thickness : t_E	$t_E = 1.3 D \left(\frac{P_d L}{E_M D} \right)^{0.4}$ for $\frac{t_E}{D} \leq 0.05$ L and D in inches	0.00283/ 0.11153	cm / in
Correction : t_{EC}	$t_{EC} = L(0.18D_i - 2.2) \times 10^{-5} - 0.19$ if $t_{EC} \geq 0$		cm / in
Maximum allowable stress : S	Seider <i>et al.</i> (2006) book p.575	15000.00	
Necessary wall thickness : $t_{W,vacuum}$	$t_W = t_E + t_{EC}$		cm / in
Necessary wall thickness : $t_{W,atmospheric}$	$t_W = \frac{0.22 (D + 18) L^2}{S D^2}$ L and D in inches	0.00283/ 0.11153	cm / in
Corrosive allowance : t_c	Seider <i>et al.</i> (2006) book p.575	0.0032/ 0.1250	cm / in
Actual wall thickness : t_s	$t_s = t_W + t_c$	0.00601/ 0.23653	cm / in
Weight of shell and two heads : W	$W = \pi (D + t_s) (L + 0.8 D) t_s \rho_{carbon}$ L and D in inches , $\rho_{carbon} = 0.284$ lb/in ³	1288.51/ 2840.67	kg / lb

Table A 112: Purchase cost of the SRC used for the solvent recovery of DMSO by Ghuge *et al.* (2010) [31].

Meaning	Formula	Results
		DMSO Ghuge <i>et al.</i> (2017)
Costs of empty vessel	$C_v = \exp\{7.2756 + 0.18255 [\ln(W)] + 0.02297 [\ln(W)]^2\}$ W in lb	\$26 360.38
Cost of platforms and ladders	$C_{PL} = 300.9 (D)^{0.63316} (L)^{0.80161}$ D and L in ft	\$9 170.83
Base costs for sieve trays	$C_{BT} = 468 \exp(0.1739 D)$ D in ft	\$742.93
Costs for installed trays	$C_T = N_T F_{TT} F_M C_{BT}$ with F_{TT} and $F_M = 1$	\$14 858.63
Purchase cost	$C_P = F_M C_V + C_{PL} + C_T$	\$50 389.84

Table A 113: Equipment purchase costs of the reflux drum of the SRC used for the solvent recovery of DMSO by Ghuge *et al.* (2010) [31].

Meaning	Formula	Results
		DMSO Ghuge <i>et al.</i> (2017)
Costs of an empty vessel	$C_v = \exp\{8.9552 - 0.2330 [\ln(W)] + 0.04333 [\ln(W)]^2\}$ W in lb, for $1000 \leq W \leq 920000$	\$ 7,322.69
Cost of platforms and ladders	$C_{PL} = 2005 (D)^{0.20294}$ D in ft	\$ 2,193.36
Purchase cost	$C_P = F_M C_V + C_{PL}$ with $F_M = 1$	\$ 9,516.04

C.9.3.2 Equipment Summary & Costs

C.9.3.2.4 Separation Task 1

Table A 114: Summary of the equipment, the important equipment characteristics and the costs for each equipment for literature process of Bastidas *et al.* (2010) using EG [30]. The total equipment costs for the year 2019 and the total permanent investment are also given.

Exchangers	Type	Area [ft ²]	Q [kW]	ΔT_{LM}		Cp
E02	Double pipe	65.99	379.63	80.95		\$ 2,480.73
E07	Shell and tube	174.49	353.44	28.50		\$ 7,842.96
E01	Shell and tube	112.92	715.00	89.09		\$ 7,666.43
E08	Double pipe	8.97	18.10	21.17		\$ 1,802.66
Reboiler EDC	Kettle	1074.97	4316.82	42.13		\$ 29,010.33
Condenser EDC	Shell and tube	929.26	3530.00	53.45		\$ 12,118.35
Reboiler SRC	Kettle	201.33	566.88	29.54		\$ 19,558.19
Condenser SRC	Shell and tube	168.82	650.44	40.42		\$ 7,819.17
					Total HE	\$ 88,298.81
Towers	Type	Diameter [ft]	Height [ft]	Volume [ft ³]	Pressure [psig]	Cp
EDC	Vertical, sieve trays	4.86	45.93	850.54	14.65	\$ 73,265.70
SRC	Vertical, sieve trays	2.79	29.53	180.35	3.77	\$ 42,427.43
					Total Towers	\$ 115,693.13
Vessels	Type	Diameter [ft]	Length [ft]	Volume [ft ³]	Pressure [psig]	Cp
Reflux drum EDC	Horizontal	3.70	11.10	119.41	14.65	\$ 15,271.33
Reflux drum SRC	Horizontal	1.38	4.13	6.15	3.77	\$ 9,730.80
					Total Vessels	\$ 25,002.13
Vacuum System	Type	Volume [ft ³]	Temperature [°C]	Flow [lb/h] or [ft ³ /min]	Pressure [torr]	Cp
Vacuum SRC	Liquid ring pump	180.35	35	11.63	195.02	\$ 19,471.83
					Total HE	\$ 19,471.83
					TOTAL 2019	\$ 301,886.08
					CTPI	\$ 1,502,487.03

Table A 115: Summary of the equipment, the important equipment characteristics and the costs for each equipment for simulated non-heat-integrated DES process. The total equipment costs for the year 2019 and the total permanent investment are also given.

Exchangers	Type	Area [ft ²]	Q [kW]	ΔT_{LM}		Cp
E01	Double pipe	33.76	168.60	70.26		\$ 2,228.55
E02	Double pipe	66.03	380.00	80.98		\$ 2,480.98
E07	Shell and tube	174.47	353.26	28.49		\$ 7,842.84
E08	Double pipe	87.02	319.10	38.47		\$ 2,593.04
E09	Double pipe	1.00	9.87	113.90		\$ 1,269.02
E10	Double pipe	12.71	65.91	54.41		\$ 1,906.00
E11	Double pipe	1.00	4.80	124.10		\$ 1,269.02
E04: Reboiler EDC	Kettle	616.40	3088.70	52.57		\$ 24,063.95
E05: Condenser EDC	Shell and tube	731.45	2750.50	52.91		\$ 11,008.01
E05: Evap 1	Horizontal tube	22.26	53.63	33.90		\$ 21,022.69
E06: Evap 2	Horizontal tube	62.93	111.58	24.95		\$ 36,467.58
					Total HE	\$ 112,151.67
Towers	Type	Diameter [ft]	Height [ft]	Volume [ft ³]	Pressure [psig]	Cp
EDC	Vertical, sieve trays	4.13	50.85	682.52	14.65	\$ 75,784.45
					Total Towers	\$ 75,784.45
Vessels	Type	Diameter [ft]	Length [ft]	Volume [ft ³]	Pressure [psig]	Cp
Reflux drum EDC	Horizontal	3.41	10.22	93.23	14.65	\$ 14,407.82
					Total Vessels	\$ 14,407.82
Vacuum System	Type	Volume [ft ³]	Temperature [°C]	Flow [lb/h] or [ft ³ /min]	Pressure [torr]	Cp
Vacuum Evap 1	Liquid ring pump	96.24	10	255.81	15.00	\$ 57,441.49
Vacuum Evap 2	Steam jet ejector	39.85	-8	25.00	2.25	\$ 9,524.40
					Total HE	\$ 66,965.89
					TOTAL 2019	\$ 327,211.44
					CTPI	\$ 1,628,531.31

Table A 116: Summary of the equipment, the important equipment characteristics and the costs for each equipment for simulated heat-integrated DES process. The total equipment costs for the year 2019 and the total permanent investment are also given.

Exchangers	Type	Area [ft ²]	Q [kW]	ΔT_{LM}		Cp
E01	Double pipe	93.87	167.91	25.17		\$ 2,624.68
E02	Shell and tube	164.03	211.00	18.10		\$ 7,799.87
E07	Shell and tube	106.34	142.26	18.82		\$ 7,664.83
E08	Double pipe	87.02	319.10	38.47		\$ 2,593.04
E09	Double pipe	0.91	9.87	113.90		\$ 1,249.82
E10	Double pipe	12.71	65.91	54.41		\$ 1,906.00
E11	Double pipe	0.54	4.80	124.10		\$ 1,151.31
E04: Reboiler EDC	Kettle	618.95	3088.55	52.35		\$ 24,092.43
E05: Condenser EDC	Shell and tube	731.39	2750.30	52.91		\$ 11,007.71
E05: Evap 1	Horizontal tube	22.26	53.63	33.90		\$ 21,022.69
E06: Evap 2	Horizontal tube	62.93	111.58	24.95		\$ 36,467.58
					Total HE	\$ 117,579.94
Towers	Type	Diameter [ft]	Height [ft]	Volume [ft ³]	Pressure [psig]	Cp
EDC	Vertical, sieve trays	4.13	50.85	682.52	14.65	\$ 75,784.45
					Total Towers	\$ 75,784.45
Vessels	Type	Diameter [ft]	Length [ft]	Volume [ft ³]	Pressure [psig]	Cp
Reflux drum EDC	Horizontal	3.41	10.22	93.23	14.65	\$ 14,407.82
					Total Vessels	\$ 14,407.82
Vacuum System	Type	Volume [ft ³]	Temperature [°C]	Flow [lb/h] or [ft ³ /min]	Pressure [torr]	Cp
Vacuum Evap 1	Liquid ring pump	96.24	10	255.81	15.00	\$ 57,441.49
Vacuum Evap 2	Steam jet ejector	39.85	-8	25.00	2.25	\$ 9,524.40
					Total HE	\$ 66,965.89
					TOTAL 2019	\$ 333,806.78
					CTPI	\$ 1,661,356.36

C.9.3.2.5 Separation Task 2

Table A 117: Summary of the equipment, the important equipment characteristics and the costs for each equipment for literature process of Zhu *et al.* (2016) using the IL [Emim]⁺[BF₄]⁻ [35]. The total equipment costs for the year 2019 and the total permanent investment are also given.

Exchangers	Type	Area [ft ²]	Q [kW]	ΔT_{LM}		Cp
E07	Double pipe	68.04	137.24	28.38		\$ 2,492.94
E08	Double pipe	93.56	188.79	21.17		\$ 2,623.26
E09	Double pipe	2.02	3.42	17.78		\$ 1,419.89
Reboiler	Kettle	315.13	2047.80	68.17		\$ 20,683.59
Condenser	Shell and tube	490.18	1851.60	53.15		\$ 9,613.57
Evap	Horizontal tube	79.92	170.41	30.00		\$ 46,900.70
					Total HE	\$ 83,733.95
Towers	Type	Diameter [ft]	Height [ft]	Volume [ft ³]	Pressure [psig]	Cp
EDC	Vertical, sieve trays	3.22	75.46	612.67	14.65	\$ 115,982.79
					Total Towers	\$ 115,982.79
Vessels	Type	Diameter [ft]	Length [ft]	Volume [ft ³]	Pressure [psig]	Cp
Reflux drum EDC	Horizontal	2.99	8.96	62.83	14.65	\$ 13,214.27
					Total Vessels	\$ 13,214.27
Vacuum System	Type	Volume [ft ³]	Temperature [°C]	Flow [lb/h] or [ft ³ /min]	Pressure [torr]	Cp
Vacuum Evap 1	Liquid ring pump	284.02	9	61.05	75.01	\$ 34,789.16
					Total HE	\$ 34,789.16
					TOTAL 2019	\$ 300,980.01
					CTPI	\$ 1,497,977.51

Table A 118: Summary of the equipment, the important equipment characteristics and the costs for each equipment for simulated non-heat-integrated DES process. The total equipment costs for the year 2019 and the total permanent investment are also given.

Exchangers	Type	Area [ft ²]	Q [kW]	ΔT_{LM}		Cp
E07	Double pipe	68.33	138.34	28.49		\$ 2,494.64
E08	Double pipe	45.97	187.70	42.83		\$ 2,341.36
E09	Double pipe	1	5.59	113.57		\$ 1,269.02
E10	Double pipe	6.11	26.81	61.74		\$ 1,695.23
E11	Double pipe	1	1.88	122.20		\$ 1,269.02
E04: Reboiler EDC	Kettle	292.47	1393.55	49.99		\$ 20,440.37
E03: Condenser EDC	Shell and tube	262.84	1163.32	62.28		\$ 8,291.03
E05: Evap 1	Horizontal tube	44.44	66.01	0.00		\$ 30,328.09
E06: Evap 2	Horizontal tube	41.42	42.54	14.45		\$ 29,218.41
					Total HE	\$ 97,347.16
Towers	Type	Diameter [ft]	Height [ft]	Volume [ft ³]	Pressure [psig]	Cp
EDC	Vertical, sieve trays	2.69	45.93	261.54	14.65	\$ 55,692.28
					Total Towers	\$ 55,692.28
Vessels	Type	Diameter [ft]	Length [ft]	Volume [ft ³]	Pressure [psig]	Cp
Reflux drum EDC	Horizontal	2.45	7.34	34.48	14.65	\$ 11,748.14
					Total Vessels	\$ 11,748.14
Vacuum System	Type	Volume [ft ³]	Temperature [°C]	Flow [lb/h] or [ft ³ /min]	Pressure [torr]	Cp
Vacuum Evap 1	Liquid ring pump	44.41	10	255.81	15.00	\$ 57,441.49
Vacuum Evap 2	Steam jet ejector	11.99	-8	16.31	2.03	\$ 8,348.53
					Total HE	\$ 65,790.01
					TOTAL 2019	\$ 280,151.78
					CTPI	\$ 1,394,315.42

Table A 119: Summary of the equipment, the important equipment characteristics and the costs for each equipment for simulated heat-integrated DES process. The total equipment costs for the year 2019 and the total permanent investment are also given.

Exchangers	Type	Area [ft ²]	Q [kW]	ΔT_{LM}		Cp
E02	Double pipe	57.91	41.80	30.83		\$ 2,429.44
E01	Shell and tube	133.72	110.65	35.34		\$ 7,700.30
E07	Double pipe	56.62	96.53	23.99		\$ 2,420.70
E08	Double pipe	45.96	187.70	42.84		\$ 2,341.27
E09	Double pipe	1.00	5.59	113.57		\$ 1,269.02
E10	Double pipe	4.56	26.81	61.74		\$ 1,617.45
E11	Double pipe	1.00	1.88	122.20		\$ 1,269.02
E04: Reboiler EDC	Kettle	260.16	1239.60	49.99		\$ 20,105.20
E03: Condenser EDC	Shell and tube	237.57	1051.50	62.28		\$ 8,153.05
E05: Evap 1	Horizontal tube	44.44	66.01	20.90		\$ 30,328.09
E06: Evap 2	Horizontal tube	41.42	42.54	14.45		\$ 29,218.41
					Total HE	\$ 106,851.95
Towers	Type	Diameter [ft]	Height [ft]	Volume [ft ³]	Pressure [psig]	Cp
EDC	Vertical, sieve trays	2.53	45.93	230.23	14.65	\$ 54,495.27
					Total Towers	\$ 54,495.27
Vessels	Type	Diameter [ft]	Length [ft]	Volume [ft ³]	Pressure [psig]	Cp
Reflux drum EDC	Horizontal	2.45	7.34	34.48	14.65	\$ 11,748.14
					Total Vessels	\$ 11,748.14
Vacuum System	Type	Volume [ft ³]	Temperature [°C]	Flow [lb/h] or [ft ³ /min]	Pressure [torr]	Cp
Vacuum Evap 1	Liquid ring pump	44.41	10	255.81	15.00	\$ 57,441.49
Vacuum Evap 2	Steam jet ejector	11.99	-8	16.31	2.03	\$ 8,348.53
					Total HE	\$ 65,790.01
					TOTAL 2019	\$ 290,245.73
					CTPI	\$ 1,444,552.97

C.9.3.2.6 Separation Task 3

Table A 120: Summary of the equipment, the important equipment characteristics and the costs for each equipment for literature process of Ghuge *et al.* (2017) using the conventional solvent DMSO [31]. The total equipment costs for the year 2019 and the total permanent investment are also given.

Exchangers	Type	Area [ft ²]	Q [kW]	ΔT_{LM}		Cp
E01	Double pipe	83.96	510.10			\$ 2,578.21
E07	Double pipe	60.36	127.77			\$ 2,445.62
E08	Double pipe	20.72	70.54			\$ 2,061.09
Reboiler EDC	Kettle	361.67	1412.80			\$ 21,195.84
Condenser EDC	Shell and tube	277.71	1051.50			\$ 8,374.24
Reboiler EDC	Kettle	174.38	1239.60			\$ 19,358.02
Condenser EDC	Shell and tube	100.00	1051.50			\$ 7,668.83
					Total HE	\$ 63,681.85
Towers	Type	Diameter [ft]	Height [ft]	Volume [ft ³]	Pressure [psig]	Cp
EDC	Vertical, sieve trays	2.30	77.10	319.38	14.65	\$ 112,163.03
SRC	Vertical, sieve trays	2.66	42.65	236.57	14.65	\$ 50,389.84
					Total Towers	\$ 162,552.86
Vessels	Type	Diameter [ft]	Length [ft]	Volume [ft ³]	Pressure [psig]	Cp
Reflux drum EDC	Horizontal	3.26	9.78	81.64	14.65	\$ 13,983.11
Reflux drum SRC	Horizontal	1.56	4.67	8.88	14.65	\$ 9,516.04
					Total Vessels	\$ 23,499.15
					TOTAL 2019	\$ 303,426.64
					CTPI	\$ 1,510,154.40

Table A 121: Summary of the equipment, the important equipment characteristics and the costs for each equipment for literature process of Ma *et al.* (2019) using the IL [Emim]⁺[N(CN)₂]⁻ [36]. Total equipment costs for the year 2019 and the total permanent investment are also given.

Exchangers	Type	Area [ft ²]	Q [kW]	ΔT_{LM}		Cp
E07	Double pipe	60.34	127.72	29.78		\$ 2,445.51
E08	Shell and tube	116.86	532.05	47.76		\$ 7,669.79
E09	Double pipe	18.72	63.06	35.35		\$ 2,027.79
E10	Double pipe	20.31	64.09	44.39		\$ 2,054.53
E11	Double pipe	1.00	3.98	124.89		\$ 1,269.02
E01	Double pipe	82.98	479.71	81.35		\$ 2,573.36
Reboiler EDC	Kettle	238.75	1480.30	65.05		\$ 19,894.06
Condenser EDC	Shell and tube	200.44	810.38	56.89		\$ 7,962.27
Evap 1	Horizontal tube	158.26	567.57	50.46		\$ 67,364.03
Evap 2	Horizontal tube	17.55	57.37	46.00		\$ 20,999.19
					Total HE	\$ 134,259.55
Towers	Type	Diameter [ft]	Height [ft]	Volume [ft ³]	Pressure [psig]	Cp
EDC	Vertical, sieve trays	2.63	50.85	276.73	14.65	\$ 63,200.28
					Total Towers	\$ 63,200.28
Vessels	Type	Diameter [ft]	Length [ft]	Volume [ft ³]	Pressure [psig]	Cp
Reflux drum EDC	Horizontal	3.16	9.48	74.22	14.65	\$ 13,693.05
					Total Vessels	\$ 13,693.05
Vacuum System	Type	Volume [ft ³]	Temperature [°C]	Flow [lb/h] or [ft ³ /min]	Pressure [torr]	Cp
Vacuum Evap 1	Liquid ring pump		25	18.78	68.85	\$ 23,027.53
Vacuum Evap 2	Steam jet ejector		-10	20.46	2.62	\$ 8,246.39
					Total HE	\$ 31,273.92
					TOTAL 2019	\$ 294,548.57
					CTPI	\$ 1,465,968.21

Table A 122: Summary of the equipment, the important equipment characteristics and the costs for each equipment for simulated non-heat-integrated DES process. The total equipment costs for the year 2019 and the total permanent investment are also given.

Exchangers	Type	Area [ft ²]	Q [kW]	ΔT_{LM}		Cp
E01	Double pipe	58.31	116.40	85.26		\$ 2,432.15
E07	Double pipe	60.36	127.80	29.79		\$ 2,445.63
E08	Shell and tube	109.79	620.00	59.25		\$ 7,665.00
E09	Double pipe	5.19	6.50	13.14		\$ 1,651.45
E10	Double pipe	12.75	54.70	60.37		\$ 1,906.96
E11	Double pipe	1.00	4.56	124.87		\$ 1,269.02
E04: Reboiler	Kettle	177.94	1193.50	70.37		\$ 19,381.73
E03: Condenser	Shell and tube	219.2377025	1026.60	65.89		\$ 8,056.61
E05: Evap 1	Horizontal tube	241.520441	732.50	42.67		\$ 74,386.07
E06: Evap 2	Horizontal tube	20.65180055	45.50	31.00		\$ 20,204.76
					Total HE	\$ 139,399.37
Towers	Type	Diameter [ft]	Height [ft]	Volume [ft ³]	Pressure [psig]	Cp
EDC	Vertical, sieve trays	2.59	50.85	268.12	14.65	\$ 62,890.52
					Total Towers	\$ 62,890.52
Vessels	Type	Diameter [ft]	Length [ft]	Volume [ft ³]	Pressure [psig]	Cp
Reflux drum EDC	Horizontal	2.74	8.23	48.59	14.65	\$ 12,540.29
					Total Vessels	\$ 12,540.29
Vacuum System	Type	Volume [ft ³]	Temperature [°C]	Flow [lb/h] or [ft ³ /min]	Pressure [torr]	Cp
Vacuum Evap 1	Liquid ring pump	97.52	35	82.36	60.00	\$ 38,633.10
Vacuum Evap 2	Steam jet ejector	24.18	-15	12.15	2.03	\$ 7,398.61
					Total HE	\$ 46,031.70
					TOTAL 2019	\$ 316,947.19
					CTPI	\$ 1,577,446.16

Table A 123: Summary of the equipment, the important equipment characteristics and the costs for each equipment for simulated heat-integrated DES process. The total equipment costs for the year 2019 and the total permanent investment are also given.

Exchangers	Type	Area [ft ²]	Q [kW]	ΔT_{LM}		Cp
E01	Shell and tube	118.05	123.17	44.57		\$ 7,671.12
E02	Double pipe	19.11	50.00	36.81		\$ 2,034.60
E07	Double pipe	46.81	77.78	23.38		\$ 2,348.16
E08	Shell and tube	109.79	620.00	59.25		\$ 7,665.00
E09	Double pipe	5.19	6.50	13.14		\$ 1,651.45
E10	Double pipe	12.75	54.70	60.37		\$ 1,906.96
E11	Double pipe	1.00	4.56	124.87		\$ 1,269.02
E04: Reboiler	Kettle	154.24	1026.40	69.82		\$ 19,245.30
E03: Condenser	Shell and tube	219.10	1025.95	65.89		\$ 8,055.89
E05: Evap 1	Horizontal tube	241.52	732.50	42.67		\$ 74,386.07
E06: Evap 2	Horizontal tube	20.65	45.50	31.00		\$ 20,204.76
					Total HE	\$ 146,438.32
Towers	Type	Diameter [ft]	Height [ft]	Volume [ft ³]	Pressure [psig]	Cp
EDC	Vertical, sieve trays	2.60	50.85	268.99	14.65	\$ 62,921.65
					Total Towers	\$ 62,921.65
Vessels	Type	Diameter [ft]	Length [ft]	Volume [ft ³]	Pressure [psig]	Cp
Reflux drum EDC	Horizontal	2.64	7.93	43.49	14.65	\$ 12,271.31
					Total Vessels	\$ 12,271.31
Vacuum System	Type	Volume [ft ³]	Temperature [°C]	Flow [lb/h] or [ft ³ /min]	Pressure [torr]	Cp
Vacuum Evap 1	Liquid ring pump	97.52	35	82.36	60.00	\$ 38,633.10
Vacuum Evap 2	Steam jet ejector	24.18	-15	12.15	2.03	\$ 7,398.61
					Total HE	\$ 46,031.70
					TOTAL 2019	\$ 325,210.53
					CTPI	\$ 1,229,295.79

C.9.3.3 Total Annual Production Costs

C.9.3.3.7 Separation Task 1

Table A 124: Utility consumption, and prices, and annual production costs of the extractive distillation of ethanol and water using EG simulated by Bastidas *et al.* (2010) [30].

Bill of Materials			Product Production: 78702 ton/year		
Utilities	Consumption (unit/kg product)	Price (\$/unit utility)	Cost (\$/kg product)	Consumption (unit/year)	Annual Costs (\$/year)
HP Steam [ton/yr]	0.00	\$14.50	\$0.00	0.00	\$0.00
MP Steam [ton/yr]	884.58	\$10.50	\$9,288.12	69618.85	\$730,997.91
LP Steam [ton/yr]	63.61	\$6.60	\$419.83	5006.34	\$33,041.84
Electricity [kWh/yr]	127.22	\$0.06	\$7.63	10012.68	\$600.76
Cooling water [m ³ /yr]	45073.49	\$0.02	\$901.47	3547394.33	\$70,947.89
Chilled water [GJ/yr]					
Refrigerant [GJ/yr]	0.00	\$5.50	\$0.00	0.00	\$0.00
Total Variable Costs					\$835,588.40

Table A 125: Utility consumption, and prices, and annual production costs of the extractive distillation of ethanol and water using ChCl:Ur (1:2) for the non-heat integrated process.

Bill of Materials			Product Production: 78702 ton/year		
Utilities	Consumption (unit/kg product)	Price (\$/unit utility)	Cost (\$/kg product)	Consumption (unit/year)	Annual Costs (\$/year)
HP Steam [ton/yr]	0.00	\$14.50	\$0.00	0.00	\$0.00
MP Steam [ton/yr]	570.42	\$10.50	\$5,989.38	44893.26	\$471,379.23
LP Steam [ton/yr]	94.08	\$6.60	\$620.90	7403.98	\$48,866.25
Electricity [kWh/yr]	120.21	\$0.06	\$7.21	9460.80	\$567.65
Cooling water [m ³ /yr]	28347.00	\$0.02	\$566.94	2230978.38	\$44,619.57
Chilled water [GJ/yr]	115.09	\$4.00	\$460.34	9057.51	\$36,230.05
Refrigerant [GJ/yr]	24.14	\$5.50	\$132.77	1899.92	\$10,449.58
Total Variable Costs					\$612,112.33

Table A 126: Utility consumption, and prices, and annual production costs of the extractive distillation of ethanol and water using ChCl:Ur (1:2) for the heat integrated process.

Bill of Materials			Product Production: 78702 ton/year		
Utilities	Consumption (unit/kg product)	Price (\$/unit utility)	Cost (\$/kg product)	Consumption (unit/year)	Annual Costs (\$/year)
HP Steam [ton/yr]	0.00	\$14.50	\$0.00	0.00	\$0.00
MP Steam [ton/yr]	570.75	\$10.50	\$5,992.84	44919.18	\$471,651.44
LP Steam [ton/yr]	30.31	\$6.60	\$200.08	2385.85	\$15,746.62

Electricity [kWh/yr]	120.21	\$0.06	\$7.21	9460.80	\$567.65
Cooling water [m ³ /yr]	25067.58	\$0.02	\$501.35	1972879.87	\$39,457.60
Chilled water [GJ/yr]	115.09	\$4.00	\$460.34	9057.51	\$36,230.05
Refrigerant [GJ/yr]	24.14	\$5.50	\$132.77	1899.92	\$10,449.58
Total Variable Costs					\$574,102.94

C.9.3.3.8 Separation Task 2

Table A 127: Utility consumption, and prices, and annual production costs of the extractive distillation of ethanol and water using the IL [Emim]⁺[BF₄]⁻ simulated by Zhu *et al.* (2016) [35].

Bill of Materials			Product Production: 30842 ton/year		
Utilities	Consumption (unit/kg product)	Price (\$/unit utility)	Cost (\$/kg product)	Consumption (unit/year)	Annual Costs (\$/year)
HP Steam [ton/yr]	0.00	\$14.50	\$0.00	0.00	\$ -
MP Steam [ton/yr]	946.50	\$10.50	\$9,938.20	29192.10	\$ 306,517.09
LP Steam [ton/yr]	73.14	\$6.60	\$482.74	2255.90	\$ 14,888.93
Electricity [kWh/yr]	324.64	\$0.06	\$19.48	10012.68	\$ 600.76
Cooling water [m ³ /yr]	48403.49	\$0.02	\$968.07	1492875.57	\$ 29,857.51
Chilled water [GJ/yr]	-	\$ -	\$ -		\$ -
Refrigerant [GJ/yr]	0.00	\$5.50	\$0.00	0.00	\$ -
Total Variable Costs					\$ 351,864.29

Table A 128: Utility consumption, and prices, and annual production costs of the extractive distillation of ethanol and water using ChCl:Ur (1:2) for the non-heat integrated process.

Bill of Materials			Product Production: 30842 ton/year		
Utilities	Consumption (unit/kg product)	Price (\$/unit utility)	Cost (\$/kg product)	Consumption (unit/year)	Annual Costs (\$/year)
HP Steam [ton/yr]	0.00	\$ 14.50	\$ -	0.00	\$ -
MP Steam [ton/yr]	663.09	\$ 10.50	\$ 6,962.40	20451.10	\$214,736.53
LP Steam [ton/yr]	49.80	\$ 6.60	\$ 328.68	1535.97	\$ 10,137.40
Electricity [kWh/yr]	434.56	\$ 0.06	\$ 26.07	13402.80	\$ 804.17
Cooling water [m ³ /yr]	28782.77	\$ 0.02	\$ 575.66	887727.19	\$ 17,754.54
Chilled water [GJ/yr]	172.73	\$ 4.00	\$ 690.92	5327.40	\$ 21,309.61
Refrigerant [GJ/yr]	24.67	\$ 5.50	\$ 135.70	760.95	\$ 4,185.25
Total Variable Costs					\$268,927.50

Table A 129: Utility consumption, and prices, and annual production costs of the extractive distillation of ethanol and water using ChCl:Ur (1:2) for the heat integrated process.

Bill of Materials			Product Production: 30842 ton/year		
Utilities	Consumption (unit/kg product)	Price (\$/unit utility)	Cost (\$/kg product)	Consumption (unit/year)	Annual Costs (\$/year)
HP Steam [ton/yr]	0.00	\$ 14.50	\$ -	0.00	\$-
MP Steam [ton/yr]	591.81	\$ 10.50	\$ 6,214.03	18252.87	\$ 191,655.14
LP Steam [ton/yr]	49.80	\$ 6.60	\$ 328.68	1535.97	\$ 10,137.40
Electricity [kWh/yr]	434.56	\$ 0.06	\$ 26.07	13402.80	\$ 804.17
Cooling water [m ³ /yr]	25385.57	\$ 0.02	\$ 507.71	782949.76	\$ 15,659.00
Chilled water [GJ/yr]	172.73	\$ 4.00	\$ 690.92	5327.40	\$ 21,309.61
Refrigerant [GJ/yr]	24.67	\$ 5.50	\$ 135.70	760.95	\$ 4,185.25
Total Variable Costs					\$243,750.56

C.9.3.3.9 Separation Task 3

Table A 130: Utility consumption, and prices, and annual production costs of the extractive distillation of IPA and water using the IL $[\text{Emim}]^+[\text{N}(\text{CN})_2]^-$ simulated by Ma *et al.* (2019) [36].

Bill of Materials			Product Production: 23654 ton/year		
Utilities	Consumption (unit/kg product)	Price (\$/unit utility)	Cost (\$/kg product)	Consumption (unit/year)	Annual Costs (\$/year)
HP Steam [ton/yr]	0.00	\$14.50	\$0.00	0.00	\$0.00
MP Steam [ton/yr]	1299.66	\$10.50	\$13,646.48	30742.75	\$322,798.86
LP Steam [ton/yr]	2.23	\$6.60	\$14.70	52.67	\$347.64
Electricity [kWh/yr]	126.65	\$0.06	\$7.60	2995.92	\$179.76
Cooling water [m ³ /yr]	71552.69	\$0.02	\$1,431.05	1692533.47	\$33,850.67
Chilled water [GJ/yr]					
Refrigerant [GJ/yr]	76.90	\$5.50	\$422.95	1819.03	\$10,004.65
Total Variable Costs					\$367,181.58

Table A 131: Utility consumption, and prices, and annual production costs of the extractive distillation of IPA and water using DMSO simulated by Ghuge *et al.* (2017) [31].

Bill of Materials			Product Production: 23654 ton/year		
Utilities	Consumption (unit/kg product)	Price (\$/unit utility)	Cost (\$/kg product)	Consumption (unit/year)	Annual Costs (\$/year)
HP Steam [ton/yr]	709.69	\$14.50	\$10,290.58	16787.38	\$243,417.05
MP Steam [ton/yr]	851.43	\$10.50	\$8,939.98	20139.96	\$211,469.55
LP Steam [ton/yr]	0.00	\$6.60	\$0.00	0.00	\$0.00
Electricity [kWh/yr]	0.00	\$0.06	\$0.00	0.00	\$0.00

Cooling water [m ³ /yr]	69432.99	\$0.02	\$1,388.66	1642393.33	\$32,847.87
Chilled water [GJ/yr]					
Refrigerant [GJ/yr]	0.00	\$5.50	\$0.00	0.00	\$0.00
Total Variable Costs					\$487,734.47

Table A 132: Utility consumption, and prices, and annual production costs of the extractive distillation of IPA and water using ChCl:TEG (1:3) for the non-heat integrated process.

Bill of Materials			Product Production: 23654 ton/year		
Utilities	Consumption (unit/kg product)	Price (\$/unit utility)	Cost (\$/kg product)	Consumption (unit/year)	Annual Costs (\$/year)
HP Steam [ton/yr]	0.00	\$14.50	\$0.00	0.00	\$0.00
MP Steam [ton/yr]	1206.50	\$10.50	\$12,668.22	28538.93	\$299,658.78
LP Steam [ton/yr]	2.55	\$6.60	\$16.85	60.38	\$398.52
Electricity [kWh/yr]	506.62	\$0.06	\$30.40	11983.68	\$719.02
Cooling water [m ³ /yr]	54710.38	\$0.02	\$1,094.21	1294139.32	\$25,882.79
Chilled water [GJ/yr]	0.00	\$4.00	\$0.00	0.00	\$0.00
Refrigerant [GJ/yr]	65.61	\$5.50	\$360.83	1551.85	\$8,535.20
Total Variable Costs					\$335,194.30

Table A 133: Utility consumption, and prices, and annual production costs of the extractive distillation of IPA and water using ChCl:TEG (1:3) for the non-heat integrated process.

Bill of Materials			Product Production: 23654 ton/year		
Utilities	Consumption (unit/kg product)	Price (\$/unit utility)	Cost (\$/kg product)	Consumption (unit/year)	Annual Costs (\$/year)
HP Steam [ton/yr]	0.00	\$14.50	\$0.00	0.00	\$0.00
MP Steam [ton/yr]	1105.74	\$10.50	\$11,610.28	26155.60	\$274,633.79
LP Steam [ton/yr]	2.55	\$6.60	\$16.85	60.38	\$398.51
Electricity [kWh/yr]	506.62	\$0.06	\$30.40	11983.68	\$719.02
Cooling water [m ³ /yr]	49896.09	\$0.02	\$997.92	1180260.36	\$23,605.21
Chilled water [GJ/yr]	0.00	\$4.00	\$0.00	0.00	\$0.00
Refrigerant [GJ/yr]	65.60	\$5.50	\$360.83	1551.84	\$8,535.10
Total Variable Costs					\$307,891.63

C.9.3.4 Total Annual Costs

C.9.3.4.10 Separation Task 1

Table A 134: TAC calculation for the extractive distillation of ethanol and water of the literature using IL, and the non-heat-integrated and heat-integrated process using ChCl:Ur (1:2).

	Bastidas <i>et al.</i> (2010) [30]	ChCl:Ur (1:2)	ChCl:Ur (1:2) HI
EDC + Reflux drum	\$ 88,537.03	\$ 90,192.27	\$ 90,192.27
Regeneration	\$ 52,158.24	\$ 57,490.26	\$ 57,490.26
Heat Exchanger	\$ 88,298.81	\$ 54,661.41	\$ 60,089.68
Vacuum system	\$ 19,471.83	\$ 66,965.89	\$ 66,965.89
TOTAL equipment for 2019	\$ 301,886.08	\$ 327,211.44	\$ 333,806.78
C_{TPI}	\$ 1,502,487.03	\$ 1,628,531.31	\$ 1,661,356.36
$C_{TPI} * i_{min}$	\$ 300,497.41	\$ 325,706.26	\$ 332,271.27
Annual Production Costs	\$ 835,588.40	\$ 612,112.33	\$ 574,102.94
TAC	\$ 1,136,085.80	\$ 937,818.59	\$ 906,374.21

C.9.3.4.11 Separation Task 2

Table A 135: TAC calculation for the extractive distillation of ethanol and water of the literature using IL, and the non-heat-integrated and heat-integrated process using ChCl:Ur (1:2).

	IL Zhu <i>et al.</i> (2016) [35]	ChCl:Ur (1:2)	ChCl:Ur (1:2) HI
EDC + Reflux drum	\$ 129,197.06	\$ 67,440.42	\$ 66,243.41
Regeneration	\$ 46,900.70	\$ 59,546.49	\$ 59,546.49
Heat Exchanger	\$ 36,833.26	\$ 37,800.67	\$ 47,305.45
Vacuum system	\$ 34,789.16	\$ 65,790.01	\$ 65,790.01
TOTAL equipment for 2019	\$ 300,980.01	\$ 280,151.78	\$ 290,245.73
C_{TPI}	\$ 1,497,977.51	\$ 1,394,315.42	\$ 1,444,552.97
$C_{TPI} * i_{min}$	\$ 299,595.50	\$ 278,863.08	\$ 288,910.59
Annual Production Costs	\$ 351,864.29	\$ 268,927.50	\$ 243,750.56
TAC	\$ 651,459.79	\$ 547,790.58	\$ 532,661.16

C.9.3.4.12 Separation Task 3

Table A 136: TAC calculation for the extractive distillation of IPA and water of the literature using IL, and the non-heat-integrated and heat-integrated process using ChCl:TEG (1:3).

	IL Ma <i>et al.</i> (2019) [36]	DMSO Ghuge <i>et al.</i> (2017) [31]	ChCl:TEG (1:3)	ChCl:TEG (1:3) HI
EDC + Reflux drum	\$ 76,893.33	\$ 126,146.13	\$ 75,430.81	\$ 75,192.96
Regeneration	\$ 88,363.22	\$ 59,905.88	\$ 94,590.83	\$ 94,590.83
Heat Exchanger	\$ 45,896.33	\$ 56,013.02	\$ 44,808.54	\$ 51,847.50
Vacuum system	\$ 31,273.92	\$ -	\$ 46,031.70	\$ 46,031.70
TOTAL equipment for 2019	\$ 294,548.57	\$ 294,109.01	\$ 316,947.19	\$ 325,210.53
C_{TPI}	\$ 1,465,968.21	\$ 1,463,780.54	\$ 1,577,446.16	\$ 1,618,572.79
$C_{TPI} * i_{min}$	\$ 293,193.64	\$ 292,756.11	\$ 315,489.23	\$ 323,714.56
Annual Production Costs	\$ 367,181.58	\$ 487,734.47	\$ 335,194.30	\$ 307,891.63
TAC	\$ 660,375.22	\$ 780,490.58	\$ 650,683.53	\$ 631,606.19